uOttawa

L'Université canadienne
Canada's university

FACULTÉ DES ÉTUDES SUPÉRIEURES ET POSTOCTORALES

uOttawa

L'Université canadienne
Canada's university

FACULTY OF GRADUATE AND POSDOCTORAL STUDIES

Dalibor Breznan

AUTEUR DE LA THÈSE / AUTHOR OF THESIS

Ph.D. (Biochemistry)

GRADE / DEGREE

Department of Biochemistry, Microbiology and Immunology

FACULTÉ, ÉCOLE, DÉPARTEMENT / FACULTY, SCHOOL, DEPARTMENT

Toxicology of Urban Particulate Matter: *In Vitro* and *In Vivo* Bioassays

TITRE DE LA THÈSE / TITLE OF THESIS

Renaud Vincent

DIRECTEUR (DIRECTRICE) DE LA THÈSE / THESIS SUPERVISOR

CO-DIRECTEUR (CO-DIRECTRICE) DE LA THÈSE / THESIS CO-SUPERVISOR

EXAMINATEURS (EXAMINATRICES) DE LA THÈSE / THESIS EXAMINERS

Keith Tanswell

Jules Blais

Illimar Altosaar

Rosalind Labow

Gary W. Slater

Le Doyen de la Faculté des études supérieures et postdoctorales / Dean of the Faculty of Graduate and Postdoctoral Studies

TOXICOLOGY OF URBAN PARTICULATE MATTER: *IN VITRO* AND *IN VIVO* BIOASSAYS

by

Dalibor Breznan

A thesis submitted to the
Faculty of Graduate and Postdoctoral Studies
in partial fulfillment of the requirements for the degree of
Doctor of Philosophy in Biochemistry

Department of Biochemistry, Microbiology and Immunology
Faculty of Medicine
University of Ottawa
Health Canada

Your file Votre référence
ISBN: 978-0-494-48390-9
Our file Notre référence
ISBN: 978-0-494-48390-9

ABSTRACT

TOXICOLOGY OF URBAN PARTICULATE MATTER: *IN VITRO* AND *IN VIVO* BIOASSAYS

by Dalibor Breznan

Exposure to air particulate matter (PM) is epidemiologically associated with increased incidence of respiratory and cardiovascular disease in humans. Although inflammation, oxidative stress and toxicity have been implicated in the pathophysiological response to air pollution, the physicochemical properties of the particles responsible for the adverse effects are yet to be elucidated. *In vitro* assays are widely used to study the toxicity of particles, however, they have not been comprehensively validated *in vivo*. This work aimed to evaluate *in vitro* cytotoxicity and inflammatory cytokine assays as screening tools for relative toxicity of PM, validate their capacity to predict toxicity of PM in BALB/*c* mice, develop a cell-interaction model for the study of the biological effects of PM, and evaluate its performance in relation to PM effects in animals. Results show that *in vitro* assays conducted in macrophage (J774A.1) and alveolar epithelial (A549) cell lines can discriminate between PM, based on their cytotoxic and inflammatory potency. SRM- and EHC-type particles were more potent than DWR1 ($PM_{2.5}$) and mineral particles both *in vitro* and *in vivo*, although PM rankings varied considerably between assays. PM with different compositions had different toxic potencies. Combinations of 2 to 4 *in vitro* assays showed a predictive potential for PM-induced effects *in vivo*, represented by bronchoalveolar lavage (BAL) neutrophilia in mice. In a co-culture, epithelial (A549) and macrophage (THP-1) cells synergistically modulate their production of pro-inflammatory cytokines (IL-1β, IL-6, IL-8, MCP-1 and TNF-α), ICAM-1 and VEGF in response to PM exposure. Cellular mediators from PM-exposed co-cultures can activate endothelial cells (HPAE) to produce cytokines (IL-6, IL-8, GM-CSF, MCP-1) and adhesion factors (ICAM-1, VCAM-1 and E-selectin). Exposure of mice to EHC-6802, DWR1 and SRM-1650 particles led to BAL neutrophilia and elevated cytokines (IL-6, KC, MIP-1α, TNF-α), with a stronger inflammatory response at 2 hrs then 24 hrs. Statistical comparison of the cell interaction model responses with PM-induced BAL neutrophilia *in vivo* shows that the co-culture model correlates well with biological effects of particles in mice. Along with its ability to simulate physiologically relevant cell-cell interactions, it is a good model for studying mechanisms of PM toxicity, and for relative toxicity screening of particles.

DEDICATION

This work is dedicated to my Granparents

.... .who loved their Grandchildren unconditionally.

pre Ninu a Starkého.

ACKNOWLEDGEMENT

The studies presented in this thesis were performed at the Inhalation Toxicology and Aerobiology laboratory, Health Canada, Tunney's Pasture, Ottawa.

First and foremost I would like to express my sincere gratitude to my supervisor, Dr. Renaud Vincent. I am especially grateful to Renaud for convincing me to become a Ph.D. student in his laboratory and for encouraging me when the going got tough. I would also like to thank him for his mentorship and for the freedom and time he gave me to further my scientific progress. His wide knowledge and his logical way of thinking have been of great value for me.

My thanks go to my Thesis Advisory Committee members, Dr. Odette Laneuville, Dr. Bruno Battistini and Dr. Rémi Aubin for their suggestions and constructive feedback that have been essential in shaping my project, and for their great career advice.

This work would not have been possible without the help from my co-workers who have invaluably contributed to these studies, as well as personally created a great and friendly working environment, over the course of my studies; Josée Guénette, DJ MacIntyre, Patrick Goegan, Erica Blais, Marcelle Phaneuf, Yunus Siddiqui, Dr. Karthikeyan Subramanian, Marc Bourbeau, Lorraine Casavant, Dr. Susantha Mohottalage, Veena Kumar, Dr. Anushuyadevi Saravanamuthu, Dr. Errol Thomson, Dr. Vinita Chauhan, Devi Ganesh, Dr. Makonnen Abebe, Miriam Dubreuil, Robert Edmonstone, Dr. Serdal Sevinc, Kevin Curtin, Dr. Mohamed Abdel Salam, Farrah Rebecca Samuels, Alain Filiatreault, Pierre Gougeon, Dr. Hari Vijai.

In particular, I would like to thank Vinita Chauhan, who introduced me to Renaud, and thus enabled my academic journey in the air pollution research field, and for being a long-time friend and a colleague, who often encouraged me to persevere through the difficult times.

I would also like to thank Dr. Prem Kumarathasan for always being there for questions, advice and interesting conversations.

I extend my profound thanks to Dr. Vas Mezl at BMI, University of Ottawa for providing me with career advice and guidance, over the course of my studies.

I would also like to thank Errol Thomson, for fueling the academic spirit at the Pasture by starting up a graduate student journal club and for the many fun and engaging environmental and scientific conversations.

I am very grateful to Carol Ann Kelly and Nicole Trudel at BMI, University of Ottawa for always keeping me informed of the important deadlines for the Ph.D., and tirelessly organizing many successful student events at the BMI Department.

I owe my deepest heartfelt thanks to my wife Eriko. For her indispensable support throughout my Ph.D. studies, for helping me focus on my goal, for being there for me during the most difficult times. Words are not enough to express my love and gratitude.

I am deeply thankful to my parents Tibor and Judith, and my sister Anna for their love, encouragement, support and their belief in me.

These studies were financially supported by the Safe Environments Programme of Health Canada (the Border Air Quality Strategy, Program on Energy Research and Development). My scholarship funding was provided by University of Ottawa, Ontario Graduate Scholarship in Science and Technology, The Natural Sciences and Engineering Research Council and the Japan Society for the Promotion of Science (Summer Fellowship in Japan). My appreciation goes to Dr. Ilona Skerjanc, at the BMI, University of Ottawa for enabling me to receive a one-time tuition assistance from the BMI Department.

TABLE OF CONTENTS

ABBREVIATIONS

A549	Alveolar epithelial cell line, human
AB	Alamar Blue
AM	Alveolar macrophage
ANOVA	Analysis of variance
AP-1	Activator protein 1
AhR	Aryl hydrocarbon receptor
ATCC	American Tissue Culture Collection
ATP	Adenosine 5'-triphosphate
BAL	Bronchoalveolar lavage
BALB/*c*	Bagg Albino inbred strain of mouse
B[a]P	Benzo[a]pyrene
BEAS-2B	Bronchial epithelial cell line 2B, human
BHT	Butylated hydroxytoluene
BrdU	5-bromo-2'-deoxyuridine
BSA	Bovine serum albumin
C57Bl/6J	Inbred strain of mouse
CAP	Concentrated ambient particles
CAT	Chloramphenicol acetyltransferase
CI	Confidence interval
CM	Conditioned medium
CO	Carbon monoxide
CYP 1A1	Cytochrome P450 1A1
DEP	Diesel exhaust particles
DETPA	Diethylene triamine pentaacetic acid
DMEM	Dulbecco's Modified Eagle Medium
DMSO	Dimethylsulfoxide
DNA	Deoxyribonucleic acid
DTNB	5,5'-dithio-bis(2-nitrobenzoic acid), Ellman's reagent

DWR1	Downsview Reference 1
ECGS	Endothelial cell growth supplement
ECV304	Endothelial, umbilical vein-derived cell line, human
EDTA	Ethylenediamine tetraacetic acid
EHC	Environmental Health Centre
EIA	Enzyme immune-assay
ELISA	Enzyme-linked immunosorbent assay
ET-1	Endothelin 1
EU	Endotoxin units
FBS	Fetal bovine serum
Fe_2O_3	Iron oxide
GM-CSF	Granulocyte-macrophage colony-stimulating factor
GSH/GSSG	Glutathione (reduced) / glutathione disulfide (oxidized)
H1L1.1c2	Hepatoma recombinant cell line, mouse
HBEC	Human bronchial epithelial cells
HEPES	4-(2-hydroxyethyl)-1-piperazineethanesulfonic acid
HepG2	Hepatocellular liver carcinoma cell line, human
HPAE	Human pulmonary artery endothelial cells
HRP	Horse-radish peroxidase
HSP-70	Heat shock protein, 70 kilodalton
HUVEC	Human umbilical vein endothelial cells
ICAM-1	Intercellular adhesion molecule 1
IL-	Interleukin-
IL-1ra	Interleukin-1 receptor antagonist
J774A.1	Monocyte/macrophage cell line/BALB/*c* mouse
KC	Keratinocyte-derived chemokine
LAL	Limulus amebocyte lysate
LDH	Lactate dehydrogenase
LPS	Lipopolysaccharide
M199	Medium 199
MCP-1	Monocyte chemoattractant protein 1

MEM	Minimal Essential Medium
MIP-1	Macrophage inflammatory protein 1
mRNA	Messenger ribonucleic acid
NADPH	Nicotinamide adenine dinucleotide phosphate (reduced)
NC	"No-Cell" control
NFκB	Nuclear Factor Kappa B
NIST	National Institute of Standards and Technology
NO	Nitric oxide
NO_2	Nitrogen dioxide
NO_x	Nitrogen oxides
PAH	Polycyclic aromatic hydrocarbons
PCB	Polychlorinated biphenyls
$PM_{2.5}$	Particulate matter with aerodynamic diameter of less than 2.5 micrometers
PM_{10}	Particulate matter with aerodynamic diameter of less than 10 micrometers
PMA	Phorbol 12-myristate 13-acetate
PMSF	Phenylmethanesulphonyl fluoride
RAIAP	Respiratory allergy and inflammation due to ambient particles
RANTES	Regulated upon activation normal T cell expressed and secreted
ROS	Reactive oxygen species
RPMI-1640	Roswell Park Memorial Institute 1640 medium
SO_2	Sulphur dioxide
SRM	Standard reference material
TCA	Tricarboxylic acid cycle
THP-1	Acute monocytic leukemia cell line, human
TiO_2	Titanium dioxide
TNF-α	Tumor necrosis factor α
UFP	Ultrafine particles
UV	Ultraviolet
VCAM-1	Vascular cell adhesion molecule 1
VEGF	Vascular endothelial growth factor
VIF	Variance inflation factor

LIST OF FIGURES

LIST OF TABLES

Main Research Aim

Much research has been done linking exposure to particulate materials in air pollution with adverse respiratory and cardiovascular outcomes, although many unknowns remain about the mechanisms behind the epidemiological observations. With increasing evidence of acute and chronic effects of air pollution particles on the cellular and organ-levels, there is a need for more extensive evaluations of the relative toxicities of the various particles in relation to their physicochemical properties and for a comprehensive *in vivo* validation of their cellular effects. As current air pollution control efforts are solely based on ambient particle mass standards, studies linking adverse effects with specific emissions could provide a body of evidence for adopting a source apportionment-based regulatory approach to protect public health.

Thus, the main aim of the thesis is to examine and compare the biologic effects of air pollution particles from different sources in cellular (mono-, co-culture) and animal models, and to assess the ability of the *in vitro* screening assays to predict particle toxicity *in vivo*. See Figure 1.1 for the outline of the PM potency analysis and assay validation.

Main Hypothesis

In vitro cytotoxicity and inflammation assays can be utilized for screening of the toxic potency of respirable particulate matter with different physico-chemical characteristics.

Sub Hypothesis # 1 (Study # 1)

In vitro screening assays are good predictors of biological effects of particulate matter *in* vivo.

Sub Hypothesis # 2 (Study # 2)

Cell interactions can modulate the effects of particulate matter *in vitro* and *in vivo*.

Specific Aims of Study # 1

- Evaluate the cytotoxic and pro-inflammatory effects of air pollution particle preparations in cell lines and establish particle potency based on the observed effects *in vitro*.

- Evaluate the toxicity of selected air pollution particles in BALB/*c* mice and establish particle potency based on the observed adverse effects *in vivo*.

- Compare potency *in vitro* with changes in critical *in vivo* endpoints of toxicity.

Specific Aims of Study # 2

- Develop an *in vitro* human pulmonary co-culture model, which enables the evaluation of the effects of cellular interactions on the release of cytotoxic and pro-inflammatory mediators by the cells challenged with air pollution particles.

- Evaluate the toxicity of a subset of $PM_{2.5}$, PM_{10} urban emissions and diesel exhaust particles in BALB/*c* mice.

- Evaluate the association of a critical *in vivo* endpoint of the biological impact of air pollution particles with the *in vitro* assay measurements obtained from the co-culture model.

Outline of PM potency analysis and assay validation

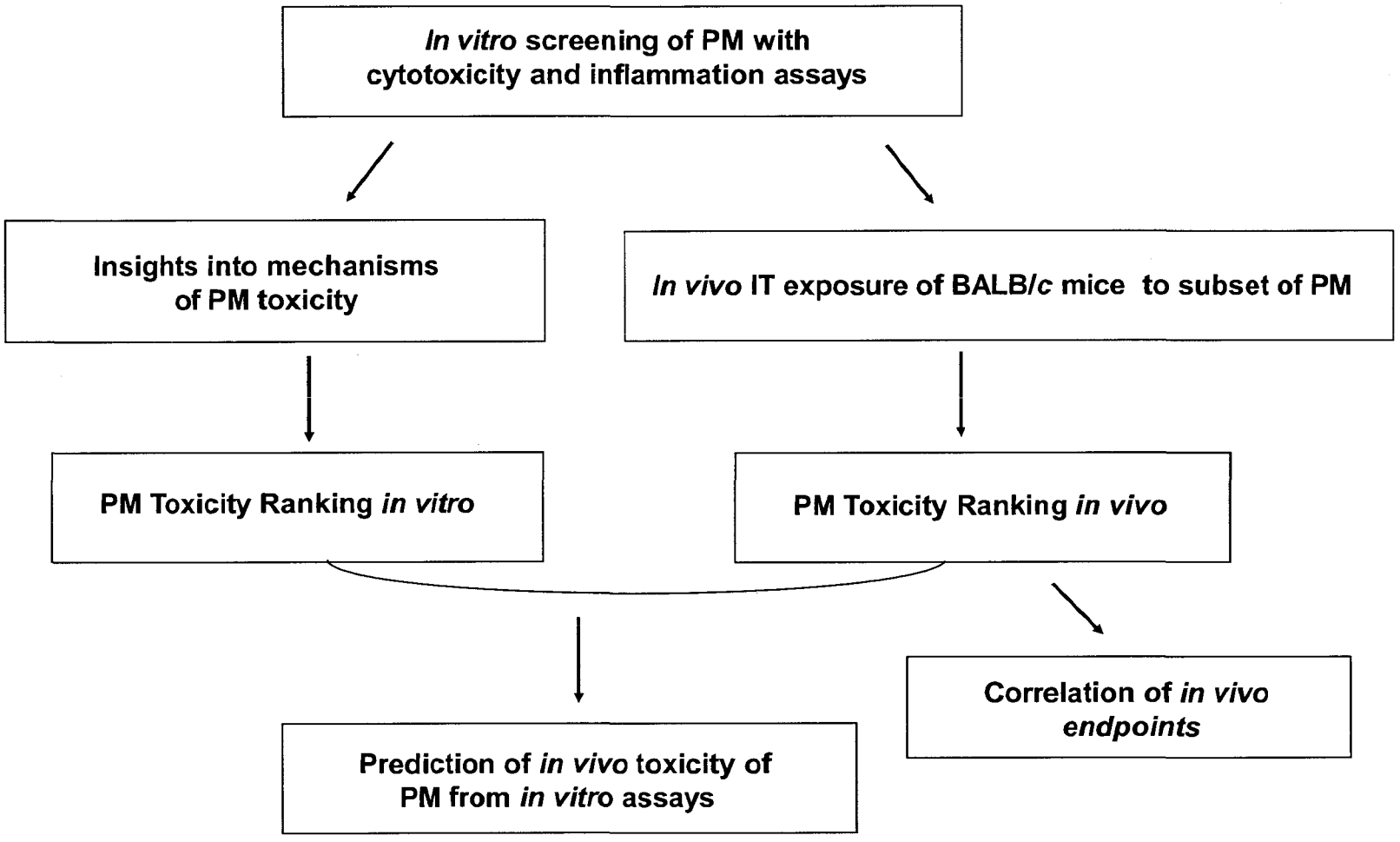

Figure 1.1. Outline of PM potency analysis and assay validation. Toxicity screening of PM is conducted using a panel of *in vitro* cytotoxicity and inflammation assays to rank the particles based on their biological effect potency. A subset of particles with a range of *in vitro* potencies is intratracheally instilled into mice. Multivariate and bivariate statistical analyses are utilized to develop and validate a model for the prediction of a critical *in vivo* endpoint from *in vitro* assays.

GENERAL INTRODUCTION

9.1 Health Effects of PM: Epidemiology, Lung Effects

9.1.1 Morbidity and Mortality

The Clean Air Act of 1956 was passed in response to the London Fog of December 1952, with the legislative aim to reduce pollution from coal burning-derived particulates. Over four days, the smog episode claimed at least 4,000 lives. Despite the lessons learned from the past, urban atmospheric pollution remains a major problem of environmental health (Brunekreef and Holgate, 2002).

In the present day, the urban air pollutants are primarily derived from fossil fuel combustion. The air pollution consists mostly of primary emissions including particulate matter (PM) and gases such as carbon monoxide (CO), sulphur dioxide (SO_2), nitrogen oxides (NO_x) emitted directly from vehicle exhausts and industrial stacks, and secondary pollutants formed from atmospheric reactions of primary emissions with sunlight and moisture, including nitrogen dioxide (NO_2), ozone, or acid rain (ammonium nitrate, NH_4NO_3; sulphuric acid, H_2SO_4; nitric acid, HNO_3).

Epidemiological studies indicate that gaseous and particulate pollutants are associated with increased respiratory and cardiovascular morbidity and mortality (Burnett *et al.*, 2000; Goldberg *et al.*, 2001). Of all these pollutants, airborne particles have been consistently shown to be associated with the observed adverse health effects (Routledge and Ayres, 2005).

The "Harvard Six Cities Study" followed a cohort of 8,000 adults living in six US cities with various levels of pollution from 1974 to 1989 and found that each 10 $\mu g/m^3$ elevation in $PM_{2.5}$ (urban particulate matter with an aerodynamic diameter of less than 2.5 μm) was associated with a 14, 19, and 21 % increased risk of all-cause, cardiopulmonary, and lung cancer mortality, respectively (Dockery *et al.*, 1993; Krewski *et al.*, 2000). The American Cancer Society Study which followed 500,000 individuals living in more than 100 US cities between 1982 and 1989 found an association of 6, 9, and 14 % increased risk of all-cause, cardiopulmonary, and lung cancer mortality, respectively, with 10 $\mu g/m^3$ increase in ambient $PM_{2.5}$ levels (Pope *et al.*, 1995; Pope *et al.*,

2002). A reanalysis of the studies conducted by Krewski and colleagues (2000) confirmed these findings.

A cohort study from the Netherlands which followed-up 5,000 adults aged 55 - 69 years over 8 years, highlighted the importance of including local sources of air pollution in the modeling of the relative risk estimates. The study found nearly a doubling of the relative risk of cardiopulmonary mortality for 10 $\mu g/m^3$ increase in traffic-related black smoke when local source-levels were compared to average background concentrations (Hoek *et al.*, 2001). The public health benefits of intervention that led to substantial reduction in air pollution levels were highlighted by a study from Clancy and colleagues (2002). The study showed 10.3 % and 15.5 % reductions in cardiovascular and respiratory mortality, respectively, after a ban on coal sales in Dublin, which resulted in a 70 % reduction in coal-burning related black smoke.

The respiratory health effects of PM from an epidemiological standpoint can be of acute or chronic nature and include increased hospitalizations due to exacerbations of diseases such as asthma (von Klot *et al.*, 2002) and chronic obstructive pulmonary disease (Schikowski *et al.*, 2005), reduced lung function (Kulkarni *et al.*, 2006), as well as increased risk of lung cancer (Beeson *et al.*, 1998).

9.1.2 Pulmonary Inflammation

Inflammation appears to be an important determinant in the observed respiratory health effects. Alveolar macrophages (AM) and airway epithelial cells play a central role in the defense from inhaled foreign materials, by generating vigorous, localized inflammatory responses in the respiratory tract. The responses involve the production and release of a range of signaling molecules, including cytokines, chemokines, prostaglandins and adhesion molecules. The magnitude of the inflammatory response is tightly controlled by these host-derived factors, which mediate pulmonary inflammation in a network involving locally resident cells, as well as recruited blood-borne leukocytes such as neutrophils and lymphocytes (Standiford *et al.*, 1999).

Depending on the specific profiles of these signaling molecules, different classes of immune cells can be recruited, ranging from eosinophils or mast cells in allergic asthma to predominantly neutrophils in non-allergic-type of inflammatory responses (Sutherland and Martin, 2003). In turn,

the recruited cells release more mediator molecules including proteases and reactive oxygen species (ROS), to aid in the elimination of the initial pulmonary insult. Excessive amount of inflammation, however, may cause localized tissue damage through apoptosis and necrosis of cells, or induce progression to disease, if sustained. This process may occur alongside tissue remodeling brought about by proliferating fibroblasts and myofibroblasts, which is of importance in the development of disease (Holgate *et al.*, 2003).

9.1.3 Airway Remodeling

A number of studies provide evidence for associations of PM exposures with airway remodeling. Lungs of individuals living in high-PM regions including São Paolo, Mexico City, or Fresno (California) evaluated from forensic death cases show great levels of airway abnormalities such as increased airway wall thickness and inflammation, or increased fibrosis and muscle in respiratory bronchioles in comparison to low-PM regions (Souza *et al.*, 1998; Pinkerton *et al.*, 2000, Churg *et al.*, 2003). Evidence for PM exposure-associated airway remodeling also comes from animal models. An investigation of the interaction of EHC-93 (Ottawa urban air particles, Environmental Health Centre, Health Canada) with ozone, in rats exposed by inhalation to the pollutants alone or in combination for 4 hrs, found evidence of acute reparative epithelial cell proliferation in the terminal bronchioles and alveolar ducts in the lungs of the animals, 32 hrs after the exposure to ozone, particles plus ozone, but not with particles alone (Vincent *et al.*, 1997a).

Airway wall remodeling, as observed in the above-described studies has been shown to be associated with chronic airflow obstruction in cigarette smokers and individuals with asthma (Pare *et al.*, 1991). The mechanisms that could be responsible for associations of exposures to high levels of PM and potential development of chronic airflow obstruction, however, remain unknown. A study utilizing an organ culture of rat tracheal explants exposed to EHC-93 particles, or diesel exhaust particles (DEP) for 7 days, provided evidence that the two types of PM directly induced expression of genes involved in fibrogenesis and actual airway wall fibrosis through nuclear factor kappa B- (NFκB) and transforming growth factor-β-mediated mechanisms (Dai *et al.*, 2003).

As evidenced by the "Harvard Six Cities", American Cancer Society Study and other studies, significant associations between air pollution and risk of lung cancer have also been observed

(Dockery *et al.*, 1993; Pope *et al.*, 1995; Beeson *et al.*, 1998). In relation to lung cancer, animal studies have supported the observed human epidemiological findings that PM, in particular, DEP can induce cancer. DEP are coated with polycyclic aromatic hydrocarbons (PAH) and nitro-aromatic hydrocarbons (nitro-PAHs), which are known DNA-adduct-forming genotoxic combustion by-products (Rosenkranz, 1995). As such, DEP are listed by the International Agency for Research on Cancer as *probably carcinogenic to humans*, as group 2A carcinogens (IARC, 1989).

9.2 Health Effects of PM: Cardiovascular Mechanisms

9.2.1 Endothelial Dysfunction

The endothelial monolayer is a physical and biological barrier that forms an interface between circulating blood in the lumen and the rest of the vascular wall. Among other functions, the endothelium regulates vascular hemodynamic homeostasis by producing vasoactive mediators such as nitric oxide (NO), endothelin-1 (ET-1), or prostacyclins (Bai *et al.*, 2007).

The notion that air pollutants may exert their effects through perturbations of vascular homeostasis was investigated in animal models. This work, pioneered by our laboratory has shown elevations of ET-1, a potent vasoconstrictor peptide in the plasma of rats exposed to EHC-93 urban air particles, or urban particles plus ozone, for 4 hrs by inhalation, followed by 20 h recovery in clean air. Alongside the augmented levels of circulating ET-1, decreased production of NO, a potent endothelium-derived vasodilator, and elevated secretion of macrophage inflammatory protein-2, a leukocyte chemoattractant protein from lung lavage cells were also observed in response to EHC-93 exposure. The co-exposure with ozone did not alter the observed ET-1 response, although it did increase the septal thickness in alveolar ducts and induced alveolar type II cell hyperplasia/hypertrophy, both signs of acute effects of pulmonary toxicants. Moreover, the lack of pronounced acute inflammation in lungs of the particle-only exposed animals suggested a potential impact of the distally distributed particles on capillary endothelial production or filtration of this vasoconstrictor peptide (Bouthillier *et al.*, 1998).

ET-1 has been associated with vascular endothelial dysfunction and adverse cardiovascular prognosis (Levin, 1995). It has been shown to play important roles in cardiovascular disorders including atherosclerosis, congestive heart failure, ischemic heart disease, as well as other

vascular disorders such as pulmonary hypertension, or stroke. A 25 % elevation of plasma ET-1 is highly predictive of congestive heart failure (Galatius-Jensen *et al.*, 1996). Moreover, ET-1 is chemotactic to monocytes, activates neutrophils and stimulates production of cytokines and growth factors, among other functions (Lüscher and Barton, 2000).

Similarly, our laboratory has shown additional evidence for plasma elevations of ET-1 in rats, 32 hrs after their exposure for 4 hrs to EHC-93 particles by nose-only inhalation, in the absence of acute lung injury. Water-leached EHC-93 particles induced increased ET-1 plasma levels 2 hrs upon exposure, with a return to basal levels 30 hrs afterwards, indicating a difference in hemodynamic effects of the urban particle when polar organic compounds and soluble elements were removed. Elevations of systemic blood pressure of the animals on day 2 after exposure to EHC-93 were also observed. The observed increase in blood pressure thus coincided with the plasma elevation of ET-1 (Vincent *et al.*, 2001).

In line with these observations, a randomized crossover trial with 25 healthy adults compared the vascular response to a 2 h inhalation of concentrated ambient fine particles (CAP) plus ozone versus the response to the inhalation of filtered air. The study found evidence of acute arterial vasoconstriction in subjects exposed to CAP (Brook *et al.*, 2002). Association between plasma ET-1 and urban air pollution was also observed in 81 children living in Mexico City, which in comparison to children from a city with low $PM_{2.5}$ displayed elevated plasma ET-1 levels and mean pulmonary arterial pressure after 7-day cumulative levels of high $PM_{2.5}$ (Calderón-Garcidueñas *et al.*, 2007).

Although mechanisms involved in the elevations of this potent vasoconstrictor associated with inhalation of air pollution particles still remain unknown, work from our laboratory has provided evidence for extensive regulation of the expression of lung endothelin system genes by PM. The observed rapid and transient transcriptional regulation is consistent with the acute plasma elevations of ET-1 (Thomson *et al.*, 2004). In line with this observation, a follow-up study by Thomson and colleagues (2005) provides further mechanistic evidence suggesting that the reported plasma elevations of ET-1 in rats exposed to PM by inhalation may result from a pulmonary spill-over of the ET-1 peptide into systemic circulation. Furthermore, the study also shows evidence for differential regulation of ET-1 in an ozone-PM co-exposure scenario in

comparison to PM-only exposure, suggestive of alternative processing of the peptide in the lungs by a potential candidate enzyme matrix metalloproteinase-2. An additional study from our laboratory examined the expression of the endothelin system in A549 human alveolar epithelial cells exposed to urban particle EHC-93 and minerals for 24 hrs. The study showed decreased expression of preproET-1 and matrix metalloproteinase-2 mRNA, as well as decreased secretion of ET-1 peptide and dysregulation of endothelin system genes involved in production and clearance of the ET-1 peptide. The findings suggested that alveolar epithelial cells (a critical target for PM_{10}-induced effects), may not be a likely source of higher pulmonary ET-1 spill-over in the circulation measured *in vivo* in response to EHC-93. A549 cells, however, released IL-8 and VEGF in response to particles, which could potentially up-regulate ET-1 production in adjacent endothelial or smooth muscle cells, in accordance with the elevated circulating levels of ET-1 (Chauhan *et al.*, 2005).

Two additional endothelin isoforms, ET-2 and ET-3, encoded by independent genes have been identified. The peptides also exert similar vasoconstrictor responses to ET-1, but show different affinities to the ET-receptor subtypes (Inoue *et al.*, 1989). Not much is known about their pulmonary regulation, however, some studies suggest alterations in circulating levels of ET-2 in aged rats exposed to highway air pollution, and of ET-3 in young, healthy rats exposed to EHC-93 urban particles by inhalation (Vincent *et al.*, 2001; Elder *et al.*, 2004).

A more recent study, examined the pulmonary gene expression levels of the three ET isopeptides in healthy rats exposed to EHC-93, ozone, or EHC-93 plus ozone. The study did not show changes in ET-2 mRNA and peptide levels, but found evidence for differential regulation of ET-1 and ET-3. The results showed a downregulation of preproET-3 in the lungs of EHC-93-ozone exposed animals, in contrast to the upregulation of preproET-1, implying that the extra-pulmonary regulation may be responsible for the sustained (>48 hrs) elevated circulating levels of ET-3 detected immediately after exposure (Thomson *et al.*, 2006).

In line with evidence of endothelin synthesis in the pituitary, rats exposed to EHC-93 particles and ozone for 4 hrs, by nose-only inhalation showed significantly increased preproET-1 and preproET-3 mRNA in the pituitary and preproET-1 in the cerebral hemispheres of the exposed animals, immediately after exposure, and 24 hrs post-exposure, although the data suggest that

the responses are more related to ozone than particles (Thomson *et al.*, 2007). The data show that ambient air pollutants may exert adverse effects on the brain.

9.2.2 Cardiovascular Disease

Several hypotheses have been proposed to explain PM-induced cardiovascular disease. Seaton and colleagues (1995) proposed that particles present in the lungs upon inhalation induced a low-grade alveolar inflammation, with release of mediators capable of increasing blood coagulability, associated with cardiovascular conditions exacerbation in susceptible individuals.

Peters and colleagues have tested this hypothesis in a cross-sectional study, by comparing measurements of plasma viscosity of individuals during an air pollution episode in Augsburg, Germany, to those made on low pollution days. They have shown odds ratios of 3.6 (95 % Confidence Interval, CI 1.6-8.1) in men and 2.3 (95 % CI 1.0-5.3) in women during the high-pollution episode in comparison to non-episode measurements, showing evidence for increased plasma viscosity in individuals in response to air pollution (Peters *et al.*, 1997).

Subsequent studies have shown PM_{10} (urban particulate matter with an aerodynamic diameter of less than 10 μm) associations with changes in additional factors involved in the coagulation pathways, such as elevated plasma levels of the acute phase protein fibrinogen, detected in myocardial infarction survivors living in six European urban areas, five days after cumulative exposure (Rückerl *et al.*, 2007). Similarly, increased plasma fibrinogen levels were detected in animal models, such as in rats with ozone-induced pulmonary inflammation, subsequently exposed to EHC-93 urban air particles, 2 days upon exposure (Ulrich *et al.*, 2002), as well as platelet activation in hamsters, 1 h after their exposure to ultrafine particles (UFP) (Nemmar *et al.*, 2003).

9.2.3 Systemic Inflammatory Response

Systemic inflammatory effects associated with episode of high air pollution have been previously documented. A comparison of white blood cell profiles in individuals that experienced an acute air pollution episode caused by forest fires in Southeast Asia during 1997 to controls showed a marked association of PM_{10} and SO_2 atmospheric pollution with elevated counts of

polymorphonuclear leukocytes for up to a few days after the episode (Tan *et al.*, 2000). Acute bone marrow stimulation with an increase in circulating polymorphonuclear leukocytes and shortened monocyte bone marrow transit time has been shown in rabbits exposed by intratracheal instillation to EHC-93 ambient particulate matter, or supernatants from AM which had been incubated in the presence of EHC-93 (Goto *et al.*, 2004).

In addition, repeated intratracheal instillation to EHC-93 caused the progression of atherosclerosis in heritable hyperlipidemic rabbits, accompanied by increased circulating polymorphonuclear leukocyte count and accelerated release of monocytes from bone marrow (Suwa *et al.*, 2002). Monocytes play a key role in the pathogenesis of atherosclerotic lesions by adhering to the arterial endothelium, migrating into the subendothelial space, and differentiating into macrophages that scavenge lipids to become foam cells (Ross, 1986).

The normal endothelium does not generally support binding of white blood cells. Activated endothelial cells, however, express adhesion molecules such as ICAM-1 or VCAM-1, which bind to various classes of leukocytes. Selectins mediate a rolling interaction of the leukocytes with the inflamed luminal endothelium, strengthened by integrin cell surface receptors. Proinflammatory cytokines expressed locally provide a chemotactic stimulus to the adherent leukocytes, directing their migration into the intima. MCP-1 appears responsible for the entry of monocytes into the intima. Once resident in the sites of inflammation, the blood-derived inflammatory cells participate and perpetuate the local inflammatory response (Libby *et al.*, 2002). Evidence has shown that primary human AM can produce inflammatory cytokines/chemokines (van Eeden *et al.*, 2001), and human endothelial cells can express adhesion factors (Yamawaki and Iwai, 2006) in response to PM_{10} or ultrafine carbon black exposures in culture.

9.2.4 Acute Phase Reactants

The hepatic release of acute phase reactants is part of an early rapid response of the innate immune system to infection or injury. The response is mediated by a number of effector molecules including cytokines IL-1β, IL-6 and TNF-α (Standiford *et al.*, 1999). Like fibrinogen, c-reactive protein is an acute phase reactant synthesized in the liver by hepatocytes. It is an

important predictor of cardiovascular disease (Albert *et al.*, 2002). A number of studies have shown associations of high PM_{10} and increased levels of plasma c-reactive protein in healthy adults and children (Peters *et al.*, 2001; Shima, 2007), although conflicting findings in healthy adults and myocardial infarction survivors have also been recently reported (Steinvil *et al.*, 2007; Rückerl *et al.*, 2007).

9.2.5 Changes in Cardiac Function

Along with changes in the systemic inflammatory profile and the clotting abilities of the blood, cardiovascular adverse outcomes may arise from alterations of autonomic function in the regulation of heart rate. Heart rate and rhythm disturbances were observed in ~3,000 subjects admitted to hospital for cardiovascular problems, during an air pollution episode in 1985 in West Germany (Wichmann *et al.*, 1989), as well as in elderly subjects in Utah Valley, that showed cardiac rhythm changes manifested as increases in their pulse rate, which were associated with elevated PM_{10} on the previous days (Pope *et al.*, 1999).

Increases in resting heart rate are an indicator of autonomic function alterations, which are a known risk factor for cardiovascular mortality and sudden death (Dyer *et al.*, 1980). In addition, heart rate variability (beat-to-beat interval) is controlled by the sympathetic and parasympathetic systems. Reductions in heart rate variability are reflective of increased influence of sympathetic stimuli, or decreased vagal parasympathetic tone, both of which increase the risk of cardiovascular morbidity and mortality (Tsuji *et al.*, 1996).

Associations between reduced heart rate variability and air pollution were shown by a number of studies. Increased levels of particulate air pollution from a steel mill were negatively associated with heart rate variability in 7 elderly subjects that underwent ambulatory electrocardiogram monitoring during the pollution episode (Pope *et al.*, 1999), as well as in elderly Boston, USA residents that showed associations of decreased heart rate variability with elevated $PM_{2.5}$, as well as ozone, suggesting a potential mechanism for the epidemiologic observations of cardiovascular morbidity and mortality (Gold *et al.*, 2000).

The observed cardiac effects have thus suggested that along with the elderly, individuals with pre-existing cardiovascular conditions are also at high risk from elevated air pollution levels. As

such, patients with myocardial infarction were found to be at greater risk of myocardial infarction onset within a few hrs, and 1 day after exposure to elevated ambient concentrations of fine particles, with odds ratios of 1.48 (95 % CI 1.09 - 2.02) for 25 $\mu g/m^3$ increase in $PM_{2.5}$ and 1.69 (95 % CI 1.13 - 2.34) associated with an increase of 20 $\mu g/m^3$ $PM_{2.5}$, before the onset, respectively (Peters *et al.*, 2001). A mortality time series study conducted using data on elderly individuals diagnosed with congestive heart failure, 1 year before death, found a positive association between daily mortality for congestive heart failure, and daily concentrations of particles and gaseous pollutants in the ambient air of Montreal, Quebec, during the period 1984-1993 (Goldberg *et al.*, 2001).

9.3 Health Effects of PM: ROS, Cell Signaling, PM Translocation

9.3.1 The Role of Oxidative Stress

Experimental evidence suggests, that oxidative stress mechanisms play a role in PM-associated health effects. Direct evidence for oxidative stress-based mechanisms come from studies showing inductions of oxidative stress via activation of cytochrome P450 in AM or epithelial cells by the organic fraction of DEP (Bonvallot *et al.*, 2001; Yin *et al.*, 2004), reduced glutathione synthesis in lung lavage cells from rats exposed to $PM_{10,}$ as well as mitochondrial damage in macrophage and epithelial cell lines treated with fine particles or UFP (Li *et al.*, 1996). Work in our laboratory has provided *in vivo* evidence for the key role of oxidative stress in cardiovascular effects of urban particles. TNF-α knockout mice exposed to EHC-93 and ozone by 90-day repeated inhalation exhibited chronic lung inflammation and increased rate of pulmonary protein nitration, which stemmed from increased rate of free radical generation in comparison to wild-type mice exposed to the air pollutants (Kumarathasan *et al.*, 2005). Furthermore, oxidative stress-induced cardiovascular effects, including increased expression of prepro ET-1 and ECE-1 mRNA and plasma ET-1 levels are abrogated in Fisher 344 rats upon a two-hour treatment with superoxide dismutase mimetic drug, *AEOL 10150* prior or post-exposure to EHC-93 and ozone by inhalation (Ganesh, 2006).

Particle-induced ROS production may originate from the particles themselves, chemicals adhered to their surface, or the interactions of the particles with cellular enzymes and organelles.

Some potential pathways of PM-induced ROS production from subcellular sources include conversion of PAH to quinones by cytochrome P450, mitochondrial damage with electron leakage in the inner membrane, quinone redox cycling by NADPH P450 reductase and NADPH oxidase, and inducible nitric oxide synthase activities in macrophages (Xia *et al.*, 2007).

Redox cycling organic chemicals and soluble transition metals have been shown to generate ROS in epithelial cells, macrophages and endothelial cells (Sagai *et al.*, 1993; Li *et al.*, 2002). The redox potential of transition metals such as copper, iron, nickel, vanadium and zinc (Gilmour *et al.*, 1996; Costa and Dreher, 1997), and their ROS-associated toxic activities have been demonstrated *in vivo* and *in vitro* (Vincent *et al.*, 1997a; Adamson *et al.*, 2000; Gurgueira *et al.*, 2002).

9.3.2 Activation of Signaling Mechanisms

Evidence further points to activation of redox-sensitive transcription factors such as NFκB, in cells exposed to particles (Baeza-Squiban *et al.*, 1999). NFκB activates the transcription of genes that regulate cytokines/chemokines and adhesion molecules leading to their increased production. Kennedy *et al.* (1998) demonstrated that PM_{10} elevated IL-6 and IL-8 production, and increased ICAM-1 gene expression in bronchial epithelial cells by a copper-dependent, NFκB-mediated mechanism. The cytokine secretion was reduced by treatment of the cells with antioxidants.

Some studies have pointed out that the soluble transition metal content may not be the only pathogenic factor behind the PM-induced adverse effects and thus sole measurements of transition metals would not completely describe the potential toxicities of particles. Ultrafine carbon black particles instilled into rats were proinflammatory, as evidenced by augmented counts of polymorphonuclear leukocytes in lung lavage, irrespective of the presence of a metal chelator. The response was accompanied by alterations of intracellular Ca^{2+} concentration (Brown *et al.*, 2000). Further support for a potential Ca^{2+}-mediated mechanism for particle-associated ROS generation was provided by a study showing that ultrafine-sized carbon black particles increased intracellular Ca^{2+} concentration, associated with increased IL-1α gene expression and TNF-α release. The cytokine responses were attenuated following treatments with calcium antagonists. (Brown *et al.*, 2004).

Mitogen-activated protein kinases are involved in signal transduction through phosphorylation of a number of proteins and transcription factors, thus regulating cell growth, differentiation, inflammation and apoptosis. P38 mitogen-activated protein kinase is induced by stress stimuli such as cytokines, heat shock, UV. P38 kinase also appears to be involved in the DEP-activated signaling and subsequent IL-8 and RANTES chemokine production in bronchial epithelial cells. The pathway appeared to be ROS-dependent, as the production of the cytokines was inhibited with an antioxidant (Hashimoto *et al.*, 2000).

9.3.3 Extrapulmonary Translocation of PM

Plausability of mechanisms for systemic impact of air ambient particle exposure is further substantiated by observations of extra-pulmonary translocation of inhaled UFP and their accumulation in organs including heart, spleen, liver and the olfactory bulb of the brain (Nemmar *et al.*, 2001; Kreyling *et al.*, 2002; Oberdörster *et al.*, 2002), although the latter appears to be related to particle-associated deterioration of the nasal mucosa and the olfactory barrier (Calderón-Garcidueñas *et al.*, 2003).

9.4 Summary

Substantial number of epidemiological and experimental studies provide evidence for the role of PM in the development and exacerbations of pulmonary and cardiovascular disease. Given the variety of multiple health effects due to PM exposure, and the complexity of PM composition, the elucidation of the exact mechanisms responsible for the adverse effects of particles remains a topic of intense ongoing research.

9.5 Air Pollution Particles: Sources, Fate in the Body

9.5.1 Sources of Particles

Particulate matter is a mixture of air-suspended solid and liquid particles of variable size, that originate from both natural and anthropogenic sources. "Thoracic" particles with an aerodynamic diameter of less than 10 μm are able to reach the lower respiratory tract. "Respirable" $PM_{2.5}$ particles (<2.5 μm) can penetrate into gas exchange regions of the lungs. Ultrafine/nano particles

(<100 nm) have been shown to translocate into the systemic circulation and deposit in major extra-pulmonary organs (Kreyling *et al.*, 2002; Oberdörster *et al.*, 2002). Moreover, particles smaller in size have a larger surface area, which would enable an increased potential for interactions with *in vivo* targets, leading to more significant adverse biological effects (Oberdörster *et al.*, 1996).

The coarse fraction particles (2.5 - 10 μm) are generated by mechanical abrasion of surfaces such as tires and roads, mining, and also include natural sources such as evaporation of sea water or windblown dust and pollen (Wilson and Suh, 1997, Bai *et al.*, 2007).

Fine particles (0.1 - 2.5 μm) are mainly formed from gases generated by fossil fuel combustion from transportation, manufacturing and power generation, and include sulphates, nitrate, organic compounds and trace elements. Solid-phase secondary pollutants such as NH_4NO_3 also represent fine particles.

The smallest, ultrafine particles are formed by nucleation resulting from condensation, or specific chemical reactions by which new particle types may be generated. Other sources of fine and ultrafine particles include forest fires, agricultural activity, wood stoves or cooking, among others. While coarse particles can settle quickly, fine and ultrafine particles can remain suspended in the air for long periods of time and be carried over long distances (Lippmann and Schlesinger, 2000).

The variability in the particle sources and their modifications within the environment are therefore determinant factors for the composition of the particle mixtures and may also play a significant role in the observed adverse health effects.

9.5.2 Clearance and Deposition

Particle deposition is dependent on the physical characteristics of the particles such as their shape, size, or density, or hygroscopy. Large, poorly soluble particles (> 10 μm) mostly deposit in the nasal passages and are cleared via mucociliary transport towards the nasopharynx. Particles that deposit in the oral passages are cleared by coughing, or by swallowing into the gastrointestinal tract. Particles, generally 5 – 10 μm in size deposit in the tracheobronchial region and are cleared by mucocilliary transport towards the oropharynx, followed by swallowing. In addition, the particles may also traverse the epithelium by endocytosis and enter the peribronchial region, where

they may be engulfed by airway macrophages, which may be removed by the mucociliary escalator, or enter the airway lumen from the bronchial or bronchiolar mucosa (Schlesinger *et al.*, 1997).

Fine particles and UFP are able to enter the alveolar region and are mostly removed by AM, interspersed on the epithelium. The particle-laden AM may be cleared via the mucocilliary system, interstitial movement to the lymphatic system, or may potentially traverse the alveolar-capillary endothelium to enter the bloodstream. Particles which are not ingested by macrophages can become trapped in perivenous, peribronchial or subpleural regions, increasing particle burden. Soluble material deposited in the nasal passages, tracheobronchial region, or alveolar region is accessible to underlying cells, and thus may be translocated by intracellular dissolution into the bloodstream via the supporting vasculature (Schlesinger *et al.*, 1995).

Studies have shown that the retention of particles in lung parenchyma was dependent on their size. An examination of lung autopsy tissues from non-smokers living in Vancouver, BC has shown that 96 % of retained PM was <2.5 μm in diameter, with UFP representing less than 5 % of the total retained PM. Accordingly, the clearance of carbon particles 100 nm in size in healthy human subjects, asthmatics or smokers was negligible, within the 24 and 72 hrs, with no significant systemic translocation (Wiebert *et al.*, 2006). Evidence shows that the translocation pathways are likely dependent on particle chemistry and surface characteristics, along with particle size. TiO_2 UFP uningested by macrophages, with low intrinsic toxicity but greater overall surface area show an increased access into the interstitium and greater lymphatic uptake than larger TiO_2 particles (Oberdörster *et al.*, 1994).

The kinetics of particle clearance in the tracheobronchial region appears to depend on a fast and slow component. The initial uptake of particles by AM is rapid (within 24 hrs of deposition), with most particles removed from the large ciliated airways (bronchi) by mucociliary clearance. The subsequent slow-phase clearance from the small airways can have half-time of several weeks to months as shown in animal models, as well as human subjects (Lay *et al.*, 1998). The mucociliary clearance of the particle-laden AM depends on the distance of the site of uptake from the distal bronchiolar terminus, as well as particle size. Uptake of particles below 0.02 μm in diameter is less effective in comparison to larger UFP, as they are not phagocytosed by AM, and may only be partially taken up with extracellular fluids by pinocytosis (Green *et al.*, 1998).

9.6 Air Pollution Particles: Size and Composition

The toxicity of PM may stem from their physical presence on the surface of the cells, or from their chemical constituents, including the adsorbed surface components, or most likely the combination of both. There is also ample evidence suggesting the importance of chemical properties of PM with respect to their biological effects. Toxicological studies have examined the PM characteristics with respect to their potential links to adverse biological health effects, providing evidence for the involvement of metals, carbon content, adsorbed organic materials, secondary inorganic and crustal constituents, as well as biogenic components in the PM.

9.6.1 Size of the Particles

PM size has been shown to be one of the key determinants of the kinetics of inhalation, deposition and elimination of the particles. The *in vivo* particle kinetics also suggest that the size distribution of the aerosol may have an impact on the type of health effects elicited. Numerous studies have shown the importance of the size metric in the evaluation of PM-associated adverse biological effects by using defined model particles, such as TiO_2 or carbon black. In general, these show that particles of smaller size have a higher pulmonary immunogenic capacity in contrast to particles of larger size, but same chemical composition and mass, and that this property correlated best with the overall greater surface area of the smaller particles available for adsorption of toxic chemicals (Oberdörster *et al.*, 1992; Li *et al.*, 1996).

Moreover, a study of fine and coarse stone particles from different rock samples showed that differences in surface area could only account for differences in biological activity (cytokine release by airway epithelial cells) of particles of the same species, but not for differences between rock species, emphasizing the importance of both surface area and surface reactivity as factors capable of inducing biological effects (Ovrevik *et al.*, 2005).

Epidemiologic studies indicate that fine particles show a greater association with mortality than larger, coarse particles (Dockery *et al.*, 1993; Burnett *et al.*, 2000; Pope *et al.*, 2002). There is, however, a good correlation between PM_{10} and $PM_{2.5}$, because $PM_{2.5}$ is a large proportion of PM_{10}. In contrast, the correlation between coarse particle fraction (2.5 – 10 μm) and $PM_{2.5}$ is lower. Thus,

although the association of $PM_{2.5}$ with mortality is stronger, PM_{10} correlate just as strongly with short-term health outcomes such as asthma, chronic obstructive pulmonary disease and respiratory admissions (Brunekreef and Forsberg, 2005).

Together these studies indicate that since the size of ambient particulate matter is not independent of their chemical composition, its toxicological evaluation is difficult. Different size fractions of air ambient PM may contain different constituents, in comparison to more homogeneous mineral particles or pure model particles, and this feature may be more important for their biological effects than the size of the particles.

9.6.2 Transition Metals

As previously discussed, soluble transition metals exert their toxic potency mainly through generation of oxidative stress via reaction such as the Fenton reaction (iron-catalyzed generation of hydroxide ion and hydroxyl free radical from hydrogen peroxide) and thus are potent chemical effectors of inflammation. As shown first in our laboratory, induction of stress genes under the transcriptional regulation from human heat shock protein 70 (HSP-70) and metallothionein IIa promoters in HepG2-derived cell lines was observed upon the exposure of cells for 18-24 hr to aqueous suspensions of urban dusts (SRM-1648, SRM-1649, EHC-93) or $PM_{2.5}$ particles. The observed effects closely correlated with amount of soluble copper in particulate preparations (Vincent *et al.*, 1997b).

A study with aquaeous extracts of PM_{10} filters collected from Utah Valley before, during and after closure of a local steel mill showed evidence of significant inductions of oxidant production (DNA damage), cytotoxicity (LDH) and inflammatory mediators (IL-6, IL-8) in bronchial epithelial cells by extracts with high metal content, specifically copper, iron and zinc in contrast to low oxidant generation and cytokine production by extracts with low metal content (Frampton *et al.*, 1999). As such, zinc in EHC-93 particles, or oil combustion emission PM were suggested to be the toxic factor responsible for pulmonary effects such as inflammation and focal fibrosis in rodents exposed to particles by intratracheal instillation (Adamson *et al.*, 2000; Kodavanti *et al.*, 2002). Studies with residual oil fly ash particles (sulphate- and transition metal-rich oil shale combustion particles) characterized by high content of zinc were also associated with higher airway

hyperreactivity and lung inflammation in rats exposed to residual oil fly ash when compared to residual oil fly ash particles with higher iron, nickel and vanadium content (Gavett *et al.*, 1997).

Nevertheless, it is clear that no one specific fraction or component of the complex mixture of particles may adequately explain all observed health effects from epidemiological studies, but the interactions of the various particle constituents alongside their physical properties may play a more important role. As previously described, fractionation of EHC-93 particles resulted in a differential hemodynamic response in rats upon inhalation of the particle, showing an acute elevation of plasma ET-1 in response to the water-leached insoluble fraction of EHC-93, and a delayed elevation of the ET-1 plasma levels 32 hrs after exposure to the un-fractionated EHC-93 containing the insoluble components along with the water-soluble elements and polar organic constituents (Vincent *et al.*, 2001) Similarly, as further observed in our laboratory, although the soluble fraction of EHC-93 was not a potent inducer of expression of endothelinergic genes in A549 cells, while the insoluble fraction and the total EHC-93 particle were, the same pattern of effects was not seen for other genes. The mRNA levels of the stress response gene HSP-70 were upregulated by EHC-93 particle, but downregulated by the insoluble fraction of the particle, and unaffected by its soluble fraction. Thus fractionation of particles may not be the ideal approach for determining the effects of particle composition on toxic potency, as the effects of the whole particle cannot be simply explained as additive effects from its subfractions (Chauhan *et al.*, 2005). Use of whole particles for evaluations of their toxic potencies, combined with multivariate statistical approaches to link them with the particle composition may represent a better approach (Vincent *et al.*, 1997b).

9.6.3 Biogenic Components

Biological components of particles include pollens, molds, spores and bacteria-derived endotoxins (eg. lipopolysaccharide). Exposure to endotoxin has long been associated with respiratory tract illnesses associated with occupational risks, for example in animal handlers (Simpson *et al.*, 1999).

Endotoxins are lipo-oligo-saccharides found in the outer membrane of Gram negative bacteria. In serum, endotoxins bind to lipopolysaccharide (LPS)-binding protein, which in turn binds the soluble or membrane bound CD14 protein present on cell membranes of monocytes/

macrophages, among other cells (Su *et al.*, 1995). The interaction of CD14 with Toll-like receptor proteins activates signal transduction pathways resulting in transcription factor activation and cytokine production (Means *et al.*, 2000).

Generally higher endotoxin levels are found in larger, coarse mode PM in comparison to smaller mode PM, which may drive their involvement with inflammation (Becker *et al.*, 2002). Accordingly, size-fractioned coarse PM induced higher levels of cytokine production by AM, compared to ultrafine or fine mode PM. The response was inhibited using antibody to CD14. In addition, AM phagocytosis of opsonized yeast and generation of yeast-induced oxidative burst by the cells was also inhibited by coarse PM more than fine PM, suggesting an association of decreased pulmonary defenses with exposure to PM (Becker *et al.*, 2003).

Similarly, a cell culture study with J774 murine macrophages exposed to PM_{10} and $PM_{2.5}$ collected from Mexico City showed that the PM_{10}-induced production of IL-6 and TNF-α cytokines by the cells was attenuated ~50-75 % using endotoxin-neutralizing protein, while $PM_{2.5}$-induced cytokine production was unaffected, likely due to higher transition metal content (Osornio-Vargas *et al.*, 2003).

In addition, some PM may act as adjuvants, with specific PM components enhancing the antigenicity of other inhaled materials, an issue relevant to allergic diseases. As such, DEP exhibit high adjuvant activity for the antigen-specific production of IgG and IgE, and enhance T helper (Th)-2 cytokine production in mice with ovalbumin-induced airway inflammation, characterized by infiltration of eosinophils and lymphocytes and increase in goblet cells in bronchial epithelium (Takano *et al.*, 1997) Thus interactions of PM with other inhaled materials may also produce adverse health outcomes.

9.6.4 Crustal Components

Crustal components of PM mostly represent inorganic elements such as aluminium, calcium, silicon, magnesium or potassium in the form of oxides and, as previously described, can form via mechanical generation and by biomass burning (Harrison and Yin, 2000). Some studies conducted with crustal materials have pointed to potential toxic effects, such as increased neutrophils in lung lavage from dogs exposed to fine particles from Boston, or bronchoconstriction in mice induced

by PM, associated with aluminium and silicon. The fine particles were concentrated using the Harvard ambient particle concentrator (Clarke *et al.*, 2000; Kobzik *et al.*, 2001). Since the elements are not present as a large fraction in PM, the researchers could not delineate with certainty a causal relationship for these elements. Thus currently there is little evidence for a significant contribution of crustal materials to the adverse health outcomes observed by epidemiology.

9.6.5 Secondary Inorganic Constituents

Sulfates and nitrates comprise the major inorganic fraction of PM. Although these chemical species have been related to adverse health outcomes from PM by epidemiology, toxicological studies are not strongly conclusive, because the ambient concentrations of sulfates were in general lower compared to exposures in controlled studies which were showing health effects (Schlesinger, 2007). While acidity of secondary inorganic sulfates may be responsible for effects associated with some adverse health outcomes related to PM, the property is unlikely to be alone responsible for the observed health effects (Dreher, 2000).

9.6.6 Carbon Content

A significant mass portion of PM is derived from combustion, and thus is enriched in elemental and organic carbon. Despite this, there has been little examination of health effects associated with carbon content of PM, although some studies provide evidence for associations of carbon content of PM with health effects. Urch and colleagues (2004) have shown negative association of elemental and organic carbon content of $PM_{2.5}$ with brachial artery diameter in adult subjects, a measure which strongly correlates with coronary vascular reactivity. Ostro *et al.* (2007) showed epidemiological associations of elemental and organic carbon content of $PM_{2.5}$ with cardiovascular mortality data from six California counties.

Studies with carbon black, low-solubility particles produced industrially from incomplete thermal decomposition of hydrocarbons showed effects similar to other insoluble particles. Namely, reduction in lung function and development of chronic bronchitis were associated with long-term occupational exposure, although they could not conclusively implicate carbon black as the causal agent behind the effects, thus a possibility that the health effects could be attributed to non-specific irritant effect of heavy dust exposure was also suggested (Gardiner *et al.*, 1993).

Experimental studies with DEP, $PM_{2.5}$ and PM_{10} increasingly indicate that the induction of oxidative stress, inflammogenicity and cellular injury may stem from the organic fraction adsorbed to the surface of the PM, enriched in organic chemicals such as PAH or quinones (Li *et al.*, 2002; Xia *et al.*, 2004; Xia *et al.*, 2007). For example, coarse and fine PM from the city of Rome are equally inflammogenic in RAW264.7 murine macrophage cell line, and their potency was consistently higher than that of carbon black particles at the same concentration, suggesting that the chemicals adsorbed to the particle surface were likely responsible for the observed effects (Pozzi *et al.*, 2003). Thus, these studies suggest that the toxic effects from DEP and some types of PM are likely due to the chemicals adsorbed to the particle's surface rather than the particle carbon core.

In contrast, a study by Yanagisawa and colleagues (2003) showed that DEP-enhanced lung injury in mice exposed to LPS was due to the carbon core of the particles, and not the organic extract fraction obtained from the washed particle. DEP are composed of carbonaceous particles, with adsorbed and condensed hydrocarbons and sulfur. The organic fraction may represent ~60 % of the DEP mass and contains PAH. Although, DEP also have the potential to form soot aggregates, with spherical cores composed of thermodynamically unstable carbon networks, with chemicals such as volatile organic compounds, sulphur and transition metals interspersed in the intranetwork spaces (Bérubé *et al.*, 2007).

9.7 Summary & Conclusion

In the present day, the associations between airborne PM pollution and adverse health effects, even at low non-episodic particle concentrations have been firmly established. The relationship between specific physicochemical properties of PM and the observed effects, however, remains unclear. Although, PM mass and size have been shown to be important factors influencing health outcomes, chemical composition appears to play an increasingly important role in the observed PM-specific increase in morbidity and mortality. Furthermore, the comparison of the biological effects between studies carries some uncertainty as to whether the observed responses can be generalized, or whether they are intrinsic to the specific model-system used. Clearly, more experimental studies are needed to elucidate the toxicological mechanisms that link specific

physicochemical characteristics of PM with biological responses *in vitro* and *in vivo*, and to examine the validity of the currently used experimental approaches.

This thesis focuses on the biological effects of particles with different composition in cell cultures and in an animal model. Both approaches are widely utilized for the study of the adverse effects of PM by employing individual endpoint assays to examine specific biological mechanisms of interest, or to examine the effects of specific particulate materials. Few attempts have been made to conduct comprehensive evaluations of multiple types of particles at various concentrations, employing a large panel of endpoints to assess various cellular functions. Such an approach can also aid in overcoming a limitation of smaller-scale studies: the difficulty in comparing with certainty observations between studies, due to questions about differences between the experimental systems used.

Furthermore, the over-reliance on either cell-based or animal-based approaches for evaluations of adverse effects of particles brings about the questions of the validity of extrapolations of biological responses between the models. This most importantly increases the uncertainty of the relevance of a specific approach to epidemiologic observations of adverse effects of air pollutants. Therefore, the thesis further focuses on a validation of the cell-based approach in a mouse model by examining the predictive ability of the *in vitro* classic endpoints of cytotoxicity and inflammation for *in vivo* biological effects of particles.

Finally, one limitation of the widely used cell-based approaches is that they examine the behaviour of cells separately. Cell-cell interactions are inherent to complex *in vivo* systems and are thus likely to play a significant role in the modulation of biological responses to inhaled particles, an aspect that remains largely unexplored. Therefore, one part of the thesis examines the role of cell-cell interactions in the particle-associated biological effects in a human co-culture model. Furthermore, the human co-culture model is validated by a comparison to an *in vivo* particle exposure of mice, and contrasted with a study of the cell types in isolation, to determine whether it provides a more accurate model of the *in situ* milieu.

Chapter 1

CORRELATION OF *IN VITRO* AND *IN VIVO* BIOASSAY RESPONSES TO PARTICULATE MATTER EXPOSURE: A MULTIVARIATE ANALYSIS

10.1.1 *In Vitro* Studies

The vast numbers of particle properties that may be associated with their adverse health effects present a challenge for experimental investigation. Therefore exposure studies in cell systems aimed at the elucidation of physicochemical properties associated with PM toxicity mechanisms that may underlie the health outcomes observed by epidemiology represent a valuable investigative approach. The studies can evaluate the influence of specific factors without the difficulties with confounding variables inherent to epidemiological studies. By enabling a control of variables such as particle size, concentration, or exposure duration, they can be used to develop dose response profiles for specific materials, and provide mechanistic support/validation of epidemiological conclusions (Schlesinger *et al.*, 2006).

In vitro studies which utilize cultured mammalian cells exposed to PM or laboratory surrogates to PM, represent an important tool for investigations of the mechanisms of particle toxicity at the cellular, biochemical and molecular levels (Fubini *et al.*, 1998). Combined with new molecular tools and "omics" approaches they make possible investigations of cellular pathways and biochemical processes resulting from cell's exposure to toxic substances. In addition, based on their relatively low cost in comparison to *in vivo* studies, they also enable rapid, high throughput screening of pollutants (Devlin *et al.*, 2005). Immortalized cell lines such as A549, BEAS-2B or J774A.1, and freshly harvested lung cells such as AM are the most commonly used cell types in these studies.

10.1.2 A549 and J774A.1 Cell Lines

A549 cells are a human immortalized cell line derived from an explanted tumor of a 58-year-old Caucasian male with a pulmonary adenocarcinoma (Giard *et al*, 1973). The cells are presumed to be of type II alveolar epithelial origin, as they carry a number of hallmarks of the cell type, such as the presence of multilamellar cytoplasmic inclusion bodies and the ability to synthesize, store and secrete lecithin with a phospholipid composition found in cells involved in pulmonary surfactant synthesis (Lieber *et al.*, 1976; Shapiro *et al.*, 1978; Nardone and Andrews, 1979). J774A.1 cells are an immortalized cell line established from a tumor of a female BALB/*c* mouse. The cells are of

monocyte/macrophage origin. They are adherent, synthesize large amounts of lysozyme, a macrophage differentiation marker and exhibit cytolysis and antibody-dependent phagocytosis (Ralph and Nakoinz, 1975; Ralph *et al.*, 1976) In addition, the cell proliferation of J774A.1 cells is inhibited by dextran sulphate or bacterial LPS (Ralph and Nakoinz, 1977). J774A.1 cells produce a free radical nitric oxide, when activated with interferon-γ and low concentration of LPS, a process which is inhibited by a pre-treatment with IL-10, but unaffected if IL-10 is added after interferon-γ activation (Cunha *et al.*, 1992).

10.1.3 Cells of the Airways & Particles

Type II alveolar pneumocytes play an important role in the pulmonary response to injury by secreting surfactant, cytokines and acting as stem cells for replacement of type I epithelial cells (Chevalier and Collet, 1972; Adamson and Bowden, 1974; Fehrenbach, 2001). Airway epithelial cells are often the first cellular layer to encounter and respond to inhaled toxicants or airborne pathogens and thus actively contribute to innate immune responses of the airways (Bals and Hiemstra, 2004). AM populate the external surface of the lung cavity and represent ~90 % of the hematopoietic cellular content of the alveolar space in the steady state (Martin and Frevert, 2005). Like their blood-borne counterparts, AM are bone marrow-derived mononuclear phagocytes (Thomas *et al.*, 1976). They play a key role in the uptake and clearance of inhaled pathogens and foreign particles, as well as dying cells (MacLean *et al.*, 1996). Together, lung epithelial cells and AM play a major role in host response to inhaled foreign particles resulting in the production and release of numerous immuno-modulatory and signaling molecules. Inflammatory mediators including chemokines and cytokines are released by AM and alveolar epithelial cells in response to pulmonary deposition of PM. The production of these molecules accompanies the concurrent uptake and clearance of the particles by the cells (Terashima *et al.*, 1997; Fujii *et al.*, 2001). The mediators are critical in the control of the local and systemic inflammatory response and their interplay influences the magnitude of the mounted response, which, if in excess, may result in excessive tissue injury and spill-over of cytokine effects into the systemic circulation (Standiford *et al.*, 1999).

Numerous *in vitro* studies of the biological effects of air pollution particles have been conducted utilizing A549 or J774A.1 cells. Although not of alveolar origin, J774A.1 cells exhibit the basic

macrophage functions such as adherence, phagocytosis or cytotoxic activity, as well as display a number of ultrastructural features common to all macrophages irrespective of their origin. Therefore they represent a useful cell type along with A549 epithelial cells for studies of basic cellular and molecular mechanisms by which PM may cause adverse effects, as well as for particle screening studies.

10.1.4 Advantages and Limitations of Cell Lines

Apart from their undeniable usefulness in toxicology and biomedical research, *in vitro* approaches do have some limitations. The major one is that the cells are removed from their complex *in vivo* environment, where they interact with neighbouring cell types, receive/send essential factors and obtain nutrients via the blood supply, thus can maintain their differentiated phenotype (Devlin *et al.*, 2005). In addition, continuous cell lines are prone to genetic instability and may be distinct from their *in vivo* counterparts from which they were derived. Neverheless, relevant cell types that retain some of their major *in vivo* functions and express specific phenotypic markers can be successfully utilized in screens of toxicants, or carefully controlled mechanistic studies. The interpretation of the findings and their relevance to *in vivo* pathophysiology, however, can only be made by their comprehensive validations with *in vivo* studies.

10.1.5 *In Vitro* Cytotoxicity Assays

Cytotoxicity assays are routinely employed in the evaluations of cell viability, i.e. the cell's ability to perform its normal functions. Cytotoxicity assays can be used to assess a number of aspects pertaining to the metabolism of normal-functioning cells, such as energy production (ATP), maintenance of plasma membrane integrity (LDH), ability to proliferate (BrdU ELISA), upkeep of enzymatic functions (Alamar Blue, WST-1), or cell death by apoptosis or necrosis. Thus cytotoxicity assays can provide information on the general mechanisms of toxicity, and provide useful tools for the screening of toxicity of ambient particulate matter. Cell type-specific aspects, such as the ability of phagocytes to ingest particles or bacteria, can also be evaluated (Zhou and Kobzik, 2007; Balduzzi *et al.*, 2004). One such study from our laboratory examined the effects of PM_{10}, $PM_{2.5}$ and mineral particles on the ability of J774A.1, WR19M.1 and RAW264.7 murine cell lines to respond to a challenge with LPS and interferon-γ by producing nitric oxide, as estimated

from cell culture supernatant nitrite. Nitric oxide is a potent radical that mediates cellular communication, as well as antimicrobial and cytotoxic activities. In general, a 2 h pre-incubation of the cells with urban particles decreased their production of nitric oxide. In contrast, silica particles increased the cellular production of NO, while TiO_2 particles were innocuous. The observed changes in NO production were directly correlated with changes in the expression of inducible NO synthase, the enzyme involved in the production of NO. The results showed that particles could modulate nitric oxide production in activated macrophages, thus potentially resulting in effects such as impaired bacterial clearance, or enhanced radical-induced cell injury (Chauhan *et al.*, 2004).

The contact of cells with particles, or their constituents may also activate signal transduction pathways resulting in the induction of transcription factors such as NFκB, or AP-1 (Kennedy *et al.*, 1998; Timblin *et al.*, 1998), thus modulating cellular functions by inducing expressions of specific, transcriptionally activated genes. Reporter gene activation assays have been widely utilized to study inductions of genes responsive to specific xenobiotics. For example, HepG2 cell-based chloramphenicol acetyltransferase (CAT)-Tox panel of assays, with CAT coding sequence under transcriptional control of mammalian stress gene regulatory sequences have been used in our laboratory to examine inductions of cytochrome P450 1A1 (CYP1A1), heat shock protein 70 (HSP-70), or human metallothionein IIa genes among others, by urban particle preparations including SRM-1648 and SRM-1649 standard materials and Ottawa dust EHC-93 (Vincent *et al.*, 1997b).

10.1.6 Cytokines

The release of cytokines represents a hallmark feature of cells' response to various molecular and particulate stimuli. Cytokines represent soluble signal transducers regulating cell differentiation, growth and death, as well as recruitment of immune cells such as neutrophils and macrophages to specific sites (Standiford *et al.*, 1999). The production of cytokines *in vitro* and *in vivo* in response to a challenge with ambient particulate matter has been documented in a large number of studies. Evidence suggests that measurements of cytokine expression by cell cultures *in vitro* are valuable for evaluation of potential adverse effects *in vivo* (Fubini *et al.*, 1998).

Airway epithelial cells have been shown to produce a number of cytokines/chemokines, including IL-1β, IL-6, IL-8, GM-CSF, MCP-1, RANTES and TNF-α. From these, IL-1β, IL-6 and TNF-α have pleiotropic proinflammatory effects, can activate B cells and monocytes, as well as induce synthesis of acute phase proteins (Mills *et al.*, 1999). GM-CSF is a chemotactic, hematopoietic growth factor capable of stimulating monocyte and granulocyte differentiation and release into circulation, as well as a cell survival factor for circulating leukocytes (Mire-Sluis and Thorpe, 1998). GM-CSF is thought to play a pivotal role in the pathophysiology of asthma (Trigg *et al.*, 1994). IL-8 is a potent neutrophil chemotactic factor (Matsushima and Oppenheim, 1989). Bronchial epithelial cells have also been shown to produce chemokines RANTES and MCP-1. RANTES is a chemoattractant for eosinophils, and MCP-1 attracts monocytes and basophils (Mills *et al.*, 1999). Alveolar macrophages release a variety of inflammatory cytokines in response to foreign materials, with TNF-α, IL-6 being the most prominent (Becher *et al.*, 2001). TNF-α from macrophages has been shown to stimulate epithelial cells to produce other inflammatory mediators and factors to further amplify the immune response to foreign materials (Imrich *et al.*, 1999).

10.1.7 *In Vitro* and *In Vivo* Toxicology and Human Risk Assessment

Human risk evaluations generally utilize an evidence-based approach, of which animal toxicological evidence is an integral part. The approach is especially important for evaluations of chronic pathology risks from prolonged exposures to toxicants, but is also important in determining acute genotoxicity and cytotoxicity risk that may arise from exposures to xenobiotics, for which *in vitro* assays can represent an ideal approach. Because *in vitro* assays are mostly short term, they need to be validated *in vivo*, in light of the previously described limitations of cell-based studies. Difficulties in quantifications of the exposures and their extrapolation to relevant tissue doses still need to be overcome. Thus, *in vivo* studies are necessary to determine reliable estimates of tissue dose over exposure time, from which human risk indices can be extrapolated (Fubini *et al.*, 1998). *In vivo* studies, however, also have limitations, such as interspecies differences in response, or the need to use doses higher than would be expected in human exposure scenarios. Potential factors behind some species differences in toxicity response to inhalable xenobiotics may be due to differences in their AM in terms of size and activity, which would critically influence the biological responses (Fubini *et al.*, 1998) Inter-strain differences in AM phagocytic functions of

mice have also been observed (Ohtsuka *et al.*, 2000). For such questions, *in vitro* experimental approaches could again prove useful alternatives to animals.

10.1.8 BALB/*c* Mouse Model

BALB/*c* mice have been extensively used in studies of inhalation and intratracheal instillation of urban particles, minerals, DEP, or other particles (Miyabara *et al.*, 1998; van Zijverden *et al.*, 2000, Steerenberg *et al.*, 2006). Obot and colleagues (2004) have shown that freshly isolated AM from bronchoalveolar lavage of healthy human subjects and of BALB/*c* mice showed similar susceptibility to $PM_{2.5}$ and to organic fractions of SRM-1648 particles, as examined by the initiation of apoptosis and necrosis due to PM. The authors concluded that BALB/*c* mice may represent a suitable model for PM toxicity studies, as it is a good predictive model for the human AM macrophages. AM are central to innate host defense from inhaled foreign materials such as PM, or pathogens.

10.1.9 Intratracheal Instillation Method

Intratracheal instillation is an alternative method to inhalation, frequently used to introduce the particles into the respiratory tract of animals. The method is advantageous when the particles are of limited quantities, as the majority of the intended dose is actually delivered to the lungs, in contrast to inhalation only, where a portion of the particles is deposited on the animal. Instillation also allows rapid delivery of multiple doses of the test material. It is therefore useful as a screening tool for ranking of particle potencies and for determining the proper dose ranges for an inhalation study (Brain *et al.*, 1976). The technique also has some limitations, such as the requirement for animal anaesthesia; the need to use a vehicle (saline or water) for test material delivery; requirement for extensive personnel training to ensure reproducible delivery; and the difference in deposition kinetics between inhalation and instillation, with less homogeneous pulmonary distribution of the test material observed with instillation (Driscoll *et al.*, 2000). Some of these issues can be minimized by increased quality assurance and by the use of better equipment for particle delivery. Use of an intrapulmonary aerosolizer minimizes the issues with bolus liquid delivery by delivering the particles in a plume of liquid aerosol, thus enabling a more uniform pulmonary distribution of the particles (PennCentury™, 2007).

10.1.10 PM Toxicity Screening Studies

Not many comprehensive particle toxicity screening studies have been conducted to validate the *in vitro* results by comparisons to biological effects *in vivo*. Seagrave *et al.* (2002, 2003) have evaluated the toxicity of combined particulate and semivolatile organic fractions of gasoline and diesel engine emissions. The relative potencies of particle fractions were assessed from dose response curves *in vitro* and compared to responses after intratracheal instillations of rats. The results of the assessment showed that for their set of particles the ranking order of potency *in vitro* and *in vivo* did not correspond very well, although the usefulness of *in vitro* assays for providing cell type-specific information on general cytotoxic mechanisms was noted. In their study, macrophages appeared more sensitive than epithelial cells, showing higher overall cytotoxicity. Becher and colleagues (2001) have analyzed the biological effects of stone particles with different metal and mineral compositions in rat type II alveolar epithelial cells and AM *in vitro*, and upon intratracheal instillation in rats by monitoring the production of proinflammatory cytokines. The authors observed good discrimination between particles in terms of their potency to induce cytokines, both *in vitro* and *in vivo*. They also observed marked cell type-specific differences in responses, and good correlation between cytokine release from the cells *in vitro* and neutrophil counts *in vivo*, in response to their most potent particle, mylonite, a mineral rich in iron and silica. The authors also examined whether the epithelial cells and macrophages would continue to show the same effects when isolated from the exposed animals. Once again, the authors showed cell-type specific cytokine release, although the particle potency order was changed.

A European-wide study RAIAP focused on the role of physicochemical particle properties in modulating the production of cytokines *in vitro*, pulmonary inflammation *in vivo*, and adjuvant potency in allergic animal models. The particles used in the study included a panel of coarse and fine PM collected from various European cities, as well as EHC-93 particles as a reference material. The *in vitro* assays of cytokine production (IL-6, IL-8, TNF-α, MIP-2) in macrophage and type II alveolar epithelial cells exposed to coarse and fine particles for 20 hrs showed high degree of correlations with inflammation endpoints (TNF-α, MIP-2, albumin, Clara cell protein 16; a bronchial mucosa-expressed anti-inflammatory mediator) measured in BAL of rats exposed for 24 hrs to the same particles by intratracheal instillation, with cell type-specific differences in the strengths of association. The authors concluded that, *in vitro* systems may be useful in predicting *in*

vivo inflammatory responses. A generally poor correlation was observed between different endpoints from respiratory and systemic allergy models in BALB/*c* mice and inflammatory parameters. Interestingly, cluster analysis of the biological effects and particle chemistry showed that allergic-type responses were associated more with combustion sources, while inflammation and toxicity showed stronger association with crustal constituents of PM (Steerenberg *et al.*, 2006).

Thus, more systematic comprehensive validation studies are required to assess the toxicity of inhaled particles, to further analyze the points of disparities and agreements between the cell-based studies and *in vivo* studies. A development of new cell culture systems that better mimic the complexities of the *in vivo* environment, as well as the need to determine which endpoint assays can provide the most biologically relevant results will be required. A choice of the *in vivo* model system for the validations that is most appropriate in relation to human risk assessment will also be of great importance.

MATERIALS AND METHODS

10.2.1 Materials and Reagents

8-Isoprostane enzyme immune-assay (EIA) kit was purchased from Cayman Chemical (Ann Arbor, MI). Alamar Blue (AB) reagent was obtained from Biosource International (Camarillo, CA). Bio-Plex Cytokine Reagent Kits and human and mouse specific Bio-Plex X-Plex cytokine assays were from Bio-Rad (Mississauga, ON). Butylated hydroxytoluene (BHT) was purchased from United States Biochemical Corporation. (Cleveland, OH). 4-(2-hydroxyethyl)-1-piperazineethanesulfonic acid (HEPES), benzo[a]pyrene (B[a]P), bovine serum albumin (BSA), diethylene triamine pentaacetic acid (DETPA), dimethylsulfoxide (DMSO), ethylenediamine tetraacetic acid (EDTA), fetal bovine serum (FBS), gentamicin, glucose, L-glutamine, pen/strep, sodium bicarbonate, trypsin-EDTA, Triton X-100 and Wright-Giemsa stain were from Sigma-Aldrich (Oakville, ON). The culture media Dulbecco's Modified Eagle Medium (DMEM), Medium 199 (M199) and Minimal Essential Medium (MEM) Alpha were purchased from Invitrogen-Gibco (Burlington, ON). Coomassie Plus reagent was from Pierce (Rockford, IL). Cell-Fixx solution was obtained from Thermo Shandon (Pittsburgh, PA). Cell culture lysis reagent, CytotTox 96 assay and the luciferase assay reagent were from Promega (Madison, WI). Isoton 2 diluent was purchased from Beckman Coulter (Mississauga, ON). ViaLight® Plus assay, Limulus Amebocyte Lysate (LAL) QCL-1000 test and luminescence-compatible clear-bottom 96-well plates were from Lonza (Walkersville, MD). Cell Proliferation ELISA, BrdU (5-bromo-2-deoxyuridine) and WST-1 reagent (4-[3-(4-Iodophenyl)-2-(4-nitrophenyl)-2H-5-tetrazolio]-1,3-benzene disulfonate) were obtained from Roche Diagnostics (Indianapolis, IN). T-75 culture flasks and 96-well plates were from Costar (Cambridge, MA). All water used was deionized/demineralized (>16 MOhms resistivity (Millipore, Bedford, MA). Sodium hydroxide and sodium chloride were purchased from BDH Inc. (Toronto, ON). Tween-80 was obtained form Nuclear-Chicago (Chicago, IL). The cell lines A549 and J774A.1 were obtained from ATCC (Manassas, VA). H1L1.1c2 cells were generously provided by Dr. Michael S. Denison (University of California, Davis, CA).

10.2.2 Particulate Materials & Endotoxin Analysis

The particulate preparations SRM-1648 (St. Louis dust, urban particulate matter), SRM-1649 (Washington dust, "organics"), SRM-1879 (Cristobalite, SiO_2) and SRM-154b (fine Titanium Dioxide; TiO_2) were obtained from the National Institute of Standards and Technology (NIST) (Gaithersberg, MD, USA). The TiO_2 particles were washed in methanol and phosphate buffered saline (PBS) to remove naphthalene contaminant (Vincent *et al.*, 1997b). DWR1 particles represent a reference mixture with equal mass of five particles from a $PM_{2.5}$ winter collection in Downsview, suburban community of Toronto (Dr. Jeffrey R. Brook, Environment Canada, Toronto, ON). The particles were collected on polyurethane foam using a high volume cascade impactor. The urban dust preparations EHC-93, EHC-98 and EHC-2000 refer to materials collected in Ottawa, ON, Canada (Vincent *et al.*, 1997a). Briefly, the EHC urban particles were recovered from bag-house filters of the single-pass air purification system of the Environmental Health Centre in Ottawa and were mechanically sieved (36 μm) to obtain finely dispersed particles. The median physical diameter of the EHC particles is 0.3 μm.

The particulate materials were weighed and resuspended in sterile particle preparation solution (Tween-80, 25 μg/ml; NaCl, 0.19 % w/v) to a final concentration of 10 mg/ml using a Dounce glass homogenizer (Nadeau *et al.*, 1987). After vortexing, the particle suspensions were sonicated in ice-cold water for 20 minutes using a Branson 1510 ultrasonic water bath (Branson, Shelton, CT) and homogenized with 25 full strokes of the homogenizer piston. The particle stocks were aliquotted into sterile centrifuge tubes with O-ring seals and sterilized in a 2L-M Isotemp water bath (Fisher Scientific, Nepean, ON) at 56°C for 30 minutes. These were kept frozen at -80°C, until use.

Prior to use, particles were routinely thawed, sonicated and mixed with the appropriate complete culture medium to make a final particle concentration of 1-2 mg/ml, and applied to the cell cultures to obtain the required final concentrations. This ensured that the concentration of the particle preparation solution in the cell cultures was no more than 10-20 % (v/v). Controls were prepared by exposing the cell cultures to the appropriate medium containing the same final concentration of the particle preparation solution, as the wells with particles. In addition, "No-Cell" (NC) controls were included in all assays performed on particle-exposed cells. NC controls

contained the highest concentration of each particle in the appropriate culture medium, added to tissue culture wells without cells. These controls ensured the monitoring of potential non-biological interference of the particles with the specific cellular assay systems, which could confound, or invalidate the measured biological and biochemical responses.

Stock samples of all particulate matter used in the experiments were analyzed for the presence of bacterial endotoxin using the chromogenic LAL test, as described by the manufacturer. Endotoxin derived from gram-negative bacteria catalyses the activation of a pro-enzyme in the Limulus Amoebocyte Lysate. The activated enzyme catalyzes the cleavage of p-nitroaniline (pNA) from a colorless substrate. The pNA released is measured photometrically at 405 nm upon stopping the reaction with glacial acetic acid (25 % (v/v). The concentrations of endotoxin in the particle samples were calculated from an *Escherichia coli* endotoxin standard curve. Endotoxin concentrations were expressed as endotoxin units per milligram of particle per ml of particle buffer. Endotoxin was measured twice independently, in triplicate. Data from one representative assay are presented (n=3).

10.2.3 Culture of A549 & J774A.1 Cells

A549, human alveolar type II epithelial cells (Caucasian male, lung carcinoma) were cultured in M199 with 2 mM L-glutamine and 10 % FBS. J774A.1, BALB/*c* murine monocyte/macrophages (female, cell sarcoma) were cultured in DMEM medium with 2 mM L-glutamine, 4.5 g/L glucose and 10 % FBS. All cells were routinely maintained in T-75 culture flasks in a humidified incubator at 37°C, 5 % CO_2, 100 % humidity) for 2-3 days. The cells were passaged using trypsin-EDTA upon reaching 80-90 % confluence, twice weekly. For all assays except BrdU Proliferation ELISA, A549 and J774A.1 cells were seeded in 96-well plates at cell densities of 4 x 10^4 and 8 x 10^4 cells/cm^2 respectively. For BrdU Proliferation assay, A549 and J774A.1 cells were seeded at 1 x 10^4 and 2 x 10^4 cells/cm^2 respectively. For the LDH assay, A549 and J774A.1 cells were cultured in serum-free media supplemented with 2 mM L-glutamine, 4.5 g/L glucose (J774A.1 cells only) and 6 mg/ml BSA. For all assays, except BrdU Proliferation ELISA, cells were cultured for 24 hrs in a humidified incubator (37°C, 5 % CO_2, 100 % humidity) prior to their exposure to particles. For BrdU Proliferation ELISA, cells were cultured for 48 hrs prior to their 24 h exposure to particles.

10.2.4 Exposure of Cells to Particles

Thawed 10 mg/ml stocks of DWR1, EHC-93, EHC-98, EHC-2000, SRM-1648, SRM-1649, Cristobalite and TiO_2 particles were sonicated in ice-cold water in a bath sonicator for 20 minutes, followed by their dilution in culture media. Nearing confluence, cells were incubated for 24 hrs with particle preparations at the concentrations of 0, 10, 20, 40, 80 and 160 $\mu g/cm^2$ in 100 μl/well (0.3 cm^2 well) of complete media. During the particle exposures, the culture media also contained pen/strep (100 U/ml penicillin-G, 100 mg/ml streptomycin) and 0.1 mg/ml gentamicin along with the described supplements. Media-only controls and NC controls were included in the exposures, as previously described (see section 10.2.2). At the end of the cell exposure, the endpoint analyses were conducted as required, as well as sample culture media aliquots were kept and stored at -40°C for additional analyses at a later time. For cytokine/chemokine analysis, identical cell exposures were performed, but cells were treated with only a subset of concentrations (0, 10, 40 and 160 $\mu g/cm^2$ in 100 μl/well) of particle suspension in culture media.

10.2.5 Intratracheal Instillation of Particles

The animal treatment protocol was reviewed and approved by the Animal Care Committee of Health Canada. Pathogen-free BALB/*c* male mice (~25 g) were purchased from Charles River (Saint-Constant, QC). Mice were housed for at least one week prior to the dose-response study. They were housed in shoe-box plexiglass cages, on woodchip bedding and maintained under HEPA air filtration at 22 +/- 2°C. They were provided with mouse chow and water *ad libitum*.

The particle preparations were thawed to room temperature prior to a 10- minute sonication. The doses of 0, 50, 100 and 250 μg of SRM-1649, EHC-2000, DWR1, TiO_2 and Cristobalite in 50 μl of 0.9 % saline with 0.005 % Tween-80 were instilled intratracheally into anaesthetized mice in supine position on an angled stand, using a MicroSprayer aerosolizer (Penn-Century, Philadelphia, PA). Sham and saline-exposed control animals were included in the study. After 24 hrs the mice were euthanized and lungs were lavaged with 0.9 % saline solution. BAL, blood, heart and lungs were harvested from the animals. Whole blood samples were spun using IEC MicroMax centrifuge (Thermo Electron, Boston, MA) at 2,000 rpm for 10 minutes to obtain plasma. All plasma and BAL fluid samples contained 20 μl of 0.3 M BHT and 0.1 M DETPA to prevent autoxidation.

The BAL and plasma samples were stored at -40°C and the tissues were immediately flash frozen and stored at -80°C. Five animals were exposed to each particle, at each dose (n=~5).

10.2.6 Cell Differential Analysis in BAL

Male BALB/*c* mice were terminally anaesthetized. The trachea was exposed and cannulated. Blood was drawn from the abdominal aorta and transferred into vacutainer tubes containing sodium EDTA (10 mg/ml) and PMSF (1.7 mg/ml), kept on ice. Next, the diaphragm was punctured and saline at 37°C was intratracheally instilled into the lungs (0.03 ml per g body weight) (Vincent *et al.*, 1996). Lungs were massaged by rubbing the thoracic cage and saline was collected, and instilled two more times to obtain the primary bronchoalveolar lavage (BAL). Three more washes with additional saline (3 ml) were performed, to obtain the secondary BAL. BAL samples were kept on ice until further processing. BAL samples were centrifuged in IEC Centra GP8R Centrifuge (Thermo Electron, Boston, MA) at 1500 rpm for 10 minutes. The cell pellets from the primary and secondary supernatants were combined, resuspended in cold PBS and a 200 μl aliquot of the cells in 10 ml of Isoton II diluent was counted using the Multisizer 3 Coulter Counter (Beckman Coulter, Ville St. Laurent, QC) to determine the number of cells per ml of BAL for each animal. The primary BAL supernatants were kept for further analysis of biochemical endpoints, while the secondary supernatants were discarded. An appropriate aliquot of 15,000 cells was taken from each BAL primary supernatant sample and made up to a final volume of 500 μl with PBS. Next, it was loaded into each sterile cytospin cuvette containing a glass slide. The cell suspensions were spun in CytoSpin 3 centrifuge (Thermo Shandon, Pittsburgh PN) at 1500 rpm for 8 minutes. The cells deposited onto the glass slides were fixed using Cell-Fixx solution and air-dried for 10 minutes. The cytospins were stored at room temperature until staining. The adhered cells were stained with the histologic stain Wright-Giemsa in Ames Hema-Tek automatic slide stainer (Miles Scientific, Naperville, IL). The cellular identity of the lavaged cells and differential counts of alveolar macrophages, neutrophils, lymphocytes, monocytes, eosinophils, basophils, band cells (immature neutrophils) and multinucleated giant cells were determined from a pair of cytospin preparations for each animal. The numbers of each cell type recovered by lavage were calculated relative to the total amount of cells.

10.2.7 Cytotoxicity Endpoints

Cell Viability and Total Protein

Cell viability of *in vitro* cultures was evaluated using Alamar Blue (AB) and WST-1 assays (Figures 1.2A, 1.2B). Alamar Blue reagent (resazurin) is an electron acceptor which is reduced to a fluorescent product (resorufin) via the innate metabolic activity of cells. The exact mechanism of the Alamar Blue reduction is not known, however, mitochondrial and cytoplasmic diaphorases or NADH dehydrogenase enzymes may be involved (O'Brien *et al.*, 2000). The exact mechanism of reduction of tetrazolium salt WST-1 is also currently unknown. Evidence, however, indicates that WST-1 dye is cleaved into soluble formazan form at the cell surface, via electron transport across the plasma membrane of dividing cells (Berridge *et al.*, 2005). In brief, after exposure of cells to particles, the spent medium was replaced with 100 μl of fresh medium with a 1:10 dilution of AB or WST-1 reagent. After a 2 h incubation at 37°C, 5 % CO_2 in a humidified incubator, the cellular reduction of AB resazurin to resorufin was measured with Cytofluor 2350 fluorometer (530/25 nm excitation, 590/35 nm emission) (Millipore, Bedford, MA), or the reduction of WST-1 tetrazolium to formazan by metabolically active cells after a 1 h incubation was measured with SpectraMax Plus spectrophotometer (Molecular Devices, Sunnyvale, CA) at the wavelength of 450 nm. After a wash with PBS, cells were stored at -40°C. Thawed cells were lysed overnight in 50 μl/well lysis buffer (0.25 N NaOH and 0.025 % Triton X-100 in ddH_2O) at room temperature with gentle shaking on a Nutator (Clay Adams, Parsippany, NJ). Upon the addition of 200 μl Coomassie Plus reagent to each well, the absorbance was quantified colorimetrically at 600 nm. The results of the Alamar Blue and WST-1 assays were expressed as fluorescence and absorbance units respectively. Total cell protein content was determined in duplicate from a BSA standard curve and expressed as μg per well. All *in vitro* data were expressed as fold change relative to control samples. For AB assay, five independent experiments were conducted, in triplicate (n=5). WST-1 assay was performed three times, with triplicate samples (n=3). Protein assay was representative of 8 experiments, with triplicate samples (n=8). For the *in vivo* experiment, total protein was analyzed directly in BALB/*c* BAL samples without the lysis step and expressed as μg protein per ml BAL, in 3 - 6 mice per treatment.

A

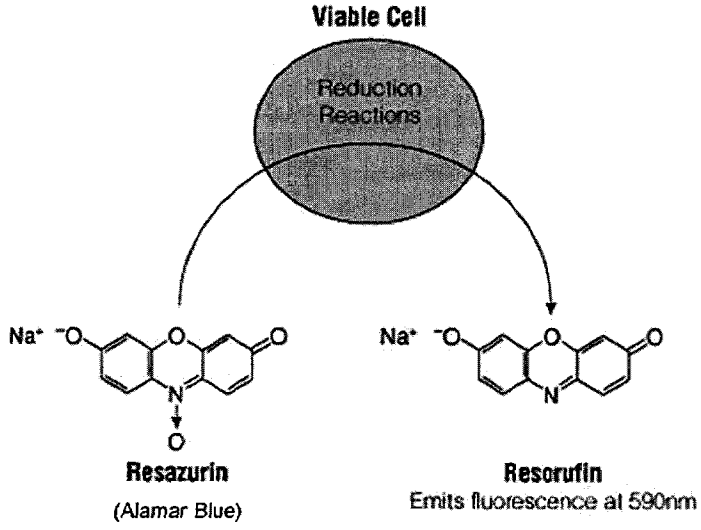

B

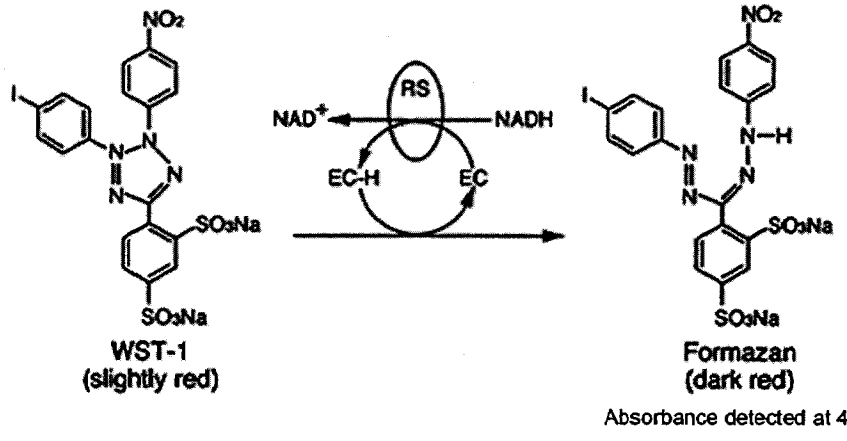

(EC = electron coupling reagent, RS = mitochondrial succinate-tetrazolium-reductase system)

Figure 1.2. The reduction of resazurin (Alamar Blue) (A) and the cleavage of the tetrazolium salt (WST-1) (B) reactions. Viable cells reduce Alamar Blue to fluorescent resorufin via mitochondrial or cytosolic enzymes. The conversion is proportional to the number of metabolically active cells. The signal is quantitated using a fluorometer (adapted from www.promega.com). The tetrazolium salt (WST-1) is cleaved to soluble formazan via an intracellular enzymatic reaction, or extracellularly, via an intermediate electron carrier such as NADH, transported across the plasma membrane. The formazan formed is directly related to the number of metabolically active cells and is quantitated by measuring its absorbance by a spectrophotometer (adapted from www.takara-bio.co.jp).

ATP Assay

Cellular ATP content was assessed upon exposure of cells to particles using the ViaLight Plus Assay. The assay is based upon bioluminescent measurement of intracellular ATP levels present in all metabolically active cells. The assay utilizes luciferase, which catalyzes the formation of light from ATP and luciferin, as a byproduct of the reaction. The emitted light intensity is linearly proportional to the ATP concentration and is measured using a luminometer. The cells were cultured in luminescence-compatible clear-bottom 96-well plates. In brief, 10 μl of cell lysis reagent was added to each well. After 10-minute incubation, 25 μl of ATP-monitoring reagent (AMR) containing firefly luciferase, luciferin, pyrophosphate, BSA and magnesium ions was added to each well. After a two-minute incubation in the dark, the cellular ATP content was determined using the LMax luminometer (Molecular Devices, Sunnyvale, CA). The data were expressed as relative light units (RLUs) and shown as fold change relative to control samples. The assay was performed three times, in triplicate (n=3).

BrdU Proliferation ELISA

DNA synthesis was assayed with the Cell Proliferation ELISA, BrdU. The kit is based on the incorporation of the pyrimidine analogue BrdU into the replicating DNA of cultured, proliferating cells. It is detected immunocytochemically after partial denaturation of double stranded DNA, with a specific anti-BrdU monoclonal antibody. It is therefore a convenient method for estimating S-phase cells in a population. Briefly, 2 hrs before the end of cell exposure to particles, 5-bromo-2-deoxyuridine (BrdU) (10 μl) was added to each 100 μl well to allow its incorporation into the DNA of proliferating cells. Upon the completion of the incubation, the cell media were removed from wells and the cells were fixed for 30 minutes at room temperature using FixDenat solution. FixDenat fixes the cells in the microtiter plate and denatures the DNA in a single step. After aspiration of FixDenat, the cells were washed with 1 ml blocking buffer (1 % BSA in PBS), followed by an incubation with 100 μl of anti-BrdU antibody conjugated with peroxidase (anti-BrdU-POD, Fab fragments) for 90 minutes at room temperature. The anti-BrdU-POD binds to the BrdU incorporated in newly synthesized, cellular DNA. After extensive washing, the cells were incubated with 100 μl of the 3,3',5,5'-tetramethylbenzidine (TMB) chromogenic substrate for 10 minutes at room temperature in the dark to detect the immune complexes. The reaction product

was quantified colorimetrically by measuring the absorbance at 370 nm using SpectraMax Plus spectrophotometer. The data were expressed in absorbance units and displayed as fold change relative to control samples. The assay was conducted three times with triplicate samples (n=3).

LDH Assay

The cytoplasmic LDH release was assessed after the incubation of cells with particles using the CytotTox 96 assay. The assay measures the presence of a stable cytosolic enzyme lactate dehydrogenase (LDH) in culture medium upon its release by cells with compromised plasma membrane integrity. The released LDH is measured by a coupled enzymatic reaction, which results in the conversion of tetrazolium salt into red formazan product, utilizing NADH diaphorase. Cells were lysed by a rapid freeze-thaw cycle. After 30-minute incubation with substrate at room temperature in the dark, LDH levels in cell-lysates and supernatants were quantified colorimetrically using SpectraMax Plus spectrophotometer at 450 nm, by monitoring NADH-coupled enzymatic reduction of tetrazolium to formazan. Results for the LDH measurement assay *in vitro* were expressed as LDH activity (rate/minute) released from the cells into the supernatant, corrected for the LDH content of the lysed cells. LDH Assay in A549 cells was conducted three times, in triplicate (n=3), and in J774A.1 cells, four times, in triplicate (n=4). The *in vitro* data were presented as fold change relative to control samples. For the *in vivo* experiment, LDH activity was analyzed directly in BALB/*c* BAL samples, without the lysis step, in 3 - 6 mice per treatment. The LDH assay results were expressed as LDH activity units per ml BAL.

AhR Activity

The presence of the aryl hydrocarbon receptor (AhR) ligands in the particulate preparations and their relative activity were assessed by monitoring dioxin response element (DRE)-driven, AhR-dependent luciferase reporter gene expression in H1L1.1c2, stably transfected recombinant mouse hepatoma cells (Garrison *et al.*, 1996).

The H1L1.1c2 cells were cultured in MEM Alpha medium supplemented with 10 % FBS and 2 mM L-glutamine at 37°C in a humidified incubator (5 % CO_2, 100 % humidity). The cells were sub-cultured bi-weekly. For the experiment, the H1L1.1c2 cells were seeded in 24-well plates at a

density of 200,000 cells per well, in 1 ml of complete media (100,000 cells/cm^2) and exposed to particulate matter at various amounts for 4 hrs, as described. A positive control containing 100 nM Benzo[a]pyrene (B[a]P) dissolved in 0.1 % DMSO in culture medium, was also included. After the incubation, the cells were washed with cold PBS, and lysed with a cell culture lysis reagent on ice, for 15 minutes. The lysates were transferred into microcentrifuge tubes and stored at -80°C until use. For the assay, the samples were thawed, briefly vortexed and centrifuged at 12,000 x g for two minutes, at 4°C. An aliquot of 25 μl from each sample was added into a luminescence compatible 96-well plate. Next, 50 μl of luciferase assay reagent were delivered into each well with an automated injector of the LMax luminometer. Luciferase activity was quantified for 15 sec, and activity was expressed as RLUs. The experiment was conducted in triplicate and repeated once. Data from one representative experiment are shown (n=3), presented as fold change relative to control samples.

10.2.8 Cytokine and Chemokine Analysis

Cell supernatants from PM-exposed A549 and J774A.1 cells (0, 10, 40, 160 μg/cm^2), as well as BAL samples from BALB/*c* mice 24 hrs after PM-instillation were assessed for the presence of cytokines and chemokines. In A549 cells, Interleukin (IL)-1β, IL-6, IL-8, IL-10, granulocyte-macrophage colony-stimulating factor (GM-CSF), macrophage inflammatory protein (MIP)-1β, monocyte chemoattractant protein (MCP)-1, and tumor necrosis factor (TNF)-α were measured. J774A.1 cell culture supernatants were assessed for the presence of IL-1α, IL-1β, IL-6, IL-10, GM-CSF, keratinocyte-derived chemokine (KC), MIP-1α, regulated upon activation normal T cell expressed and secreted (RANTES) and TNF- α. The profile of IL-1α, IL-1β, IL-4, IL-5, IL-6, IL-10, GM-CSF, KC, MIP-1α, RANTES and TNF-α was determined in BAL samples collected from mice. The simultaneous quantification of cytokine levels was performed using the Bio-Plex liquid suspension array system (Bio-Rad Laboratories, Mississauga, ON), according to manufacturer's recommended procedure. Cytokine standards were used for quantification. The Bio-Plex assay is based on the principles of capture-sandwich immunoassay, with cytokines binding to color-coded polystyrene beads conjugated with monoclonal antibodies specific for a target cytokine followed by a binding to biotinylated detection antibodies directed against a different cytokine epitope "sandwiched" around the cytokines. The complex is detected with

streptavidin-phycoerythrin by a multi-laser reader capable of analysis of multiple cytokines per sample. In brief, cell culture supernatants and BAL supernatants were thawed on ice and spun at 3,000 rpm in an Eppendorf 5417R Microcentrifuge (Mississauga, ON) for 5 minutes, at 4°C. After this initial step, 50 μl of samples were incubated with 50 μl of microbeads labeled with antibodies to the specific cytokines in a 96-well filter plate for 30 minutes. Samples were washed after the incubation and were incubated with the 25 μl of detection antibody cocktail for 30 minutes, each antibody specific to a single cytokine. This step was followed by another wash step, and the beads were incubated with 50 μl of streptavidin-phycoerythrin for 10 minutes, again washed, and the concentration of each cytokine was determined using the array reader. All incubations were done with the filter plate covered with aluminium foil, with agitation on a Barnstead 4625 Titer Plate Shaker (Barnstead International, Dubuque, IO) at room temperature.

The data were analyzed using the Bio-Plex Manager™ software with 5PL curve fitting. The value of each cytokine/chemokine in medium without cells was subtracted from values obtained from the media of controls and particle-treated cells, as a background. Blocker protein (0.5 % BSA) was added to the BAL supernatants prior to analysis. The cytokines/chemokines in cell culture supernatants were analyzed in three samples per treatment, each from independent experiments (n=3). BAL cytokine/chemokine analysis was performed in samples from all animals (n= ~5). All data were expressed in pg per ml of culture supernatants, or BAL.

10.2.9 8-Isoprostane EIA in BAL

8-Isoprostaglandin-2α (8-Isoprostane) in BALB/*c* mouse plasma samples from whole blood collected in vacutainers containing EDTA was quantitated using the competitive EIA kit. The assay detects the presence of the 8-isoprostane eicosanoid immunocytochemically. 8-isoprostane is a potent pulmonary and renal vasoconstrictor, which represents a reliable marker of oxidative stress and antioxidant deficiency. Prior to performing the assay, the mouse plasma samples were purified, to improve the consistency of results. Briefly, a C_{18} *Sep Pak* cartridge (Waters, Millford, MA) was pre-treated by washes with methanol and ddH_2O, using a 1 cc syringe. Next, 250 μl of plasma sample was added to each cartridge, followed by a ddH_2O wash of the C_{18} cartridge. The samples were eluted in three one ml fractions of methanol. The purified samples were dried under a constant flow of N_2 and stored at -80°C until use. Prior to use, the plasma samples were

reconstituted in 1x EIA buffer and 50 μl of each sample was assayed in the EIA 96-well plate. In brief, the assay is based on the competition of 8-isoprostane with a constant amount of 8-isoprostane-alkaline phosphatase conjugate for 8-isoprostane-specific rabbit antiserum binding sites. The antibody-8-isoprostane complex binds to the wells coated with monoclonal anti-rabbit IgG. After washing, 5,5'-dithio-bis(2-nitrobenzoic acid) (Ellman's reagent, DTNB) is added and the enzymatic reaction product is detected using a spectrophotometer at 412 nm. The concentration of 8-isoprostane in the samples (4 - 6 mice per treatment) was expressed in pg/ml of plasma, as determined by interpolation from a standard curve.

10.2.10 Statistical Analyses

All data are expressed as mean ± standard error of the mean (SEM). The effects of the particles in treated cells and animals were tested for statistical significance by 2-way analysis of variance (ANOVA) with PARTICLE (DWR1, EHC-93, EHC-98, EHC-2000, SRM-1648, SRM-1649, Cristobalite, TiO_2) and CONCENTRATION (0, 10, 20, 40, 80, 160 $\mu g/cm^2/100\mu l$ media), as factors for *in vitro* cell exposure experiments, or PARTICLE (SRM-1649, EHC-2000, DWR1, Cristobalite, TiO_2) and DOSE (0, 50, 100, 250 μg), as factors for *in vivo* experiment samples. Cytokine/chemokine levels in culture supernatants of cells exposed to particles were analyzed by 2-way ANOVA with PARTICLE (DWR1, EHC-93, EHC-98, EHC-2000, SRM-1648, SRM-1649, Cristobalite, TiO_2) and CONCENTRATION (0, 10, 40, 160 $\mu g/cm^2/100\mu l$ media) as factors. Where the data were not normally distributed, or did not meet equal variance, log, ln, square root, or reciprocal transformations were applied, or the data were rank-transformed, as suggested by Conover *et al.* (1981). Seaman *et al.* (1994) have shown that the 2-way ANOVA used hereby is not affected adversely by interaction in contrast to other designs using ranked data. The differences between groups were determined with *post hoc* comparisons using the Holm-Sidak method. $P < 0.05$ was considered to be statistically significant. Statistical comparisons between vehicle and sham controls from the *in vivo* experiment were done by Student's t-test. Non-normally distributed control data were analyzed by Mann-Whitney Rank Sum test. $P < 0.05$ was considered to be statistically significant. The comparisons of sham vs. vehicle controls were done separately, as they had to be excluded from the ANOVA to satisfy the requirements for a factorial ANOVA design. Statistical analyses were performed using the Sigma-Stat 3.0 software (Systat Software Inc., Chicago, IL). ANOVA results are summarized in Tables A-1 to A-4.

Multivariate and Bivariate Statistics

All statistical analyses were performed using SigmaStat 3.0 (Systat Software Inc., Chicago, IL) and Minitab 15 Statistical Software for Windows (Minitab Inc., State College, PA). Multiple regression 'best subsets' analysis was employed to assess the association between predictor variables (up to 22 *in vitro* assay endpoints) and the dependent variable (BAL neutrophil counts). For the analysis, the *in vitro* endpoint assays were represented by particles matching the *in vivo* set of particles. Namely, EHC-2000, SRM-1649, DWR1, TiO_2 and Cristobalite at nil, low, medium and high concentrations (0, 10, 40 and 160 $\mu g/cm^2/100\ \mu l$ media) were matching the nil, low, medium and high *in vivo* particle doses (0, 50, 100 and 250 $\mu g/50\ \mu l$ of saline). This technique allows a systematic search of the different combinations of predictor variables, selecting those subsets that best contribute to the variation of the dependent variable. Best subsets regression identified combinations of variables with the highest value of R for each number of parameters in the model. Variance inflation factor (VIF) was used to aid the model selection and to detect multicollinearity of variables, which could confound the analysis. VIF measures the inflation of a regression coefficient for an independent variable due to redundant information in other independent variables. Models containing variables with any VIF exceeding 10 or with sum of all VIFs exceeding 10 were rejected (Chatterjee *et al.*, 2000). Additionally, Mallows' C_p statistic was used as a stopping rule for best subsets regression, to detect over-fitting of the regression model. C_p is a gauge of the bias introduced into the estimate of the dependent variable when independent variables are omitted from the regression equation. The optimal value for C_p is equal to the number of parameters (independent variables in the subset plus constant; $C_p = p = k+1$ and $2p > C_p > p$; or $C_p < p$) (Mallows, 1973; Hocking, 1976; Daniel and Wood, 1980). Because there were more predictor variables than dependent variable observations, the data were analyzed in two predictor subsets, CYTOTOXICITY (all *in vitro* endpoint assays) and INFLAMMATION (all cytokine/chemokine *in vitro* assays) (Table 1.1). Furthermore, to verify the validity of the best models, a number of regressions were conducted with variables randomly selected from the two subsets, to ensure that the final models truly represented the best subsets. Regressions categorized by cell type were also conducted for the same purpose. In order to verify the strength of the relationships of the *in vitro* predictor variables and the *in vivo* dependent variable when only urban particle responses are considered, the analyses were repeated with data sets from all subsets without the responses to mineral dusts Cristobalite and TiO_2. This approach was used to evaluate

the potential impact of mineral dust responses on the model selection of the best predictor variables.

The relationship between BAL neutrophil counts and all other *in vivo* endpoints (15 *in vivo* measures) assessed in BALB/*c* mice exposed to particles was examined by using the Pearson Product Moment Correlation. The analysis was performed with variables comprised of responses to all particles, and with variables excluding the responses to mineral dusts Cristobalite and TiO_2. The strength of pairwise associations between BAL neutrophil counts and the other variables was represented by a correlation coefficient and the significance of the association was based on the p values. For *in vivo* endpoints, the subsets of variables were CYTOTOXICITY (*in vivo* biochemical endpoints and cell differential counts) and INFLAMMATION (all cytokine/chemokine *in vivo* assays) (Table 1.1).

Potency Estimation and Ranking

Based on the best fit, two equations were used for the particle potency estimation for specific sets of data. The modified power equation, $y = ab^x$, was used to express the particle concentration response curve, or beta potency estimation for each particle, for all *in vitro* cytotoxicity assays, with the exception of AhR assay. The equation was log-transformed ($\log y = \log a + x \log b$) to linearize the endpoint responses, where x is the concentration of the particles; log(y) is the measured endpoint response in logarithmic scale at each concentration over control; log(a) is the expected endpoint response in logarithmic scale when there are no particles and log(b) is the beta potency estimate of endpoint response in logarithmic scale from a unit increase in particles.

For all *in vitro* and *in vivo* cytokine/chemokine assays, *in vivo* biochemical endpoints, BAL cell counts and AhR assay, the equation $y = (x + 1)^a$ provided the best fit, where y is the ratio of endpoint response for a given particle concentration/dose to the value in the control cells; x is the particle concentration/dose and a is the slope of the endpoint response curve and represents the beta potency estimate of the specific particle (Vincent *et al.*, 1997b).

Particle responses were grouped into endpoint categories (Table 1.1), and the relative rankings of particles with respect to their beta potency values for different endpoints were compared. Beta

potency values across the endpoints within each category were equally scaled, by dividing the potency estimate of each endpoint by the largest observed potency value for that endpoint (adapted from Seagrave *et al.*, 2002). Potency estimates were determined using CurveExpert software version 1.3 (Hixson, TN). The potency estimates are listed in Tables A-4 to A-6, A-7 to A-8).

Table 1.1. Subsets for multivariate and bivariate analysis of *in vitro* and *in vivo* responses to particles

Cytotoxicity *in vitro*		Inflammation *in vitro*		Cytotoxicity *in vivo*	Inflammation *in vivo*
Alamar Blue	A,J	IL-1α	J	LDH	IL-1α
WST-1	A,J	IL-1β	J	8-Isoprostane	IL-1β
ATP	A,J	IL-6	A,J	Total Protein	IL-5
BrDU ELISA	A,J	IL-8	A	Total Cells	IL-6
LDH	A,J	IL-10	J	Macrophages	KC
Total Protein	A,J	GM-CSF	A,J	Band Cells	MIP-1α
AhR Assay	H	MCP-1	A	Lymphocytes	RANTES
		RANTES	J		TNF-α
		TNF-α	J		

in vitro assays: A - A549; J – J774A.1; H – H1L1;
in vivo assays: BALB/c BAL, except 8-Isoprostane (BALB/c blood plasma)

See Figures 1.3A and 1.3B for schematic descriptions of the *in vitro* and *in vivo* experimental approaches.

A

In Vitro PM Potency Analysis

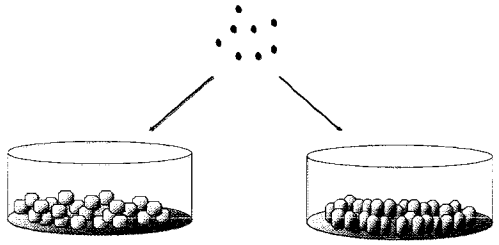

J774A.1 mouse macrophages

A549 human lung epithelial cells

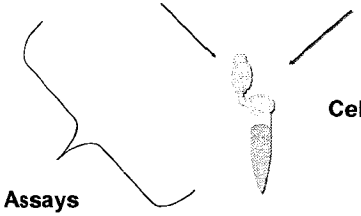

Cell culture supernatants

Cytotoxicity Assays

Cell viability (Alamar Blue, WST-1)
Cell membrane damage (LDH)
Metabolic activity (ATP)
Cell proliferation (BrDU Prolif.)

Bioplex cytokine / chemokine analysis

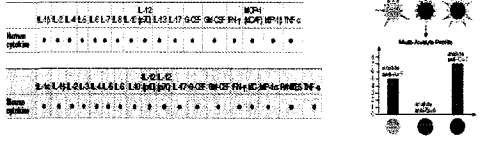

B

In Vivo IT-PM Exposure of Balb/c Mice

Particulate matter

Balb/c mice

24 hrs

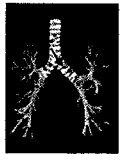

Bronchoalveolar lavage

Cell differential counts

LDH, Isoprostane,
Protein Assay

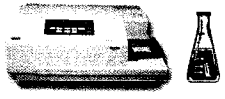

Bioplex cytokine / chemokine analysis
(BAL, blood plasma)

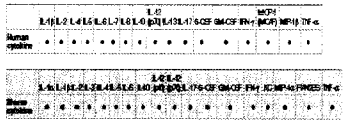

Figure 1.3. Schematic representations of the *in vitro* and *in vivo* experimental approaches. A549 and J774A.1 cells were exposed to urban particulate matter <10 μm, <2.5 μm in aerodynamic diameter (PM_{10}, $PM_{2.5}$) and mineral particles in culture media for 24 hours. Cell culture supernatants and cell lysates were collected, and a range of cytotoxicity and inflamation endpoints were analysed (A). BALB/*c* mice were exposed to urban PM and mineral particles by intratracheal instillation. After 24 hours, animals were sacrificed and bronchoalveolar lavage, blood and tissues were collected for downstream analysis of a range of cytotoxicity and inflammation endpoints (B).

RESULTS

10.3.1 Effects of Particles in Cell Lines

In this study I have examined the effects of a number of urban dust particles (EHC-93, EHC-98, EHC-2000, SRM-1648, SRM-1649), mineral standards (Cristobalite and TiO_2) and fine particulate matter (DWR1) *in vitro* in two cell lines, A549 human alveolar epithelial cells and J774A.1 murine macrophage cells by utilizing a panel of cytotoxicity assays and critical inflammation endpoints. The cytotoxicity panel comprised of assays for determination of cell viability (Alamar Blue, WST-1, total protein), plasma membrane damage (LDH), energy metabolism (ATP), cell proliferation (BrdU ELISA), and gene activation (AhR assay) (Figures 1.4 - 1.7). The inflammation endpoints included a number of cytokines and chemokines previously identified in the literature on cellular responses to particulate matter and minerals (IL-1α, IL-1β, IL-6, IL-8/KC, IL-10, GM-CSF, MCP-1, MIP-1α, MIP-1β, RANTES, TNF-α) (Figures 1.8 - 1.10). Particle potency estimates (slopes of the particle concentration-response curves) and particle rank order were then determined for all cytotoxicity and inflammation endpoints that were examined (Tables A-5, 6 in the appendix). For ease of comparison, the beta potency estimates were uniformly scaled by maximal potency for each particle per endpoint and presented in the two subsets representative of overall cytotoxicity and inflammation response (Figures 1.11A, 1.11B). The statistical significance values of all measured responses are present in Tables A-1 and A-2.

10.3.2 Cytotoxicity *In Vitro*

The cell viability was assessed using Alamar Blue and WST-1 assays. Statistically significant responses that were particle type- and concentration-dependent were observed for both assays in A549 and J774A.1 cells (Figures 1.4A-D, Table A-1). Although both assays are used to assess cell metabolic activity, differential responses to PM were seen between the assays, with WST-1 assay showing bi-phasic effects. The differences between the two assays were more striking in A549 cells, while J774A.1 cells responded to particles more similarly. The Alamar Blue assay showed consistent particle concentration-dependent decrease in metabolic activity of A549 cells. WST-1 assay showed more variability in A549 response to particles. Interestingly, while both assays identified TiO_2 to be the most potent particle (Table A-5), its effect on the metabolic activity of

A549 cells was opposite, with a decreasing response in Alamar Blue assay and an increasing response in WST-1 assay. In J774A.1 cells, Alamar Blue assay showed more variability in response to particles in comparison to A549 cells, with low particle concentration-induced stimulation observed with a number of particle exposures. Both assays identified EHC-93 to be the most potent particle in J774A.1 cells. The cell viability assays identified DWR1 to be the least potent particle. Interestingly, while Alamar Blue assay showed a significant weak response to DWR1 in both cell lines, WST-1 assay showed higher sensitivity for the DWR1 fine particle mixture. The assay revealed a more marked cell response to DWR1, with a statistically significant decrease in metabolic activity of A549 cells (at 160 $\mu g/cm^2$ well) in comparison to a significant increase in metabolic activity of J774A.1 cells exposed to the particle (main PM and CONC effects). A decrease in total protein was observed at higher concentrations of a number of urban particles in both cell lines. The mineral dusts caused more loss of protein in A549 cells in comparison to J774A.1 cells (main PM and CONC effects) (Figures 1.6C, 1.6D, Table A-1). It must be noted, however, that some loss of protein may have resulted from the fact that the cells were rinsed in PBS after the endpoint assays were performed.

ATP assay provided a tool to assess the overall state of energy metabolism in the two cell lines. Higher concentrations of a number of the urban dusts induced decreases in intracellular ATP production in both cell lines, with an overall higher potency of the SRM- urban particles in comparison to the EHC- urban particles (main PM and CONC effects) (Figures 1.5C, 1.5D, Table A-1). The ATP assay identified SRM-1648 and SRM-1649 particles as most potent, while DWR1 particle showed low potency ranking in both cell lines (Table A-5).

The ability of cells to proliferate was assessed using BrdU ELISA. The assay revealed significant inhibitory effects of the majority of particles on J774A.1 cell proliferation, with the exception of DWR1 particle, which did not overall affect the ability of J774A.1 cells to proliferate (main PM and CONC effects) (Figure 1.5B, Table A-1). A549 cells were less affected by particles in their ability to proliferate (Figure 1.5A, Table A-1), although significant differences between particles were observed (main PM and CONC effects). Interestingly, BrdU ELISA and Alamar Blue assay showed similarities in particle potency ranking in A549 cells, with the TiO_2 and SRM-1649 particles showing most potency and Cristobalite showing least potency in both assays. SRM-1649 and DWR1 ranked as the most and least potent particles respectively in J774A.1 cells (Table A-5).

To assess the integrity of the cell membrane after exposure of cells to particles, LDH assay was conducted. The assay revealed a distinct difference in effect between the two cell lines (Figures 1.6A, 1.6B). In A549 cells, the majority of the particles induced a significant increase in LDH activity in cell supernatants that was concentration- and particle type-dependent with the exception of DWR1, which overall, in general, did not induce a release of LDH. In J774A.1 cells, small significant changes in LDH activity in cell supernatants were detected for majority of the particles, when compared to control. Significant increase in LDH activity in J774A.1 cell supernatants was seen with highest doses of all urban dusts and Cristobalite. SRM-1649 and DWR1 were ranked the most potent and least potent particles respectively in A549 cells. In J774A.1 cells, EHC-93 ranked highest in potency, followed by SRM-1649, while DWR1 and TiO_2 had the lowest potency ranks. Interestingly, in A549 cells TiO_2 particles were moderately potent in inducing LDH release (Table A-5).

A comparison of the particle potency estimates in the ligand-activated AhR signaling assay showed clear differences in beta potencies of the urban particles, fine particle DWR1 and the mineral dusts (Table A-5), with all urban dusts showing a scaled potency estimate above 0.89, in contrast to DWR1 with a potency estimate of 0.58 and the mineral dusts Cristobalite and TiO_2 with slightly negative potency estimates (-0.11 and -0.15 respectively). Overall, the urban dusts were significantly more potent in inducing AhR-dependent gene expression than DWR1 and the mineral dusts Cristobalite and TiO_2. In addition, comparison of the inductions of the AhR-responsive luciferase gene expression by urban dust particles revealed that the SRM- particles were more potent than EHC- particles (Figure 1.7).

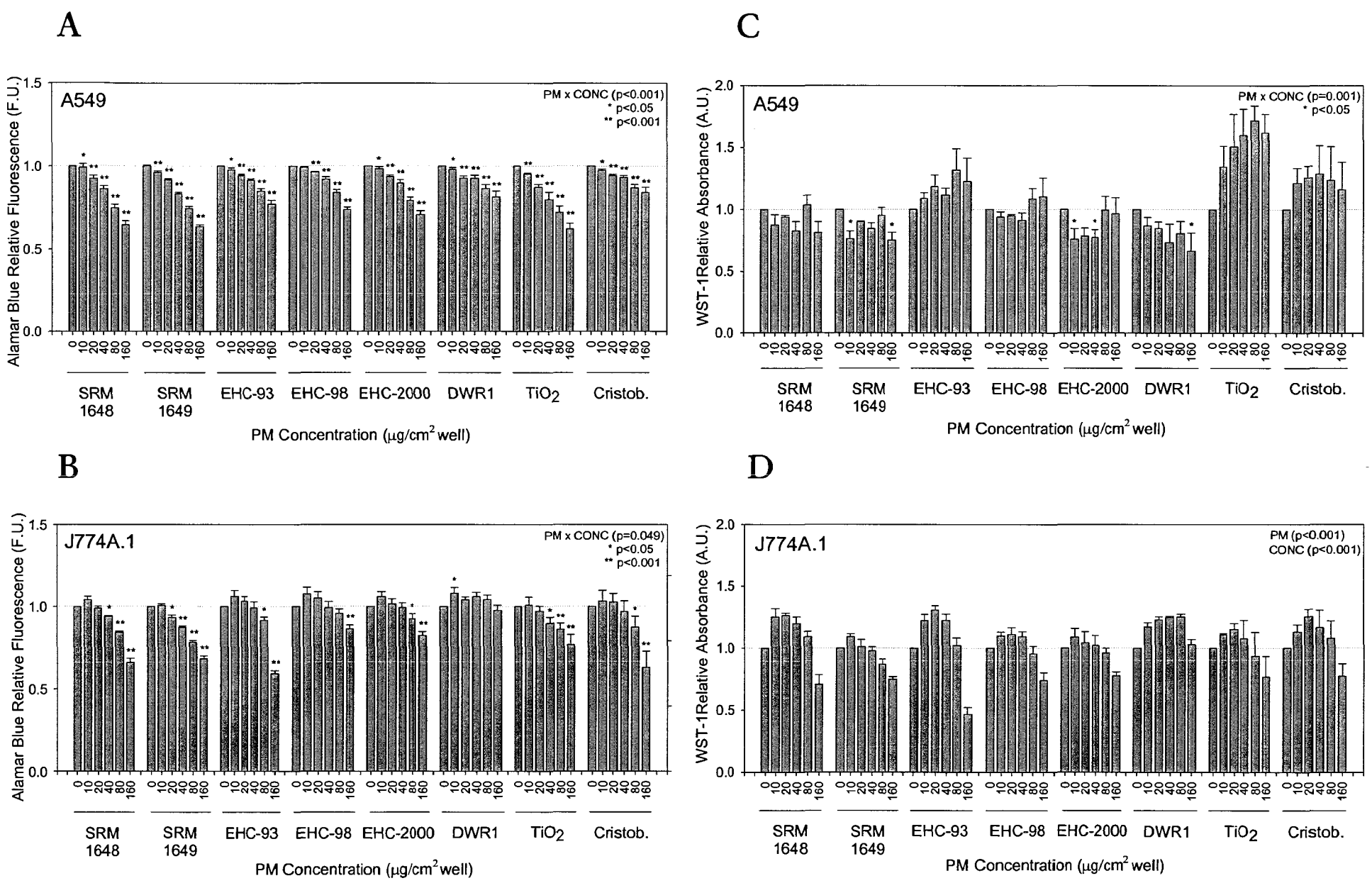
A
A549
PM x CONC (p<0.001)
* p<0.05
** p<0.001
Alamar Blue Relative Fluorescence (F.U.)
1.5
1.0
0.5
0.0
0 10 20 40 80 160
SRM 1648
SRM 1649
EHC-93
EHC-98
EHC-2000
DWR1
TiO2
Cristob.
PM Concentration (μg/cm2 well)
C
A549
PM x CONC (p=0.001)
* p<0.05
WST-1Relative Absorbance (A.U.)
2.0
1.5
1.0
0.5
0.0
PM Concentration (μg/cm2 well)
B
J774A.1
PM x CONC (p=0.049)
* p<0.05
** p<0.001
Alamar Blue Relative Fluorescence (F.U.)
PM Concentration (μg/cm2 well)
D
J774A.1
PM (p<0.001)
CONC (p<0.001)
WST-1Relative Absorbance (A.U.)
PM Concentration (μg/cm2 well)

Figure 1.4. Cellular metabolic activity of A549 human epithelial cells and J774A.1 murine macrophages exposed for 24 hrs to particle preparations. Rate of reduction of Alamar Blue reagent was measured fluorometrically (A, B). Rate of reduction of WST-1 dye was measured photometrically (C, D). Values are presented as mean ± standard error for both assays (Alamar Blue, n = 5; WST-1, n = 3). PM x CONC interactions were observed for all assays except WST-1 assay in J774A.1 cells. PM and CONC main effects were obtained for WST-1 assay in J774A.1 cells. Asterisks above bars represent particle concentration effects significantly different from control, where PM x CONC interaction was observed (2-way ANOVA).

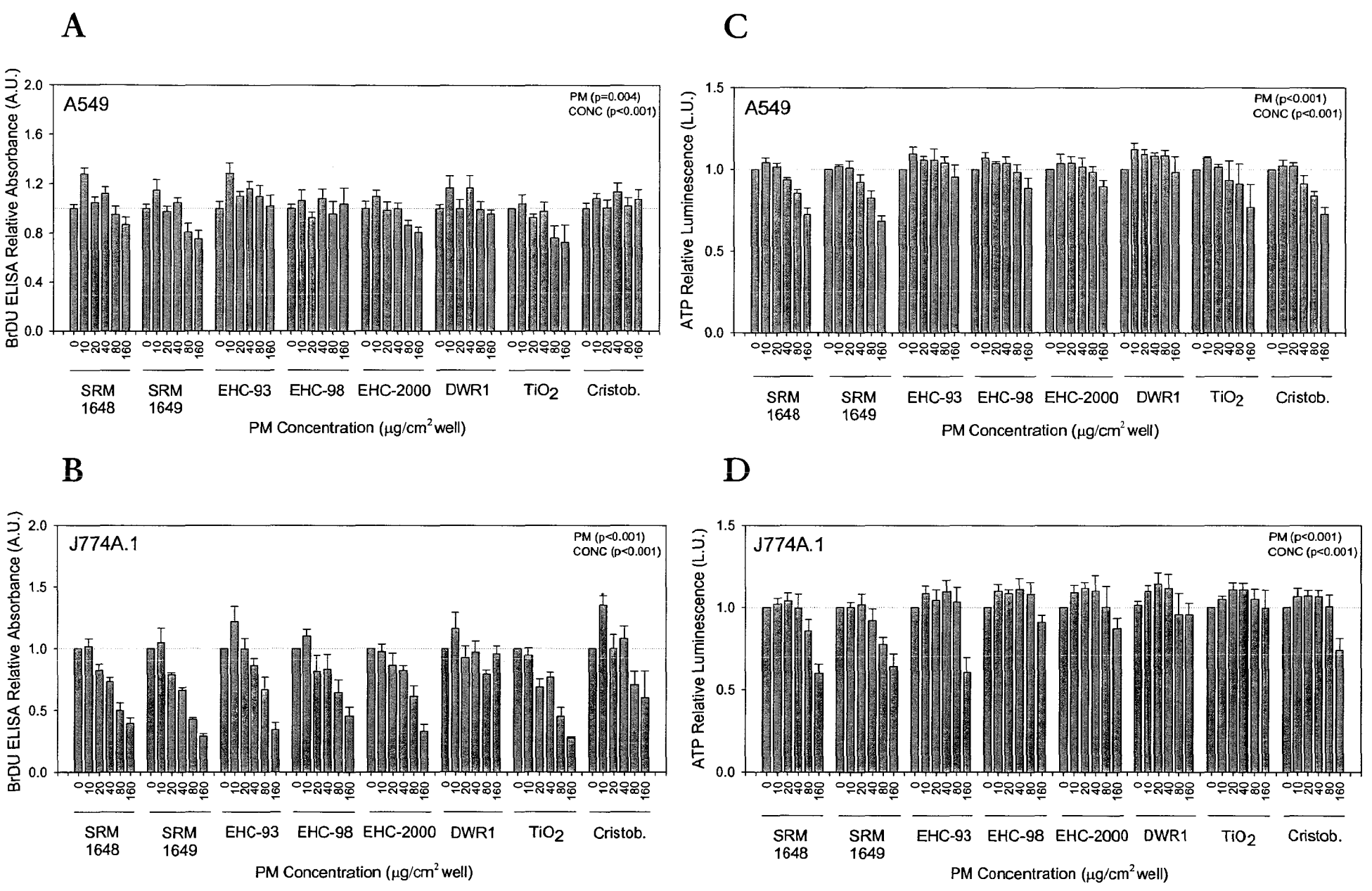
A
A549
PM (p=0.004)
CONC (p<0.001)
BrDU ELISA Relative Absorbance (A.U.)
2.0
1.6
1.2
0.8
0.4
0.0
0 10 20 40 80 160
SRM 1648
SRM 1649
EHC-93
EHC-98
EHC-2000
DWR1
TiO2
Cristob.
PM Concentration (μg/cm² well)
C
A549
PM (p<0.001)
CONC (p<0.001)
ATP Relative Luminescence (L.U.)
1.5
1.0
0.5
0.0
SRM 1648
SRM 1649
EHC-93
EHC-98
EHC-2000
DWR1
TiO2
Cristob.
PM Concentration (μg/cm² well)
B
J774A.1
PM (p<0.001)
CONC (p<0.001)
BrDU ELISA Relative Absorbance (A.U.)
2.0
1.5
1.0
0.5
0.0
SRM 1648
SRM 1649
EHC-93
EHC-98
EHC-2000
DWR1
TiO2
Cristob.
PM Concentration (μg/cm² well)
D
J774A.1
PM (p<0.001)
CONC (p<0.001)
ATP Relative Luminescence (L.U.)
1.5
1.0
0.5
0.0
SRM 1648
SRM 1649
EHC-93
EHC-98
EHC-2000
DWR1
TiO2
Cristob.
PM Concentration (μg/cm² well)

Figure 1.5. Proliferation and ATP content of A549 human epithelial cells and J774A.1 murine macrophages exposed for 24 hrs to particle preparations. Quantitative determination of cellular DNA synthesis was performed using colorimetric BrdU ELISA (A, B). Intracellular ATP content was measured by a luciferase-luciferin based assay (C, D). Values are presented as mean ± standard error (n = 3). PM x CONC main effects were observed for all assays (2-way ANOVA).

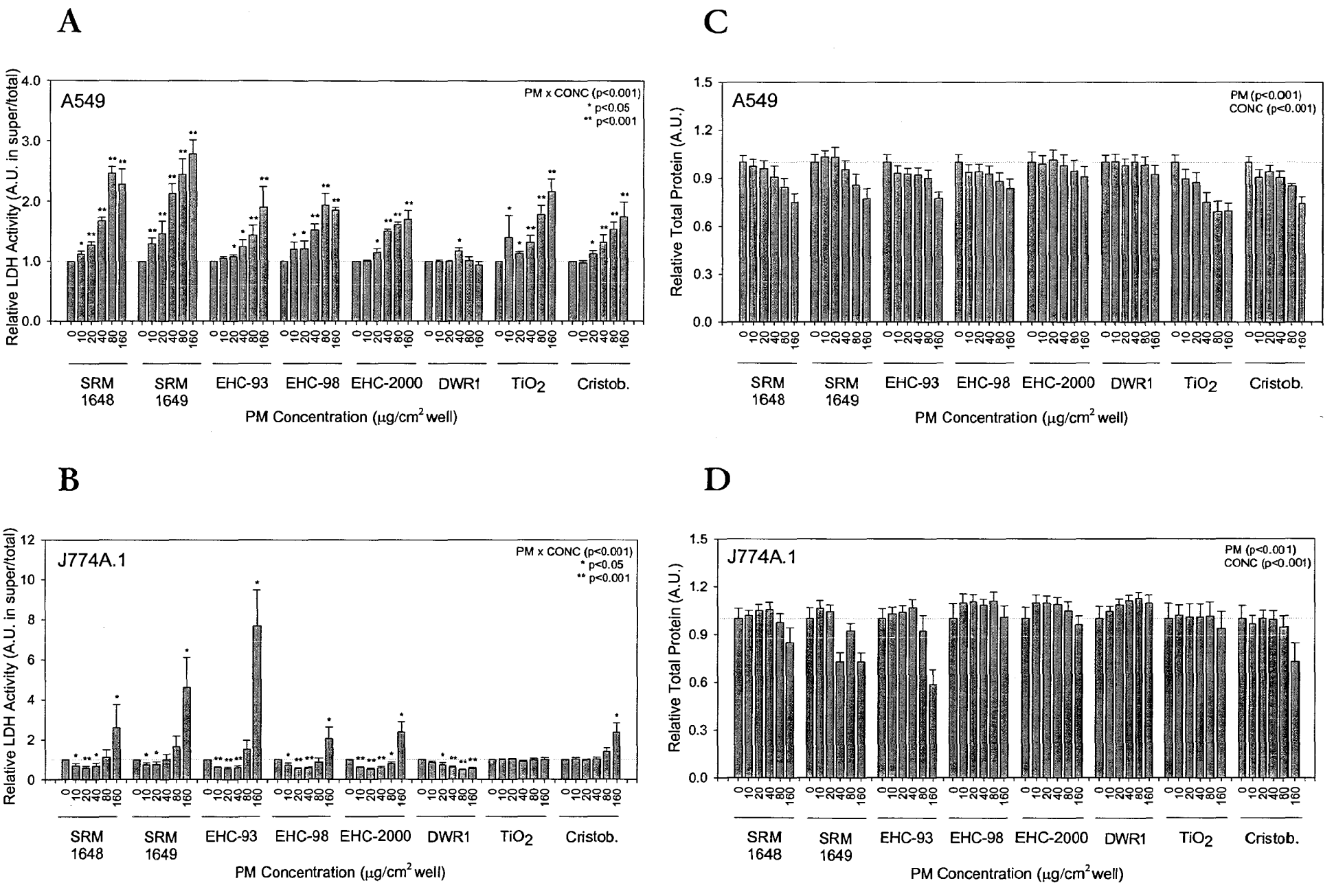
A
A549
PM x CONC (p<0.001)
* p<0.05
** p<0.001
Relative LDH Activity (A.U. in super/total)
SRM 1648
SRM 1649
EHC-93
EHC-98
EHC-2000
DWR1
TiO2
Cristob.
PM Concentration (μg/cm2 well)
C
A549
PM (p<0.001)
CONC (p<0.001)
Relative Total Protein (A.U.)
B
J774A.1
PM x CONC (p<0.001)
* p<0.05
** p<0.001
D
J774A.1
PM (p<0.001)
CONC (p<0.001)

Figure 1.6. Lactate Dehydrogenase (LDH) release into cell culture supernatants and total protein content of A549 human epithelial cells and J774A.1 murine macrophages exposed for 24 hrs to particle preparations. LDH release was measured colorimetrically by a Cytotox 96 assay (A, B). The data represent LDH activity in the cell culture supernatants, corrected for intracellular LDH content. Total protein of PBS-rinsed monolayers was determined colorimetrically from cell lysates, by Coomassie assay (C, D). Values are presented as mean ± standard error (n = 3). PM x CONC interactions were observed for the LDH assay. PM and CONC main effects were obtained for the Coomassie assay. Asterisks above bars represent particle concentration effects significantly different from control, where PM x CONC interaction was observed (2-way ANOVA).

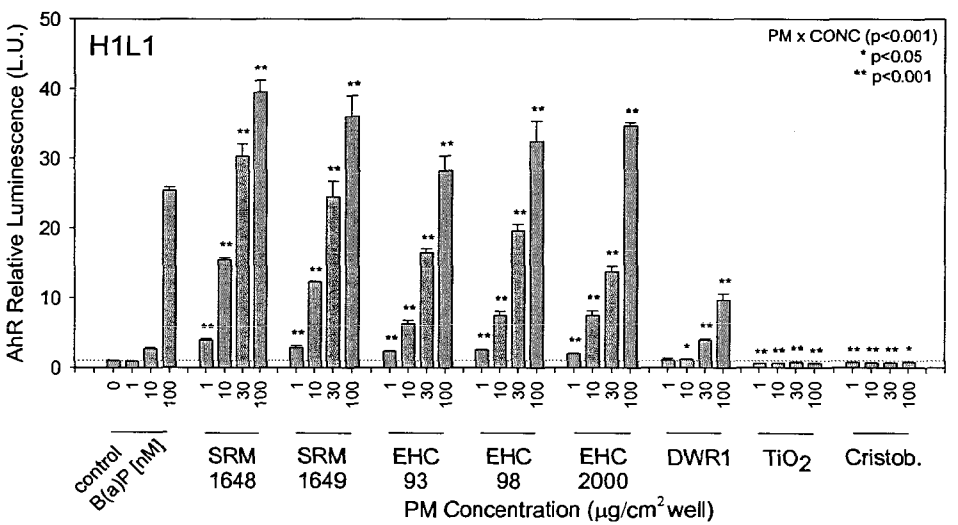
H1L1
PM x CONC (p<0.001)
* p<0.05
** p<0.001
AhR Relative Luminescence (L.U.)
50
40
30
20
10
0
0 1 10 100
1 10 30 100
control
B(a)P [nM]
SRM 1648
SRM 1649
EHC 93
EHC 98
EHC 2000
DWR1
TiO2
Cristob.
PM Concentration (μg/cm2 well)

Figure 1.7. Luciferase activity of H1L1.1c2 cells exposed for 24 hrs to particles. The luciferase activity in the H1L1.1c2 cells was assessed using Promega luciferase assay reagent. B[a]P is present for reference (positive control) and was not included in the ANOVA to maintain the factorial design. All values are presented as mean ± standard error (n = 3). PM x CONC interaction was obtained for AhR assay. Asterisks above bars represent particle concentration effects significantly different from control (2-way ANOVA).

10.3.3 Inflammation *In Vitro*

A cytokine/chemokine profile was determined for A549 and J774A.1 cells exposed to particles. Different cytokine profiles were seen between the two cell lines upon particle exposure, as well as differences in cytokine responses to specific particles were observed (Figures 1.8 – 1.10). In J774A.1 cells pro-inflammatory cytokines IL-1α, IL-1β, IL-6, GM-CSF, RANTES and TNF-α showed significant particle concentration-dependent increases in response to most particles, while anti-inflammatory cytokine IL-10 decreased upon exposure to particles. Significant differences in response to the various particles were also observed. Significant 2-way particle type- and concentration-dependent interactions were observed in IL-6, GM-CSF, RANTES and TNF-α levels in J774A.1 cells (Figures 1.9C, 1.10B, 1.10C). In A549 cells IL-6, IL-8, GM-CSF and MCP-1 increased significantly in response to a number of particles (Figures 1.8A-D), while the other cytokines including IL-10 were undetected, or unchanged. Significant 2-way interaction was observed in MCP-1 levels in A549 cells, while the changes in IL-6, IL-8 and GM-CSF were particle concentration dependent, with IL-8 chemokine also showing particle type-dependent differences in response. Compared to A549 cells, J774A.1 cells released more cytokines at higher magnitudes when exposed to particles. The comparison of the ranking of particle potencies for the release of cytokines revealed high level of similarity in ranking between the pro-inflammatory cytokines IL-1α, IL-1β, IL-6, GM-CSF, RANTES and TNF-α in J774A.1 cells, with EHC-2000 and EHC-98 ranked as most potent particles and DWR1 and the mineral dusts Cristobalite and TiO_2 as least potent particles, with the rest of the urban dusts showing intermediate potency (Table A-6). The particles SRM-1649, EHC-98 and EHC-93 were the most potent inhibitors of the anti-inflammatory cytokine IL-10, while the fine particle DWR1 and Cristobalite had the least effect on IL-10 levels in J774A.1 cells (Figure 1.9D). TNF-α showed the largest changes in magnitude between the particles compared to control (91 ± 8.4 pg/ml), with 212 ± 76.4 pg/ml detected in supernatants of J774A.1 cells exposed to 160 $\mu g/cm^2$ Cristobalite, versus 32,393 ± 3,607 pg/ml detected in J774A.1 supernatants upon exposure of cells to 160 $\mu g/cm^2$ of EHC-98. Interestingly, while most urban particles ranked highly for inducing TNF-α release, the urban particle EHC-93 showed significantly less induction of TNF-α, more comparable to the mineral dusts and DWR1 (Figure 1.10C). In A549 cells, SRM-1649 and the minerals represented particles

with the highest overall ranking of potency estimates in contrast to DWR1, which showed consistently lowest ranking for all cytokines detected in A549 cells (Table A-6).

10.3.4 Endotoxin Content of Particles

As shown in Table 1.2, the endotoxin content of the urban particles and fine particle DWR1 was comparable (~18 - 23 EU/mg particle), with the exception of SRM-1649 that contained less endotoxin (12.08 ± 0.76 EU/mg particle). No endotoxin was detected in the mineral dust preparations (TiO_2, Cristobalite) and the particle preparation buffer. An extraction of EHC-93 in water showed that the majority of the endotoxin content of the urban particle was associated with the water-insoluble fraction, with only 2.9 ± 0.2 EU/mg particle associated with the water-soluble fraction.

Table 1.2. Endotoxin content of particle preparations.

Particle	Endotoxin Content (EU/mg particle/ml buffer)
DWR1	18.00 ± 0.88
EHC-93	20.01 ± 0.30
EHC-93*sol*	2.90 ± 0.20
EHC-98	22.31 ± 0.15
EHC-2000	23.36 ± 0.02
SRM-1648	23.20 ± 0.07
SRM-1649	12.08 ± 0.76
TiO_2	n.d.
Cristobalite	n.d.
Particle Buffer	n.d.

n.d. – not detected

10.3.5 Ranking of *In Vitro* Particle Potency

As seen in Figures 1.11A and 1.11B, differences in response to particles were observed between the two cell lines, for both cytotoxicity and inflammation subsets of endpoints. Overall, cytotoxicity endpoints appeared to show less cell line-specific differences in potency compared to endpoints indicative of inflammation, when the proximity of the averages of the potency estimates for particles in the two subsets was compared (horizontal bars).

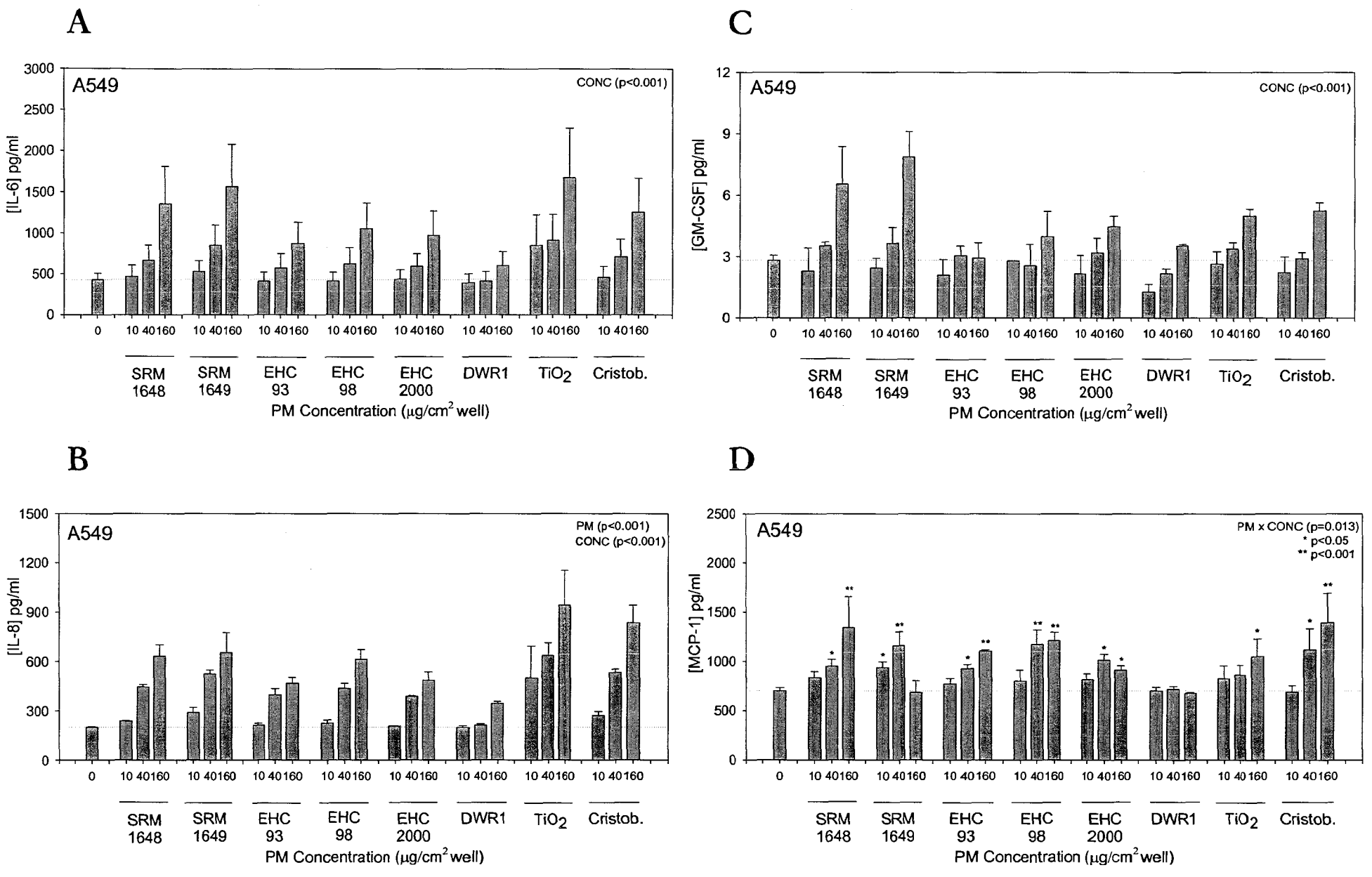
A
A549
CONC (p<0.001)
[IL-6] pg/ml
3000
2500
2000
1500
1000
500
0
0 10 40160 10 40160 10 40160 10 40160 10 40160 10 40160 10 40160 10 40160
SRM 1648
SRM 1649
EHC 93
EHC 98
EHC 2000
DWR1
TiO2
Cristob.
PM Concentration (μg/cm2 well)
C
A549
CONC (p<0.001)
[GM-CSF] pg/ml
12
9
6
3
0
0 10 40160 10 40160 10 40160 10 40160 10 40160 10 40160 10 40160 10 40160
SRM 1648
SRM 1649
EHC 93
EHC 98
EHC 2000
DWR1
TiO2
Cristob.
PM Concentration (μg/cm2 well)
B
A549
PM (p<0.001)
CONC (p<0.001)
[IL-8] pg/ml
1500
1200
900
600
300
0
0 10 40160 10 40160 10 40160 10 40160 10 40160 10 40160 10 40160 10 40160
SRM 1648
SRM 1649
EHC 93
EHC 98
EHC 2000
DWR1
TiO2
Cristob.
PM Concentration (μg/cm2 well)
D
A549
PM x CONC (p=0.013)
* p<0.05
** p<0.001
[MCP-1] pg/ml
2500
2000
1500
1000
500
0
0 10 40160 10 40160 10 40160 10 40160 10 40160 10 40160 10 40160 10 40160
SRM 1648
SRM 1649
EHC 93
EHC 98
EHC 2000
DWR1
TiO2
Cristob.
PM Concentration (μg/cm2 well)

Figure 1.8. Interleukin (IL)-6 (A), IL-8 (B), Granulocyte-Macrophage Colony-Stimulating Factor (GM-CSF) (C) and Monocyte Chemoattractant Protein (MCP)-1 (D) levels in cell culture supernatants of A549 human epithelial cells exposed for 24 hrs to particle preparations. Cytokine and chemokine levels were determined by Bio-Plex assay. Values are presented as mean ± standard error (n = 3). For IL-6, IL-8 and GM-CSF, main effects only, were obtained. PM x CONC interaction was observed for MCP-1 data. Asterisks above bars represent particle concentration effects significantly different from control, where PM x CONC interaction was observed (2-way ANOVA).

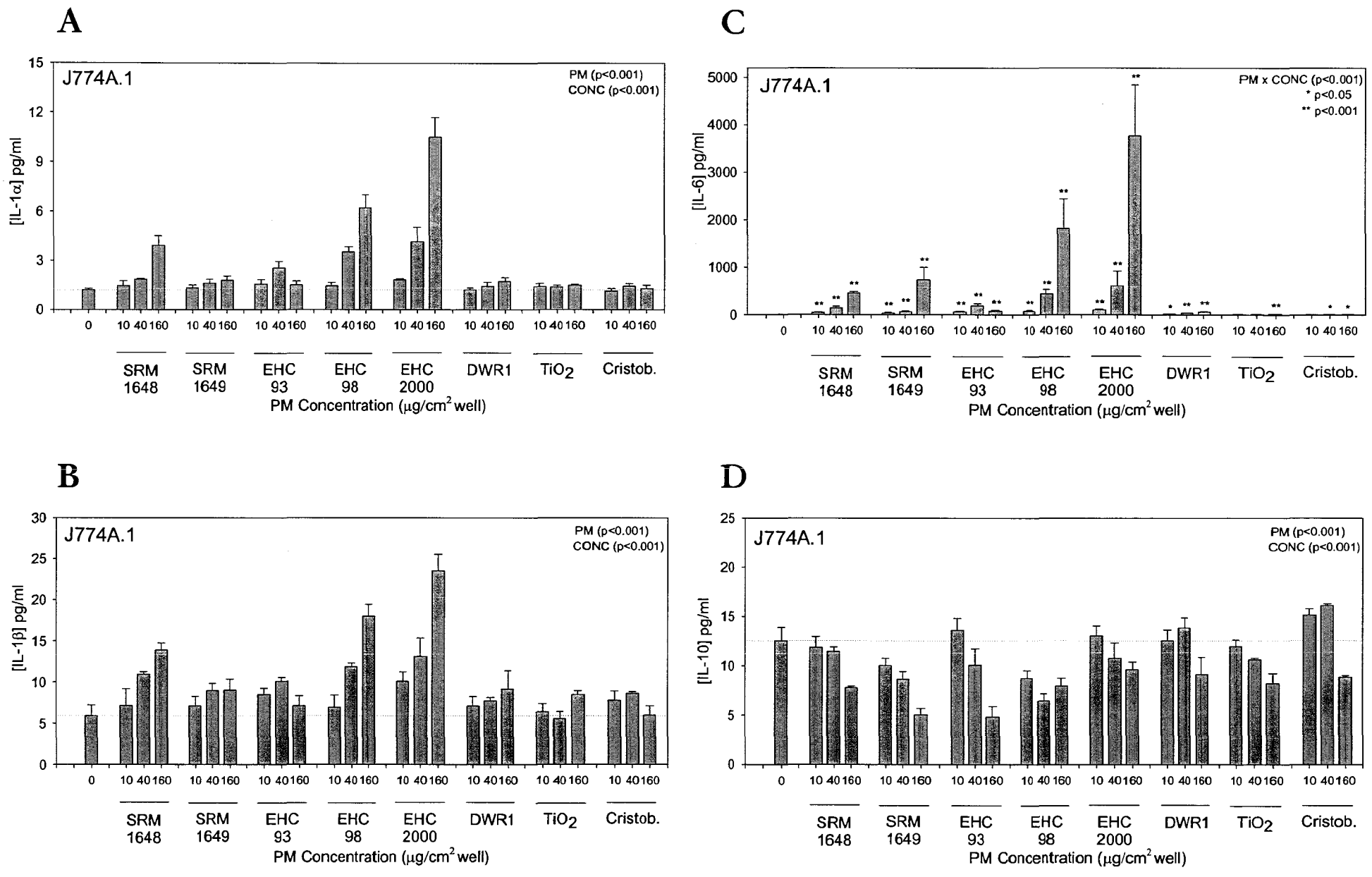
A
J774A.1
PM (p<0.001)
CONC (p<0.001)
[IL-1α] pg/ml
0 3 6 9 12 15
0 10 40 160 10 40 160 10 40 160 10 40 160 10 40 160 10 40 160 10 40 160 10 40 160
SRM 1648
SRM 1649
EHC 93
EHC 98
EHC 2000
DWR1
TiO2
Cristob.
PM Concentration (μg/cm2 well)
C
J774A.1
PM x CONC (p<0.001)
* p<0.05
** p<0.001
[IL-6] pg/ml
0 1000 2000 3000 4000 5000
PM Concentration (μg/cm2 well)
B
J774A.1
PM (p<0.001)
CONC (p<0.001)
[IL-1β] pg/ml
0 5 10 15 20 25 30
PM Concentration (μg/cm2 well)
D
J774A.1
PM (p<0.001)
CONC (p<0.001)
[IL-10] pg/ml
0 5 10 15 20 25
PM Concentration (μg/cm2 well)

Figure 1.9. Interleukin (IL)-1α (A), IL-1β (B), IL-6 (C) and IL-10 (D) levels in cell culture supernatants of J774A.1 human murine macrophages exposed for 24 hrs to particle preparations. Cytokine levels were determined by Bio-Plex assay. Values are presented as mean ± standard error (n = 3). For IL-1α, IL-1β and IL-10, PM and CONC main effects were found. PM x CONC interaction was observed for IL-6 data. Asterisks above bars represent particle concentration effects significantly different from control, where PM x CONC interaction was observed (2-way ANOVA).

A

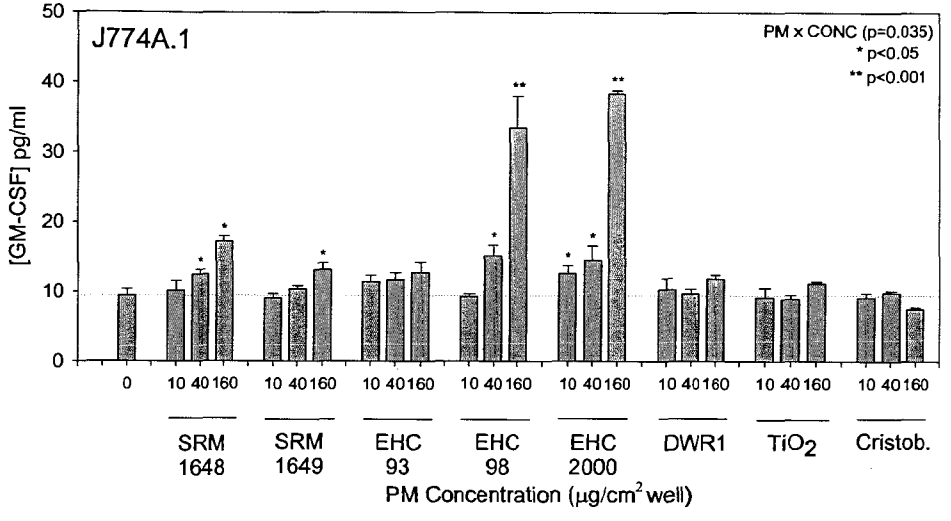
J774A.1
PM x CONC (p=0.035)
* p<0.05
** p<0.001
[GM-CSF] pg/ml
0
10
20
30
40
50
0 10 40 160 10 40 160 10 40 160 10 40 160 10 40 160 10 40 160 10 40 160 10 40 160
SRM 1648
SRM 1649
EHC 93
EHC 98
EHC 2000
DWR1
TiO2
Cristob.
PM Concentration (µg/cm2 well)

C

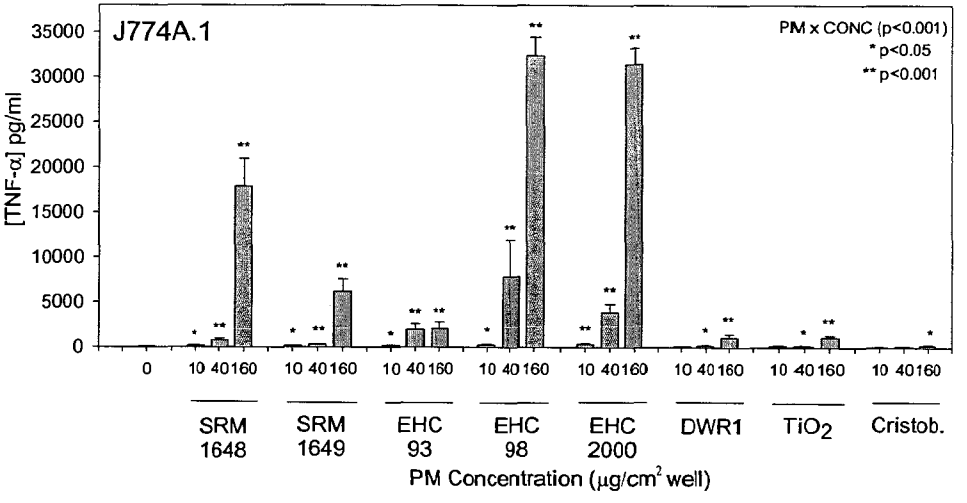
J774A.1
PM x CONC (p<0.001)
* p<0.05
** p<0.001
[TNF-α] pg/ml
0
5000
10000
15000
20000
25000
30000
35000
0 10 40 160 10 40 160 10 40 160 10 40 160 10 40 160 10 40 160 10 40 160 10 40 160
SRM 1648
SRM 1649
EHC 93
EHC 98
EHC 2000
DWR1
TiO2
Cristob.
PM Concentration (µg/cm2 well)

B

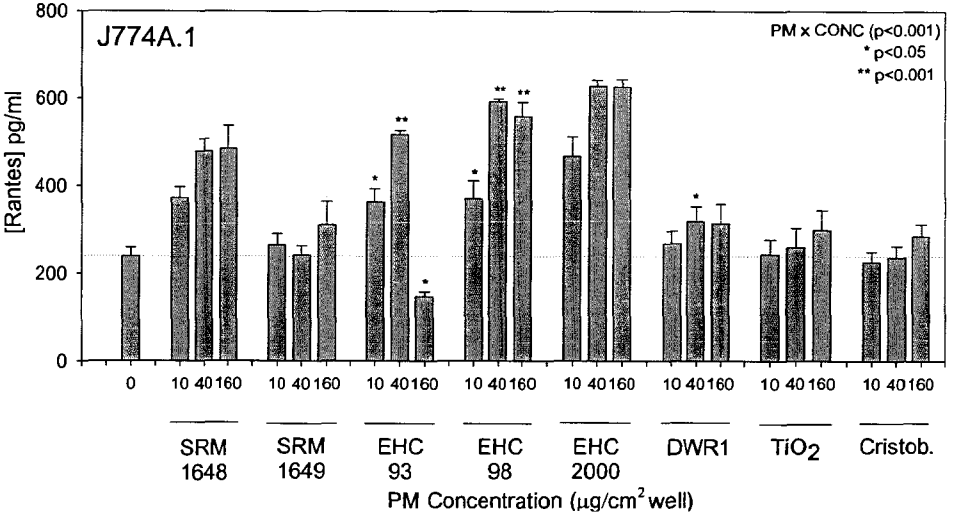
J774A.1
PM x CONC (p<0.001)
* p<0.05
** p<0.001
[Rantes] pg/ml
0
200
400
600
800
0 10 40 160 10 40 160 10 40 160 10 40 160 10 40 160 10 40 160 10 40 160 10 40 160
SRM 1648
SRM 1649
EHC 93
EHC 98
EHC 2000
DWR1
TiO2
Cristob.
PM Concentration (µg/cm2 well)

Figure 1.10. Granulocyte-Macrophage Colony-Stimulating Factor (GM-CSF) (A), Regulated upon Activation Normal T cell Expressed and Secreted (RANTES) (B), Tumor Necrosis Factor (TNF)-α (C) levels in cell culture supernatants of J774A.1 human murine macrophages exposed for 24 hrs to particle preparations. Cytokine and chemokine levels were determined by Bio-Plex assay. All values are presented as mean ± standard error (n = 3). For all assays, PM x CONC interactions were obtained. Asterisks above bars represent particle concentration effects significantly different from control (2-way ANOVA).

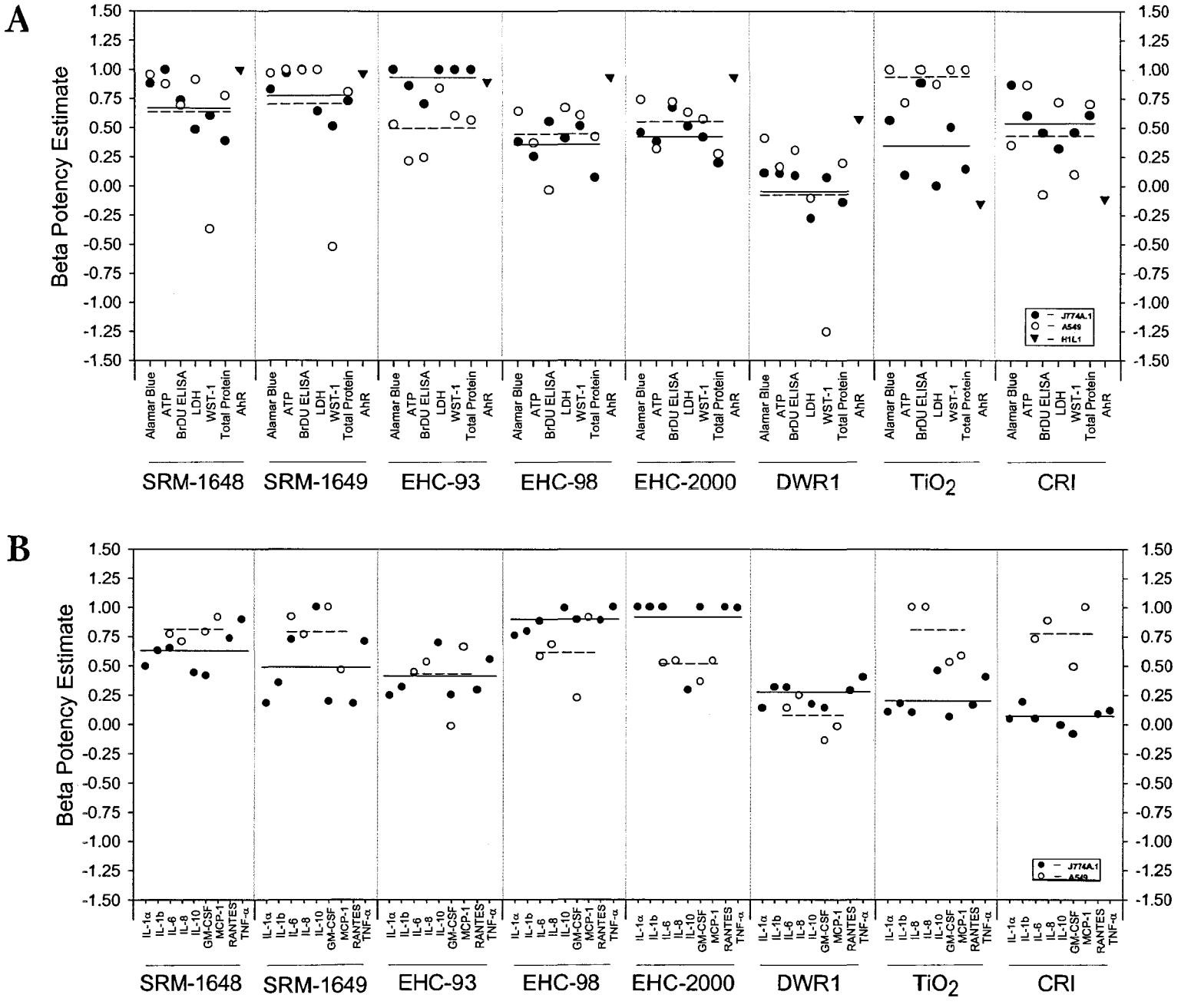
A
Beta Potency Estimate
1.50
1.25
1.00
0.75
0.50
0.25
0.00
-0.25
-0.50
-0.75
-1.00
-1.25
-1.50
Alamar Blue
ATP
BrDU ELISA
LDH
WST-1
Total Protein
AhR
J774A.1
A549
H1L1
SRM-1648
SRM-1649
EHC-93
EHC-98
EHC-2000
DWR1
TiO2
CRI
B
Beta Potency Estimate
IL-1α
IL-1b
IL-6
IL-8
IL-10
GM-CSF
MCP-1
RANTES
TNF-α
J774A.1
A549
SRM-1648
SRM-1649
EHC-93
EHC-98
EHC-2000
DWR1
TiO2
CRI

Figure 1.11. Ranking comparison of *in vitro* beta potencies. Beta potency estimates for *in vitro* cytotoxicity assays listed in Table A-5 and cytokines listed in Table A-6 were scaled to the maximal potency for each endpoint. Relative potencies for each particle are shown for all potency estimates within the two endpoint categories; A) *in vitro* cytotoxicity assays and B) *in vitro* cytokine/chemokine assays. Solid circles represent beta potencies obtained from assays performed in J774A.1 cells, empty circles represent endpoints from all assays performed in A549 cells and triangle represents beta potencies of the AhR assay in H1L1.1c2 cells. Horizontal line indicates the average of the relative beta potency estimates for the two cell lines (solid line - J774A.1; dashed line - A549) (method adapted from Seagrave *et al.*, 2002).

The overall average ranking order of particles for cytotoxicity endpoints measured in J774A.1 cells was EHC-93 >SRM-1649 >SRM-1648 >Cristobalite >EHC-2000 >EHC-98 >TiO_2 >DWR1. The average ranking of particle potencies for the inflammation subset as estimated from cytokine/chemokine measurements was EHC-2000 >EHC-98 >SRM-1648 >SRM-1649 >EHC-93 >DWR1 >TiO_2 >Cristobalite. For A549 cells, the average ranking order for the endpoints of the cytotoxicity index was TiO_2 >SRM-1649 >SRM-1648 >EHC-2000 >EHC-93 >EHC-98 > Cristobalite >DWR1 and the average ranking order of the potency estimates for the inflammation index was SRM-1648 >SRM-1649 >TiO_2 >Cristobalite >EHC-98 >EHC-2000 >EHC-93 >DWR1. The ranking order of the gene activation AhR assay in H1L1.1c2 cells was SRM-1648 >SRM-1649 >EHC-2000 >EHC-98 >EHC-93 >DWR1 >Cristobalite >TiO_2. Overall, SRM- and EHC-type urban particles appeared to be more potent in eliciting cytotoxic and inflammatory responses than fine particle DWR1 ($PM_{2.5}$) and mineral dusts Cristobalite and titanium dioxide. A comparison of the scaled potency estimates for all assays of the cytotoxicity subset showed that the measurement of cell viability in A549 cells using the WST-1 assay produced most discrimination between particles, when considering the magnitude of the difference between the most potent and least potent particle in each assay. The assay, however, also appeared to be the most different from the rest of the assays, as indicated by its distance from the average particle potency estimate. For J774A.1 cells, measurement of cytoplasmic LDH leakage from cells produced highest discrimination among particles. The LDH assay was also well consistent with the overall average of the scaled beta potency estimates determined for each particle. A comparison of the endpoints of the inflammation subset indicated that measurement of GM-CSF cytokine in cell supernatants showed best discrimination among particles in both cell lines. In A549 cells, concentration main effect only was detected for GM-CSF data by 2-way ANOVA, thus in this study the assay cannot be considered as best endpoint for particle potency ranking in A549 cells.

10.3.6 Effects of Particles in Mice

The effects of a subset of particles comprised of urban dusts (EHC-2000, SRM-1649), mineral standards (Cristobalite and TiO_2) and fine particulate mixture (DWR1) were examined *in vivo* upon their intra-tracheal instillation into the lungs of BALB/*c* mice. The particles were selected on the basis of their overall potency ranking in the *in vitro* assays, to encompass a wide range of their

effects in cells. After a 24 h exposure, the mice were sacrificed and a number of endpoints were assessed in BAL and blood plasma of the animals, to obtain an overview of the extent of cytotoxicity and inflammation induced by the various particles *in vivo*. A panel of biochemical endpoints (LDH, 8-isoprostane, total protein) and cell differential counts in BAL (total cells, neutrophils, macrophages, band cells, lymphocytes, eosinophils, monocytes, basophils and multinucleated giant cells) were assessed as an index of cytotoxicity (Figures 1.12, 1.13). The extent of inflammation was determined from the measurements of a number of cytokines/chemokines in BAL (IL-1α, IL-1β, IL-5, IL-6, IL-10, KC, GM-CSF, MIP-1α, RANTES, TNF-α) (Figures 1.14 - 1.16). Particle potency estimates (slopes of the dose-response curves) *in* vivo and particle potency rank order were determined for all cytotoxicity and inflammation endpoints that were examined (Tables A-7, A-8). For ease of comparison, the beta potency estimates were uniformly scaled by maximal potency for each particle per endpoint and presented in the two subsets representative of overall cytotoxicity and inflammation response (Figures 1.17A, 1.17B). The statistical significance of all measured responses was summarized in Tables A-3 and A-4.

10.3.7 Toxicity *In Vivo*

Intratracheal instillation of particles in BALB/*c* mice with 24 h exposure caused mild, acute cytotoxicity, as evidenced by lack of pronounced changes in plasma isoprostane and BAL LDH, total protein or total cell count (Figures 1.12A-D) that would be expected in the presence of a strong acute toxic response. 8-isoprostane levels in blood plasma of the exposed animals showed significant differences that were particle dose-dependent when compared to the control animals, with mostly bi-phasic effects (DOSE main effects, $p < 0.001$) (Figure 1.12B). Amount of total protein in BAL was significantly different with respect to particle dose (DOSE main effect, $p < 0.001$) and showed an overall trend of a dose response with increases upon exposure to the particles (Figure 1.12C). The differences in response between particles were not significant for these two endpoints. The total number of cells in BAL did not significantly change upon exposure to particles. LDH levels in BAL were borderline significantly different at the highest dose of particles only (DOSE main effect, $p=0.041$), while differences in BAL LDH induced by the various particles, with the exception of EHC-2000 were also significant (PM main effect, $p=0.009$). Overall, LDH showed a trend of increase in comparison to the controls, with the exception of DWR1. An increase in neutrophil influx (PM x DOSE interaction, $p=0.004$) and a

drop in alveolar macrophages (DOSE main effect, $p<0.001$; PM main effect, $p=0.034$) were consistent with particle challenge and clearance in the animals (Figures 1.13A, 1.13B). Number of band cells and lymphocytes were significantly higher for all particle doses in comparison to control animals (DOSE main effect, $p<0.001$), with no differences between various particle treatments and with high variability in measurements (Figures 1.13C, 1.13D). Table A-7 lists the ranked beta potency estimates for the individual assays comprising the *in vivo* cytotoxicity subset. Five of the eight endpoints of the cytotoxicity subset identified the urban dust SRM-1649 as most potent and six out of eight endpoints showed DWR1 to be the least potent of the particles. EHC-2000 was shown to have intermediate potency by five of the seven endpoints. No significant differences between sham and saline-vehicle control treated animals were observed with respect to the measured endpoints.

10.3.8 Inflammatory Mediators in Mice

Significant particle type- and dose-dependent increases in pro-inflammatory mediators IL-6, KC and MIP-1α in BAL were observed in response to a number of particles (PM x DOSE interactions) (Figures 1.14D, 1.15B, 1.15D). The amounts of IL-1α, IL-1β and TNF-α in BAL were also significantly higher with respect to the dose of the particles, as well as showing differences in response between the different particles (DOSE main effect, $p<0.001$; PM main effect, $p<0.001$) (Figures 1.14A, 1.14B, 1.16). The cytokine IL-5 significantly increased in an overall response to the medium (100 μg) and high (250 μg) doses of particles, while the chemokine RANTES was found to increase in response to the low (50 μg) dose (DOSE main effect, $p<0.001$), without dependence on particle type (Figures 1.14C, 1.15C). The changes in the amount of IL-10 in response to particles were not significant (Figure 1.15A). Comparison of the particle potency ranking based on the cytokine/chemokine assays of the inflammation subset with that based on the endpoints of the cytotoxicity subset revealed overall similarities in responses. Urban dust EHC-2000 was identified to be the first or second most potent particle by seven of the nine assays followed by SRM-1649 in the first or second place, as shown by five of the nine assays. DWR1 had the least effect in inducing increases in BAL cytokines, as shown by five out of nine assays. Interestingly, the ranking of the particles based on their potency in inducing IL-10 changes in BAL was opposite to that of the rest of the assays, identifying DWR1 as second most potent particle

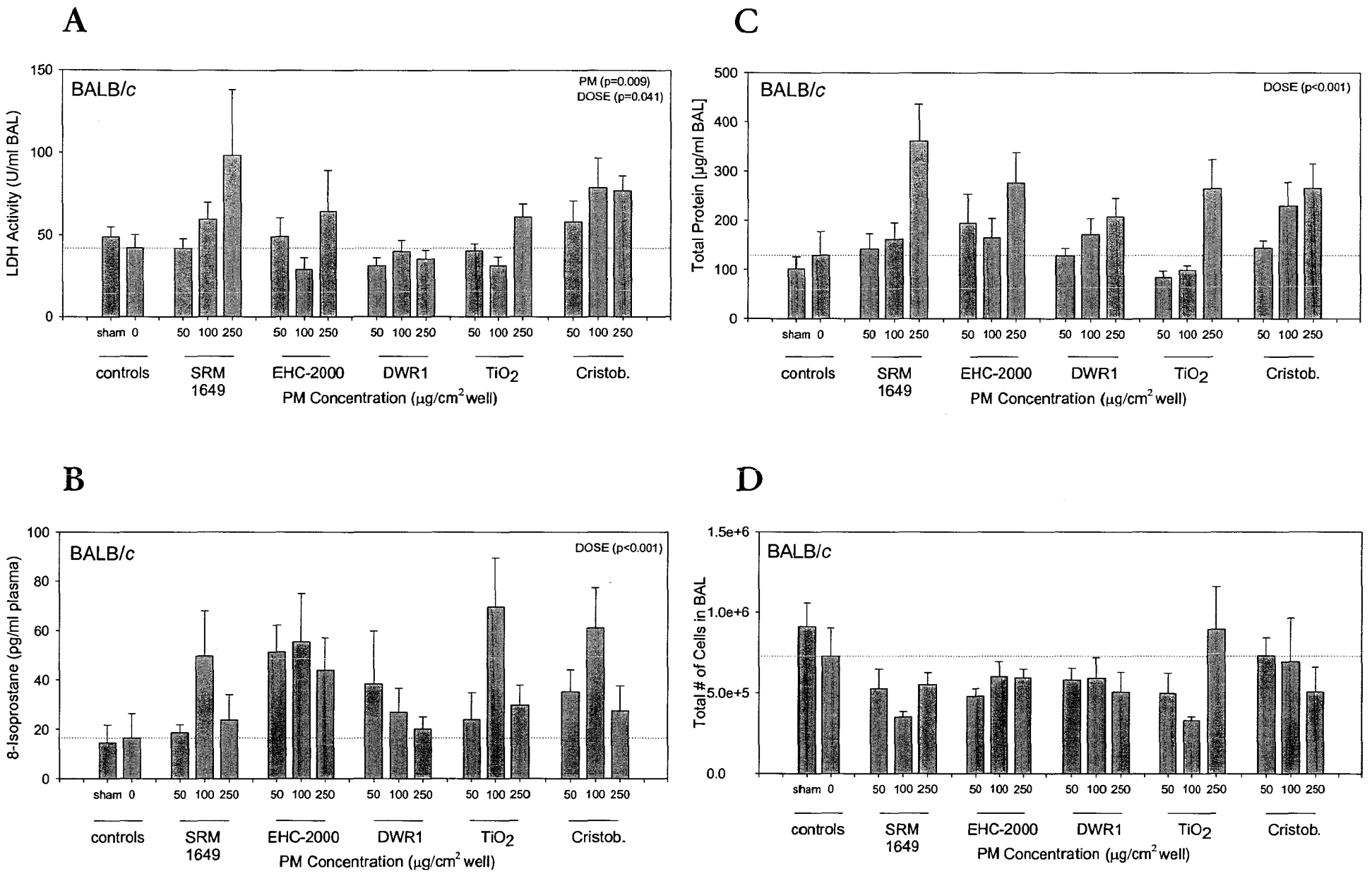
A
BALB/c
PM (p=0.009)
DOSE (p=0.041)
LDH Activity (U/ml BAL)
150
100
50
0
sham 0
50 100 250
controls
SRM 1649
EHC-2000
DWR1
TiO2
Cristob.
PM Concentration (μg/cm2 well)
C
BALB/c
DOSE (p<0.001)
Total Protein [μg/ml BAL]
500
400
300
200
100
0
B
BALB/c
DOSE (p<0.001)
8-Isoprostane (pg/ml plasma)
100
80
60
40
20
0
D
BALB/c
Total # of Cells in BAL
1.5e+6
1.0e+6
5.0e+5
0.0

Figure 1.12. LDH levels (A) in bronchoalveolar lavage fluid (BAL), 8-Isoprostane levels (B) in blood plasma, total protein levels (C) and total cell count (D) in BAL of BALB/*c* mice exposed to particulate matter for 24 hrs by intratracheal instillation. LDH levels were measured colorimetrically by a Cytotox 96 assay. 8-Isoprostane levels in plasma were determined using an enzyme immune-assay. Total protein was determined colorimetrically from BAL samples, by Coomassie Assay. Total cell counts were determined from cytospin preparations of BAL. Values are presented as mean ± standard error (n=~5). Main effects were observed for LDH, 8-isoprostane and total protein endpoints by 2-way ANOVA. Total cell counts showed changes without statistical significance.

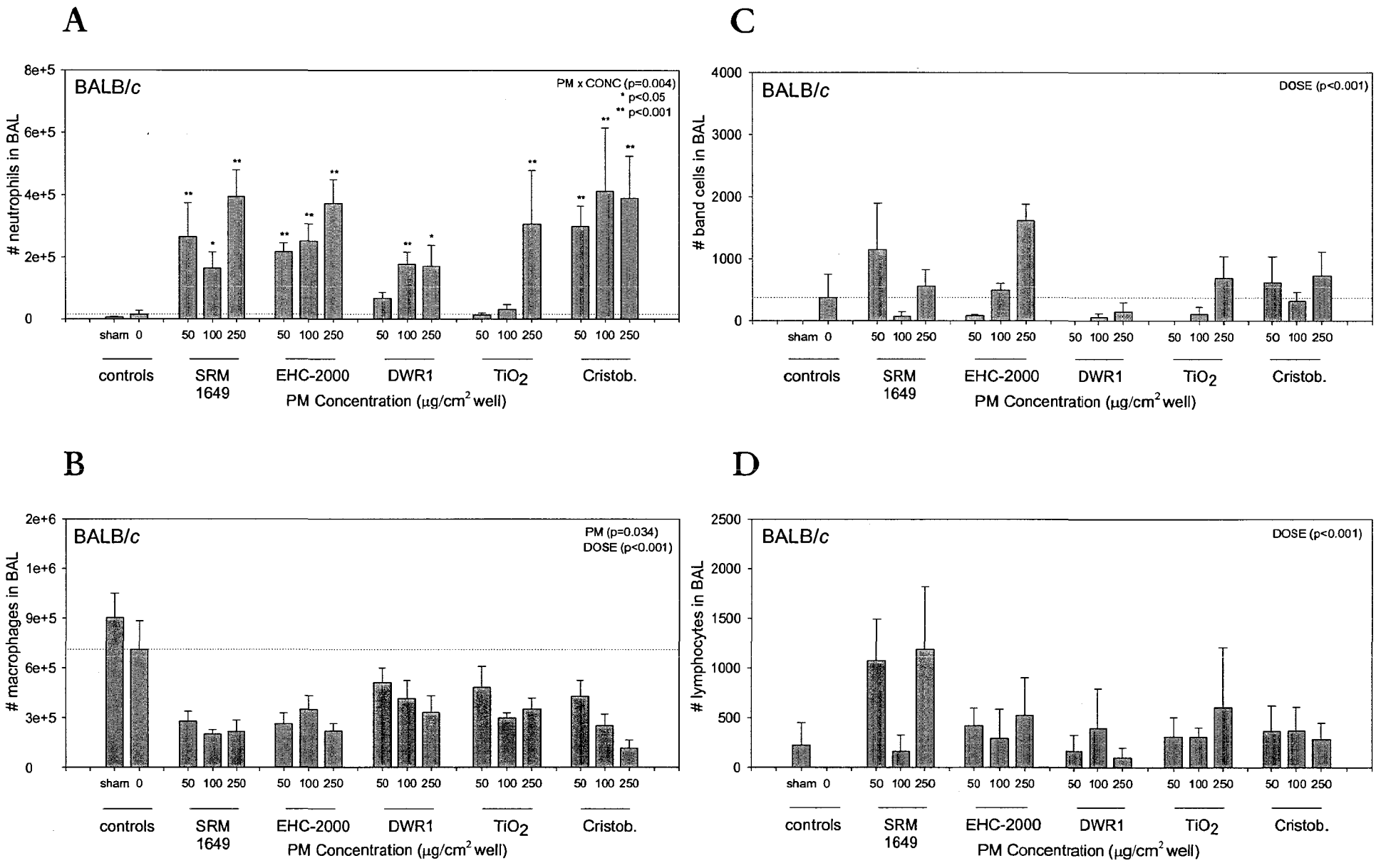
A
BALB/c
PM x CONC (p=0.004)
* p<0.05
** p<0.001
# neutrophils in BAL
8e+5
6e+5
4e+5
2e+5
0
sham 0
50 100 250
controls
SRM 1649
EHC-2000
DWR1
TiO2
Cristob.
PM Concentration (µg/cm2 well)
C
BALB/c
DOSE (p<0.001)
band cells in BAL
4000
3000
2000
1000
0
B
BALB/c
PM (p=0.034)
DOSE (p<0.001)
macrophages in BAL
2e+6
1e+6
9e+5
6e+5
3e+5
0
D
BALB/c
DOSE (p<0.001)
lymphocytes in BAL
2500
2000
1500
1000
500
0

Figure 1.13. Neutrophil (A), macrophage (B), band cell (C) and lymphocyte (D) cell counts in bronchoalveolar lavage (BAL) fluid of BALB/*c* mice exposed to particulate matter for 24 hrs by intratracheal instillation. Cell counts were determined from cytospin preparations of BAL. Values are presented as mean ± standard error (n=~5). PM x DOSE interaction was obtained for neutrophil cell counts. Asterisks above bars represent dose effects significantly different from control, where PM x CONC interaction was observed. Main effects were observed for macrophage, band cell and lymphocyte cell counts by 2-way ANOVA (not shown).

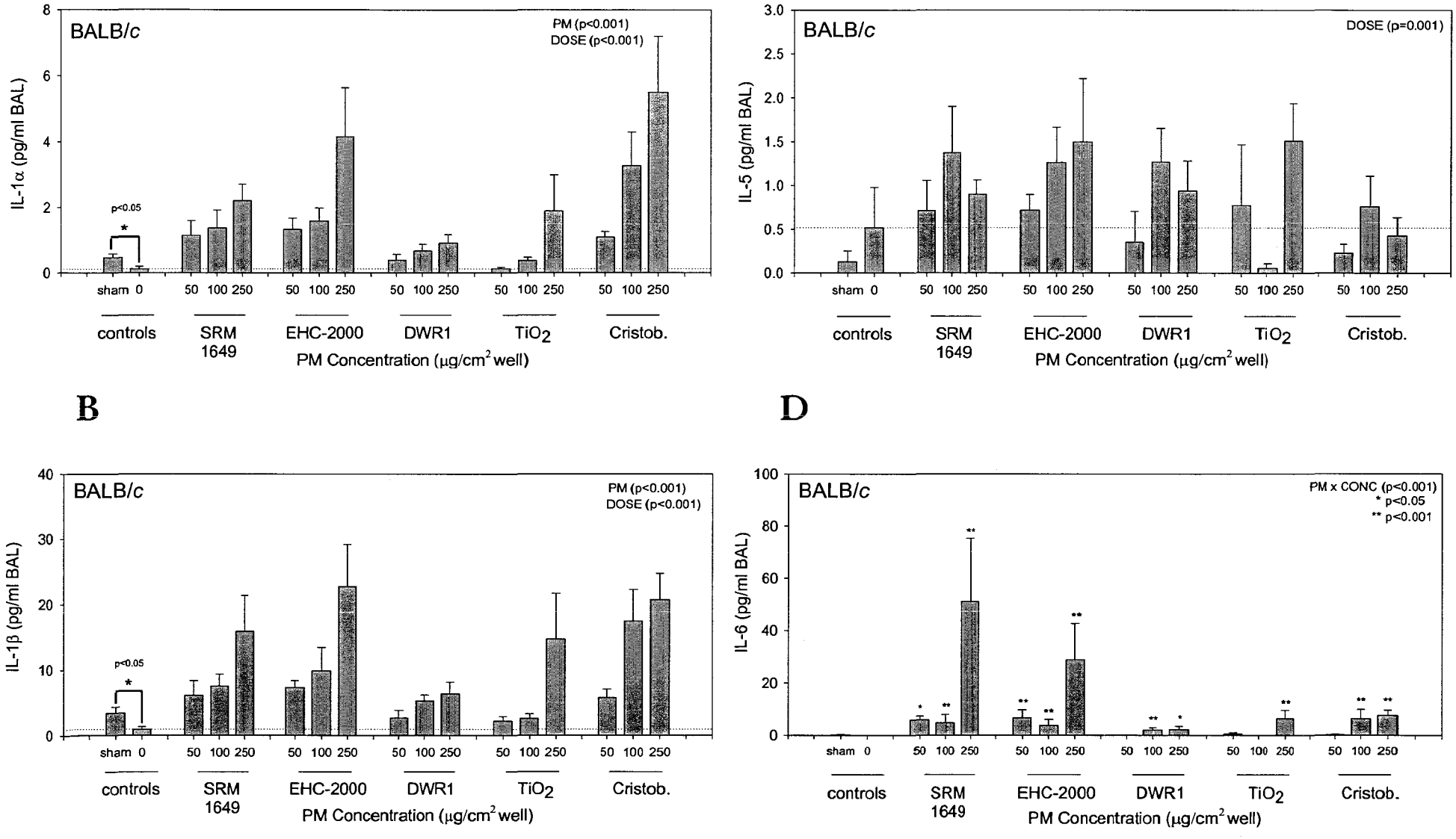
A
BALB/c
PM (p<0.001)
DOSE (p<0.001)
IL-1α (pg/ml BAL)
p<0.05
*
sham 0
50 100 250
controls
SRM 1649
EHC-2000
DWR1
TiO2
Cristob.
PM Concentration (μg/cm2 well)
C
BALB/c
DOSE (p=0.001)
IL-5 (pg/ml BAL)
B
BALB/c
PM (p<0.001)
DOSE (p<0.001)
IL-1β (pg/ml BAL)
D
BALB/c
PM x CONC (p<0.001)
* p<0.05
** p<0.001
IL-6 (pg/ml BAL)

Figure 1.14. Interleukin (IL)-1α (A), IL-1β (B), IL-5 (C) and IL-6 (D) levels in bronchoalveolar lavage (BAL) fluid of BALB/*c* mice exposed to particulate matter for 24 hrs by intratracheal instillation. Cytokine levels in BAL were determined by Bio-Plex assay. Values are presented as mean ± standard error (n=~5). Main effects were obtained for IL-1α, IL-1β and IL-5. PM x DOSE interaction was obtained for IL-6 data. Asterisks above bars represent dose effects significantly different from control, where PM x CONC interaction was observed (2-way ANOVA). Statistically significant difference between the sham and control animals were observed for IL-α and IL-1β levels in BAL by a Student's t-test (*P <0.05).

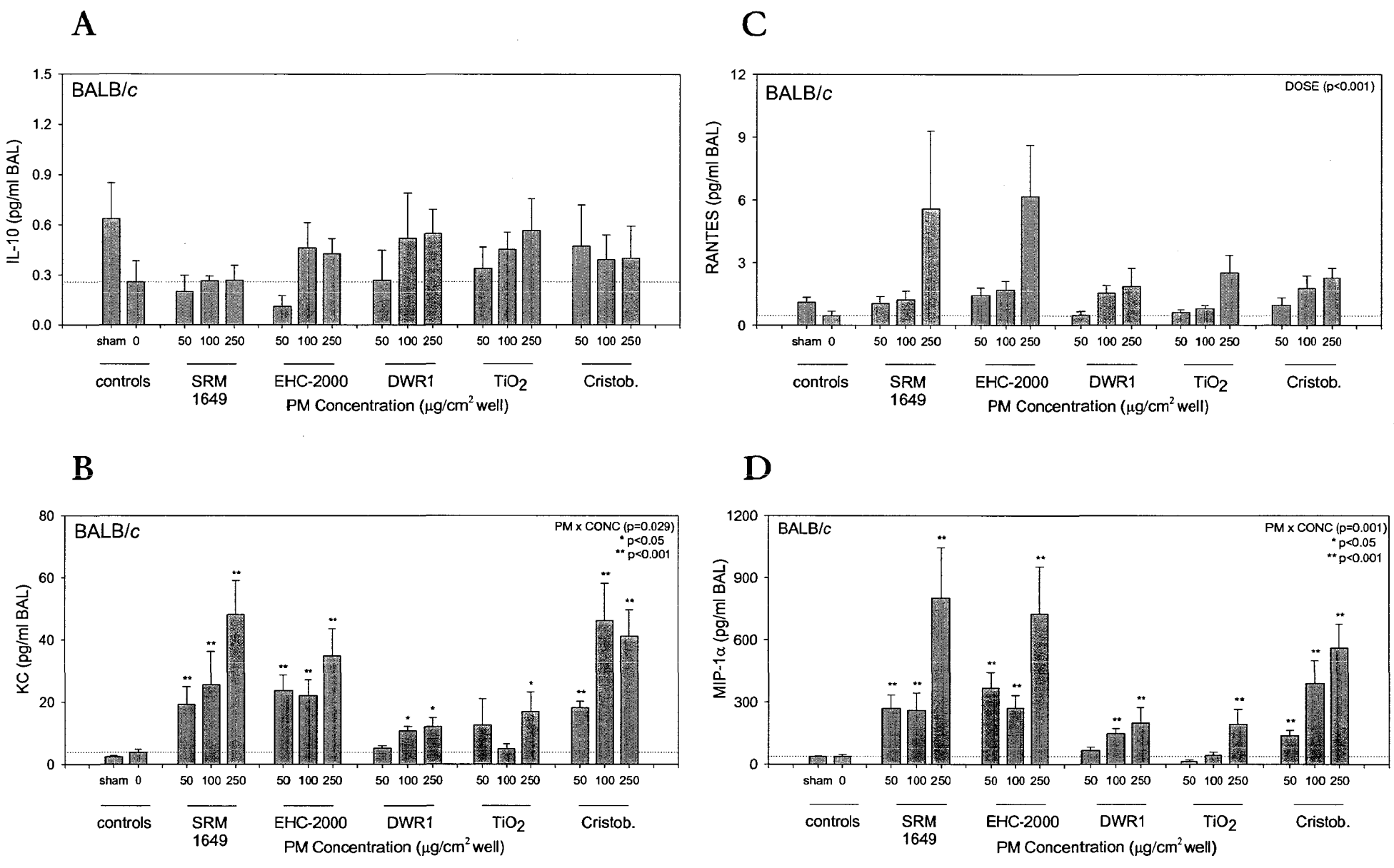
A
BALB/c
IL-10 (pg/ml BAL)
1.5
1.2
0.9
0.6
0.3
0.0
sham 0
50 100 250
controls
SRM 1649
EHC-2000
DWR1
TiO2
Cristob.
PM Concentration (μg/cm2 well)
C
BALB/c
DOSE (p<0.001)
RANTES (pg/ml BAL)
12
9
6
3
0
B
BALB/c
PM x CONC (p=0.029)
* p<0.05
** p<0.001
KC (pg/ml BAL)
80
60
40
20
0
D
BALB/c
PM x CONC (p=0.001)
* p<0.05
** p<0.001
MIP-1α (pg/ml BAL)
1200
900
600
300
0

Figure 1.15. Interleukin (IL)-10 (A), Keratinocyte-derived Chemokine (KC) (B), Macrophage Inflammatory Protein (MIP)-1α (C) and Regulated upon Activation Normal T cell Expressed and Secreted (RANTES) (D) levels in bronchoalveolar lavage (BAL) fluid of BALB/*c* mice exposed to particulate matter for 24 hrs by intratracheal instillation. Cytokine and chemokine levels in BAL were determined by Bio-Plex assay. Values are presented as mean ± standard error (n = ~5). IL-10 levels in BAL were not statistically different. PM x DOSE interaction was obtained for KC and MIP-1α. Asterisks above bars represent dose effects significantly different from control, where PM x CONC interaction was observed. Main effects were obtained for RANTES (2-way ANOVA).

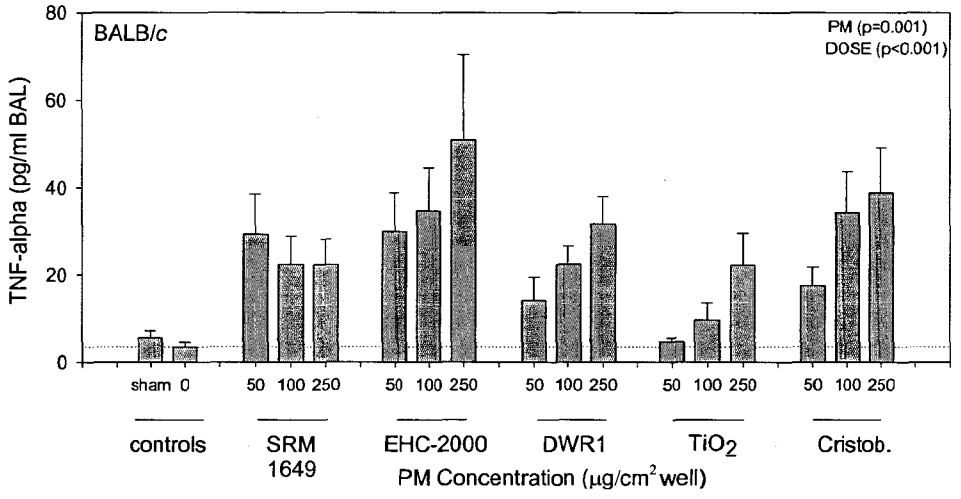
BALB/c
PM (p=0.001)
DOSE (p<0.001)
TNF-alpha (pg/ml BAL)
80
60
40
20
0
sham 0
50 100 250
50 100 250
50 100 250
50 100 250
50 100 250
controls
SRM 1649
EHC-2000
DWR1
TiO2
Cristob.
PM Concentration (µg/cm2 well)

Figure 1.16. Tumor Necrosis Factor (TNF)-α levels in bronchoalveolar lavage (BAL) fluid of BALB/*c* mice exposed to particulate matter for 24 hrs by intratracheal instillation. TNF-α levels in BAL were determined by Bio-Plex assay. PM and DOSE main effects were obtained for TNF-α by 2-way ANOVA. Values are presented as mean ± standard error (n=~5).

and SRM-1649 as the least potent of the particles (Table A-8). No significant differences between sham- and saline vehicle control-treated animals were observed with respect to the majority of the measured endpoints, with the exception of the IL-1α and IL-1β cytokines, where the levels of the two cytokines were significantly higher in sham animals in comparison to vehicle controls (IL-1α $p=0.040$; IL-1β $p=0.027$) (Figures 1.14A, 1.14B).

10.3.9 Ranking of *In Vivo* Particle Potency

As seen in Figures 1.17A and 1.17B, endpoints in both, cytotoxicity and inflammation subsets were generally consistent in scaled particle potency estimates, with most values between 0.4 and 1.0. The differences between the particles appeared to be more distinct when determined from the cytotoxicity subset of endpoints, in contrast to the inflammation subset, where less differences in averages of the scaled endpoints for each particle were seen. The overall ranking of the particles based on the average of *in vivo* cytotoxicity potency estimates for each particle was SRM-1649 >EHC-2000 >Cristobalite >TiO_2 >DWR1. The ranking of the particles as determined from the average of the scaled beta potency estimates of endpoints of the inflammation subset was EHC-2000 >Cristobalite >SRM-1649 >TiO_2 >DWR1.

10.3.10 Prediction of PM-Induced BAL Neutrophilia by *In Vitro* Assays

Best subsets multiple regression analysis was conducted to develop a model for the association between the *in vitro* assay predictor variables of the cytotoxicity and inflammation subsets and the neutrophil counts determined from bronchoalveolar lavage samples of BALB/*c* mice exposed to particles *in vivo*. BAL neutrophil counts represented the critical endpoint for the overall *in vivo* pathogenic response of animals exposed to air pollution particles by a pulmonary pathway. Table 1.3 summarizes the models determined by the analysis to represent the best predictors of the *in vivo* BAL neutrophil counts when responses to the complete set of particles were included. Best subsets regression analysis with predictor variables of the cytotoxicity subset identified three potential models for the prediction of BAL neutrophil counts. The best of the three models comprised of Alamar Blue and BrdU ELISA in A549 cells and LDH assay in J774A.1 cells, with the three assays explaining 73 % of the variability in BAL neutrophil counts. Although the p value for the LDH assay in J774A.1 cells was above 0.05 ($P=0.146$), the variable was included in the

model as it appreciably improved the R value of the model without negatively affecting the VIF and C_p model selection criteria, a 5 % increase in comparison to model # 2 comprised of Alamar Blue and BrdU ELISA assays. The regression analysis with *in vitro* inflammation subset identified two models predictive of BAL neutrophil counts; model # 1 with IL-6 assay in A549 cells (R = 0.56) and model # 2 comprised of IL-8 assay in A549 cells and IL-1β assay in J774A.1 cells (R = 0.71). The models had acceptable p and VIF values, although the C_p values were inflated. To select the best models for the prediction of BAL neutrophil counts from both, inflammation and cytotoxicity subsets, the best predictor variables that were selected from the two subsets were combined in a new best subsets regression analysis. The analysis selected three models comprised of *in vitro* assay combinations with best ability to predict *in vivo* BAL neutrophil counts. All three models comprised of IL-1β assay in J774A.1 cells and IL-8 assay in A549 cells. Model # 1 also included the WST-1 assay in A549 cells, model # 2 included BrdU ELISA assay in A549 cells and model # 3 also included BrdU ELISA in A549 cells and LDH assay in J774A.1 cells. The first two models explained 76 % of the variability in BAL neutrophil counts. The highest variability in BAL neutrophil counts, 82 % was explained by the third model. Model # 3 also best fitted the model selection criteria, with acceptable p, VIF and C_p values, although the LDH assay in J774 cells had a borderline non-significant p value of 0.061. Comparison of models # 2 and # 3, revealed that the inclusion of this variable provided an overall improvement in the predictive ability (6 % increase) and in significance of the variables (decreased p values) of model # 3. Best subsets regressions with randomly selected variables and variables categorized by cell type verified indicated that the best model selection was valid, with no random model showing an R value above that of the selected best models.

Table 1.4 summarized the best subsets model selection for the prediction of BAL neutrophil counts with a data set without the responses to mineral dusts Cristobalite and TiO_2. The analysis produced a set of best subsets models that were notably different from those obtained with a complete data set of *in vitro* variables including responses to all particles. In addition, the *in vitro* subsets of assays without the mineral dusts were better predictors of *in* vivo BAL neutrophil counts in comparison to the *in* vitro assays including responses to all particles. Due to the reduction of the amount of *in vitro* data, the predictor variables of the cytotoxicity and inflammation subsets had to be further categorized by cell type to conduct the best subsets

regressions, with a total of four best subsets regressions conducted to obtain the potential best *in vitro* predictors of the BAL neutrophils count. The assays selected by the four regressions were included in a final best subsets regression to identify the best combination of *in vitro* assays contributing to the variation of BAL neutrophil counts. Two models were identified, model # 1 comprised of WST-1 assay in A549 cells and AhR assay in H1L1.1c2 cells and Model # 2 comprised of WST-1 assay in A549 cells, AhR assay in H1L1.1c2 cells and RANTES in J774A.1 cells. A combination of WST-1 assay (A549) and AhR assay (H1L1.1c2) explained 93 percent of variability in BAL neutrophil counts. Addition of RANTES assay (J774A.1) improved the prediction of the model by 3 % (R = 0.96). The models had acceptable VIF, C_p values and variable p values. Although RANTES assay in model # 2 was borderline non-significant (p=0.051), it was included in the model, as it provided an increase in R value without affecting the other selection criteria. The effect of mineral dusts on the predictive ability of the *in vitro* assay combinations was best illustrated by the AhR assay in H1L1.1c2 cells. A comparison of the best subsets regressions with and without the cellular responses to the Cristobalite and TiO_2 showed that in the absence of the minerals, AhR assay explained 95 % of variability in BAL neutrophil counts in comparison to only 48 % when mineral dusts were included in the data sets. Consequently, in the absence of the minerals, the AhR assay became a good predictor of BAL neutrophil counts and was included in the selection of final best subsets models (Tables 1.3, 1.4). Best subsets regressions with randomly chosen variables did not produce models with R values higher than those of the two best selected models.

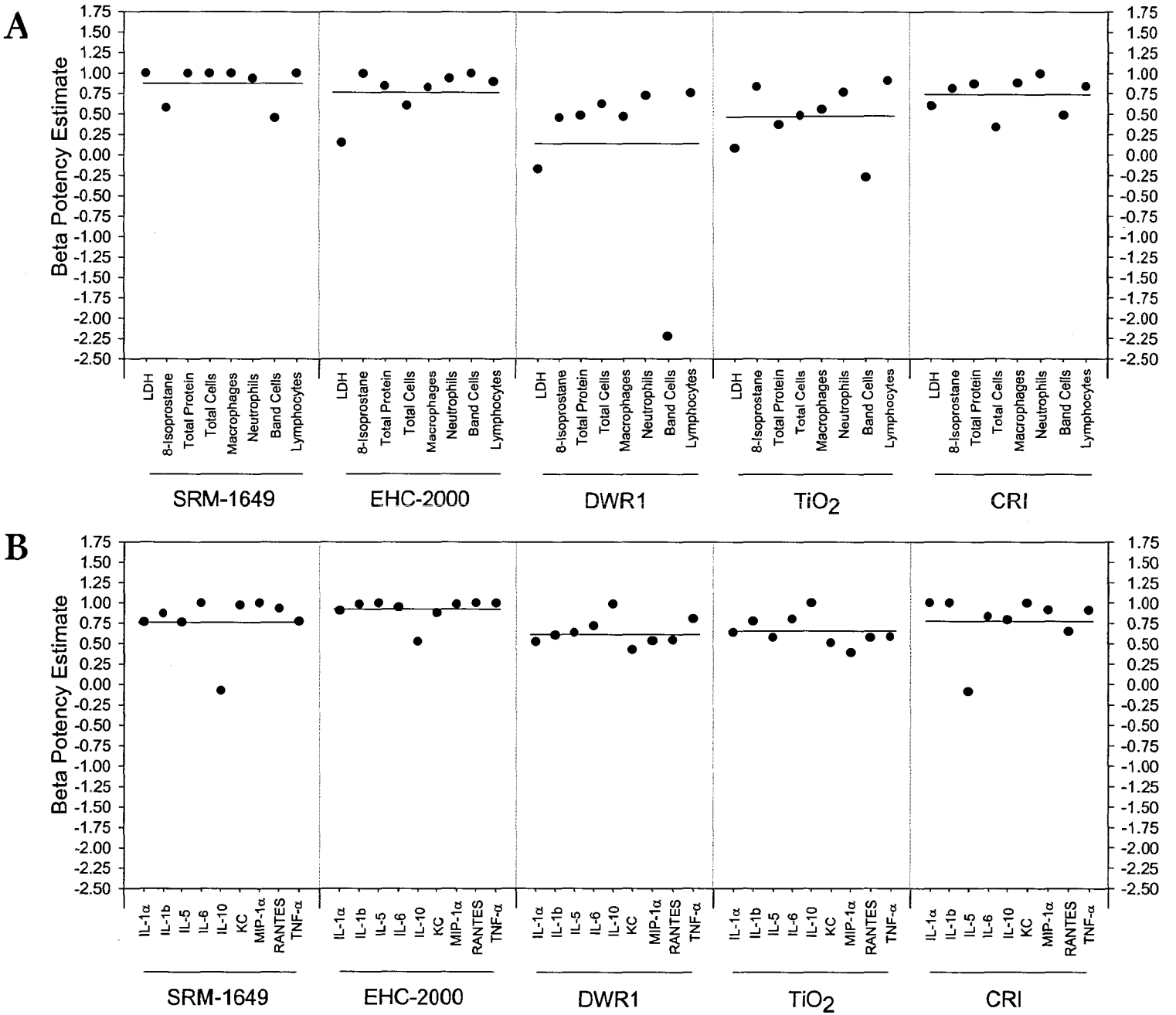
A
Beta Potency Estimate
1.75
1.50
1.25
1.00
0.75
0.50
0.25
0.00
-0.25
-0.50
-0.75
-1.00
-1.25
-1.50
-1.75
-2.00
-2.25
-2.50
LDH
8-Isoprostane
Total Protein
Total Cells
Macrophages
Neutrophils
Band Cells
Lymphocytes
SRM-1649
EHC-2000
DWR1
TiO2
CRI
B
Beta Potency Estimate
IL-1α
IL-1b
IL-5
IL-6
IL-10
KC
MIP-1α
RANTES
TNF-α
SRM-1649
EHC-2000
DWR1
TiO2
CRI

Figure 1.17. Ranking comparison of *in vivo* beta potencies. Beta potency estimates for *in vivo* biochemical endpoints and BAL cell counts listed in Table A-7 and cytokines listed in Table A-8 were scaled to the maximal potency for each endpoint. Relative potencies for each particle are shown for all potency estimates within the two endpoint categories; A) *in vivo* cytotoxicity endpoints and B) *in vivo* cytokine/chemokine assays. Horizontal line indicates the average of the relative beta potency estimates for all endpoints per particle (method adapted from Seagrave *et al.*, 2002).

Table 1.3. Best subsets regression models for the prediction of *in vivo* BALB/*c* neutrophil counts from *in vitro* assays of the cytotoxicity and inflammation subsets (complete data set).

Variable	Coef.	Std. Error	t	P	VIF	Cp
***In vitro* cytotoxicity vs. *in vivo* neutrophil counts**						
Model # 1	R = 0.58					6.870
Constant	801866.433	210282.241	3.813	0.001	0.000	
A549 AB	-696750.172	233530.077	-2.984	0.008	1.000	
Model # 2	R = 0.68					4.178
Constant	588782.342	218079.738	2.700	0.015	0.000	
A549 AB	-1248289.209	339425.055	-3.678	0.002	2.510	
A549 BrDU	699082.041	333703.439	2.095	0.051	2.510	
Model # 3	R = 0.73					3.860
Constant	288558.298	287452.630	1.004	0.330	0.000	
A549 AB	-1087879.789	343223.615	-3.170	0.006	2.769	
A549 BrDU	792324.465	327027.691	2.423	0.028	2.601	
J774 LDH	52147.870	34100.201	1.529	0.146	1.586	
***In vitro* inflammation vs. *in vivo* neutrophil counts**						
Model # 1	R = 0.56					178.2
Constant	26347.757	60563.545	0.435	0.669	0.000	
A549 IL-6	92170.550	32086.026	2.873	0.010	1.000	
Model # 2	R = 0.71					127.269
Constant	-86481.230	69887.208	-1.237	0.233	0.000	
J774 IL-1β	95379.890	37671.350	2.532	0.021	1.018	
A549 IL-8	65137.093	22491.713	2.896	0.010	1.018	
***In vitro* cytotoxicity and inflammation (A549) vs. *in vivo* neutrophil counts**						
Model # 1	R = 0.56					6.751
Constant	801866.433	210282.241	3.813	0.001	0.000	
A549 AB	-696750.172	233530.077	-2.984	0.008	1.000	
Model # 2	R = 0.70					3.414
Constant	236354.884	98676.992	2.395	.028	0.000	
A549 WST-1	-271137.041	112583.255	-2.408	0.028	1.456	
A549 IL-8	109555.105	27254.468	4.020	<0.001	1.456	

Variable	Coef.	Std. Error	t	P	VIF	Cp
Model # 3	R = 0.74					3.574
Constant	547446.367	272355.503	2.010	0.062	0.000	
A549 AB	-578813.493	218731.906	-2.646	0.018	1.139	
A549 WST-1	-144681.250	95752.757	-1.511	0.150	1.109	
***In vitro* cytotoxicity and inflammation (J774A.1) vs. *in vivo* neutrophil counts**						
Model # 1	R = 0.55					99.051
Constant	810000.767	226569.184	3.575	0.002	0.000	
J774 AB	-666079.451	237657.803	-2.803	0.012	1.000	
Model # 2	R = 0.68					74.733
Constant	586115.830	227730.767	2.574	0.020	0.000	
J774 IL-1β	88915.462	39597.967	2.245	0.038	1.045	
J774 AB	-563382.078	219580.208	-2.566	0.020	1.045	
AhR assay (H1 L1) vs. *in vivo* neutrophil counts						
Model # 1	R = 0.48					2.000
Constant	131847.924	36490.342	3.613	0.002	0.000	
H1L1 AhR	6315.026	2714.618	2.326	0.032	1.000	
Best model selection						
Model # 1	R = 0.76					3.239
Constant	89368.407	120773.902	0.740	0.470	0.000	
A549 WST-1	-195586.360	112451.541	-1.739	0.101	1.670	
A549 IL-8	93550.515	26812.298	3.489	0.003	1.620	
J774 IL-1β	71681.425	38127.679	1.880	0.078	1.168	
Model # 2	R = 0.76					3.989
Constant	-573044.111	299964.802	-1.910	0.074	0.000	
J774 IL-1b	119255.131	38619.926	3.088	0.007	1.182	
A549 IL-8	86227.067	24879.310	3.466	0.003	1.376	
A549 BrDU	406637.042	244449.736	1.663	0.116	1.586	
Model # 3	R = 0.82					4.462
Constant	-800435.244	296388.799	-2.701	0.016	0.000	
A549 BrDU	589646.904	241109.989	2.446	0.027	1.843	
J774 LDH	59419.799	29274.038	2.030	0.061	1.524	
J774 IL-1β	114504.384	35406.132	3.234	0.006	1.187	
A549 IL-8	75124.213	23407.172	3.209	0.006	1.455	

Table 1.4. Best subsets regression models for the prediction of *in vivo* BALB/*c* neutrophil counts from *in vitro* assays of the cytotoxicity and inflammation subsets (data set without minerals).

Variable	Coef.	Std. Error	t	P	VIF	Cp
***In vitro* cytotoxicity (A549) vs. *in vivo* neutrophil counts**						
Model # 1	R = 0.80					21.215
Constant	940398.735	182690.015	5.148	<0.001	0.000	
A549 AB	-853871.261	202508.215	-4.216	0.002	1.000	
Model # 2	R = 0.88					12.602
Constant	748514.969	175451.430	4.266	0.002	0.000	
A549 AB	1261709.182	247804.227	-5.092	<0.001	2.117	
A549 ATP	582231.258	256943.291	2.266	0.050	2.117	
Model # 3	R = 0.96					2.501
Constant	954773.128	122309.359	7.806	<0.001	0.000	
A549 AB	1240676.986	155475.019	-7.980	<0.001	2.119	
A549 ATP	753176.310	167089.036	4.508	0.002	2.277	
A549 WST-1	-460432.839	119315.879	-3.859	0.005	1.192	
***In vitro* cytotoxicity (J774A.1) vs. *in vivo* neutrophil counts**						
Model # 1	R = 0.76					-0.0734
Constant	480049.047	86495.767	5.550	<0.001	0.000	
J774 BrDU	-356145.596	96862.705	-3.677	0.004	1.000	
Model # 2	R = 0.81					-0.0734
Constant	140284.457	245427.906	0.572	0.582	0.000	
J774 BrDU	-585091.852	180872.718	-3.235	0.010	3.890	
J774 WST-1	527960.819	359515.731	1.469	0.176	3.890	
AhR assay (H1 L1) vs. *in vivo* neutrophil counts						
Model # 1	R = 0.95					2.000
Constant	69413.755	28746.592	2.415	0.036	0.000	
H1L1 AhR	8789.902	1657.652	5.303	<0.001	1.000	
***In vitro* inflammation (A549) vs. *in vivo* neutrophil counts**						
Model # 1	R = 0.76					0.0973
Constant	-30909.562	62353.12	-0.49	0.631	0.000	
A549 IL-8	127694.286	34843.297	3.665	0.004	1.000	

Variable	Coef.	Std. Error	t	P	VIF	Cp
***In vitro* inflammation (J774A.1) vs. *in vivo* neutrophil counts**						
Model # 2	R = 0.68					23.951
Constant	564504.400	135588.677	4.163	0.002	0.000	
J774 IL-10	-447891.316	152918.918	-2.929	0.015	1.000	
Model # 2	R = 0.88					7.736
Constant	366694.368	109819.250	3.339	0.009	0.000	
J774 IL-10	-420122.514	105993.612	-3.964	0.003	1.006	
J774 RANTES	119837.992	34688.680	3.455	0.007	1.006	
Best model selection						
Model # 1	R = 0.93					5.018
Constant	-189729.113	179608.284	-1.056	0.322	0.000	
H1L1 AhR	8067.371	1301.906	6.197	<0.001	1.041	
A549 WST-1	-389749.482	138914.610	-2.806	0.021	1.041	
Model # 2	R = 0.96					2.653
Constant	320833.182	107656.955	2.980	0.018	0.000	
J774 RANTES	6328.509	24585.348	2.291	0.051	1.230	
H1L1 AhR	6968.411	1175.339	5.929	<0.001	1.249	
A549 WST-1	-368417.049	114869.205	-3.207	0.012	1.048	

10.3.11 Correlation of PM-Induced BAL Neutrophilia with Other Responses in Mice

To examine the relationship of BAL neutrophil counts with the *in vivo* endpoints measured in BALB/c mice exposed to particles EHC-2000, DWR1, SRM-1649, TiO_2 and Cristobalite for 24 hrs, Pearson Product Moment Correlations were conducted (Table 1.5). From the endpoints representing the cytotoxic response of the animals to particle exposure, LDH, total protein, macrophage, band cells and lymphocyte counts determined in BAL fluid were significantly correlated with BAL neutrophil counts. From the assays, BAL total protein showed the highest association with neutrophil counts (R=0.83). BAL macrophage counts were negatively correlated with neutrophil counts with ~80 % similarity in the overall response to particle instillations. An examination of the pairwise associations of BAL neutrophil counts with the endpoints

representing the inflammatory response of the animals to particles showed that all cytokines with the exception of IL-5 and IL-10 were significantly correlated with neutrophil counts. From these, pro-inflammatory mediators IL-1β and KC showed the strongest significant associations with BAL neutrophil counts, with an above 90 % degree of similarity. All endpoints of the inflammation subset were positively correlated with neutrophil counts.

To evaluate the degree of contribution of the biologic responses of the animals to mineral dusts to those of the urban particles, Pearson Product Moment Correlations were repeated with a dataset excluding the responses to TiO_2 and Cristobalite from all endpoints (Table 1.6). The analysis revealed that by excluding all of the measured animal responses to minerals, the relationship between neutrophil counts and the other endpoints representing the cytotoxic and inflammatory response to urban particles was strengthened. This was manifested by an overall increase in the number of statistically significant endpoints which were highly correlated ($R>0.75$) with neutrophil counts in BAL, from 8 to 10 variables, as well as in the improvement in the correlations for some of the endpoints. From the endpoints comprising the cytotoxicity subset, lymphocyte and macrophage counts in BAL, as well as total protein showed the highest correlations with neutrophil counts ($R>0.75$). All significant measures with the exception of macrophage counts were positively correlated with neutrophil counts. From the inflammation subset of measures, the cytokines IL-1α, IL-1β, IL-6, TNF-α and chemokines KC, MIP-1α and RANTES were highly correlated with neutrophil counts, with a correlation coefficient above 0.75. From all the assays, IL-1β, KC and MIP-1α showed above 90 % similarity to neutrophil counts. From all significant measures, only LDH showed a marked decrease in its strength of association with neutrophil counts, when mineral dust responses were excluded from the variables.

Table 1.5. Pearson Product Moment Correlation of BAL neutrophil counts with other *in vivo* measures of biological responses to a set of particles (EHC-2000, DWR1, SRM-1649, TiO_2, Cristobalite) in BALB/*c* mice.

Subset	Endpoint	24 hr TP	
		Correlation Coefficient[2]	P value
Cytotoxicity[1]	LDH	**0.756**	0.0001
	8-Isoprostane	0.321	0.168
	Total protein	**0.827**	0.000007
	Total cells	-0.021	0.928
	Macrophages	**-0.797**	0.00003
	Band Cells	**0.547**	0.012
	Lymphocytes	**0.668**	0.001
Inflammation[1]	IL-1α	**0.847**	0.000002
	IL-1β	**0.912**	0.00000002
	IL-5	0.416	0.068
	IL-6	**0.604**	0.0048
	IL-10	0.323	0.165
	KC	**0.902**	0.00000006
	MIP-1α	**0.845**	0.000003
	RANTES	**0.722**	0.0003
	TNF-α	**0.847**	0.000002

1Endpoints within the subsets were measured in BAL of BALB/*c* mice exposed to PM
2 Statistically significant Correlation Coefficients are shown in bold ($p<0.050$)

Table 1.6. Pearson Product Moment Correlation of BAL neutrophil counts with other *in vivo* measures of biological responses to a set of particles (EHC-2000, DWR1, SRM-1649) in the absence of responses to mineral dusts TiO_2 and Cristobalite in BALB/*c* mice.

Subset	Endpoint	24 hr TP	
		Correlation Coefficient[2]	P value
Cytotoxicity[1]	LDH	**0.616**	0.033
	8-Isoprostane	0.387	0.214
	Total protein	**0.824**	0.001
	Total cells	-0.486	0.109
	Macrophages	**-0.871**	0.0002
	Band Cells	0.560	0.058
	Lymphocytes	**0.815**	0.001
Inflammation[1]	IL-1α	**0.866**	0.0003
	IL-1β	**0.907**	0.00005
	IL-5	**0.638**	0.026
	IL-6	**0.789**	0.002
	IL-10	0.182	0.571
	KC	**0.922**	0.00002
	MIP-1α	**0.927**	0.00001
	RANTES	**0.848**	0005
	TNF-α	**0.829**	0.0008

1Endpoints within the subsets were measured in BAL of BALB/*c* mice exposed to PM
2 Statistically significant Correlation Coefficients are shown in bold ($p<0.050$)

DISCUSSION

In this study, cytotoxicity endpoint assays and inflammatory cytokine profiling were evaluated as screening tools for toxic potencies of ambient particulate matter and mineral dusts *in vitro* in human alveolar type II-like epithelial cell line (A549) and mouse macrophage cell line (J774A.1). The further goals were to determine which assays were useful in assessing the differences in the relative potencies of the particles in cells and in mice exposed to a subset of particles, and last, to determine if *in vitro* assays can usefully reflect the biological effects of particles in BALB/*c* mice *in vivo*. The results have shown that the assays are useful for discrimination between toxic potencies of particles, especially when the particles under study are of the same class. Observations from some cell viability assays, such as Alamar Blue and WST-1, however, need to be interpreted with caution, due to the yet undefined nature of their underlying assay mechanisms. Thus the use of multiple independent assays is recommended, combined with extensive validation of each assay system. Cytokines *in vitro* were also useful in discriminating between toxicities of particles, especially urban air particles. Cytokine profiles were clearly cell type-associated. In general, the *in vitro* and *in vivo* relative potency estimates were comparable, identifying SRM- and EHC-type particles as more potent then minerals and DWR1 particles, although the particle potency rankings between the assays varied considerably. Instillation of a subset of particles into the lungs of BALB/*c* mice resulted in elevated BAL neutrophil counts, accompanied by increased levels of BAL cytokines and by generally unremarkable changes in biochemical markers, a profile consistent with mild, acute pulmonary inflammation, 24 hrs after exposure. Combinations of 2 to 4 *in vitro* cytotoxicity and inflammation assays showed high predictive potential for particle induced effects *in vivo*, which were represented by elevated BAL neutrophil counts in mice exposed to particles. The predictive ability of the *in vitro* assays for *in vivo* particle-induced toxicity is improved when particles with more similar compositions are evaluated, likely reflecting a more unified set of mechanisms that govern their biological effects.

Results from Alamar Blue and WST-1 assays indicate that there were considerable differences in the cell metabolic activities between the two assays, when responses to the same particles were evaluated. While the Alamar Blue assay mostly revealed particle-associated reductions in metabolic activity in both cell types, the metabolic measurements obtained from the WST-1 assay were more variable and showed increases in response to a number of the particles. Particle controls (without

the presence of cells) did not show any evidence of interference of test materials with the two assays. Currently, the metabolic activities observed in the case of the reduction of the two dyes cannot be clearly defined. These may involve a number of enzymes, and may occur in different subcellular locations, on the plasma membrane, or extracellularly via a chemical reaction. The reduction of Alamar Blue (resazurin) to pink fluorescent resorufin was postulated to occur through mitochondrial enzyme activity (De Fries and Mitsuhashi, 1995). Further studies have provided evidence for efficient reductions of Alamar Blue by hepatic post-mitochondrial (cytosol and microsomes), as well as mitochondrial fractions isolated by differential centrifugation, suggesting the involvement of a variety of non-mitochondrial enzymes (Gonzales *et al.*, 2001). Furthermore, O'Brien and colleagues (2000) found no evidence of mitochondrial reduction of Alamar Blue, by confocal microscopy. In semen, the diaphorase complex of enzymes was identified, as the enzyme likely responsible for the reduction of resazurin (Zalata *et al.*, 1998). Diaphorases are a series of enzymes, which include dihydrolipoamine dehydrogenase, NAD(P)H:quinine oxidoreductase and flavin reductase, with a localization in the mitochondria and cytoplasm. Thus it is difficult to conclude whether the particle-associated reductions of Alamar Blue in both cell types represent inhibitions of specific enzymes, or reflect the overall metabolic state of the cells. In contrast, the WST-1 assay may measure phenomena that are distinct from those detected by the Alamar Blue assay. The WST-1 dye has a net negative charge therefore its uptake across the plasma membrane may be difficult. Thus, reduction of WST-1 tetrazolium salt to colored formazan was proposed to occur extracellularly, by trans-plasma membrane transport, via an intermediate electron carrier. NADH derived mainly from the mitochondrial TCA cycle was proposed to be the likely cellular reductant, acting through membrane ubiquinone redox cycling mechanism (Berridge *et al.*, 2005). Interestingly, WST-1 reduction is extensively inhibited (~80 %) by superoxide dismutase, suggesting that oxygen may be an additional electron acceptor involved in the reduction of WST-1 dye, via superoxide (Berridge *et al.*, 1996). This suggests that the dye could be utilized in measurements of cellular superoxide production. The presence of superoxide and its contribution to WST-1 reduction in the study was not assessed. In future studies, superoxide dismutase could be added to cells treated with particles prior to WST-1 assay measurements, to determine the extent of superoxide contribution to the detected cellular activity. ROS, such as superoxide can be generated upon interaction of particles with target cells, during particle-elicited inflammation, or by intrinsic generation from particles or their adsorbed

constituents (Schins and Knaapen, 2007). Interestingly, fine TiO_2, low solubility, low-inflammogenic material, produced the highest increase in metabolic activity in A549 cells, as detected by WST-1 assay. The reason for this is currently not known. The particle is intrinsically not potent in ROS production (Janssen *et al.*, 1994; Park *et al.*, 2007, Xia *et al.*, 2006), although ultrafine TiO_2 particles have been shown to induce toxic, inflammatory effects *in* vitro and *in vivo*, thought to relate to their large surface area (Singh *et al.*, 2007). It may be possible that the WST-1 assay measured some metabolic activity associated with the rapid uptake of the mineral aggregates by A549 cells. Rapid cellular uptake of fine and ultrafine TiO_2 has been observed by others (Singh *et al.*, 2007). As the results from the assays indicate, the exact mechanisms governing the cellular metabolism of these commercial cell viability dyes may significantly differ, and are yet to be elucidated. Thus the use of multiple cell viability/cytotoxicity endpoints is recommended, to get a more accurate representation of the overall biological impact of the particulate materials on specific target cells.

Loss of total protein was observed in cells. It was mostly associated with highest concentrations of several particles, potentially reflecting a degree of cytotoxicity due to the high-concentrations exposures to particles resulting in apoptosis and/or necrosis. It must be noted, however, that some loss of total protein was likely due to the rinsing of the monolayers after the endpoint assays were performed. Due to the loss of protein from the PBS wash, the results from the *in vitro* cytotoxicity assays were not corrected for the total protein, as the supernatant aliquots were collected for quantitation prior to the PBS wash. Although the changes in total protein could partially affect the biphasic responses, there is no straight forward, direct correlation between the cytotoxic assay responses to particle exposures and the observed changes in total protein (eg. Alamar Blue assay, J774A.1 exposure to TiO_2, Figures 1.4B, 1.6D).

J774A.1 cells showed higher sensitivity to particles in comparison to A549 cells, when cell proliferation was assessed by BrdU ELISA that measured the incorporation of the synthetic thymidine analog into DNA. The observation was in line with studies carried out with Mexico City PM_{10} particles in J774A.1 and A549 cells, which showed higher susceptibility in the J774A.1 cells by Crystal Violet assay, a nuclear stain utilized in determinations of cell proliferation and detection of viable cells in culture (Alfaro-Moreno *et al.*, 2002). PM_{10} urban particles and TiO_2 showed the highest effect on proliferation of J774A.1 cells, in comparison to DWR1 particles. Phagocytic cells

may be especially susceptible to particle-induced toxicity due to the increased intracellular particle load resulting from their active engulfment of particles. Although J774A.1 cells share a number of common functional, morphological and biochemical features with primary blood, or alveolar macrophages, more cautious interpretation of the *in vitro* results in the J774A.1 cell line with respect to the *in vivo* situation is required. While the J774A.1 cells are capable of DNA synthesis and proliferation, the primary macrophages are in contrast terminally differentiated.

The metabolic energy source ATP was used as an indicator of mitochondrial cellular stress response in epithelial cells and macrophages. The results indicate that urban particles SRM-1648 and SRM-1649 were most potent in ATP depletion from both cell lines, mainly at higher concentrations of the particles. The effect may be due to the presence of high iron content in the particles. A comparison of the elemental composition of the particles revealed that the SRM particles contain ~1.5-2.5 fold more iron then most of the EHC urban particles, on μg/g PM basis. Additionally, fine PM mixture DWR1 contained ~30-50 fold less iron on μg/g PM basis. DWR1 did not cause depletion of ATP levels in A549 and J774A.1 cells. Mitochondria are especially susceptible to oxidative stress, and iron content of particles has been linked to excessive hydroxyl radical generation through the Fenton reaction (Xia *et al.*, 2007). Wilson and colleagues (2002) showed that the addition of iron salts to J774A.1 cells incubated with ultrafine carbon black particles potentiated ATP depletion in the cells. Cristobalite-associated ATP depletion in cells was also observed in the current work. Oxidative stress generation by crystalline silica has been widely documented *in vivo* and *in vitro* (Fubini *et al.*, 2003, Balduzzi *et al.*, 2004). Interestingly, slightly increased cellular ATP content was observed in both cell lines exposed to EHC particles and DWR1. Cruz *et al.* (2007) have recently reported that addition of exogenous ATP to AM cultures induced the production of ROS. Free radicals in turn activated the phosphoinositide-3 kinase-signaling pathway, which resulted in augmented secretion of proinflammatory cytokines and upregulation of genes involved in glutathione synthesis. Thus, the release of extracellular ATP may be a novel mechanism for cellular adaptation to exposure to oxidants, or inflammation and secretion of cytokines. The differential response of cells to the various particles observed in the ATP assay may reflect both, adaptive and cytotoxic cellular mechanisms. Further investigation is required to determine the constituents and/or physical properties of the particles driving the different responses.

The LDH assay shows that PM_{10} urban particles induce cytotoxicity in A549 and J774A.1 cells, as evidenced by leakage of LDH from the cells. LDH leakage reflects compromised cellular plasma membrane integrity, with subsequent cell death by necrosis. SRM1648, SRM-1649 and EHC-93 induced highest levels of cytotoxicity in both cell lines, although the cytotoxic mechanisms are likely different. A549 cells showed concentration-dependent increases in cytotoxicity in comparison to J774A.1 cells, where the cytotoxicity was apparent only at high concentrations of the PM_{10} urban particles. The data suggest that A549 epithelial cells are more sensitive to particle exposures than J774A.1 macrophage cells, in terms of susceptibility to irreversible membrane damage. Further investigation is required to determine which particle properties may be responsible for the observed effects. Similarly, Li and colleagues (2002) have shown that BEAS-2B bronchial epithelial cells were more susceptible to apoptosis/necrosis then THP-1 macrophages upon exposures to organic DEP extracts. The observations correlated with a more substantial decline in cellular GSH/GSSG ratio in BEAS-2B cells, perturbation of mitochondrial permeability and a decrease in intracellular ATP. BEAS-2B cells also showed an inability to convert N-acetylcysteine to protective GSH. Cytotoxicity-associated bioenergetic depletion (ATP) and LDH release, with subsequent cell death by necrosis have been previously described in cell cultures treated with metals such as cadmium, iron or zinc, and have been attributed to metal-induced ROS generation (López *et al.*, 2003; Steinebach and Wolterbeek *et al.*, 1993; Robb *et al.*, 1999).

As previously stated, the physical and chemical properties of the air pollution particles are intimately connected, making their relative contributions to a specific adverse biological activity often difficult to evaluate. Also, such is the case in the evaluations of the particle properties with respect to their cytotoxic potential. Just as specific chemical constituents may be the likely candidates behind the observed biological effects, physical interactions of the particles with cells may also be involved. Besides the previously described potential of biological toxicity due to the presence of chemicals adsorbed to the particle's surface (see general introduction), the irregularity of the surface of insoluble particulates at the molecular level may modulate particle cytotoxicity via surface-associated ROS formation. Reductants produced by inflammatory cells may react at the surface of the particles to generate free radicals (Donaldson *et al.*, 1996). In addition, cytotoxic responses may simply result from the physical contact of cells with insoluble particles, in which case membrane damage would be the most direct result of such encounters, with a consequence

of cell death by necrosis and the release of cytoplasmic molecules into the extracellular medium (Fubini *et al.*, 1998).

The high toxic potential of aromatic chemical compounds in DEP, PM_{10}, or UFP has been noted in several studies (Arrieta *et al.*, 2003; Xia *et al.*, 2004). ROS production induced by organic chemical constituents in PM, such as quinones and PAHs has been postulated to play a central role in perturbations of cellular organelle functions essential for cell survival (eg. mitochondrial respiration), thus leading to disease and secondary consequences of PM-induced cellular damage (Xia *et al.*, 2007).

The AhR assay (measuring the CYP1A1 gene activity) was utilized to detect the presence of high-affinity AhR agonists, such as PAHs or PCBs in the PM preparations. The inducible CYP1A1 gene activity plays a direct role in toxicity (Nebert *et al.*, 2000) and has been shown to result in ROS-associated oxidative stress (Elbekai *et al.*, 2004). Based on the assay, SRM and EHC particles induced significant concentration-dependent activations of DNA binding *in vitro*, indicative of a presence of AhR agonists in the urban PM samples. The fine PM mixture DWR1 also exhibited agonist activity, although it was ~10 fold less in comparison to PM_{10} particles, suggesting that the particle has a smaller content of chemicals capable of acting as AhR ligands. Similarly, activities of SRM urban particles and EHC-93 consistent with the presence of PAHs were previously observed in our laboratory, in HepG2 cells harbouring stress genes, with a chloramphenicol acetyltransferase under transcriptional regulation of a number of mammalian promoters and response elements, including CYP1A1 promoter and xenobiotic response element among others (Vincent *et al.*, 1997b). Additionally, CYP1A1-related enzyme activity has been previously observed in organic extracts of PM_{10} from various sites in Mexico and has also been linked to the PAH content of the particles (Arrieta *et al.*, 2003). One limitation of the H1L1.1c2-based assay is that its luciferase signal is transient in nature and peaks at 4 hrs, after which it rapidly declines, owing to the presence of several residues in the luciferase gene, coding for a peroxisomal targeting sequence (Han *et al.*, 2002). Endogenous ligands capable of activating the AhR receptor have been previously described, with prostaglandins, among others, acting as weak agonists for the AhR (Seidel *et al.*, 2001). Because they are metabolically less stable, their potential production by the cells could somewhat overestimate the observed AhR activity of the preparations. Stimulation of prostaglandin E2 production by fibroblasts *in vitro*, exposed to PM_{10} (Alfaro-Moreno *et al.*, 2002),

as well as in AM exposed to silica and TiO_2 minerals have been previously demonstrated (Kuhn *et al.*, 1993). Minute induction of luciferase activity was also observed with the mineral particle suspensions. The mineral particles contain no PAHs, thus it may be possible that the signal is due to weak activation of the AhR signal transduction pathway by endogenous AhR ligands such as prostaglandins.

The sensitivity of cytokine expression in inflammatory responses of cells exposed to air pollution particles has made their analysis very useful for discrimination of toxicities of varieties of particles. In relation to insoluble particles, cytokine expression of immune phagocytes, especially macrophages has been the major focus of the studies. More recent studies have also implicated epithelial cells in airway host defense and have noted their ability to produce immunomodulatory mediators such as cytokines (Mills *et al.*, 1999). Cytokine profiling in A549 epithelial cells exposed to a variety of air pollution particles revealed high, particle concentration-dependent expressions of IL-6, IL-8 and MCP-1 cytokines/chemokines after 24 hrs exposure. Additionally, low expression of GM-CSF was also detected. The finding is in agreement with numerous studies that have demonstrated PM_{10}, or mineral particle-stimulated expressions of these cytokines in alveolar epithelial cells such as A549, or bronchial epithelial cells (Stringer *et al.*, 1996; Mills *et al.*, 1999; Fujii *et al.*, 2001; Hetland *et al.*, 2000). Our laboratory has also previously shown increased secretion of IL-8, alongside vascular endothelial growth factor (VEGF) in A549 cells exposed to EHC-93, its insoluble fraction or Cristobalite (Chauhan *et al.*, 2005). Although the cytokines were generated in high quantities, the A549 cellular responses did not enable clear discrimination between the various particle types, with PM_{10} and mineral particles mostly inducing comparable cytokine responses, with the exception of DWR1, which did not appear to stimulate appreciable cytokine secretion. These pro-inflammatory mediators play significant roles in the recruitment, activation, and/or promotion of survival of immune effector cell types including neutrophils, monocytes/macrophages and granulocytes among others (Mills *et al.*, 1999; van Eeden *et al.*, 2005). The epithelial cells may thus play an important role in initiating and potentiating pulmonary inflammatory defense by cytokine-mediated communication with immune effector cell types.

J774A.1 macrophages produced a variety of cytokines in response to particle challenge. The PM_{10} urban particles induced strong secretion of TNF-α and IL-6, and moderate secretion of RANTES. Additionally, the cells induced IL-1α, IL-1β and GM-CSF. The responses were particle

type and concentration-dependent, illustrating the great sensitivity of the J774A.1 cytokine analysis for discriminating between the various particle types (ie. PM_{10} vs $PM_{2.5}$ vs minerals), as well as between particles of the same class. Unexpectedly, concentration-dependent inhibition of IL-10 was observed in response to each particle. IL-10 is an anti-inflammatory cytokine, which inhibits cell mediated (Th1-type) immunity and promotes the development of Th2-type immune responses. The cytokine deactivates neutrophils and macrophages, and suppresses cytokines such as TNF-α, interferon-γ and a number of chemokines (Standiford *et al.*, 1999). To date not much is known about the role of IL-10 in the modulation of cellular responses to particles. Although, some evidence from studies with healthy human subjects and asthmatics exposed to DEP, and with mice challenged with silica supports the association of elevated IL-10 plasma levels with the asthma phenotype, as well as with elevations of profibrotic cytokines (Stenfors *et al.*, 2004; Barbarin *et al.*, 2005). The observation of IL-10 supression in J774A.1 cells exposed to particles may be indicative of a dysregulation of a feedback mechanism required to protect the cells from excessive production of proinflammatory cytokines, associated with cytotoxicity. Johannessen and colleagues (2005) showed strong suppression of IL-10 levels, accompanied by increased TNF-α in culture supernatants of human monocytic cell line Mono Mac 6 challenged with mold-derived mycotoxins. The presence of small amounts of mycotoxins in "real world" urban particles is a possibility, however, the observation of IL-10 supressions in response to mineral dusts do not support such a view.

Comparison of proinflammatory cytokine secretion in J774A.1 macrophages exposed to minerals and PM_{10} urban particles may suggest the involvement of biogenic materials in the cytokine responses. Endotoxin-associated induction of proinflammatory cytokines TNF-α, IL-1 and IL-6 can be inhibited by polymyxin B in AM exposed to urban particles (Dong *et al.*, 1996). Some studies, however, have shown only partial inhibition of cytokines such as TNF-α by polymyxin B in macrophages exposed to coarse and fine urban particles. The authors suggested that some endotoxin may be embedded in particles and thus not be inhibited by the antibiotic (Huang *et al.*, 2002). As to whether such fraction would be bioavailable for cellular recognition, remains to be determined. Thus other components may also be responsible for the proinflammatory cytokine production in macrophage cells exposed to particles. In support of this, all PM_{10} particles in the study contained comparable trace amount of endotoxin (~20 EU/mg PM), however, they showed

large differences in cytokine productions, including endotoxin-responsive TNF-α and IL-6. Furthermore, DWR1 contained ~12 EU/mg PM of endotoxin, however, it showed very poor ability to induce cytokines in J774A.1, which was more comparable with that of TiO_2 and Cristobalite, both of which contained no endotoxin. In addition, as showed by van Eeden and colleagues, the trace levels of endotoxin present in EHC-93 ambient particulate material were insufficient to induce mRNA expression of proinflammatory genes in human bronchial epithelial cells (HBEC) exposed to the particles (Fujii *et al.*, 2001), as well as instillation of a similar amount of endotoxin into the lungs of rabbits did not stimulate their bone marrow, a measure of systemic inflammatory response (Mukae *et al.*, 2000). Thus, although endotoxin plays a role in the induction of cytokines, it does not appear to be the major constituent responsible for the significant cytokine stimulations in J774A.1 cells exposed to PM_{10} in this study. As described previously, PM-associated production of ROS may play a significant role in the signaling pathways leading to the expression of proinflammatory cytokine genes via activation of redox-sensitive transcription factors such as NFκB (Baeza-Squiban *et al.*, 1999), or via Ca^{2+}-mediated mechanisms (Brown *et al.*, 2004). More work is needed to identify the particle constituents responsible for the PM_{10}-associated cytokine inductions.

Intratracheal instillations of particles in BALB/*c* mice were conducted to assess the *in vivo* effects of the particles. The study showed that, 24 hrs after exposure, all particles induced an acute influx of neutrophils into the lungs. Of all the cellular and biochemical parameters tested, neutrophil counts in the BAL appeared to be the most sensitive endpoint. The response was accompanied by a decrease in the number of AM in the BAL, consistent with the AM-associated clearance of the particles from the lungs. The observations were in agreement with other studies, showing that the neutrophil counts in BAL were the most sensitive endpoint detected upon instillation of a variety of particles including urban particles (Dick *et al.*, 2003), or minerals (Yuen *et al.*, 1996). The remaining endpoints were less sensitive, including slight elevations in LDH and dose-dependent changes in total protein and 8-isoprostane concentrations, and lymphocyte and band cell counts in BAL. Similar findings were also reported by others (Dick *et al.*, 2003; Happo *et al.*, 2007). The overall pattern was consistent with a generally low, acute inflammatory response associated with particle exposure.

Overall, urban particles and the minerals elicited higher responses in the mice then DWR1 $PM_{2.5}$ particles. This suggests that the particles may have acted through distinct *in vivo* mechanisms, likely associated with the differences in their chemical composition and/or physical properties. The assessment of cytokine/chemokine levels in BAL upon particle instillations revealed a particle-type associated heterogeneity in the various cytokine responses. MIP-1α showed the highest sensitivity from all of the cytokines/chemokines measured. MIP-1α is an LPS-inducible macrophage chemoattractant, also involved in wound repair (DiPietro *et al.*, 1998). Evidence for high expression of MIP-1α induced from particulate matter comes from intratracheal instillation studies with rats exposed to silica and TiO_2 (Driscoll *et al.*, 1993), or allergic mice with atopic dermatitis exposed to DEP (Inoue *et al.*, 2006). The highest levels of MIP-1α were observed in BAL of mice exposed to the SRM-1649 and EHC-2000 particles and mineral Cristobalite. Although MIP-1α is LPS-inducible, the high level of secretion of the chemokine in animals exposed to Cristobalite suggests that endotoxin, metals, or organic chemicals present in the particles are not the sole determinants of inflammatory responses in these animals. Additionally, significant inductions of TNF-α, KC, IL-1α and IL-1β, with similar pattern of particle potency were observed. IL-6 and RANTES were also elevated in BAL in response to particle exposures, with only the highest dose (250 μg) of the SRM-1649 and EHC-2000 urban particles inducing highest secretion. Exposure of mice to particles did not alter IL-10 levels in the BAL of the animals. Additionally, dose-dependent increase in Th2-type cytokine IL-5 was also detected in BAL of mice exposed to particles, although the responses were highly variable and not particle-type dependent. Increases in BAL cytokines TNF-α, IL-6 and KC have been recently documented in C57Bl/6J mice exposed by intratracheal instillation to size-fractionated urban particles collected from a number of European cities, as measured at various time points. The authors observed highest levels of the three cytokines in BAL upon exposures to fine and coarse particle fractions, after 4 hrs. Significant differences were also found for several particles at 12 and 24 hrs, although the magnitude of the cytokine levels was significantly lower compared to 4 hrs after exposure (Happo *et al.*, 2007).

Examination of the *in vitro* cytotoxicity and inflammation ranking of the particles showed that the responsiveness of endpoint assays is particle type- and cell type-dependent. Overall, the urban particles were more potent than the minerals and DWR1, although A549 epithelial cells appeared

more sensitive to mineral exposures (especially TiO_2), than J774A.1 macrophage cells. One may speculate that macrophages may be less sensitive to cytotoxic damage from "more inert", insoluble particles such as TiO_2, due to their roles as professional phagocytes. This appears to be supported by observations from assays such as LDH or ATP, which indicate that the epithelial cells may be more sensitive to necrosis-type damage. Thus in light of the observations, the biological "inertness" of fine TiO_2 particles needs to be further examined. Although fine TiO_2 is frequently utilized in the air pollution studies as a generally innocuous control particle, some studies have linked the mineral with genotoxicity and tumor formation in animal models, most frequently in rats. The mechanisms behind the carcinogenicity of poorly soluble particles with low toxicity are currently unknown, however, studies point to the involvement of persistent lung inflammation and compromised antioxidant responses, in relation to the surface area metric (Borm *et al.*, 2004).

Difficulties with potency estimations arise when the assay responses to particles are bi-phasic, as is the case for WST-1 assay. Therefore, the negative potencies would also need to be considered as high potency, i.e. some particles induce, while others inhibit the same specific cellular response. Better mathematical modeling for bi-phasic responses needs to be developed. The assays also provide good discrimination between particles of the same class, i.e. various PM_{10} particles. The need to consider the duality of the biological effects of urban particles is apparent by comparing the overall responses of the cytotoxic and inflammatory subsets of assays. The cytotoxicity and inflammation endpoints appear to show considerable differences in the average potency rankings of the urban particles. EHC-98 and EHC-2000 appear to be more potent in inducing an inflammatory response, and less potent in causing overall cytotoxicity in both cell lines, while the overall cytotoxic and inflammatory responses of the SRM-type particles are more comparable. Furthermore, EHC-93 particles are stronger inducers of cytotoxicity, especially in J774A.1 cells, and weaker inducers of overall cytokine inflammatory response. Comparison of the AhR assay response with the beta potency estimates for the PM_{10} urban particles suggests that there may be a potential relation between PAH content and inflammatory responses, as determined by cytokine profiling, and that this relation is stronger than that between PAHs and cytotoxicity endpoints *in vitro*. Thus the analysis of the associations of cytotoxic and inflammatory responses with physicochemical characteristics of the particles using multifactorial statistical approaches such as principal component analysis, or multiple linear regressions may provide useful insights into the relative contributions of the particle characteristics to specific biological response. DWR1 particles

appear to exert least cytotoxic and inflammatory effects *in* vitro, in comparison to the other particles. DWR1 represents a $PM_{2.5}$ mixture with equal mass of randomly chosen particles from the winter collection in Toronto. Chemical content of DWR1 is dominated by chloride (10 fold higher in comparison to PM_{10} particles), potassium, and sulfate, and has several fold lower content of elements such as copper, iron, nickel, vanadium and zinc, widely associated with urban pollution, in comparison to PM_{10} particles. Thus fine particle mixture DWR1 may not be a good surrogate for urban $PM_{2.5}$, which may reflect its relatively low potency in most of the cytotoxic endpoint assays and cytokine assays. Indeed, the particles were collected in Downsview, a suburban area of Toronto. As the data illustrate, the scaled comparison of particle potencies may also be very useful in evaluations of similarities/differences in relative potencies of particles in different types of cells, such as cells derived from different tissues, or cell lines in comparison to primary cells.

Determination of general toxicity *in vivo* was made by evaluating the summated indices within the cytotoxicity and inflammation subsets of assays. The potency estimates of the individual assays, within the cytotoxicity, or inflammation subsets were generally in good agreement. SRM-1649 particles were more cytotoxic, and less inflammogenic, in comparison to EHC-2000, which showed the reverse. This was in good agreement with the *in vitro* cytotoxicity and inflammation ranking in J774A.1 macrophages, but not so much A549 epithelial cells. The negative beta potency observed with band cell counts in BAL of mice exposed to TiO_2 and DWR1 was reflected by the band cell numbers below those in the control animals, however, as the ANOVA statistical analysis of the band cell counts only showed a significant dose main effect, the band cell potency estimates should not be considered as significantly different from those of the other particles. Additionally, lowest beta potency of DWR1 particles was observed in a number of *in vivo* and *in vitro* assays, with the exception of the cytokine assays in J774A.1 cells, which showed that DWR1 was slightly more potent than the Cristobalite and TiO_2 minerals in inducing cytokine increases in the macrophages, specifically IL-6, RANTES, and TNF-α, which overall were the highest responding cytokines in J774A.1 cells.

Validation of the panel of *in vitro* assays in the BALB/*c* mouse model was performed using a best subset regression, to identify a combination of *in vitro* cytotoxicity and inflammation (cytokines) endpoints which best describe/predict the responses of the critical *in vivo* endpoint, neutrophil

counts in BAL of the mice exposed to particles by intratracheal instillation. The analysis showed that models with 3 to 4 variables showed a very good ability to predict the BAL neutrophil count *in vivo*. From these, the 4 variable model comprised of linear combinations of BrdU and IL-8 measures in A549 epithelial cells, and LDH and IL-1β measures in J774A.1 macrophages proved effective in predicting BAL neutrophil counts in BALB/*c* mice, with an R value of 0.82. Comparison of the scaled beta potency estimates revealed that, in general, the mineral responses showed greatest variability in beta potency estimates of endpoints between the two cell types in both cytotoxicity and inflammation subsets. Based on this observation, and the fact that the minerals were most different in their physicochemical characteristics from the rest of the particles (PM_{10}, $PM_{2.5}$), best subset regressions were repeated without the mineral responses present in the data set. The best predictive models for *in vivo* BALB/*c* BAL neutrophil counts now contained 2 to 3 variables, which represented endpoints that were different from those obtained in the regression analysis of the complete data set, and which showed a significantly improved R value of 0.96. The new analysis showed that the linear combinations of measures of AhR assay in H1L1.1c2 cells, WST-1 assay in A549 cells and RANTES chemokine levels in J774A.1 cell culture supernatants were highly predictive of *in vivo* neutrophil counts in BALB/*c* BAL. Therefore, the use of mineral particles as "positive" and "negative" controls in studies evaluating the toxic potencies of urban particles may not be appropriate, in light of their significantly distinct physicochemical properties from those of atmospheric particles, as they may hinder the predictive ability of a model whose purpose is to provide a screening tool for urban air particles.

Bivariate linear correlations of the various inflammatory, biochemical, and cell differential endpoints with neutrophil counts in BAL revealed that a number of the measurements were significantly correlated with neutrophils in BAL when dose response values from the whole set of particles were considered. These included LDH, total protein, macrophages, band cells and lymphocytes. Additionally, IL-1α, IL-1β, IL-6, KC, MIP-1α, RANTES and TNF-α were also significantly correlated with lung lavage neutrophils. The comparison of the scaled *in vivo* beta potency estimates showed that the mineral particle responses were somewhat more variable than those of the urban particles, when band cell responses were excluded, although to a somewhat lesser degree than was observed for the *in vitro* assays. Therefore, the correlation analysis was repeated without the mineral particle data to determine its impact on the associations between the

lavage neutrophils and the other *in vivo* endpoints. After excluding the mineral responses from the lung data set, associations of BAL neutrophils with macrophages, lymphocytes, IL-1α, IL-5, IL-6, KC, MIP-1α and RANTES have improved, while those with LDH, total protein and IL-1β have somewhat decreased, with the exception of LDH relationship with neutrophils, which showed a more marked decrease in the correlation coefficient. The results indicate that a number of the *in vivo* biological responses to urban particles show improved correlation with lung lavage neutrophil counts when responses to particles of a different class are excluded. This suggests that *in vivo* toxicity screening of particles with comparable physicochemical characteristics may be more appropriate, as the mechanisms driving the biological effects of different classes of particles may be distinct and of low relevance to one another.

Chapter 2

BIOLOGICAL EFFECTS OF PARTICULATE MATTER: *IN VITRO* HUMAN CO-CULTURE MODEL

11.1.1 Airway Cell Interactions & Lung Defense

In vitro studies are an important tool for elucidating the mechanisms by which air pollutants damage cells. The major limitation of *in vitro* studies is that cells are removed from their complex *in vivo* environment in which they interact with neighbouring cells, as well as receive and send factors by blood and lymph supply. Nevertheless, many basic cellular processes and pathways underlying the cell's responses to toxic materials are activated in a comparable manner *in vitro* and *in vivo*. Thus, cellular co-culture models have been used to more realistically simulate the complexity of the *in vivo* micro-environments by enabling interactions between cell types native to specific organ systems.

In the lungs, the inhaled materials deposited in the pulmonary micro-environment are displaced through surface forces of the surfactant at the air liquid interface into close proximity to airway epithelial cells and cells associated with lung defense, such as AM and dendritic cells (Gehr *et al.*, 2006). Most of the deposited materials are removed via the mucociliary epithelium of the conducting airways and by the phagocytosis of the materials by AM, and to a smaller extent by airway epithelial cells (Baeza-Squiban *et al.*, 1999). Both AM and epithelial cells interact and participate in the inflammatory response to the inhaled materials by producing mediators such as cytokines/chemokines, which can mobilize and activate leukocytes from the circulation and enable their adhesion, and degranulation in the inflamed site (Takizawa *et al.*, 1998). Evidence for the importance of the cell-cell interactions in the context of pulmonary inflammation comes from a study by Stříž and coworkers (2001), who showed that the co-culture of THP-1 macrophages or primary peripheral blood monocytes with A549 epithelial cells resulted in epithelial cell-mediated stimulus for expression of adhesion factor CD54 (ICAM-1), and the MHC class II cell surface receptor on monocytes and THP-1 macrophages, as well as CD14 (co-receptor involved in the recognition of LPS) and CD11b (integrin involved in cell adhesion) on THP-1 cells, as detected by immunocytochemistry and flow cytometry.

Other studies have demonstrated the importance of epithelial cells in the process. HTB54 lung epithelial cells pre-treated with TNF-α and subsequently exposed to Boston $PM_{2.5}$ particles

showed elevated production of IL-8 in response to the particles. The IL-8 production by epithelial cells was augmented in a co-culture with neutrophils. The response was markedly decreased upon treatment of the particles with antioxidant and a metal chelator, showing the role of oxidative stress induced by transition metals present in the particles. The study showed that cytokine priming and interactions with neutrophils can augment lung epithelial cell inflammatory responses to air pollution particles (Ning *et al.*, 2004). Similarly, Tao and Kobzik (2002) provided evidence of interaction between normal rat AM and RLE-6TN rat alveolar type II epithelial cells. An increase in TNF-α and MIP-2 was observed when the co-culture, but not macrophage mono-culture was exposed to various concentrations of TiO_2, silica, residual oil fly ash or urban air particles for 24 hrs. Epithelial cells did not produce these cytokines. No enhancement in cytokine levels was seen when macrophages were incubated with rat fetal fibroblasts prior to particle exposure, thus the interaction was epithelial cell-macrophage specific. The co-culture also synergistically increased basal levels of the cytokines in comparison to macrophage mono-culture.

11.1.2 Cellular Crosstalk & Cytokines

The importance of cytokines in the cell-cell interactions in relation to exposures to air pollution particles was demonstrated in our laboratory. Conditioned media from AM that were harvested from rats, and incubated for 24 hrs on transwell inserts in the presence of a variety of particle preparations (PM_{10}, $PM_{2.5}$, minerals) induced stronger responses in HepG2 reporter CAT-gene cell lines in comparison to media incubated with the particles alone. The gene responses that were assessed included xenobiotic-, metal-, stress-, and cytokine-responsive promoters in control of the transcription of CAT gene. The data suggested that the macrophages played a role of a modifier of particle potency towards other target cells via production of cellular mediators, whereby the extent of the response was particle-composition dependent (Goegan *et al.*, 1998).

In addition, Jiménez *et al.* (2002) showed that A549 cells treated with conditioned medium from primary human monocyte-derived macrophages exposed to PM_{10} particles showed enhanced NFκB and AP-1 activity, as well as increased IL-8 mRNA expression and protein levels. The effect was partially mediated by TNF-α present in the conditioned medium, as pre-incubation of the media with anti-TNF-α antibody significantly reduced the production of IL-8 by A549 cells. The lack of complete inhibition, however, suggested that other mediators produced by the PM_{10}-

exposed macrophages were present in the conditioned medium, which enhanced the IL-8 production by A549 cells. The conditioned medium also enhanced neutrophil chemotactic activity. As shown by a Fujii and colleagues (2002), the soluble mediators produced by PM_{10}-induced interaction of AM with airway epithelial cells can stimulate the bone marrow of rabbits to mobilize and recruit circulating inflammatory cells, when conditioned media from AM/HBEC co-cultures, containing the mediators are intravenously introduced into the animals. No effect was observed when supernatants from HBEC mono-cultures were used, demonstrating a potential for mediators produced via localized pulmonary inflammation induced by PM_{10} to initiate a systemic inflammatory response.

The complexity of the cellular interactions is further illustrated by a finding that conditioned medium containing cell-derived membrane fragments shed by eukaryotic cells upon activation or during apoptosis, in this case by monocyte/macrophages, can up-regulate IL-8, MCP-1 and ICAM-1 mRNA expression and protein production by alveolar epithelial cells (A549) and IL-8 production by bronchial epithelial cells (BEAS-2B). Ultrafiltration and ultracentrifugation of the material abolished the effect, showing that the cell fragments, rather than the soluble material were responsible for it, thus suggesting a potential role for cell-derived membrane fragments in modulating the innate immunity of the airway epithelium in health and disease (Cerri *et al.*, 2006).

11.1.3 Endothelial Cells

The stimulatory effects caused by urban air particles are not restricted to the interaction of the airway epithelium with AM, but are likely to subsequently affect underlying tissues of the lungs such as the endothelium, via the soluble mediators generated by the initial encounter of the lung tissues with the inhaled material. Thus in the context of the pulmonary vascular endothelium forming a regulated interface between the lung airspace and systemic circulation, and based on its central role in numerous pathologies associated with endothelial dysfunction, its potential involvement in the PM-induced inflammation and toxicity needs to be explored. As the distance between the pneumocytes lining the alveolar lumen and the basement membrane of the endothelial cells of the underlying capillaries is small, this thin gas-exchange fluid region, where the AM are also present, is the site for communication between the cell types (Cormack and Ham, 1987).

A co-culture model of BEAS-2B human bronchial epithelial cells grown on a transwell support (apical compartment) and ECV304 human umbilical vein endothelial cells cultured on the bottom (basolateral compartment) of the well was used to study the damaging effects of ozone on airway tissue by exposing BEAS-2B cells to ozone. The study showed augmented production of IL-6 and IL-8 cytokines from co-cultures exposed to air or ozone above those observed with mono-cultures, as well as increased expression of ICAM-1 in the endothelial cells grown in the co-culture, but not ECV304 monoculture, providing evidence for communication between epithelial and endothelial cells in co-culture (Mögel *et al.*, 1998).

11.1.4 Cell Interaction Models for PM Effects

As has been made apparent by an increasing body of evidence, lung inflammatory responses associated with the inhaled air pollution particles may not only present a potential for development or exacerbation of pulmonary disorders such as asthma, or chronic obstructive pulmonary disease, but are also demonstrating a potential to induce a systemic response characterized by the stimulation of the hematopoietic system, which could influence pre-existing conditions, such as triggering of cardiovascular events in subjects with heart conditions (van Eeden *et al.*, 2005). As evidenced by the described studies, *in vitro* co-culture systems are proving to be a useful tool in studying the biological effects of urban air particles. Additionally, the added level of biological complexity inherent to the co-culture models versus their mono-culture counterparts may make them a more appropriate tool for screening of urban air particles, aimed at associating the physicochemical properties of the PM with their toxic potency ranking, in effect providing a higher degree of physiological relevance.

11.1.5 THP-1, A549 & HPAE cells

THP-1 cells are a monocytic cell line derived from the peripheral blood of a 1 year-old male with acute monocytic leukaemia. THP-1 cells produce lysozyme and have IgG Fc receptors on their cell surface, among other distinct monocytic markers (Tsuchiya *et al.*, 1980). The cells can differentiate into macrophage-like cells upon induction with phorbol 12-myristate 13-acetate (PMA) and are capable of phagocytosis of latex beads or sheep erythrocytes (Tsuchiya *et al.*, 1982). Although not of pulmonary origin, their ability to differentiate into macrophages with phagocytic activity and

their human origin has established their use in research on the biological effects of urban air pollutants such as carbon black, diesel, or PM_{10} (Don Porto Carero *et al.*, 2001; Sevastyanova *et al.*, 2007). Primed THP-1 cells also produce reactive oxygen- and nitrogen- species in response to a challenge such as silica, endotoxin, or atherogenic chylomicron remnants (Chen *et al.*, 1996; Bentley *et al.*, 2007). THP-1 cells have also been used to examine the cytotoxic effects of silica and hematite (Fe_2O_3) particles on mono- and co-cultures of THP-1 cells with A549 alveolar epithelial cells, as determined by measurements of plasma membrane integrity (LDH) and cytokine production (IL-6, IL-8) (Wottrich *et al.*, 2004). Finally, the expression pattern of THP-1 cells co-cultured with airway epithelial cells is comparable to that of activated human AM (Stříž *et al.*, 1993).

Primary cultures of normal human pulmonary artery endothelial (HPAE) cells were isolated from the lumen of the pulmonary artery of a 33 years old male. The cells have the potential to reach 29 population doublings before the onset of senescence (ATCC, 2007). The human alveolar type II epithelial cell line (A549) has been previously described in detail (see section 10.1.2).

Overall, the described body of evidence demonstrates that interactions between different cell types in their local pulmonary environment may play a potentially important role in modulating one another's phenotype and functions in steady state, as well as during pulmonary inflammation (Stříž *et al.*, 2001). In addition, the unique profile of mediators produced via these interactions would be able to influence other cell types of the lung, including pulmonary endothelial cells, or smooth muscle cells. Thus, a *in vitro* co-culture system may be well suited to more realistically mimic "*in situ*-like" conditions by enabling the aspect of intercellular communication between the different cell types, as well as enable a versatile system for ranking particle toxic potencies with an added degree of physiological relevance. These features can make the co-culture model superior to widely utilized mono-culture approaches for the study of biological effects of particulate matter.

11.2.1 Materials and Reagents

Alamar Blue (AB) reagent was obtained from Biosource International (Camarillo, CA). Bio-Plex cytokine reagent kits and human and mouse specific Bio-Plex X-Plex cytokine assays were from Bio-Rad (Mississauga, ON). 2-Mercaptoethanol, 4-(2-hydroxyethyl)-1-piperazineethanesulfonic acid (HEPES), bovine serum albumin (BSA), dimethylsulfoxide (DMSO), endothelial cell growth supplement (ECGS), fetal bovine serum (FBS), gelatin from porcine skin, gentamicin, glucose, heparin, L-glutamine, pen/strep, phorbol 12-myristate 13-acetate (PMA), sodium bicarbonate, trypsin-EDTA, Triton X-100 were from Sigma-Aldrich (Oakville, ON). Endothelin-1 (ET-1) and big ET-1 EIA assays were from Assay Designs (Ann Arbor, MI). Human vascular endothelial growth factor (VEGF) Beadmates™ and Beadlyte® Human Multi-Cytokine Beadmaster™ kits were purchased from Upstate-Millipore (Bedford, MA). Human Cardiovascular Disease (CVD) Panel 1 LINCO*plex* kit containing beads for soluble E-selectin, Intercellular Adhesion Molecule (ICAM)-1, and Vascular Cell Adhesion Molecule (VCAM)-1 analytes were purchased from Linco-Millipore (Bedford, MA). The culture media Roswell Park Memorial Institute (RPMI)-1640 and Ham's F12 Nutrient Mixture with Kaighn's Modification (F12K) were obtained from Invitrogen-Gibco (Burlington, ON). Coomassie Plus reagent was from Pierce (Rockford, IL). Isoton 2 diluent was purchased from Beckman Coulter (Mississauga, ON). Limulus Amebocyte Lysate (LAL) QCL-1000 test was from Lonza (Walkersville, MD). T-25 and T-75 culture flasks, 24-well and 96-well plates were from Costar (Cambridge, MA). All water used was deionized/demineralized (>16 MOhms resistivity (Millipore, Billerica, MA). Sodium chloride and sodium pyruvate were purchased from BDH Inc. (Toronto, ON). Tween-80 was obtained form Nuclear-Chicago (Chicago, IL). THP-1 and A549 cell lines and HPAE-26 cells were obtained from ATCC (Manassas, VA).

11.2.2 Particulate Materials & Endotoxin Analysis

The particulate preparations SRM1650b (diesel particulate matter), SRM-1879 (Cristobalite, SiO_2) and SRM-154b (titanium dioxide; TiO_2) were obtained from the National Institute of Standards and Technology (Gaithersberg, MD). The urban dust preparation EHC-93 was collected in

Ottawa, ON, Canada (Vincent *et al.*, 1997a). EHC-6802 is a new reference mixture comprised of an equal mass of EHC-96, EHC-98, EHC-2000 and EHC-2002 particles. DWR1 $PM_{2.5}$ reference particles from the Trans-Canada collection were also utilized in this study. The preparation of the particulate material stocks for *in vitro* studies has been described previously (see section 10.2.2).

All controls described previously (see section 10.2.2) were also included in the co-culture study experiments. In this study, the HPAE-26 cells were exposed to the No-Cell (NC) control media generated from the mono-culture exposures, along with the mono-culture conditioned media (CM) from PM-exposed mono-cultures. The purpose of the NC controls in this study was to detect the contribution of potential particle "carry-over" from mono-cultures and co-cultures to the measurements of the biological and biochemical endpoints in HPAE cells, thus allowing differentiation between CM-induced effects and potential confounding direct particle carry-over effects.

Stock samples of all particulate matter used in the experiments were analyzed for the presence of bacterial endotoxin using the chromogenic LAL test, as described previously (see section 10.2.2).

11.2.3 A549 and THP-1 Mono-cultures

A549 and THP-1 Mono-cultures

A549 cells were originally maintained in M199 medium supplemented with 2 mM L-glutamine and 10 % FBS. For the experiments, cells were first pre-adapted with a 50:50 (v/v) mixture of M199:RPMI-1640 complete media for one week, and subsequently cultured in complete RPMI-1640 medium. The cells were maintained in T-75 culture flasks in a humidified incubator at 37°C, 5 % CO_2, 100 % humidity for 2-3 days. They were passaged bi-weekly, using trypsin-EDTA. For the experiments, the A549 cells were seeded in 24-well plates at 20,000 cells/cm^2 and cultured until confluence in 1 ml of RPMI-1640 medium supplemented with 2 mM L-glutamine and 10 % FBS, in one ml media per well, for 48 hrs, before their exposure to particles. THP-1 monocytes were cultured in RPMI-1640 medium supplemented with 2 mM L-glutamine and 10 % FBS. The cells were maintained in suspension, at a concentration not exceeding 1 x 10^6 cells per ml, and passaged bi-weekly by centrifugation. For the experiments, the THP-1 cells were seeded at 200,000 cells/cm^2 and cultured in one ml RPMI-1640 medium containing 2 mM L-glutamine, 10 % FBS

and 10 ng/ml PMA. PMA was used to induce monocytic differentiation into macrophages, and facilitate macrophage attachment to the surface of the wells. The cells were cultured for 24 hrs before their exposure to particles.

A549 and THP-1 Co-culture

For the co-culture experiments, THP-1 cells were first seeded in 24-well plates at 100,000 cells/cm^2, in one ml of complete RPMI-1640 medium and cultured for 24 hrs in the presence of 10 ng/ml PMA in the media. After one day, the spent media were aspirated and one ml of A549 cell suspension of 80,000 cells/ml (40,000 cells/cm^2) in complete RPMI-1640 media (without PMA) was added on top of the differentiated THP-1 macrophage monolayer in each well. The cells were incubated for additional 24 hrs, before their exposure to particles.

11.2.4 Exposure of Cells to Particles

Thawed 10 mg/ml stocks of DWR1, EHC-93, EHC-6802, SRM-1650, Cristobalite and TiO_2 particles were prepared as described previously (see section 10.2.2). The spent media were aspirated and 0, 10, 30 and 100 μg/cm^2 (2 cm^2 well) of particles in one ml of complete RPMI-1640 media also containing antibiotics, as previously described were added to the cells. The cells were then incubated for 24 hrs. Media-only controls and NC controls were included in the exposures, as previously described (see section 10.2.2). Three independent experiments were conducted, with duplicate plates per experiment. For each experiment, the culture supernatants from the two samples for each treatment were combined (n=3) and centrifuged at 12,000 rpm for 5 minutes, at 8°C, to remove cell debris and leftover particles. After the cell exposures, the cell viability and protein assays were conducted and the collected purified supernatants were aliquoted and kept at -40°C for further analyses and as CM for HPAE cell exposures.

11.2.5 Culture of HPAE Cells

HPAE cells were initially cultured in F12K medium containing 2 mM L-glutamine, 0.1 mg/ml heparin, 0.03 mg/ml ECGS and 10 % FBS in a T-25 flask. After reaching confluence, the cells were sub-cultured into T-75 flasks and adapted to RPMI-1640 medium by first growing them in complete 50:50 (v/v) F12K:RPMI-1640 medium mixture for one week, followed by subsequent

cultures in complete RPMI-1640 medium containing described supplements. The cells were sub-cultured bi-weekly, by passaging with trypsin-EDTA. For experiments, the cells were seeded at 80,000 cells/ml (40,000 cells/cm^2) in 24-well plates in complete RPMI-1640 medium. The cells were grown to ~90 % confluence (24 hrs) before their exposure to CM. All cell culture dishes were pre-coated with 0.1 % sterile porcine gelatine in ddH_2O, to facilitate cell attachment. The HPAE cells were generally viable for 15 population doublings after thawing, before the onset of senescence. Only viable cells were used in the experiments.

11.2.6 Exposure of HPAE Cells to Conditioned Media

Frozen supernatants from A549 cells, THP-1 cells, or A549/THP-1 Co-cultures exposed to particles were thawed for 20 minutes in a 37 °C water-bath. 700 µl of CM were mixed with 300 µl of fresh complete RPMI-1640 medium (70:30 ratio), for a total of one ml added per well, after the spent medium was aspirated. The medium also contained antibiotics (100 U/ml penicillin-G, 100 mg/ml streptomycin and 0.1 mg/ml gentamicin) along with the described supplements. The cells were exposed to all CM from particle-exposed cells, as well as media-only controls and NC controls. The cells were incubated for 24 hrs with the CM in a humidified incubator. At the end of the incubation, cell viability and protein assays were conducted and the cell culture supernatants were collected, aliquoted and kept at -40°C for further analyses.

The CM from A549 and THP-1 mono-cultures and co-culture contained a variety of biomolecular products of these cells. To determine the production of the analyte of interest by HPAE cells upon their exposure to the CM, 70 % of the amount of that analyte present in the CM prior to the incubation was subtracted from the overall amount of the analyte measured in the HPAE cell culture supernatants at the end of the incubations. Loss of the specific analyte due to its half-life or degradation rate was assumed negligible, as the CM were frozen immediately upon collection and used immediately after thawing. All samples were utilized simultaneously and thawed once only.

See Figure 2.1 for a schematic description of the *in vitro* co-culture model.

All cell types utilized in the study presented in this chapter were of human origin, as the purpose of the *in vitro* approach was to utilize a human co-culture model for cell interaction to improve the level of human relevance of the study.

11.2.7 Co-culture Model Validation

Cell plating densities used in the co-culture model experiments were chosen after validation of growth properties of all the cell types used in the study. Each of the cell types was cultured at a number of cell densities before the optimal number of cells was established for each cell type for both, mono-cultures and co-culture.

11.2.8 Intratracheal Instillation of Particles

The animal treatment protocol was reviewed and approved by the Animal Care Committee of Health Canada. The animals were maintained, as previously described (see section 10.2.5).

The particle preparations were thawed and allowed to reach room temperature prior to a 10-minute sonication. The doses of 0, 50 and 250 μg of SRM-1650, EHC-6802 and DWR1 in 50 μl of 0.9 % saline with 0.005 % Tween-80 were instilled intratracheally into anaesthetized BALB/*c* mice (male, ~25 g) in supine position on an angled stand using a MicroSprayer aerosolizer. Naïve, sham and vehicle-exposed control animals were included in the study. After 2 and 24 hrs, the mice were euthanized with isoflurane and lungs were lavaged with 0.9 % saline solution. Harvesting and processing of all of the samples was done as previously described (see section 10.2.5). Six to eight animals were exposed to each particle, at each dose (n= ~7). The *in vivo* experimental approach and procedures were similar to those used in the first study (Figure 1.3B), with difference including additional endpoints in BAL and blood plasma, additional controls, two time points and exposures to different set of particles.

11.2.9 Cell Differential Analysis in BAL

The cell differential analysis of the BAL fluid from the treated animals was conducted, as previously described (see section 10.2.6). The number of each cell type recovered by lavage was then determined from a pair of cytospin preparations for each animal and calculated relative to the total amount of cells.

11.2.10 Viability & Total Protein

Cell viability of *in* vitro cultures was evaluated using the Alamar Blue (AB) assay, as described previously (see section 10.2.7). The protein assay of cell cultures and BAL samples from *in vivo* exposures were also performed as previously described (see section 10.2.7). AB and protein assays

(cell cultures) were representative of three independent experiments with one measurement per treatment (n=3). Protein assay (BAL samples) was representative of 6 to 8 animals per treatment (n=~7).

11.2.11 Cytokine and Chemokine Analysis

Cell culture supernatants from A549 and THP-1 mono-culture and co-culture exposures to particles, as well as cell culture supernatants from HPAE-26 cell exposures to CM from these mono- and co-cultures were analyzed for the presence of IL-1β, IL-5, IL-6, IL-8, IL-10, GM-CSF, MCP-1 and TNF-α. Inflammatory mediators IL-1α, IL-1β, IL-5, IL-6, IL-10, GM-CSF, KC, MIP-1α, RANTES and TNF-α were quantified in BAL fluid and blood plasma of treated BALB/*c* mice. The analysis was conducted as previously described (see section 10.2.8). Cell culture supernatants and BAL fluid samples were analyzed directly, while plasma samples were diluted 1:4 in Bio-Plex sample diluent prior to analysis. The value of each analyte in medium without cells was subtracted from values obtained from the media of controls and particle-treated cells, as a background. The cytokines/chemokines in cell culture supernatants were analyzed in three samples per treatment, each from independent experiments (n=3). BAL cytokine/chemokine analysis was performed in samples from all animals (n=~7). Plasma cytokines/chemokines were analyzed in a subset of animals only (n=3), due to limiting plasma volumes. All data were expressed in pg per ml of culture supernatants, or BAL.

11.2.12 Adhesion Factors

Cell culture supernatants from particle-exposed A549 and THP-1 mono-cultures and co-cultures and cell culture supernatants from HPAE-26 cell exposed to CM, as well as BAL samples from BALB/*c* mice dosed with particles were assayed for the presence of soluble ICAM-1, VCAM-1 and E-selectin adhesion factors using a LINCO*plex* CVD1 kit and the Bio-Plex array reader. The

protocol was performed as recommended by the manufacturer and was similar to the previously outlined procedure used in the analysis of cytokines/chemokines (see section 10.2.8), with the exception of an overnight incubation of samples with antigen-coated beads, in contrast to 30-minute incubation for cytokines/chemokines. The plate was incubated in the dark, with agitation on IKA KS 130 Basic plate shaker (Clarkson-IKA, Chula Vista, CA) at 4°C. The adhesion factors in cell culture supernatants were analyzed in three samples per treatment, each from independent experiments (n=3). BAL adhesion factor analysis was performed in samples from all animals (n=~7). All data were expressed in pg per ml of culture supernatants, or BAL.

11.2.13 Vascular Endothelial Growth Factor

Vascular Endothelial Growth Factor (VEGF) levels in cell culture supernatants form particle-exposed A549 and THP-1 mono-cultures and co-cultures and supernatants from HPAE-26 cell exposed to CM were quantified using the VEGF Beadmates™ and Beadlyte® Human Multi-Cytokine Beadmaster™ kits and the Bio-Plex array reader. Manufacturer's recommended protocol was used for the analysis, similar to the previously described analysis of cytokines/chemokines (see section 10.2.8). VEGF in cell culture supernatants were analyzed in three samples per treatment, each from independent experiments (n=3). Data were expressed in pg/ml.

11.2.14 Endothelin EIA

Release of Endothelin (ET)-1 and big ET-1 from particle-treated A549, THP-1 cells, A549/THP-1 co-cultures and HPAE endothelial cells exposed to CM was measured in cell culture supernatants by ELISA. The protocol was similar for both analytes, with the exception of some assay conditions. For the ET-1 assay, the samples were incubated with the polyclonal antibody to ET-1 for 1 hr and all incubations with antibodies were done at 37°C, while for the big ET-1 assay, the samples were incubated overnight with the polyclonal antibody to big ET-1, with all incubations performed at 4°C. Briefly, 100 μl of samples and endothelin standards in culture media were added to 96-well microtiter plate pre-coated with primary antibody. The plate contents were mixed by tapping, and the appropriate incubation followed. After extensive washing with a wash buffer, 100 μl of a horse-radish peroxidase (HRP)-conjugated rabbit polyclonal antibody directed against ET-1 or big ET-1 was added (1:30 dilution), followed by a 30 minute incubation

at the appropriate temperature, in the dark. After extensive washing with the wash buffer, 100 μl of TMB substrate and hydrogen peroxide was added to each well. Following a 30-minute incubation at room temperature in the dark, 100 μl stop solution (1N sulphuric acid in water) was added to each well. The color developed by the enzyme reaction was measured at 450 nm in a SpectraMax Plus plate reader. The concentrations of ET-1 and big ET-1 were calculated from a standard curve prepared from recombinant ET-1 and big ET-1 standards (Assay Designs). Three samples per treatment, each from independent experiments were analyzed (n=3). Data were expressed in pg/ml.

11.2.15 Statistical Analyses

All data are expressed as mean ± standard error of the mean (SEM). The effects of the particle concentration and dose responses of the cells subjected to particles or CM and animals exposed to particles as measured by the various assays were tested for statistical significance by 2-way Analysis Of Variance (ANOVA). The factors of the ANOVA for *in vitro* co-culture study experiments included PARTICLE (DWR1, EHC-93, EHC-6802, SRM-1650, Cristobalite, TiO_2) and CONCENTRATION (0, 10, 30, 100 $\mu g/cm^2$/ml media). The ANOVA factors for *in vivo* experiment samples were PARTICLE (SRM-1650, EHC-6802, DWR1) and DOSE (0, 50, 250 μg). ANOVA analysis was performed as previously described (see section 10.2.10) ANOVA results are summarized in Tables A-9 to A-14. Statistical comparisons between vehicle, naïve and sham controls from the *in vivo* experiment were done by a 1-way ANOVA analysis, with Holm-Sidak multiple comparisons test, or Kruskal-Wallis 1-way ANOVA on Ranks, with Dunn's test for multiple pair-wise comparisons. $P < 0.05$ was considered to be statistically significant (Table A-15).

Bivariate Statistics

Pearson Product Moment Correlations were performed as previously described. The analysis was used to assess the correlation between the critical endpoint BAL neutrophil counts at 2 and 24 hr time points and *in vitro* assay responses to particles (64 *in vitro* assay measures) and the other *in vivo* endpoints analyzed in the BALB/*c* mice intra-tracheally exposed to particles (26 *in vivo* measures per time point). For the analysis, the *in vitro* endpoint assays were represented by combined set of response to particles matching the *in vivo* set of particles. Specifically, EHC-6802, SRM-1650 and

DWR1 at nil, low and high particle concentration (0, 30 and 100 $\mu g/cm^2/ml$ media) were chosen to match the nil, low and high *in vivo* particle doses (0, 50 and 250 $\mu g/50\ \mu l$ of saline). The *in vitro* data were grouped into three predictor subsets CYTOTOXICITY (Alamar Blue assay, AhR assay), ENDOTHELIAL ACTIVATION (VEGF, Endothelins, Adhesion Factors) and INFLAMMATION (cytokines/chemokines) (Table 2.1). The *in vivo* variable subsets were CYTOTOXICITY (*in vivo* biochemical endpoints and cell differential counts), ENDOTHELIAL ACTIVATION (adhesion factors in BAL) PULMONARY INFLAMMATION (all cytokine/chemokine measured in BAL) and SYSTEMIC INFLAMMATION (all cytokines/chemokines measured in blood plasma) (Table 2.2).

Table 2.1. Subsets for multivariate analysis of *in vitro* predictors of BAL neutrophil response to particles

Cytotoxicity *in vitro*		Inflammation *in vitro*		Endothelial Activation *in vitro*	
Alamar Blue	(A,T,C,H_A,H_T,H_C)	IL-1β	(T,C,H_C)	VEGF	(A,T,C)
AhR Assay	(H)	IL-6	(A,T,C,H_A,H_T,H_C)	big ET-1	(A,T,C,H_A,H_T,H_C)
		IL-8	(A,T,C,H_A,H_T,H_C)	ET-1	(A,T,C,H_A,H_T,H_C)
		IL-10	(T,C,H_C)	ICAM-1	(T,C,H_A,H_T,H_C)
		GM-CSF	(T,C,H_T,H_C)	VCAM-1	(T,H_A,H_T,H_C)
		MCP-1	(A,T,C,H_A,H_T,H_C)	E-Selectin	(H_T,H_C)
		TNF-α	(T,C,H_T,H_C)		

direct PM exposure: A - A549; T - THP-1; H - H1L1, C - A549/THP-1 Co-culture
conditioned media exposure: H_A - HPAE (A549), H_T - HPAE (THP-1), H_C – HPAE Co-culture

Table 2.2. Subsets for bivariate analysis of the association of BAL neutrophil response (2 and 24 hour timepoints) with other *in vivo* measures of biological effects of particles

Cytotoxicity *in vivo**	Endothelial Activation *in vivo**	Pulmonary Inflammation *in vivo**	Systemic Inflammation *in vivo***
LDH	ICAM-1	IL-1α	IL-1α
Total Protein	VCAM-1	IL-5	IL-1β
Total Cells		IL-6	IL-5
Macrophages		IL-10	IL-6
Band Cells		GM-CSF	IL-10
Lymphocytes		KC	GM-CSF
		MIP-1α	KC
		TNF-α	MIP-1α
			RANTES
			TNF-α

*BAL, ** Blood plasma

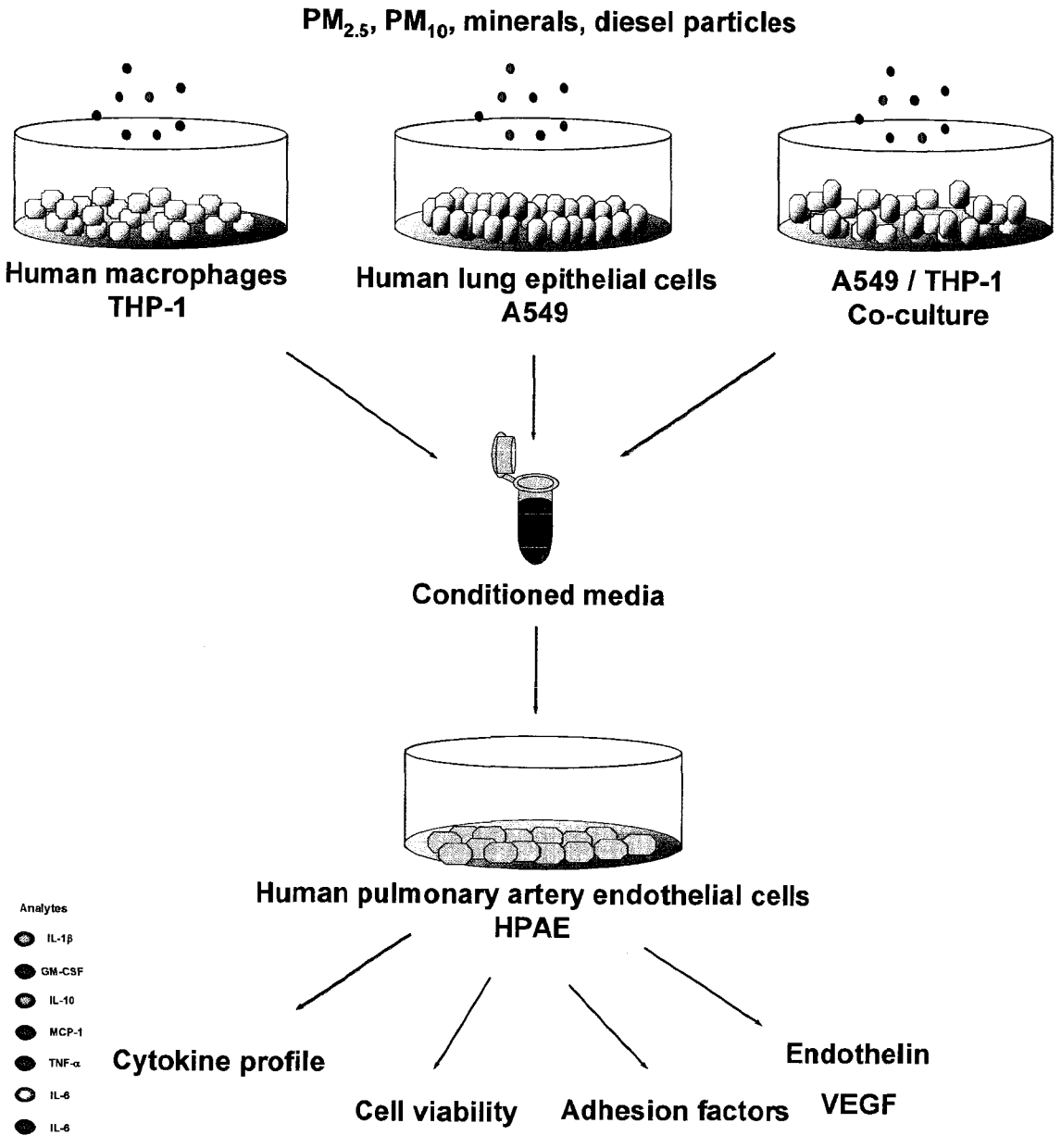
PM2.5, PM10, minerals, diesel particles
Human macrophages
THP-1
Human lung epithelial cells
A549
A549 / THP-1
Co-culture
Conditioned media
Human pulmonary artery endothelial cells
HPAE
Analytes
IL-1β
GM-CSF
IL-10
MCP-1
TNF-α
IL-6
IL-6
Cytokine profile
Cell viability
Adhesion factors
Endothelin
VEGF

Figure 2.1. Schematic representation of the *in vitro* cell interaction model. After a 24 h exposure of A549 and THP-1 cell mono- and co-cultures to particulate matter <10 μm, <2.5 μm in aerodynamic diameter (PM_{10}, $PM_{2.5}$), minerals and diesel particles, conditioned media were collected, centrifuged, and added to HPAE for 24 hrs.

RESULTS

11.3.1 Co-culture Model

In this work, the effects of urban particle preparations (EHC-93, EHC-6802), mineral standards (Cristobalite and TiO_2), diesel particles (SRM-1650) and fine particulate matter (DWR1) were studied *in vitro* in a human co-culture model. Human alveolar epithelial cells (A549) and human macrophages (THP-1) were cultured together, as well as separately. The mono-cultures and co-cultures of the cells were directly exposed to particle preparations in media for 24 hrs, before the profiles of the desired endpoints were determined in the cell lysates and cell culture supernatants. In the next step of the model, human pulmonary artery endothelial cells (HPAE) were incubated for 24 hrs with the mono-culture- and co-culture CM obtained from these cell exposures, before cell lysates and cell supernatants were analyzed for the presence of the endpoints of interest. This approach enabled the assessment of the indirect effects of the particle preparations on the endothelium through the various mediators present in the CM from mono-cultures and co-cultures of cells directly exposed to particles. The levels of the analytes released into the medium by HPAE cells were determined as the difference of the specific analytes measured in the HPAE cell supernatants minus the potential contribution from A549 or THP-1 mono-culture production remaining within the CM, and were presented as such.

A panel of endpoints was examined in the model. The endpoints were categorized into three subsets based on the general biological roles of the chosen analytes, or their involvement in specific processes. The CYTOTOXICITY subset included the Alamar Blue as a measure of overall cell metabolic activity and the AhR assay as a measure of specific pollutant-induced gene activation, as well as the assessment of total protein content (Figures 2.2 - 2.6). ENDOTHELIAL ACTIVATION subset comprised of a number of mediators of the vascular endothelium including big ET-1, ET-1, VEGF, ICAM-1, VCAM-1 and E-selectin (Figures 2.7 – 2.18). The INFLAMMATION subset consisted of cytokines and chemokines IL-1β, IL-5, IL-6, IL-8, IL-10, GM-CSF, MCP-1 and TNF-α (Figures 2.19 - 2.32). The statistical significance of the measured responses was summarized in Tables A-9 to A-11.

11.3.2 Cytotoxicity *In Vitro*

Metabolic activity of A549 cells was slightly lower upon their exposure to particles for 24 hrs (Figure 2.2A). The differences in metabolic activity between particles were not significant, however, overall 10 $\mu g/cm^2$ and 100 $\mu g/cm^2$ amount of the particles significantly affected the A549 cell viability in comparison to control cells. In THP-1 cells, significant differences were observed in the effects of particles on their metabolic activity, with Cristobalite causing a decrease in cell viability in comparison to EHC-93, EHC-6802, SRM-1650 and DWR1 particles (Figure 2.2C). The effects were particle concentration-independent. All particles with the exception of diesel particles SRM-1650 significantly affected cell viability of the A549/THP-1 co-cultures, with small bi-phasic effects on cell metabolic activity manifested as increases at low- and medium-, and decreases at high concentration of the particles in comparison to control. (Figure 2.3A). Exposure of HPAE cells to A549 or THP-1 CM resulted in slight decrease in HPAE metabolic activity without significant differences between particles (Figures 2.2B, 2.2D). The decreases were overall significant at the medium and high concentration particle exposures. Overall decrease of HPAE metabolic activity was observed when cells were incubated with co-culture CM for 24 hrs (Figure 2.3B). The effect was particle type-independent and appeared only at low and medium concentration of the particles.

Slight decrease in total protein amount was observed in A549 cells exposed to EHC-93 and Cristobalite particle preparations (Figure 2.4A). In THP-1 cells, some variability in total protein amount was observed, with increased total protein when cells were exposed to medium or high concentrations of diesel, EHC-6802 and DWR1. High concentration of Cristobalite significantly reduced total protein in THP-1 cells (Figure 2.4C). No significant changes in total protein were observed in co-cultures exposed to particles and in HPAE cells incubated with A549- or THP-1 CM (Figures 2.4B, 2.4D, 2.5A). An overall particle concentration-induced decrease in total cell protein of HPAE cells incubated with co-culture CM was observed (Figure 2.5B).

A comparison of the particle potency estimates in the ligand-activated AhR signaling assay revealed significant differences in responses of urban particles, fine particle DWR1, the mineral dusts and diesel particles (Figure 2.6). Diesel particles caused the highest inductions of the AhR

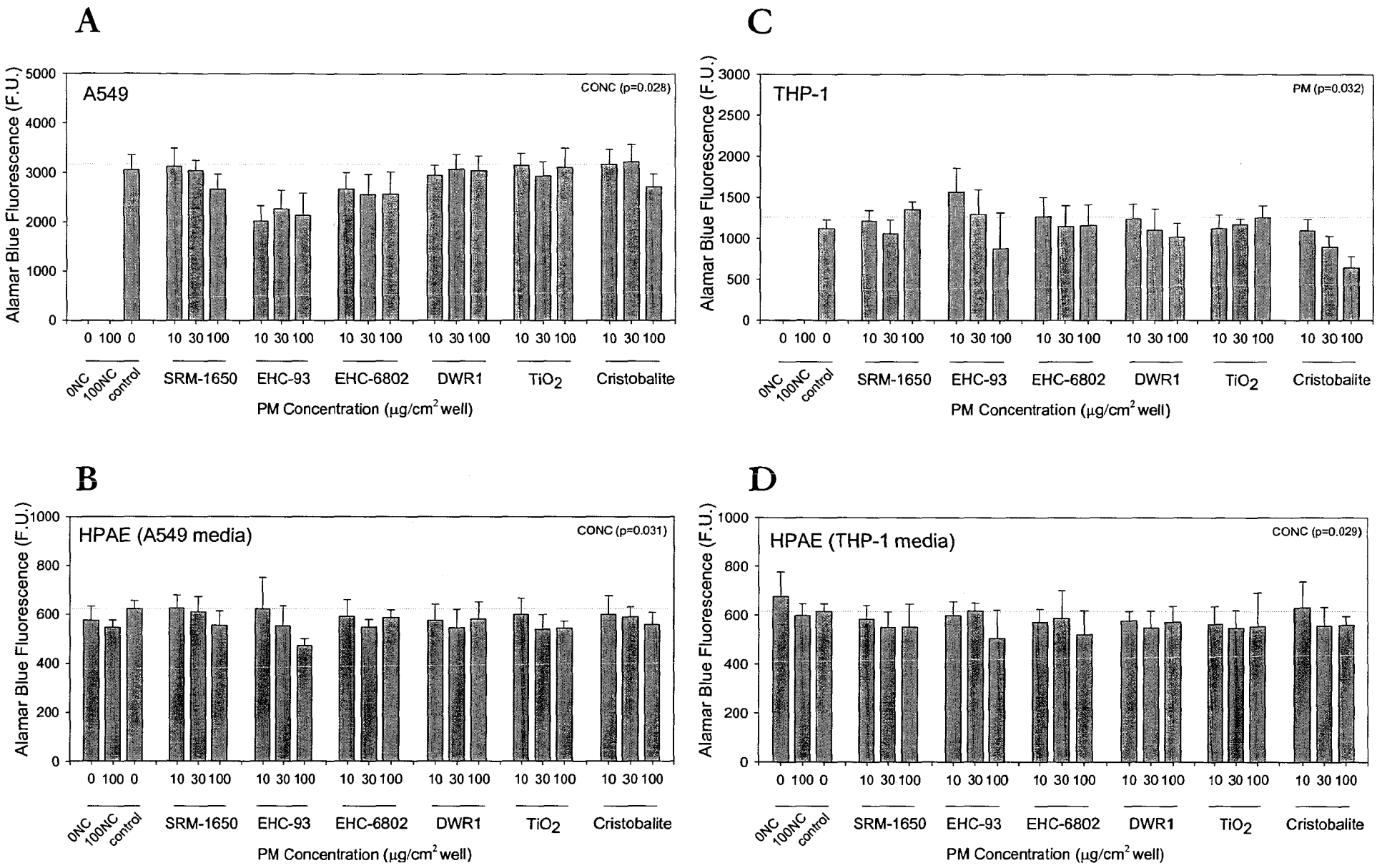
A
A549
CONC (p=0.028)
Alamar Blue Fluorescence (F.U.)
0 1000 2000 3000 4000 5000
0 100 0 10 30 100 10 30 100 10 30 100 10 30 100 10 30 100 10 30 100
0NC 100NC control
SRM-1650
EHC-93
EHC-6802
DWR1
TiO2
Cristobalite
PM Concentration (μg/cm2 well)
C
THP-1
PM (p=0.032)
Alamar Blue Fluorescence (F.U.)
0 500 1000 1500 2000 2500 3000
0 100 0 10 30 100 10 30 100 10 30 100 10 30 100 10 30 100 10 30 100
0NC 100NC control
SRM-1650
EHC-93
EHC-6802
DWR1
TiO2
Cristobalite
PM Concentration (μg/cm2 well)
B
HPAE (A549 media)
CONC (p=0.031)
Alamar Blue Fluorescence (F.U.)
0 200 400 600 800 1000
0 100 0 10 30 100 10 30 100 10 30 100 10 30 100 10 30 100 10 30 100
0NC 100NC control
SRM-1650
EHC-93
EHC-6802
DWR1
TiO2
Cristobalite
PM Concentration (μg/cm2 well)
D
HPAE (THP-1 media)
CONC (p=0.029)
Alamar Blue Fluorescence (F.U.)
0 200 400 600 800 1000
0 100 0 10 30 100 10 30 100 10 30 100 10 30 100 10 30 100 10 30 100
0NC 100NC control
SRM-1650
EHC-93
EHC-6802
DWR1
TiO2
Cristobalite
PM Concentration (μg/cm2 well)

Figure 2.2. Cellular metabolic activity of A549 epithelial cells (A), THP-1 macrophages (C) exposed for 24 hrs to particle preparations and HPAE endothelial cells incubated with A549- or THP-1-conditioned media (B, D). Rate of reduction of Alamar Blue reagent was measured fluorometrically. Values are presented as mean ± standard error (n=3). Main effects were obtained for cell viability data from A549 cells, THP-1 cells and HPAE cells incubated with A549- or THP-1-conditioned media, as determined by 2-way ANOVA.

A

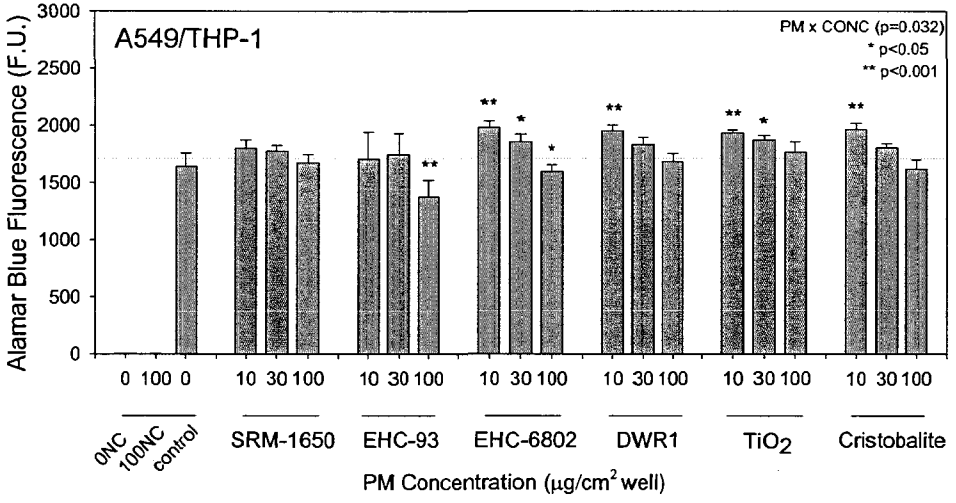
A549/THP-1
PM x CONC (p=0.032)
* p<0.05
** p<0.001
Alamar Blue Fluorescence (F.U.)
3000
2500
2000
1500
1000
500
0
0 100 0
10 30 100
10 30 100
10 30 100
10 30 100
10 30 100
10 30 100
10 30 100
0NC
100NC
control
SRM-1650
EHC-93
EHC-6802
DWR1
TiO2
Cristobalite
PM Concentration (μg/cm2 well)

B

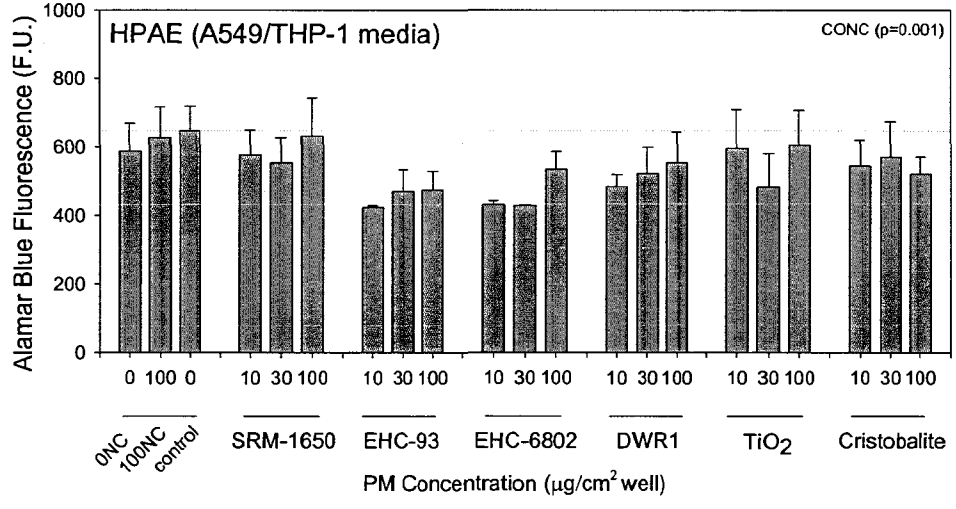
HPAE (A549/THP-1 media)
CONC (p=0.001)
Alamar Blue Fluorescence (F.U.)
1000
800
600
400
200
0
0 100 0
10 30 100
10 30 100
10 30 100
10 30 100
10 30 100
10 30 100
10 30 100
0NC
100NC
control
SRM-1650
EHC-93
EHC-6802
DWR1
TiO2
Cristobalite
PM Concentration (μg/cm2 well)

Figure 2.3. Cellular metabolic activity of A549/THP-1 co-cultures exposed for 24 hrs to particle preparations (A), as well as HPAE endothelial cells incubated with co-culture-conditioned media (B). Rate of reduction of Alamar Blue reagent was measured fluorometrically. Values are presented as mean ± standard error (n=3). PM x CONC interaction was observed for cell viability of co-cultures. Asterisks above bars represent effects significantly different from control where PM x CONC interaction was observed. Main effects were obtained for cell viability of HPAE cells incubated with co-culture-conditioned media, as determined by 2-way ANOVA.

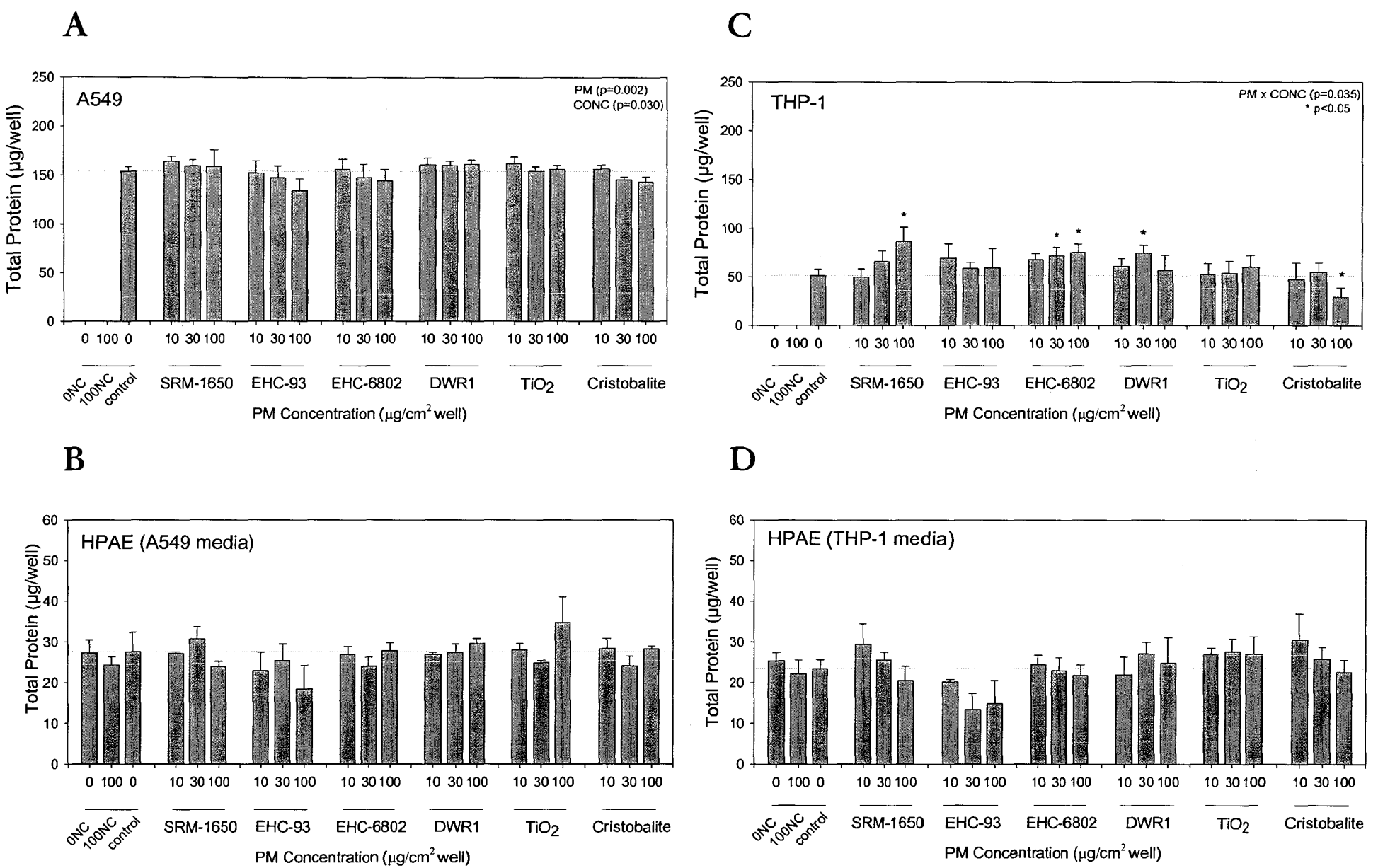
A
A549
PM (p=0.002)
CONC (p=0.030)
Total Protein (µg/well)
0 50 100 150 200 250
0 100 0
10 30 100
0NC
100NC
control
SRM-1650
EHC-93
EHC-6802
DWR1
TiO2
Cristobalite
PM Concentration (µg/cm2 well)
C
THP-1
PM x CONC (p=0.035)
* p<0.05
B
HPAE (A549 media)
0 10 20 30 40 50 60
D
HPAE (THP-1 media)

Figure 2.4. Total protein amount in A549 epithelial cells (A), THP-1 macrophages (C) exposed for 24 hrs to particle preparations and HPAE endothelial cells incubated with A549- or THP-1-conditioned media (B, D). Total protein content of PBS-rinsed monolayers was determined colorimetrically from cell lysates, by Coomassie assay. Values are presented as mean ± standard error (n=3). Main effects were observed for total protein amount in A549 cells exposed to particles. PM x CONC interaction was obtained for the total protein data from THP-1 cells. Asterisks above bars represent effects significantly different from control where PM x CONC interaction was observed. Total protein amounts in HPAE cells incubated with A549- or THP-1-conditioned media were not statistically different as shown by 2-way ANOVA.

A

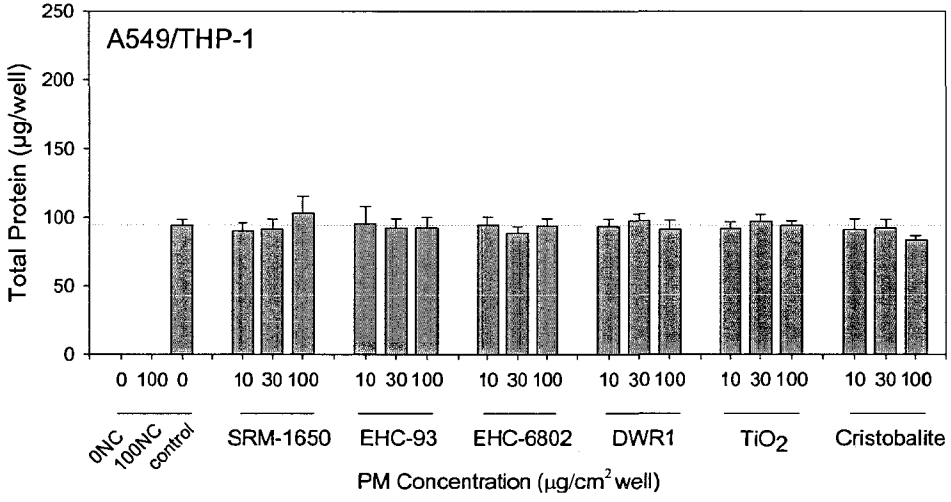
A549/THP-1
Total Protein (µg/well)
250
200
150
100
50
0
0 100 0
10 30 100
10 30 100
10 30 100
10 30 100
10 30 100
10 30 100
0NC
100NC
control
SRM-1650
EHC-93
EHC-6802
DWR1
TiO2
Cristobalite
PM Concentration (µg/cm2 well)

B

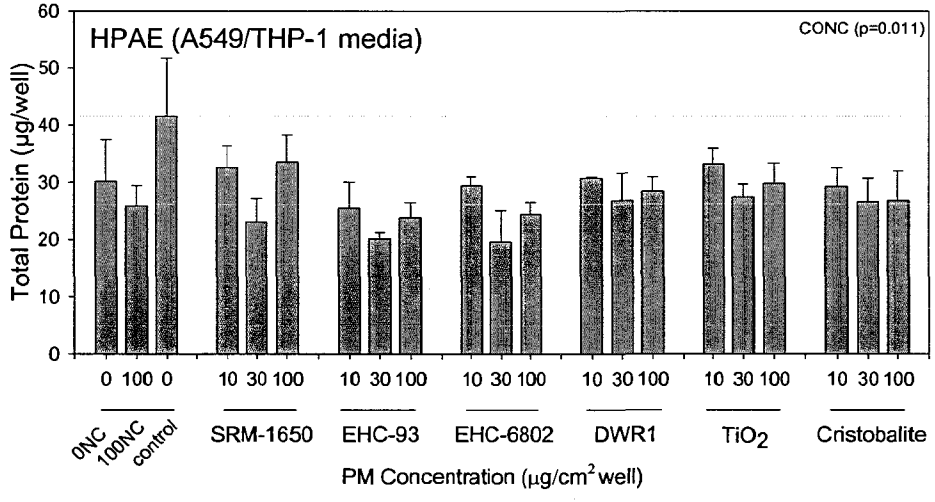
HPAE (A549/THP-1 media)
CONC (p=0.011)
Total Protein (µg/well)
60
50
40
30
20
10
0
0 100 0
10 30 100
10 30 100
10 30 100
10 30 100
10 30 100
10 30 100
0NC
100NC
control
SRM-1650
EHC-93
EHC-6802
DWR1
TiO2
Cristobalite
PM Concentration (µg/cm2 well)

Figure 2.5. Total protein amount in A549/THP-1 co-cultures exposed for 24 hrs to particle preparations (A) and HPAE endothelial cells incubated with co-culture-conditioned media (B). Total protein content of PBS-rinsed monolayers was determined colorimetrically from cell lysates by Coomassie Assay. Values are presented as mean ± standard error (n=3). Differences in total protein amount in co-cultures exposed to particles were not statistically significant. CONC main effect was observed for total protein amount in HPAE cells incubated with co-culture-conditioned media, as found by 2-way ANOVA.

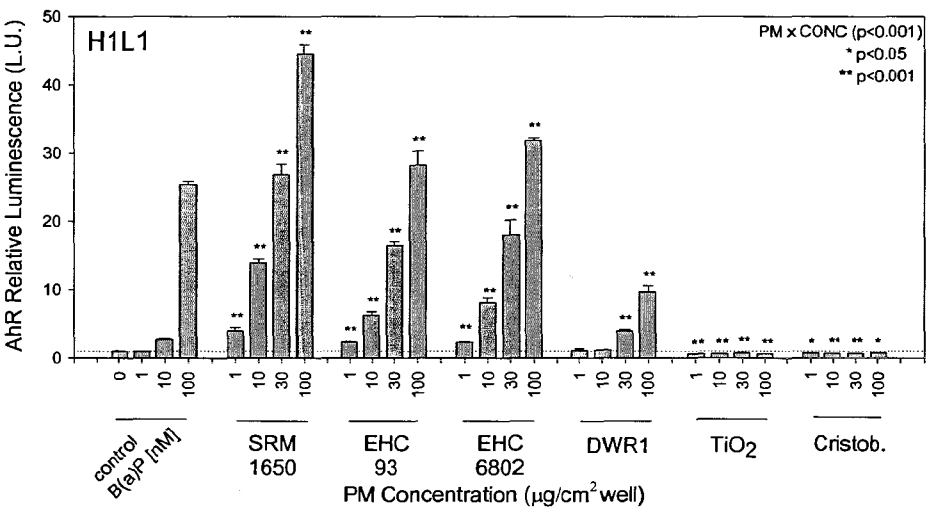
H1L1
PM x CONC (p<0.001)
* p<0.05
** p<0.001
AhR Relative Luminescence (L.U.)
50
40
30
20
10
0
0 1 10 100
1 10 30 100
1 10 30 100
1 10 30 100
1 10 30 100
1 10 30 100
1 10 30 100
control B(a)P [nM]
SRM 1650
EHC 93
EHC 6802
DWR1
TiO2
Cristob.
PM Concentration (µg/cm2 well)

Figure 2.6. Luciferase activity of H1L1.1c2 cells exposed for 24 hrs to particles. The luciferase activity of the H1L1.1c2 cells was assessed using Promega luciferase assay reagent. B[a]P is present for reference (positive control) and was not included in the ANOVA to maintain the factorial design. All values are presented as mean ± standard error (n = 3). PM x CONC interaction was obtained for AhR assay. Asterisks above bars represent particle concentration effects significantly different from control (2-way ANOVA).

receptor activity, followed by the responses from urban dusts EHC-6802 and EHC-93. The response induced by fine particle mixture DWR1 was intermediate, and the response of the mineral dusts was minimal.

11.3.3 Mediators of Endothelial Activation *In Vitro*

Adhesion Factors

A549 epithelial cells did not produce detectable amounts of the adhesion factor ICAM-1, while THP-1 cells produced a basal level of ~1,000 pg/ml of ICAM-1 (Figures 2.7A, 2.7C). Statistically significant ICAM-1 increase was observed in THP-1 cells exposed to all particles with the exception of SRM-1650, in comparison to controls. The urban particles were most potent inducers of ICAM-1, followed by DWR1 and the mineral dusts. The amount of ICAM-1 in the supernatants of A549/THP-1 co-cultures was lower in comparison to THP-1 cells, with basal levels of ICAM-1 measured in co-cultures, ~ 200 pg/ml. The ICAM-1 levels significantly increased in response to particle exposures, although overall they remained about 2-fold lower in comparison to THP-1 cells (Figure 2.8A). The pattern of particle effects in co-cultures was similar to that seen in THP-1 cells, with higher amounts of ICAM-1 detected in supernatants of cells exposed to DWR1, EHC-93 and EHC-6802 in comparison to the mineral dusts. HPAE cells incubated in control media produced ICAM-1 with levels around 600 - 700 pg/ml (Figures 2.7B, 2.7D, 2.8B). Conditioned media from A549 cells, which were exposed to particle preparations did not induce changes in HPAE ICAM-1 production (Figure 2.8B). The pattern of particle effects in HPAE cells incubated with THP-1 CM was identical to that observed in THP-1 cells, with comparable levels of ICAM-1. (Figure 2.8D). The pattern of effects of particles in HPAE cells incubated with co-culture CM was also very similar to that seen in co-cultures exposed directly to particles, with overall ~2-fold higher ICAM-1 levels in HPAE cells (Figure 2.8B). A549 cells and A549/THP-1 co-cultures did not produce detectable amounts of VCAM-1 (Figures 2.9A, 2.10A). While no VCAM-1 was detected in control THP-1 cells, it was measured in THP-1 cell supernatants upon exposure to EHC-93, EHC-6802 and DWR1 particles (Figure 2.9C). HPAE cells produced VCAM-1 in control media (~100-200 pg/ml). No changes in VCAM-1 production with respect to particle incubations were induced from A549 CM in HPAE cells (Figure 2.9B). HPAE cells incubated in THP-1- or co-culture CM showed augmented production of VCAM-1,

with comparable levels. (Figure 2.9D, 2.10B). The ranking of particle potency was similar between the two exposures, with most VCAM-1 detected in CM in response to urban particles and DWR1, followed by mineral dusts and diesel particles. Soluble E-selectin protein was not detected in cell culture supernatants of A549 or THP-1 mono-cultures and co-cultures exposed to particles, as well as in HPAE cells incubated with A549-conditoned media (Figures 2.11A-C, 2.12A). HPAE cells released substantial amounts of E-selectin into culture supernatants in response to THP-1- or co-culture CM (Figures 2.11D, 2.12B). The pattern of particle effects was again similar to that observed for ICAM-1 and VCAM-1 adhesion factors in THP-1, co-culture, or HPAE cells incubated with THP-1- or co-culture CM. E-selectin was not detected in HPAE cells incubated with THP-1-conditoned media controls but was observed with co-culture CM control incubations (Figures 2.11D, 2.12B).

Endothelin

ET-1 precursor, big ET-1 was detected in the supernatants of A549, THP-1 and HPAE cells. In all exposures, with the exception of direct exposure of THP-1 cells to particles, no significant differences in big ET-1 levels were detected. The basal amount of ET-1 production in A549 cells was ~ 40 pg/ml, which was comparable to that in HPAE cells (40-50 pg/ml). THP-1 cells produced small amount of big ET-1 in response to EHC-93, EHC-6802, DWR1 and Cristobalite only, with no detectable basal levels (Figure 2.13C). Interestingly, A549/THP-1 co-cultures produced about 3-fold less big ET-1 than A549 mono-cultures. Although not statistically significant, there was a trend of increase in big ET-1 levels in supernatants from the co-cultures exposed to EHC-6802 (Figure 2.14A). A comparison of ET-1 levels in cell culture supernatants in each exposure showed no statistically significant differences in ET-1 levels (Figures 2.15A-C, 2.16A-B), with the exception of HPAE cells incubated with CM from THP-1 cells exposed to EHC-93, EHC-6802 and DWR1, which showed a significantly higher response in comparison to SRM-1650 and the minerals (PM main effect, $p < 0.001$). Particle treatments also increased ET-1 in a concentration-dependent manner (CONC main effect, $p < 0.001$). Overall, the production levels of ET-1 in co-cultures were around 1.5-fold lower than those detected in A549 cell culture supernatants (Figures 2.15A, 2.16A). Small amounts of ET-1 were overall detected in THP-1 cell culture supernatants in response to particle exposures (~1-5 pg/ml) (Figure 2.15C). The presence of signal in No-Cell controls indicated that the majority of the low level of ET-1 signal detected in

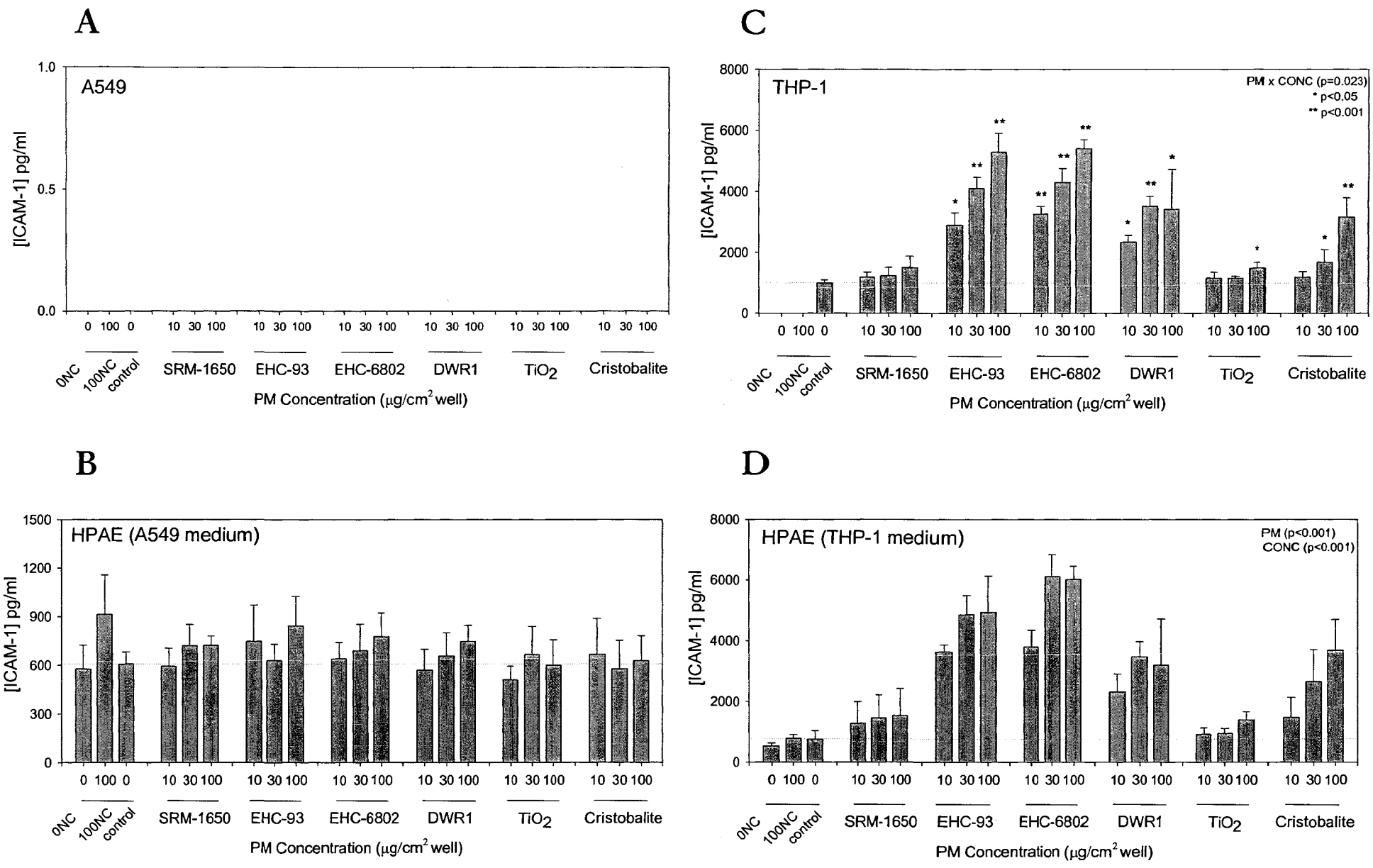
A
A549
[ICAM-1] pg/ml
1.0
0.5
0.0
0 100 0
10 30 100
0NC
100NC control
SRM-1650
EHC-93
EHC-6802
DWR1
TiO2
Cristobalite
PM Concentration (μg/cm2 well)
C
THP-1
PM x CONC (p=0.023)
* p<0.05
** p<0.001
8000
6000
4000
2000
0
B
HPAE (A549 medium)
1500
1200
900
600
300
D
HPAE (THP-1 medium)
PM (p<0.001)
CONC (p<0.001)

Figure 2.7. Intercellular Adhesion Molecule (ICAM)-1 levels in cell culture supernatants of A549 epithelial cells (A), THP-1 macrophage cells (C) exposed for 24 hrs to particle preparations, as well as HPAE endothelial cells incubated with A549- or THP-1-conditioned media (B, D). Levels of the adhesion factor were determined by Bio-Plex assay. For HPAE cells, the ICAM-1 levels produced are presented as the difference of ICAM-1 in the cell supernatants minus the potential contribution from A549 or THP-1 mono-culture production within the conditioned media. Values are presented as mean ± standard error (n=3). ICAM-1 was not detected in A549 cell supernatants. PM x CONC interaction was obtained for ICAM-1 levels in THP-1 supernatants. Asterisks above bars represent effects significantly different from control where PM x CONC interaction was observed. Differences in levels of ICAM-1 in supernatants of HPAE cells incubated with A549-conditioned media were not statistically significant. Main effects were seen for ICAM-1 levels in supernatants of HPAE cells incubated with THP-1-conditioned media by 2-way ANOVA.

A

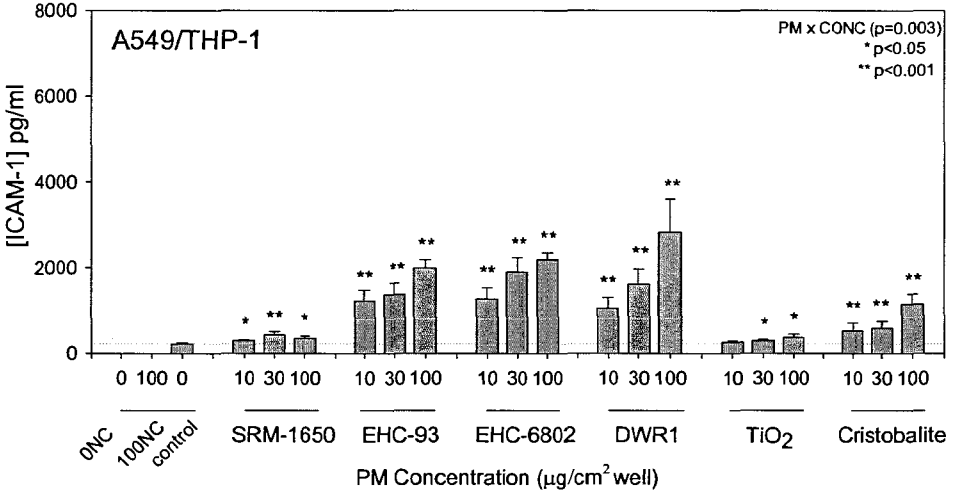
A549/THP-1
PM x CONC (p=0.003)
* p<0.05
** p<0.001
[ICAM-1] pg/ml
8000
6000
4000
2000
0
0 100 0
10 30 100
10 30 100
10 30 100
10 30 100
10 30 100
10 30 100
0NC
100NC control
SRM-1650
EHC-93
EHC-6802
DWR1
TiO2
Cristobalite
PM Concentration (µg/cm2 well)

B

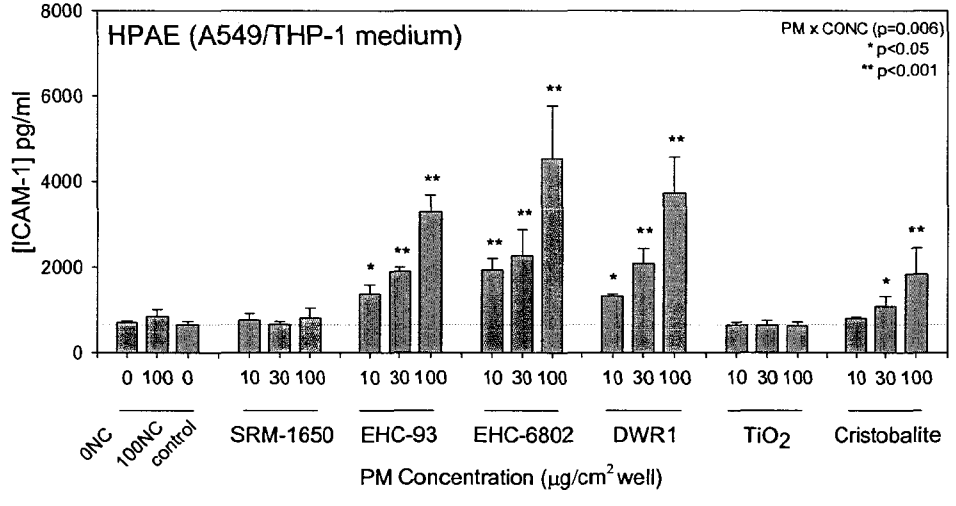
HPAE (A549/THP-1 medium)
PM x CONC (p=0.006)
* p<0.05
** p<0.001
[ICAM-1] pg/ml
8000
6000
4000
2000
0
0 100 0
10 30 100
10 30 100
10 30 100
10 30 100
10 30 100
10 30 100
0NC
100NC control
SRM-1650
EHC-93
EHC-6802
DWR1
TiO2
Cristobalite
PM Concentration (µg/cm2 well)

Figure 2.8. Intercellular Adhesion Molecule (ICAM)-1 levels in cell culture supernatants of A549/THP-1 co-cultures exposed for 24 hrs to particle preparations (A), as well as HPAE endothelial cells incubated with co-culture-conditioned media (B). Levels of the adhesion factor were determined by Bio-Plex assay. For HPAE cells, the ICAM-1 levels produced are presented as the difference of ICAM-1 in the cell supernatants minus the potential contribution from A549/THP-1 co-culture production within the conditioned media. Values are presented as mean ± standard error (n=3). PM x CONC interaction was obtained for ICAM-1 levels in co-culture supernatants, as well as in supernatants of HPAE cells incubated with co-culture-conditioned media by 2-way ANOVA. Asterisks above bars represent effects significantly different from control.

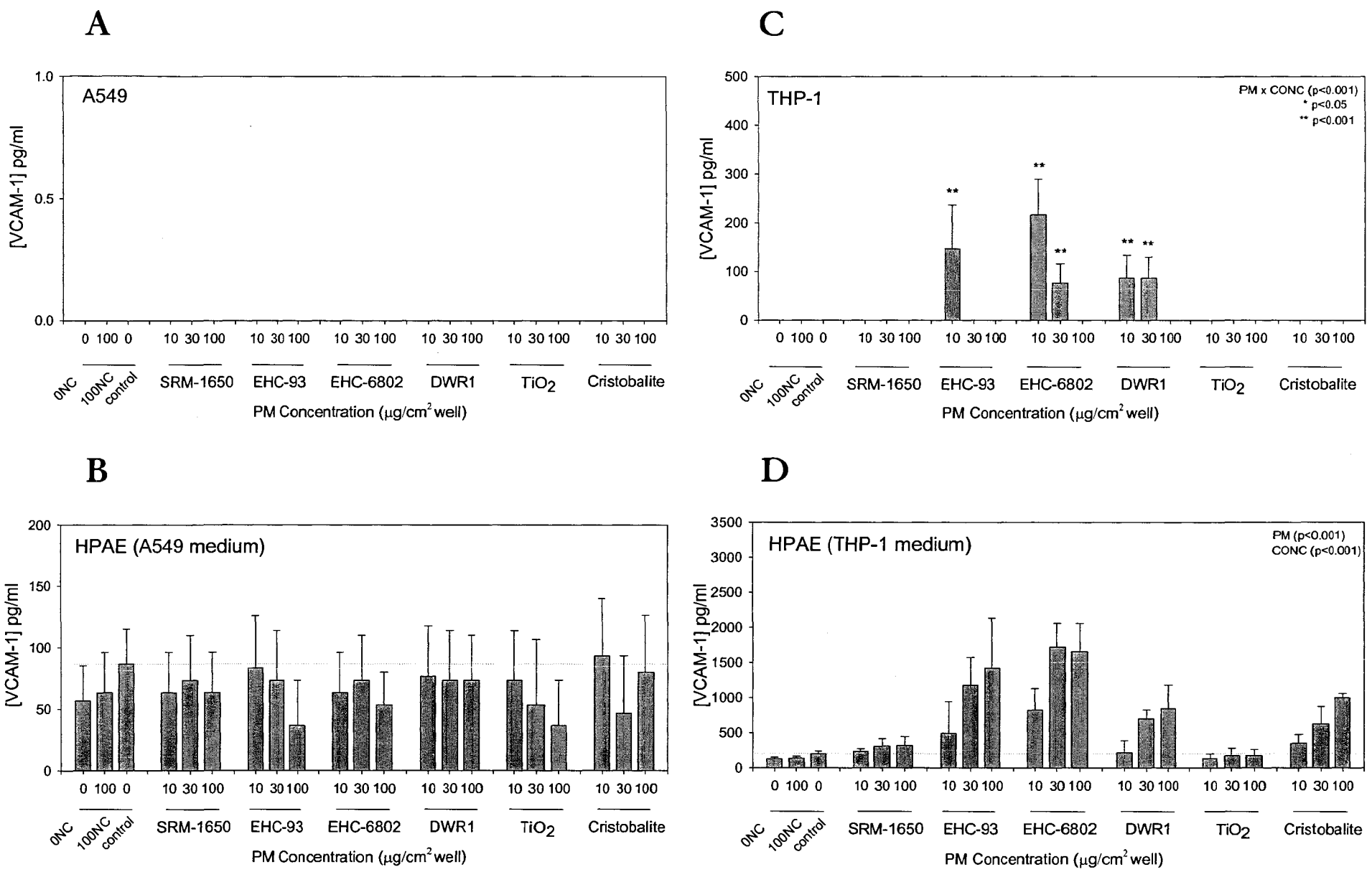
A
A549
[VCAM-1] pg/ml
1.0
0.5
0.0
0 100 0
10 30 100
0NC
100NC control
SRM-1650
EHC-93
EHC-6802
DWR1
TiO2
Cristobalite
PM Concentration (μg/cm2 well)
C
THP-1
PM x CONC (p<0.001)
* p<0.05
** p<0.001
500
400
300
200
100
0
**
B
HPAE (A549 medium)
200
150
100
50
0
D
HPAE (THP-1 medium)
PM (p<0.001)
CONC (p<0.001)
3500
3000
2500
2000
1500
1000
500

Figure 2.9. Vascular Cell Adhesion Molecule (VCAM)-1 levels in cell culture supernatants of A549 epithelial cells (A), THP-1 macrophage cells (C) exposed for 24 hrs to particle preparations, as well as HPAE endothelial cells incubated with A549- or THP-1-conditioned media (B, D). Levels of the adhesion factor were determined by Bio-Plex assay. For HPAE cells, the VCAM-1 levels produced are presented as the difference of VCAM-1 in the cell supernatants minus the potential contribution from A549 or THP-1 mono-culture production within the conditioned media. Values are presented as mean ± standard error (n=3). VCAM-1 was not detected in A549 cell supernatants. PM x CONC interaction was obtained for VCAM-1 levels in THP-1 supernatants. Asterisks above bars represent effects significantly different from control where PM x CONC interaction was observed. Differences in VCAM-1 levels in supernatants of HPAE cells incubated with A549-conditioned media were statistically insignificant. Main effects were observed in supernatants of HPAE cells incubated with THP-1-conditioned media by 2-way ANOVA.

A

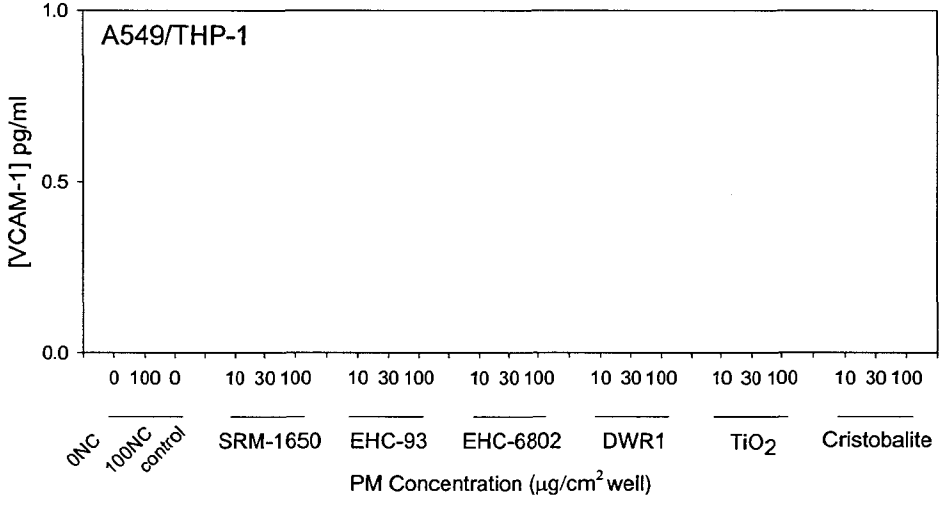
A549/THP-1
[VCAM-1] pg/ml
1.0
0.5
0.0
0 100 0
10 30 100
10 30 100
10 30 100
10 30 100
10 30 100
10 30 100
0NC
100NC control
SRM-1650
EHC-93
EHC-6802
DWR1
TiO2
Cristobalite
PM Concentration (μg/cm2 well)

B

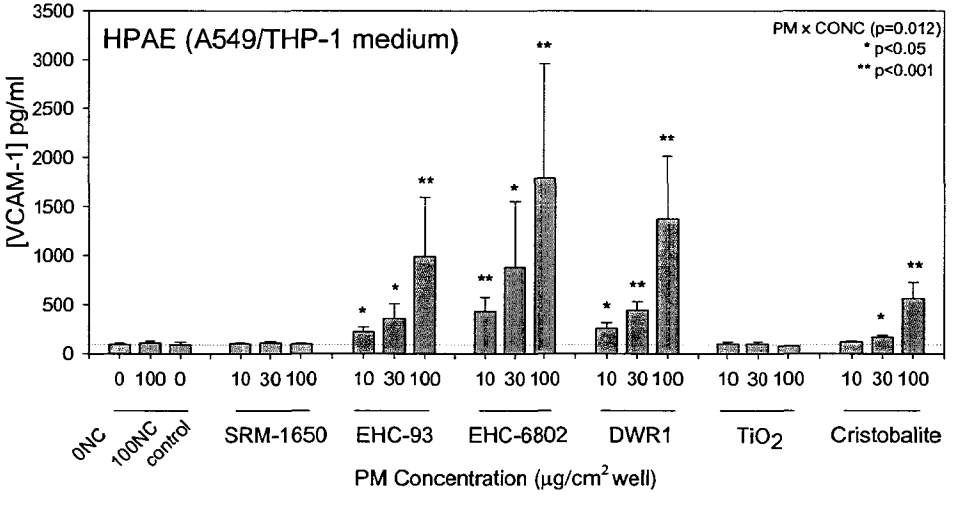
HPAE (A549/THP-1 medium)
PM x CONC (p=0.012)
* p<0.05
** p<0.001
[VCAM-1] pg/ml
3500
3000
2500
2000
1500
1000
500
0
0 100 0
10 30 100
10 30 100
10 30 100
10 30 100
10 30 100
10 30 100
0NC
100NC control
SRM-1650
EHC-93
EHC-6802
DWR1
TiO2
Cristobalite
PM Concentration (μg/cm2 well)

Figure 2.10. Vascular Cell Adhesion Molecule (VCAM)-1 levels in cell culture supernatants of A549/THP-1 co-cultures exposed for 24 hrs to particle preparations (A), as well as HPAE endothelial cells incubated with co-culture-conditioned media (B). Levels of the adhesion factor were determined by Bio-Plex assay. For HPAE cells, the VCAM-1 levels produced are presented as the difference of VCAM-1 in the cell supernatants minus the potential contribution from A549/THP-1 co-culture production within the conditioned media. Values are presented as mean ± standard error (n=3). VCAM-1 was not detected in co-culture cell supernatants. PM x CONC interaction was obtained for VCAM-1 levels in supernatants of HPAE cells incubated with co-culture-conditioned media by 2-way ANOVA. Asterisks above bars represent effects significantly different from control where PM x CONC interaction was observed.

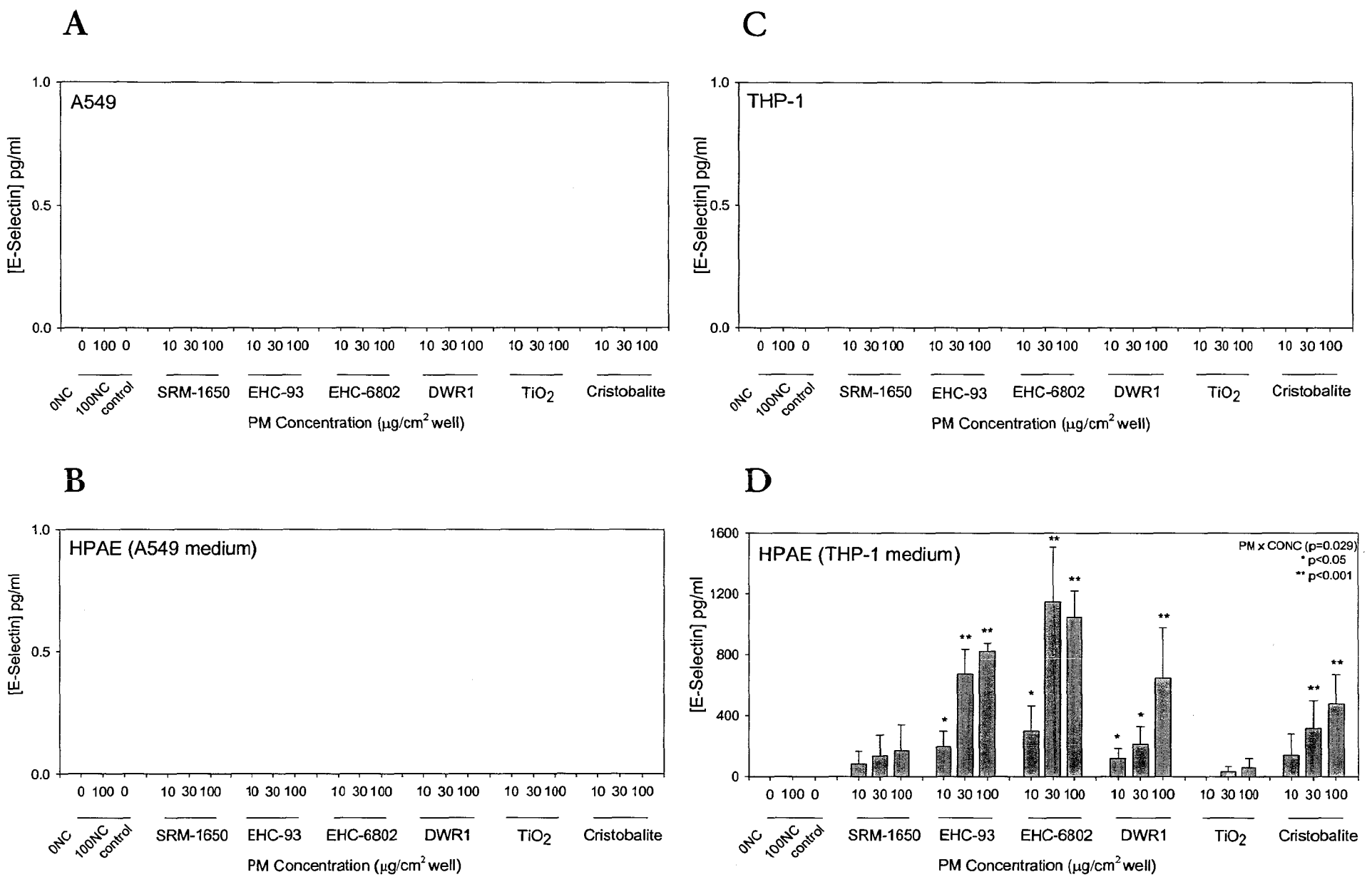
A
A549
[E-Selectin] pg/ml
1.0
0.5
0.0
0 100 0
10 30 100
0NC
100NC control
SRM-1650
EHC-93
EHC-6802
DWR1
TiO2
Cristobalite
PM Concentration (μg/cm2 well)
C
THP-1
B
HPAE (A549 medium)
D
HPAE (THP-1 medium)
PM x CONC (p=0.029)
* p<0.05
** p<0.001
1600
1200
800
400
0

Figure 2.11. Endothelial-leukocyte adhesion molecule (E-selectin) levels in cell culture supernatants of A549 epithelial cells (A), THP-1 macrophage cells (C) exposed for 24 hrs to particle preparations, as well as HPAE endothelial cells incubated with A549- or THP-1-conditioned media (B, D). Levels of the adhesion factor were determined by Bio-Plex assay. For HPAE cells, the E-selectin levels produced are presented as the difference of E-selectin in the cell supernatants minus the potential contribution from A549 or THP-1 mono-culture production within the conditioned media. Values are presented as mean ± standard error (n=3). E-selectin was not detected in supernatants of A549, THP-1 and HPAE cells incubated with A549-conditioned media. PM x CONC interaction was obtained for E-selectin levels in supernatants of HPAE cells incubated with THP-1-conditioned media by 2-way ANOVA. Asterisks above bars represent effects significantly different from control, where PM x CONC interaction was observed.

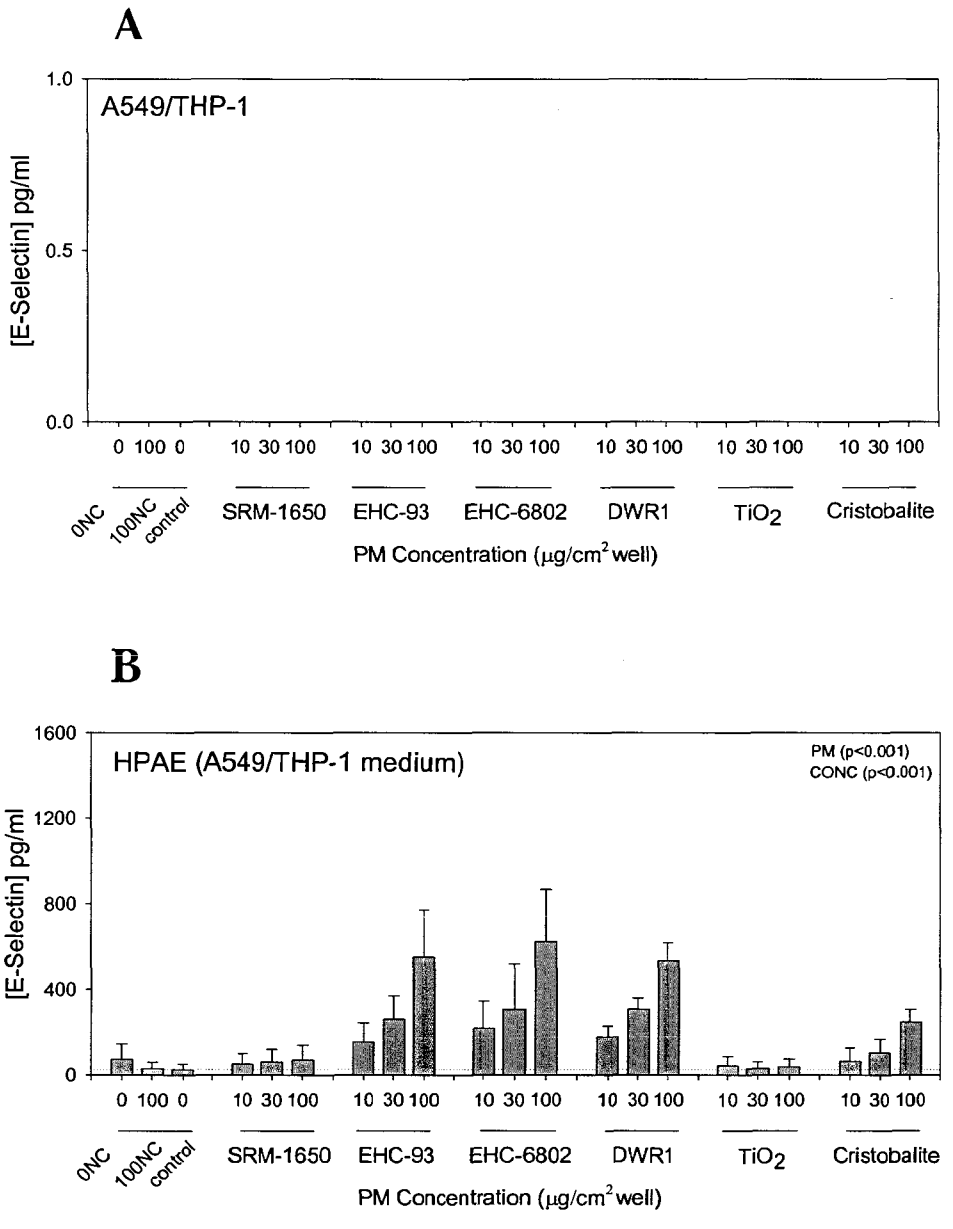
A
A549/THP-1
[E-Selectin] pg/ml
1.0
0.5
0.0
0 100 0
10 30 100
10 30 100
10 30 100
10 30 100
10 30 100
10 30 100
0NC
100NC control
SRM-1650
EHC-93
EHC-6802
DWR1
TiO2
Cristobalite
PM Concentration (μg/cm2 well)
B
HPAE (A549/THP-1 medium)
PM (p<0.001)
CONC (p<0.001)
[E-Selectin] pg/ml
1600
1200
800
400
0
0 100 0
10 30 100
10 30 100
10 30 100
10 30 100
10 30 100
10 30 100
0NC
100NC control
SRM-1650
EHC-93
EHC-6802
DWR1
TiO2
Cristobalite
PM Concentration (μg/cm2 well)

Figure 2.12. Endothelial-leukocyte adhesion molecule (E-selectin) levels in cell culture supernatants of A549/THP-1 co-cultures exposed for 24 hrs to particle preparations (A), as well as HPAE endothelial cells incubated with co-culture-conditioned media (B). Levels of the adhesion factor were determined by Bio-Plex assay. For HPAE cells, the E-selectin levels produced are presented as the difference of E-selectin in the cell supernatants minus the potential contribution from A549/THP-1 co-culture production within the conditioned media. Values are presented as mean ± standard error (n=3). E-selectin was not detected in co-culture cell supernatants. Main effects were observed for E-selectin levels in supernatants of HPAE cells incubated with co-culture-conditioned media by 2-way ANOVA.

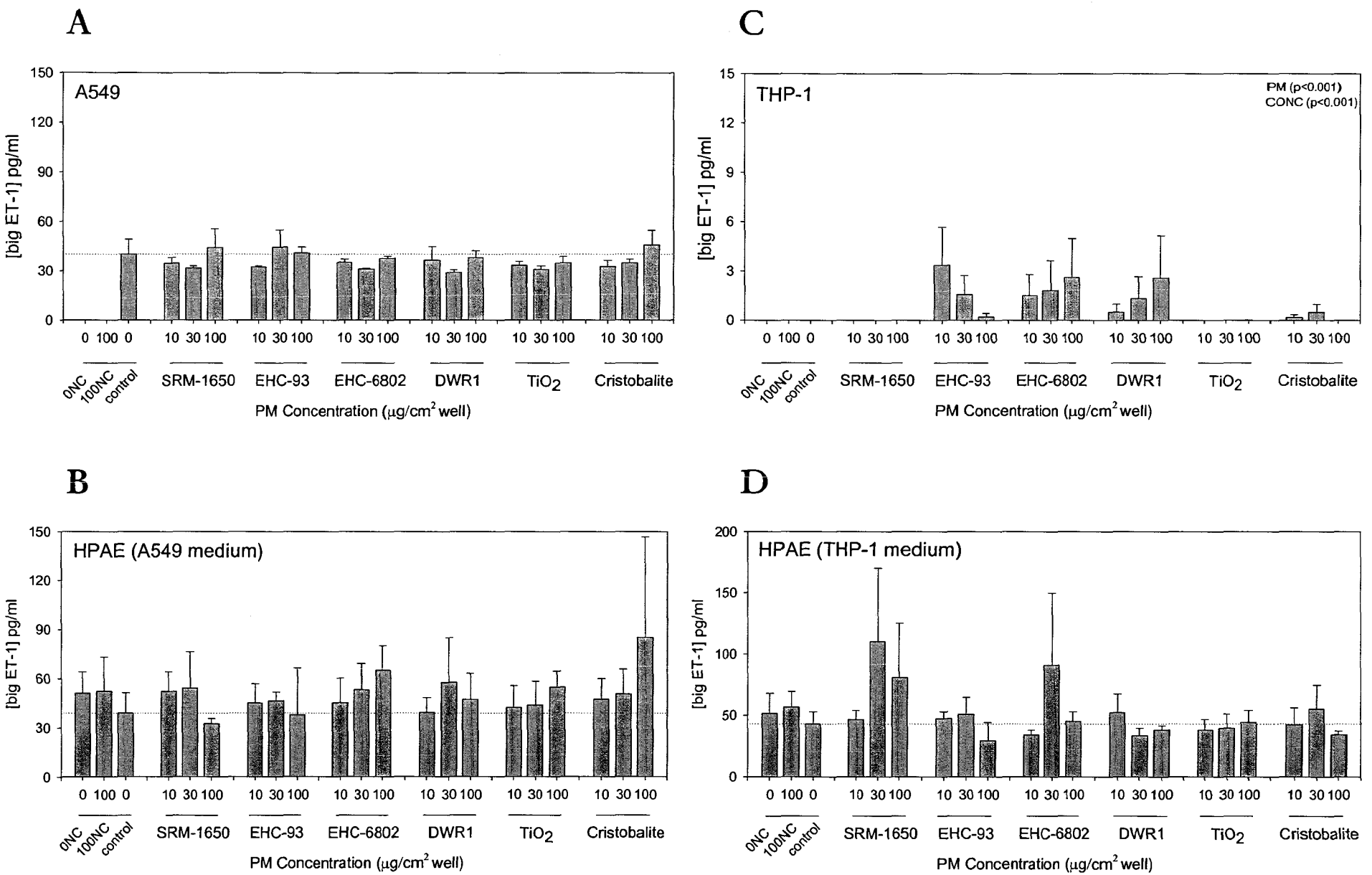
A
A549
[big ET-1] pg/ml
150
120
90
60
30
0
0 100 0
10 30 100
0NC
100NC
control
SRM-1650
EHC-93
EHC-6802
DWR1
TiO2
Cristobalite
PM Concentration (μg/cm² well)
C
THP-1
PM (p<0.001)
CONC (p<0.001)
15
12
9
6
3
0
B
HPAE (A549 medium)
D
HPAE (THP-1 medium)
200
150
100
50

Figure 2.13. Big Endothelin (ET)-1 levels in cell culture supernatants of A549 epithelial cells (A), THP-1 macrophage cells (C) exposed for 24 hrs to particle preparations, as well as HPAE endothelial cells incubated with A549- or THP-1-conditioned media (B, D). Levels of the ET-1 precursor were determined by colorimetric ELISA. For HPAE cells, the big ET-1 levels produced are presented as the difference of big ET-1 in the cell supernatants minus the potential contribution from A549 or THP-1 mono-culture production within the conditioned media. Values are presented as mean ± standard error (n=3). Differences in big ET-1 levels in supernatants of A549 cells and those of HPAE cells incubated with A549- or THP-1-conditioned media were not statistically significant. Main effects were obtained in cell media of THP-1 cells exposed to particles, as determined by 2-way ANOVA.

A

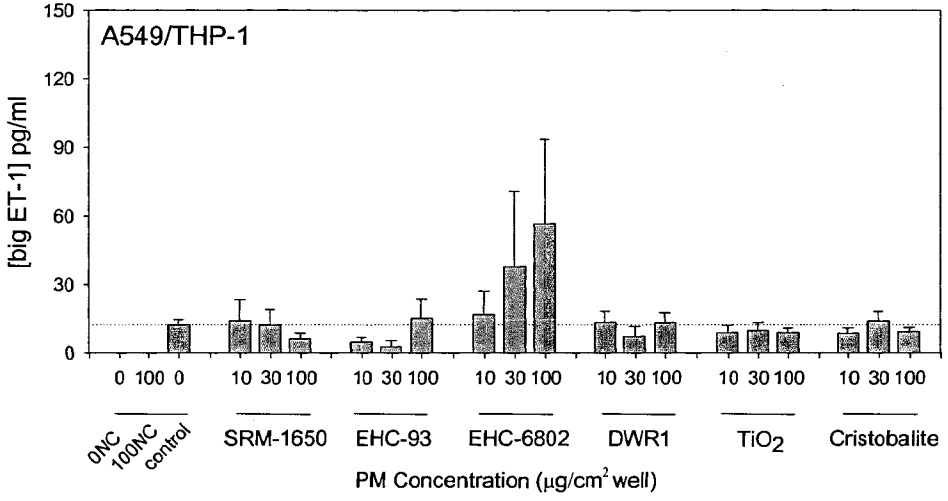
A549/THP-1
[big ET-1] pg/ml
150
120
90
60
30
0
0 100 0
10 30 100
10 30 100
10 30 100
10 30 100
10 30 100
10 30 100
0NC
100NC
control
SRM-1650
EHC-93
EHC-6802
DWR1
TiO2
Cristobalite
PM Concentration (µg/cm² well)

B

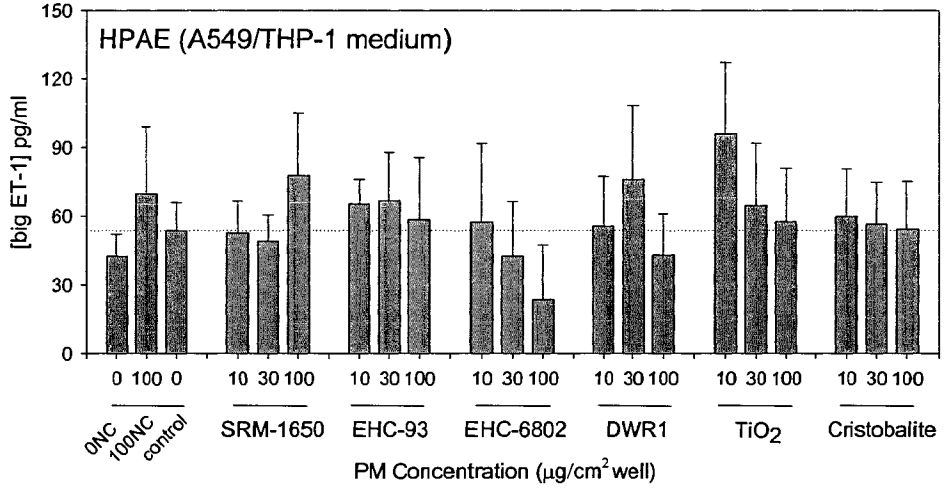
HPAE (A549/THP-1 medium)
[big ET-1] pg/ml
150
120
90
60
30
0
0 100 0
10 30 100
10 30 100
10 30 100
10 30 100
10 30 100
10 30 100
0NC
100NC
control
SRM-1650
EHC-93
EHC-6802
DWR1
TiO2
Cristobalite
PM Concentration (µg/cm² well)

Figure 2.14. Big Endothelin (ET)-1 levels in cell culture supernatants of A549/THP-1 co-cultures exposed for 24 hrs to particle preparations (A), as well as HPAE endothelial cells incubated with co-culture-conditioned media (B). Levels of the ET-1 precursor were determined by colorimetric ELISA. For HPAE cells, the big ET-1 levels produced are presented as the difference of big ET-1 in the cell supernatants minus the potential contribution from A549/THP-1 co-culture production within the conditioned media. Values are presented as mean ± standard error (n=3). Differences in big ET-1 levels produced by co-cultured cells and by HPAE cells incubated with co-culture-conditioned media were not statistically significant (2-way ANOVA).

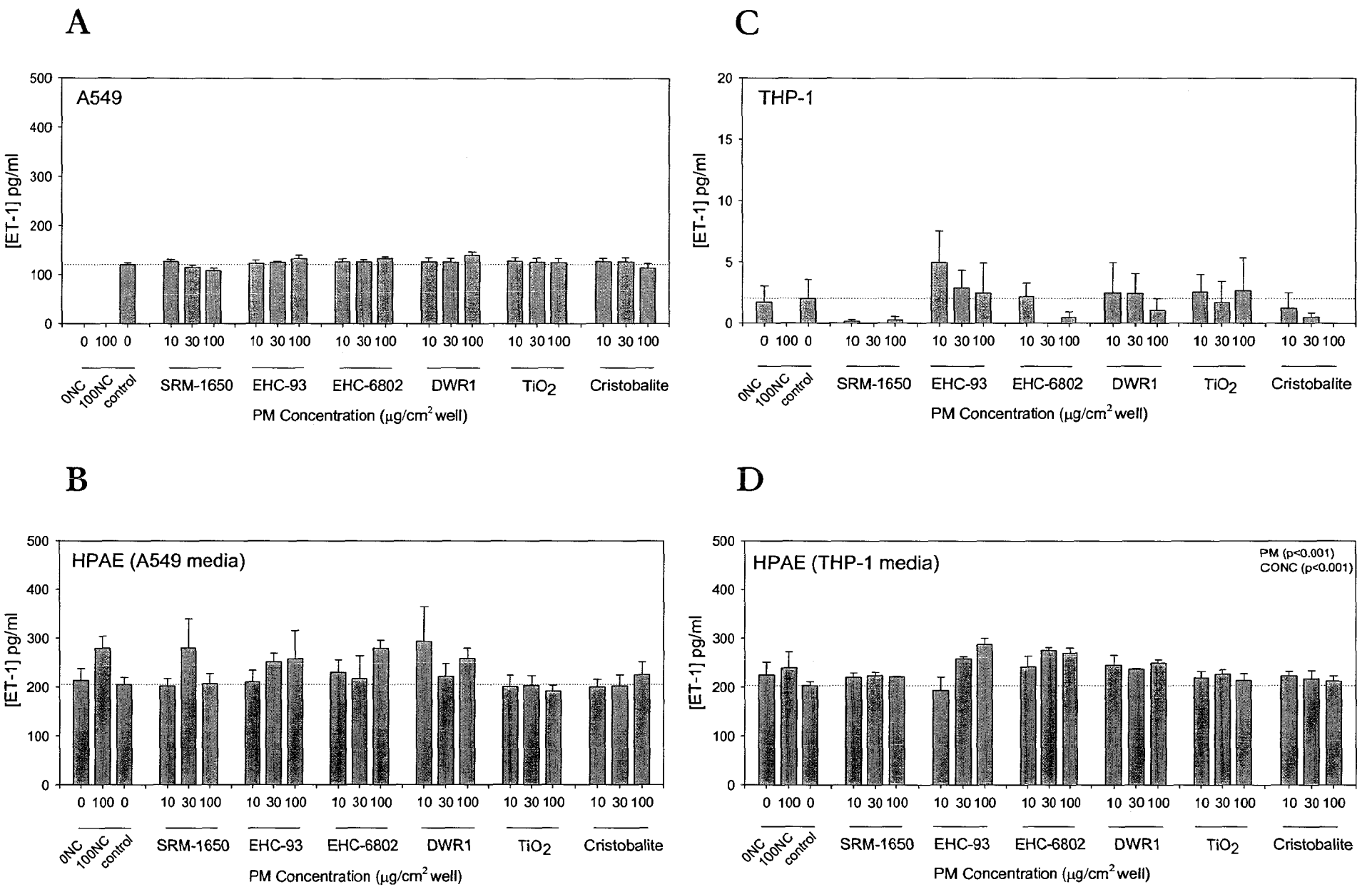
A
A549
[ET-1] pg/ml
500
400
300
200
100
0
0 100 0
10 30 100
0NC
100NC
control
SRM-1650
EHC-93
EHC-6802
DWR1
TiO2
Cristobalite
PM Concentration (μg/cm2 well)
C
THP-1
20
15
10
5
0
B
HPAE (A549 media)
D
HPAE (THP-1 media)
PM (p<0.001)
CONC (p<0.001)

Figure 2.15. Endothelin (ET)-1 levels in cell culture supernatants of A549 epithelial cells (A), THP-1 macrophage cells (C) exposed for 24 hrs to particle preparations, as well as HPAE endothelial cells incubated with A549- or THP-1-conditioned media (B, D). Levels of the vasoconstrictor were determined by colorimetric ELISA. For HPAE cells, the ET-1 levels produced are presented as the difference of ET-1 in the cell supernatants minus the potential contribution from A549 or THP-1 mono-culture production within the conditioned media. Values are presented as mean ± standard error (n=3). Differences in ET-1 levels in supernatants of A549, THP-1 cells and those of HPAE cells incubated with A549-conditioned media were not statistically significant. Main effects were obtained in supernatants of HPAE cells incubated with THP-1-conditioned media exposed to particles, as determined by 2-way ANOVA.

A

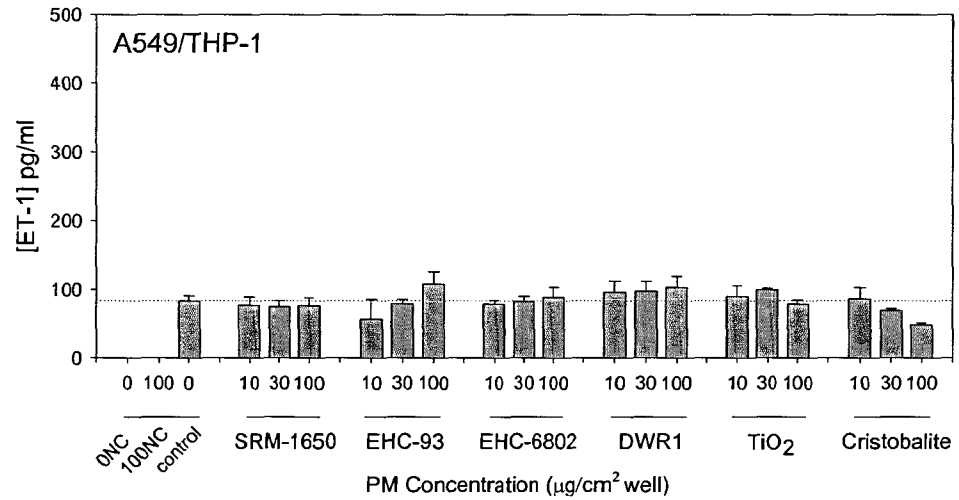
A549/THP-1
[ET-1] pg/ml
500
400
300
200
100
0
0 100 0
10 30 100
10 30 100
10 30 100
10 30 100
10 30 100
10 30 100
0NC
100NC
control
SRM-1650
EHC-93
EHC-6802
DWR1
TiO2
Cristobalite
PM Concentration (μg/cm² well)

B

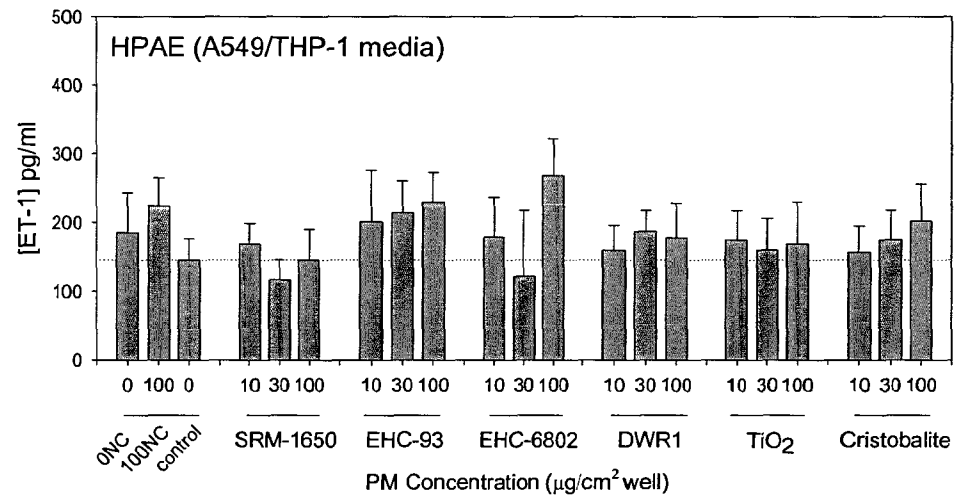
HPAE (A549/THP-1 media)
[ET-1] pg/ml
500
400
300
200
100
0
0 100 0
10 30 100
10 30 100
10 30 100
10 30 100
10 30 100
10 30 100
0NC
100NC
control
SRM-1650
EHC-93
EHC-6802
DWR1
TiO2
Cristobalite
PM Concentration (μg/cm² well)

Figure 2.16. Endothelin (ET)-1 levels in cell culture supernatants of A549/THP-1 co-cultures exposed for 24 hrs to particle preparations (A), as well as HPAE endothelial cells incubated with co-culture-conditioned media (B). Levels of the vasoconstrictor were determined by colorimetric ELISA. For HPAE cells, the ET-1 levels produced are presented as the difference of ET-1 in the cell supernatants minus the potential contribution from A549/THP-1 co-culture production within the conditioned media. Values are presented as mean ± standard error (n=3). Differences in ET-1 levels produced by co-cultured cells and by HPAE cells incubated with co-culture-conditioned media were not statistically significant (2-way ANOVA).

THP-1 cells may be likely attributed to non-specific background. The basal levels of ET-1 in HPAE cells were ~200 pg/ml.

Vascular Endothelial Growth Factor

A549 cells produced ~500 pg/ml of VEGF basally, in comparison to ~300 pg/ml produced by THP-1 cell controls (Figures 2.17A, 2.17C). A549 cells showed significant overall increases in VEGF production in response to all concentrations of particles (CONC main effect, $p < 0.001$). The changes in VEGF levels observed in THP-1 cell culture supernatants showed significant dependence on particle type, with EHC-93, EHC-6802 and DWR-1 displaying an overall increase in VEGF levels in comparison to diesel SRM-1650 and Cristobalite. TiO_2 particles also increased VEGF levels in comparison to diesel particles (Figure 2.17C). When A549 and THP-1 cells were cultured together, significant particle type- and concentration-dependent increases in VEGF levels were detected in cell culture supernatants from all particles. EHC-93, EHC-6802 and DWR1 showed highest potencies in inducing VEGF, which were comparable in magnitude, between these particles. The overall magnitude of VEGF production was similar between the co-culture and mono-cultures of the cells (Figure 2.18A). No VEGF was detected in HPAE cell cultures incubated with any CM (Figures 2.17 B, 2.17D, 2.18B).

11.3.4 Inflammation *In Vitro*

Interleukin 1β

IL-1β was not detectable in the culture supernatants of A549 cells (Figure 2.19A). Differences in IL-1β levels in the culture supernatants from HPAE endothelial cells incubated with A549- or THP-1 CM were not statistically significant. The levels measured were of very small magnitude and high variability (Figures 2.19B, 2.19D). In contrast, THP-1 cells produced substantial amounts of IL-1β in response to particle exposures, with significant particle type- and concentration-dependence. The urban particle EHC-6802 was most potent in increasing IL-1β levels, followed by EHC-93, DWR1, SRM-1650, Cristobalite and TiO_2. Comparable pattern of particle effects on IL-1β levels was seen in A549/THP-1 co-cultures. Interestingly, the co-culture of A549 and THP-1 cells showed substantially decreased levels of IL-1β released into cell culture supernatants in

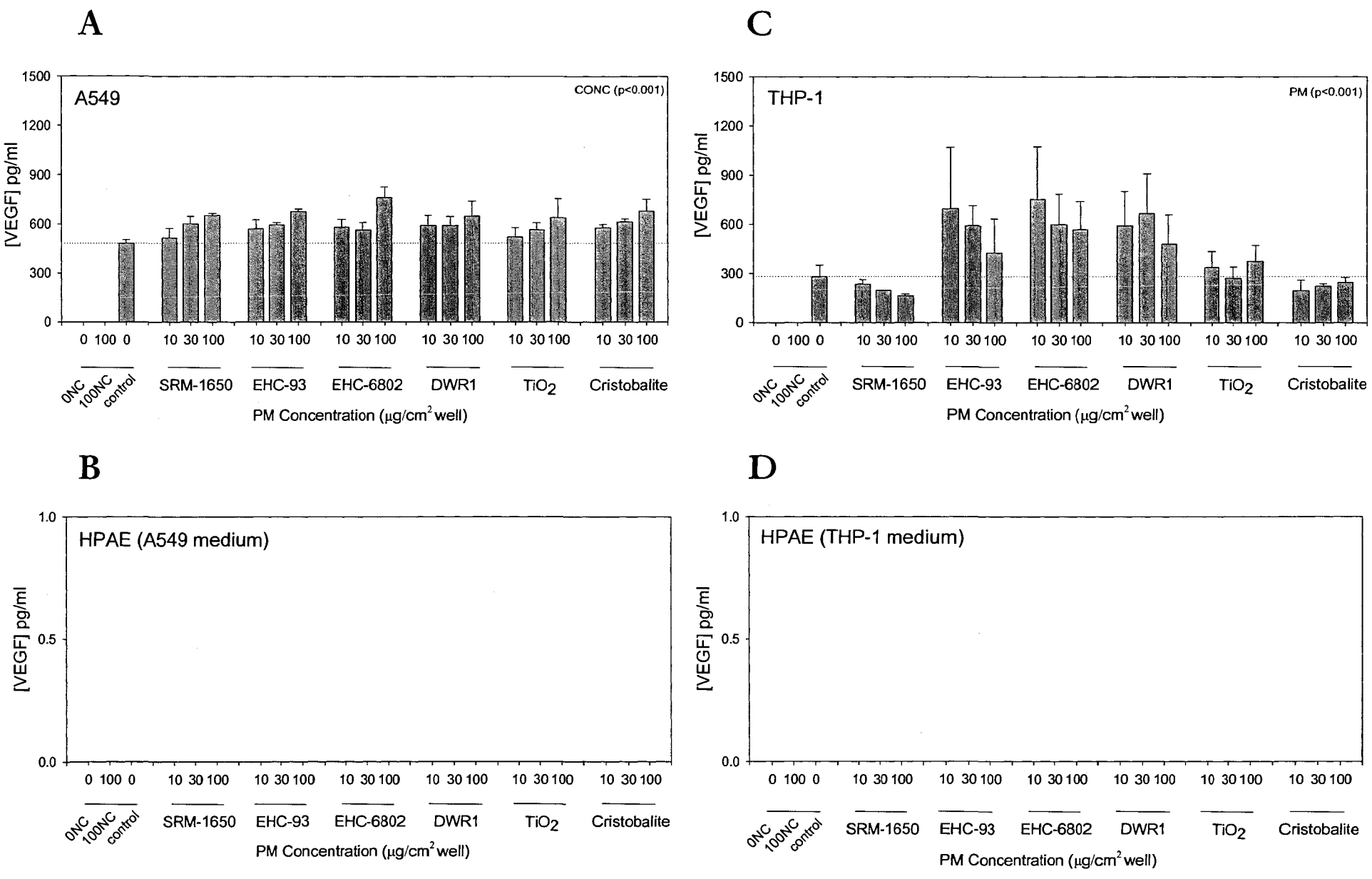
A
A549
CONC (p<0.001)
[VEGF] pg/ml
1500
1200
900
600
300
0
0 100 0
10 30 100
0NC
100NC
control
SRM-1650
EHC-93
EHC-6802
DWR1
TiO2
Cristobalite
PM Concentration (µg/cm2 well)
C
THP-1
PM (p<0.001)
B
HPAE (A549 medium)
1.0
0.5
0.0
D
HPAE (THP-1 medium)

Figure 2.17. Vascular Endothelial Growth Factor (VEGF) levels in cell culture supernatants of A549 epithelial cells (A), THP-1 macrophage cells (C) exposed for 24 hrs to particle preparations, as well as HPAE endothelial cells incubated with A549- or THP-1-conditioned media (B, D). Levels of the growth factor were determined by Bio-Plex assay. For HPAE cells, the VEGF levels produced are presented as the difference of VEGF in the cell supernatants minus the potential contribution from A549 or THP-1 mono-culture production within the conditioned media. Values are presented as mean ± standard error (n=3). Main effects were obtained for VEGF levels in A549 and THP-1 cell supernatants by 2-way ANOVA. VEGF was not present in supernatants of HPAE cells incubated with A549- or THP-1-conditioned media.

A

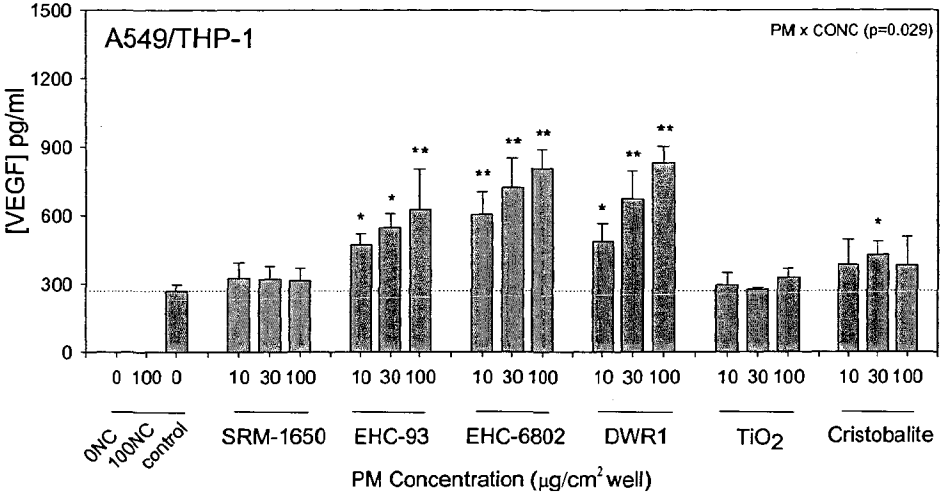
A549/THP-1
PM x CONC (p=0.029)
[VEGF] pg/ml
1500
1200
900
600
300
0
0 100 0
10 30 100
10 30 100
10 30 100
10 30 100
10 30 100
10 30 100
0NC
100NC
control
SRM-1650
EHC-93
EHC-6802
DWR1
TiO2
Cristobalite
PM Concentration (µg/cm² well)

B

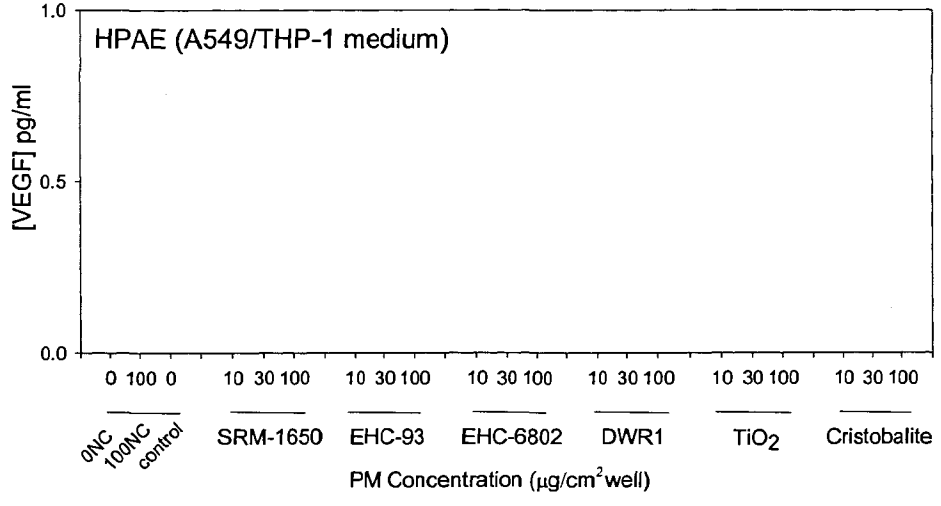
HPAE (A549/THP-1 medium)
[VEGF] pg/ml
1.0
0.5
0.0
0 100 0
10 30 100
10 30 100
10 30 100
10 30 100
10 30 100
10 30 100
0NC
100NC
control
SRM-1650
EHC-93
EHC-6802
DWR1
TiO2
Cristobalite
PM Concentration (µg/cm² well)

Figure 2.18. Vascular Endothelial Growth Factor (VEGF) levels in cell culture supernatants of A549/THP-1 co-cultures exposed for 24 hrs to particle preparations (A), as well as HPAE endothelial cells incubated with co-culture-conditioned media (B). Levels of the growth factor were determined by Bio-Plex assay. For HPAE cells, the VEGF levels produced are presented as the difference of VEGF in the cell supernatants minus the potential contribution from A549/THP-1 co-culture production within the conditioned media. Values are presented as mean ± standard error (n=3). PM x CONC interaction was obtained for VEGF levels in co-culture supernatants by 2-way ANOVA. Asterisks above bars represent effects significantly different from control, where PM x CONC interaction was observed. VEGF was not present in supernatants of HPAE cells incubated with co-culture-conditioned media.

response to particles, in comparison to THP-1 mono-cultures (Figures 2.19A, 2.19C, 2.20A). Small amounts of IL-1β (<6 pg/ml) were detectable in all treatments except that with co-culture CM from Cristobalite exposure. The measurements showed high variability and were not statistically significant (Figure 2.20B).

Interleukin 6

Only very small amounts of IL-6, which were particle concentration-dependent were detected in A549 cell culture supernatants upon 24 hr exposure to the particles (<25 pg/ml) (Figure 2.21A). In this experiment, a trend of increase in IL-6 was detected for diesel particles and Cristobalite in A549 cells supernatants. THP-1 cells also showed particle type- and concentration-dependent increases in IL-6 production, which overall were also small in magnitude (<15 pg/ml) (Figure 2.21C). When A549 and THP-1 cells were cultured together, IL-6 production markedly increased in cells exposed to particles, in comparison to the mono-cultures. The highest response was observed with EHC-6802, EHC-93, DWR1 and Cristobalite particles in up to 800 pg/ml detectable in the supernatants of A549 cells exposed to the high concentration of DWR1, although basal level of IL-6 remained low (~7 pg/ml) (Figure 2.22A). HPAE cells produced substantial basal amounts of IL-6 (Figures 2.21B, 2.21D, 2.22B). Overall, the IL-6 levels in HPAE cells incubated with A549- or co-culture CM did not show statistically significant differences between treatments. In HPAE cells incubated with THP-1 CM, an overall effect of particle amount in comparison to control with an increasing trend in IL-6 levels was detected (Figure 2.21D).

Interleukin 8

Cristobalite and diesel particles induced highest increases in IL-8 in A549 cells, with a 16- and 10-fold difference in the IL-8 levels induced by the highest concentration of the two particles respectively, in comparison to control (Figure 2.23A). THP-1 cells were highly responsive to the urban particle EHC-6802, with a significant increase in IL-8 levels in comparison to the control, and the other particle exposures (Figure 2.23C). In A549/THP-1 co-cultures, a significant pattern of responses to particle exposures was observed, with similarity to THP-1 response to particles.

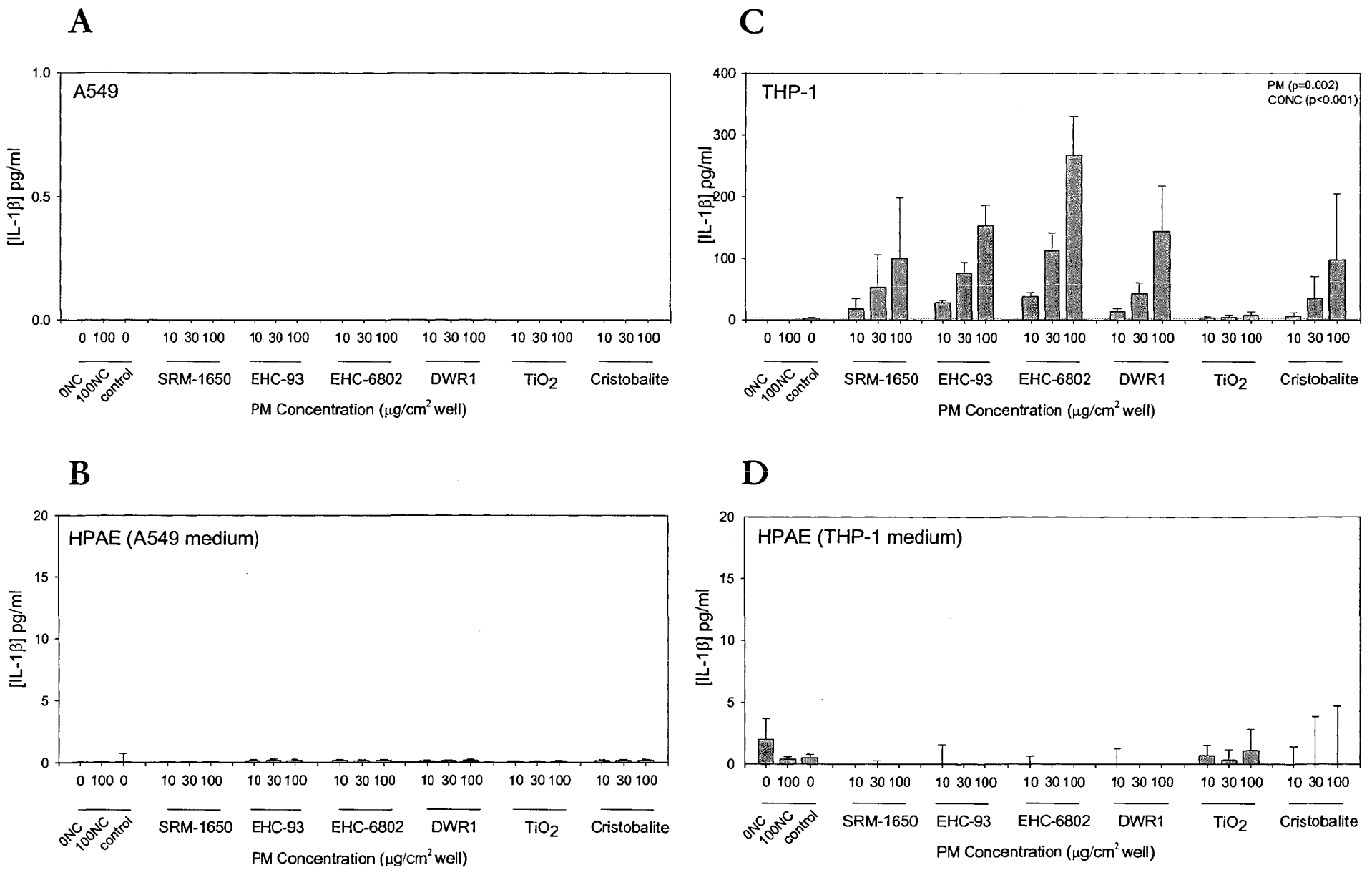
A
A549
[IL-1β] pg/ml
1.0
0.5
0.0
0 100 0
10 30 100
0NC
100NC
control
SRM-1650
EHC-93
EHC-6802
DWR1
TiO2
Cristobalite
PM Concentration (μg/cm2 well)
C
THP-1
PM (p=0.002)
CONC (p<0.001)
400
300
200
100
0
B
HPAE (A549 medium)
20
15
10
5
0
D
HPAE (THP-1 medium)

Figure 2.19. Interleukin (IL)-1β levels in cell culture supernatants of A549 epithelial cells (A), THP-1 macrophage cells (C) exposed for 24 hrs to particle preparations, as well as HPAE endothelial cells incubated with A549- or THP-1-conditioned media (B, D). Levels of the cytokine were determined by Bio-Plex assay. For HPAE cells, the IL-1β levels produced are presented as the difference of IL-1β in the cell supernatants minus the potential contribution from A549 or THP-1 mono-culture production within the conditioned media. Values are presented as mean ± standard error (n=3). IL-1β was not present in supernatants of A549 cells. Differences in IL-1β levels in supernatants from HPAE cells incubated with A549- or THP-1-conditioned media were not statistically significant. Main effects were obtained for THP-1 cell supernatants by 2-way ANOVA.

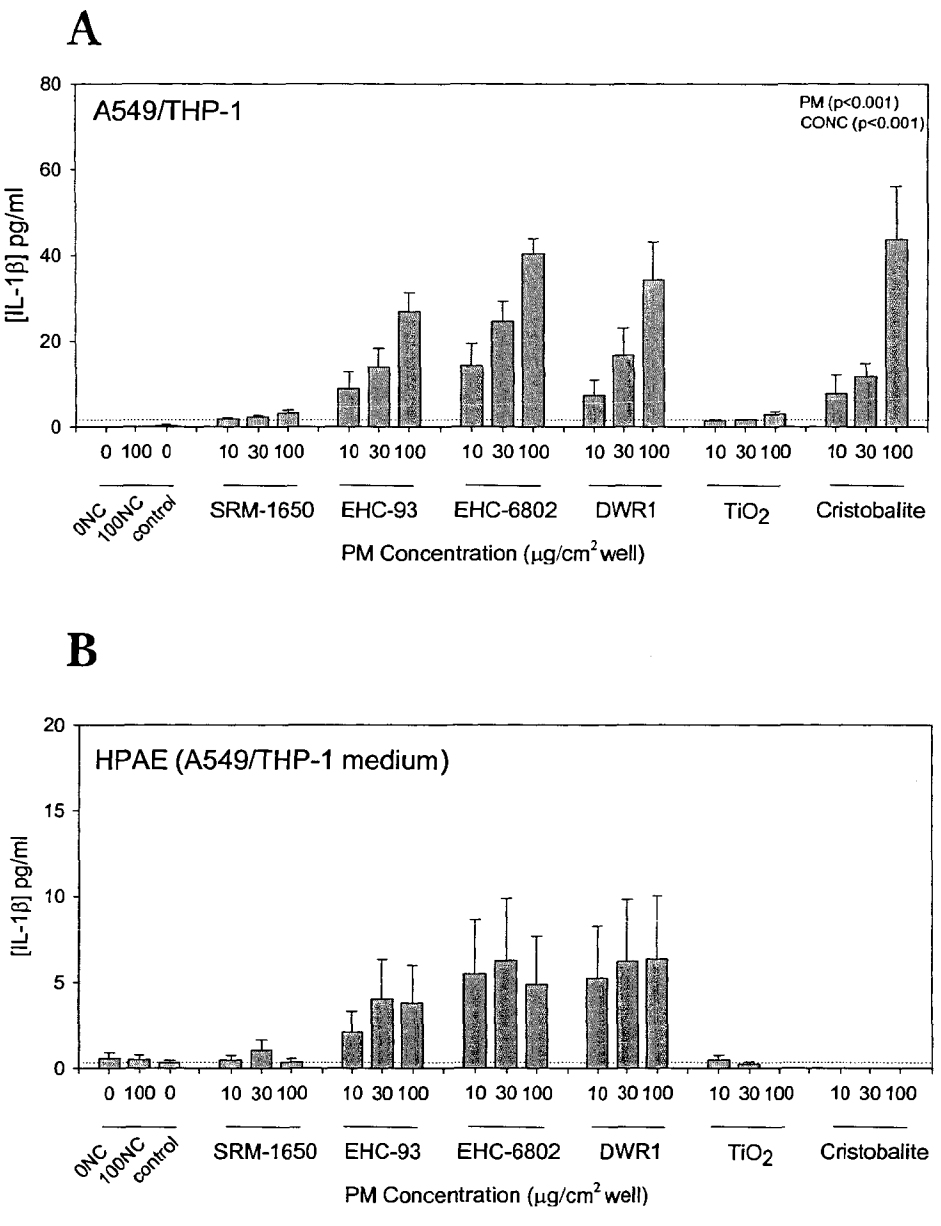
A
A549/THP-1
PM (p<0.001)
CONC (p<0.001)
[IL-1β] pg/ml
80
60
40
20
0
0 100 0
10 30 100
10 30 100
10 30 100
10 30 100
10 30 100
10 30 100
0NC
100NC
control
SRM-1650
EHC-93
EHC-6802
DWR1
TiO2
Cristobalite
PM Concentration (μg/cm2 well)
B
HPAE (A549/THP-1 medium)
[IL-1β] pg/ml
20
15
10
5
0
0 100 0
10 30 100
10 30 100
10 30 100
10 30 100
10 30 100
10 30 100
0NC
100NC
control
SRM-1650
EHC-93
EHC-6802
DWR1
TiO2
Cristobalite
PM Concentration (μg/cm2 well)

Figure 2.20. Interleukin (IL)-1β levels in cell culture supernatants of A549/THP-1 co-cultures exposed for 24 hrs to particle preparations (A), as well as HPAE endothelial cells incubated with co-culture-conditioned media (B). Levels of the cytokine were determined by Bio-Plex assay. For HPAE cells, the IL-1β levels produced are presented as the difference of IL-1β in the cell supernatants minus the potential contribution from A549/THP-1 co-culture production within the conditioned media. Values are presented as mean ± standard error (n=3). Main effects were obtained for THP-1 cell supernatants by 2-way ANOVA. Differences in IL-1β levels produced by HPAE cells incubated with co-culture-conditioned media were not statistically significant.

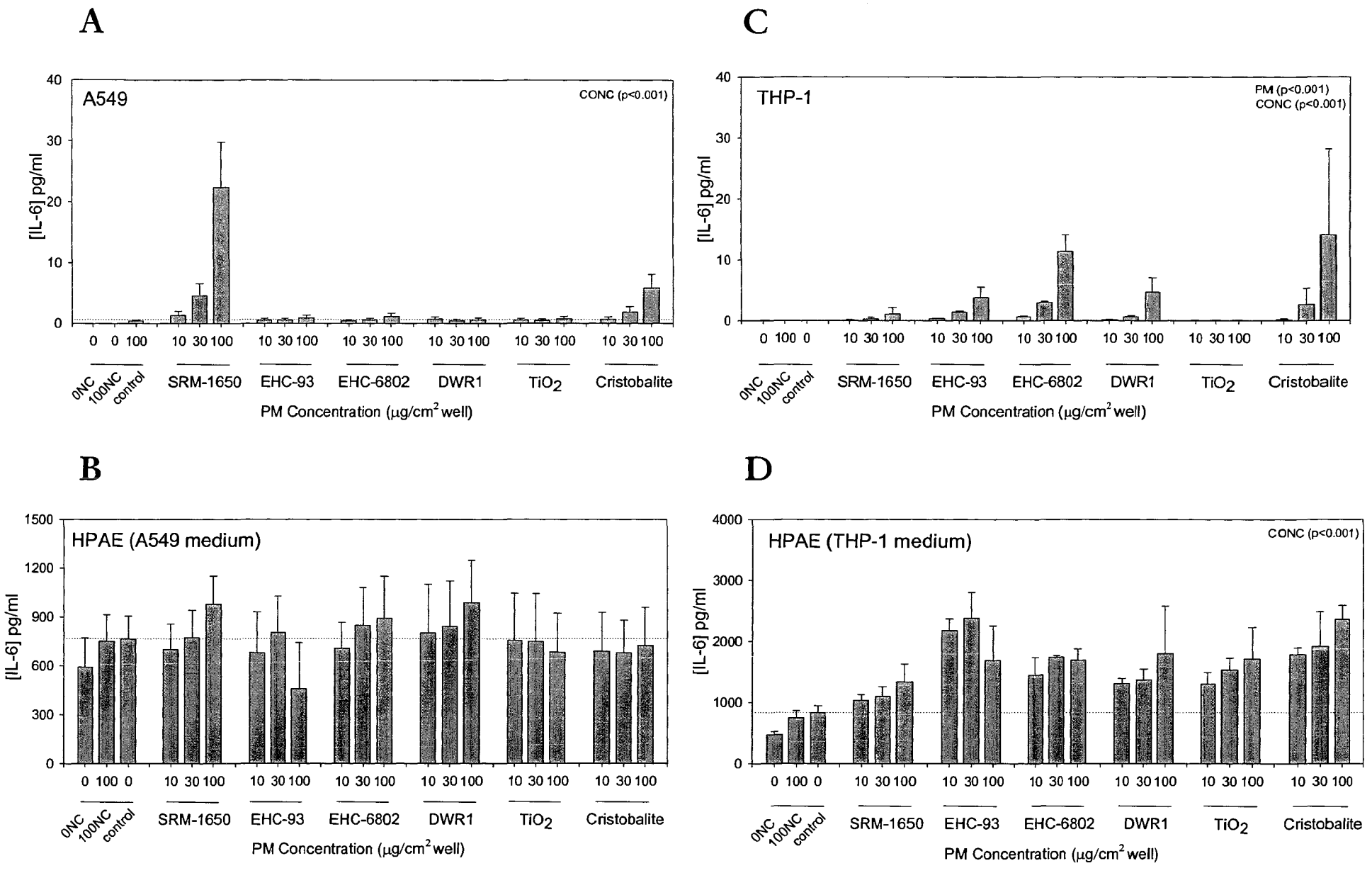
A
A549
CONC (p<0.001)
[IL-6] pg/ml
0 0 100 10 30 100 10 30 100 10 30 100 10 30 100 10 30 100 10 30 100
0NC 100NC control
SRM-1650
EHC-93
EHC-6802
DWR1
TiO2
Cristobalite
PM Concentration (μg/cm2 well)
C
THP-1
PM (p<0.001)
CONC (p<0.001)
[IL-6] pg/ml
0 100 0 10 30 100 10 30 100 10 30 100 10 30 100 10 30 100 10 30 100
0NC 100NC control
SRM-1650
EHC-93
EHC-6802
DWR1
TiO2
Cristobalite
PM Concentration (μg/cm2 well)
B
HPAE (A549 medium)
[IL-6] pg/ml
0 100 0 10 30 100 10 30 100 10 30 100 10 30 100 10 30 100 10 30 100
0NC 100NC control
SRM-1650
EHC-93
EHC-6802
DWR1
TiO2
Cristobalite
PM Concentration (μg/cm2 well)
D
HPAE (THP-1 medium)
CONC (p<0.001)
[IL-6] pg/ml
0 100 0 10 30 100 10 30 100 10 30 100 10 30 100 10 30 100 10 30 100
0NC 100NC control
SRM-1650
EHC-93
EHC-6802
DWR1
TiO2
Cristobalite
PM Concentration (μg/cm2 well)

Figure 2.21. Interleukin (IL)-6 levels in cell culture supernatants of A549 epithelial cells (A), THP-1 macrophage cells (C) exposed for 24 hrs to particle preparations, as well as HPAE endothelial cells incubated with A549- or THP-1-conditioned media (B, D). Levels of the cytokine were determined by Bio-Plex assay. For HPAE cells, the IL-6 levels produced are presented as the difference of IL-6 in the cell supernatants minus the potential contribution from A549 or THP-1 mono-culture production within the conditioned media. Values are presented as mean ± standard error (n=3). Main effects were obtained for IL-6 levels in A549 and THP-1 cell supernatants, as well as the supernatants of HPAE cells incubated with THP-1-conditioned media, as determined by 2-way ANOVA. Differences in IL-6 levels in supernatants of HPAE cells incubated with A549-conditioned media were not statistically significant.

A

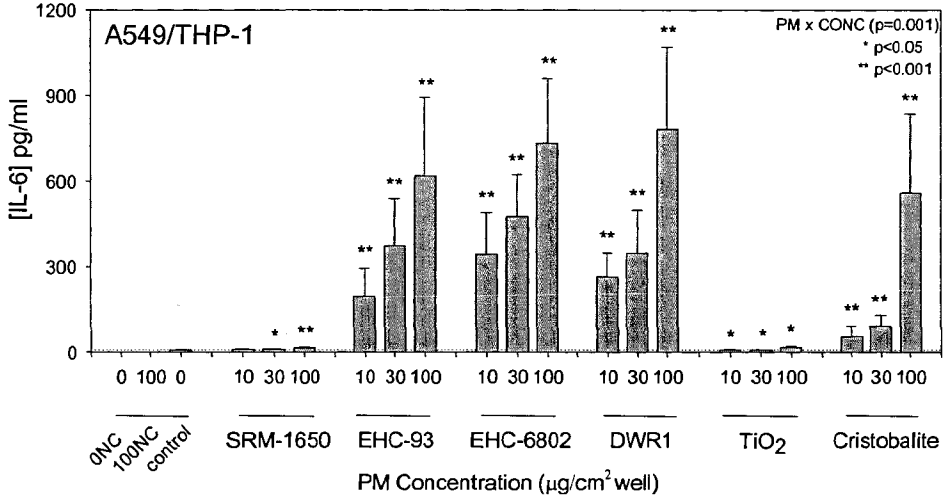
A549/THP-1
PM x CONC (p=0.001)
* p<0.05
** p<0.001
[IL-6] pg/ml
1200
900
600
300
0
0 100 0
10 30 100
10 30 100
10 30 100
10 30 100
10 30 100
10 30 100
0NC
100NC
control
SRM-1650
EHC-93
EHC-6802
DWR1
TiO2
Cristobalite
PM Concentration (μg/cm2 well)

B

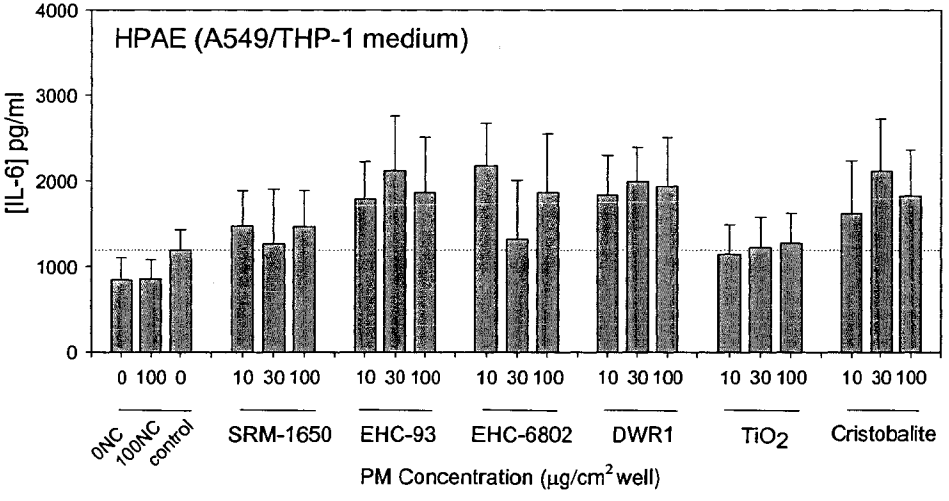
HPAE (A549/THP-1 medium)
[IL-6] pg/ml
4000
3000
2000
1000
0
0 100 0
10 30 100
10 30 100
10 30 100
10 30 100
10 30 100
10 30 100
0NC
100NC
control
SRM-1650
EHC-93
EHC-6802
DWR1
TiO2
Cristobalite
PM Concentration (μg/cm2 well)

Figure 2.22. Interleukin (IL)-6 levels in cell culture supernatants of A549/THP-1 co-cultures exposed for 24 hrs to particle preparations (A), as well as HPAE endothelial cells incubated with co-culture-conditioned media (B). Levels of the cytokine were determined by Bio-Plex assay. For HPAE cells, the IL-6 levels produced are presented as the difference of IL-6 in the cell supernatants minus the potential contribution from A549/THP-1 co-culture production within the conditioned media. Values are presented as mean ± standard error (n=3). PM x CONC interaction was obtained for IL-6 levels in co-culture supernatants by 2-way ANOVA. Asterisks above bars represent effects significantly different from control, where PM x CONC interaction was observed. Differences in IL-6 levels produced by HPAE cells incubated with co-culture-conditioned media were not statistically significant.

The magnitude of the IL-8 response of co-cultures was lower for majority of the particles (Figures 2.23C, 2.24A). Differences in IL-8 between the various incubations with A549 CM were not statistically significant (Figure 2.23B). In HPAE cells incubated with THP-1 CM, a significant overall effect of the particles at medium and high concentrations was seen, with higher amount of IL-8 in comparison to the control (Figure 2.23D). In HPAE cells incubated with co-culture CM, the IL-8 levels and pattern of particle effects were comparable to those from direct exposures of co-cultures to particles, with a decreased response to the highest concentrations of EHC-6802 and DWR1 and an increased response to the highest concentration of EHC-93 in HPAE cells in comparison to the A549/THP-1 co-culture (Figure 2.24B).

Interleukin 10

A549 cells did not produce detectable levels of IL-10 cytokine (Figure 2.25A). In THP-1 cells, small but significant amounts of IL-10 were detected in response to particle exposures. No IL-10 production was detected in supernatants from control cells. The highest significant production of IL-10 was detected in THP-1 cells exposed to EHC-6802 and EHC-93 particles, followed by DWR1, Cristobalite and diesel particles. A549/THP-1 co-cultures produced more IL-10 than THP-1 mono-cultures, with a pattern of particle response similar to that of THP-1 cells (Figure 2.26A). Very small amounts of IL-10 cytokine were detected in HPAE cell supernatants upon incubations with A549- and THP-1 CM. Small amount of IL-10 (<3 pg/ml) was present in HPAE cell supernatants after incubations with co-culture CM from EHC-93, EHC-6802 and DWR1 exposures (Figure 2.26B).

Granulocyte-Macrophage Colony-Stimulating Factor

GM-CSF was not detectable in the supernatants of A549 cells exposed to particles or control media (Figure 2.27A). Small amount of GM-CSF was measured in THP-1 cell culture supernatants upon particle exposures, with highest concentration of Cristobalite inducing the strongest response in GM-CSF release, followed by EHC-6802, EHC-93, DWR1, SRM-1650 and TiO_2 particles (Figure 2.27C). The simultaneous culture of A549 and THP-1 cells augmented the overall production of GM-CSF in response to the particles. The co-culture responses to particles were significantly different from control, with particle type- and concentration-dependence.

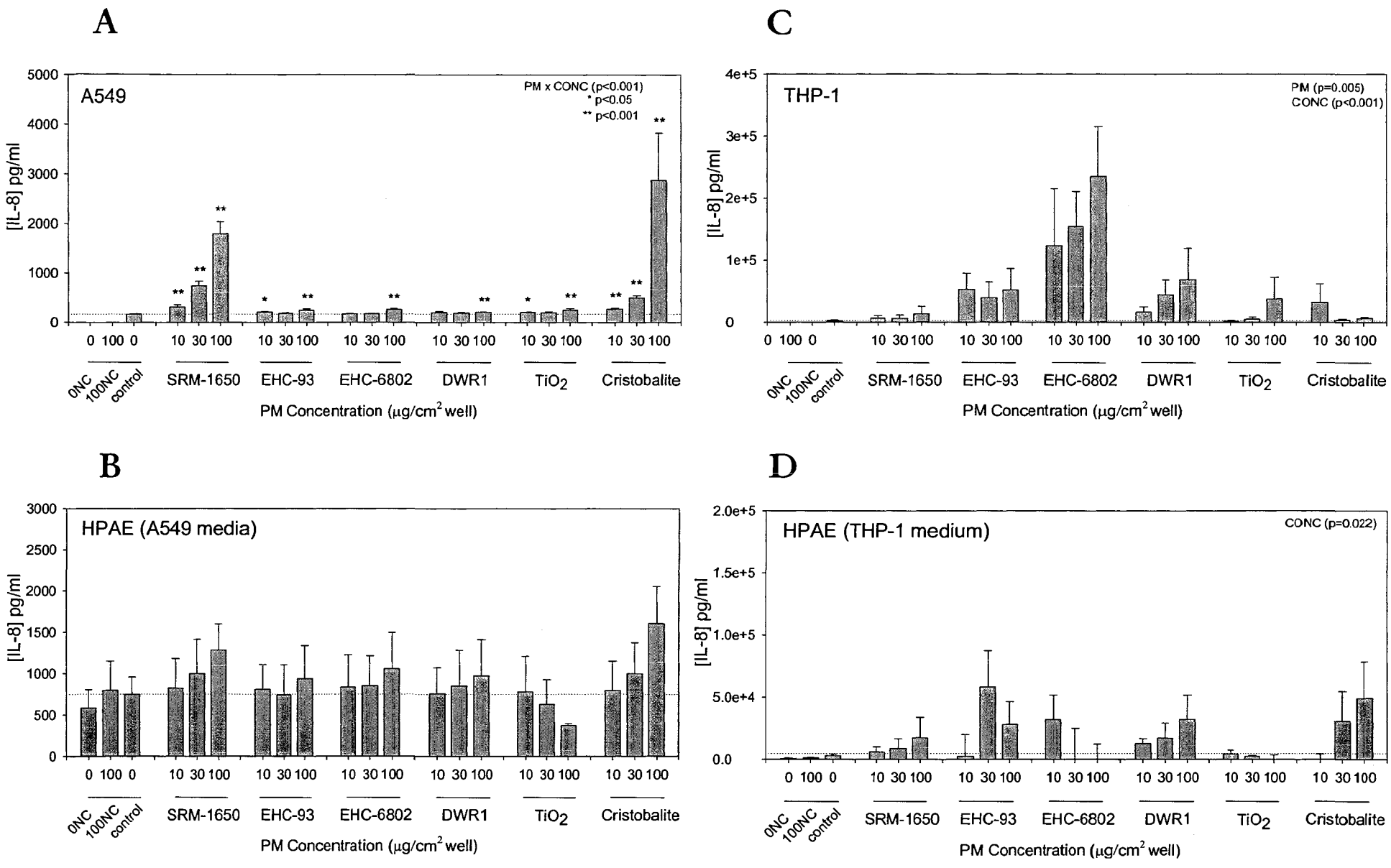
A
A549
PM x CONC (p<0.001)
* p<0.05
** p<0.001
[IL-8] pg/ml
5000
4000
3000
2000
1000
0
0 100 0
10 30 100
0NC
100NC
control
SRM-1650
EHC-93
EHC-6802
DWR1
TiO2
Cristobalite
PM Concentration (μg/cm2 well)
C
THP-1
PM (p=0.005)
CONC (p<0.001)
4e+5
3e+5
2e+5
1e+5
0
B
HPAE (A549 media)
3000
2500
2000
1500
1000
500
0
D
HPAE (THP-1 medium)
CONC (p=0.022)
2.0e+5
1.5e+5
1.0e+5
5.0e+4
0.0

Figure 2.23. Interleukin (IL)-8 levels in cell culture supernatants of A549 epithelial cells (A), THP-1 macrophage cells (C) exposed for 24 hrs to particle preparations, as well as HPAE endothelial cells incubated with A549- or THP-1-conditioned media (B, D). Levels of the chemokine were determined by Bio-Plex assay. For HPAE cells, the IL-8 levels produced are presented as the difference of IL-8 in the cell supernatants minus the potential contribution from A549 or THP-1 mono-culture production within the conditioned media. Values are presented as mean ± standard error (n=3). PM x CONC interaction was obtained for IL-8 levels in A549 cell supernatants. Asterisks above bars represent effects significantly different from control, where PM x CONC interaction was observed. Main effects were obtained for IL-8 levels in THP-1 cell supernatants, as well as the supernatants of HPAE cells incubated with THP-1-conditioned media, as determined by 2-way ANOVA. Differences in IL-8 levels in supernatants of HPAE cells incubated with A549-conditioned media were not statistically significant.

A

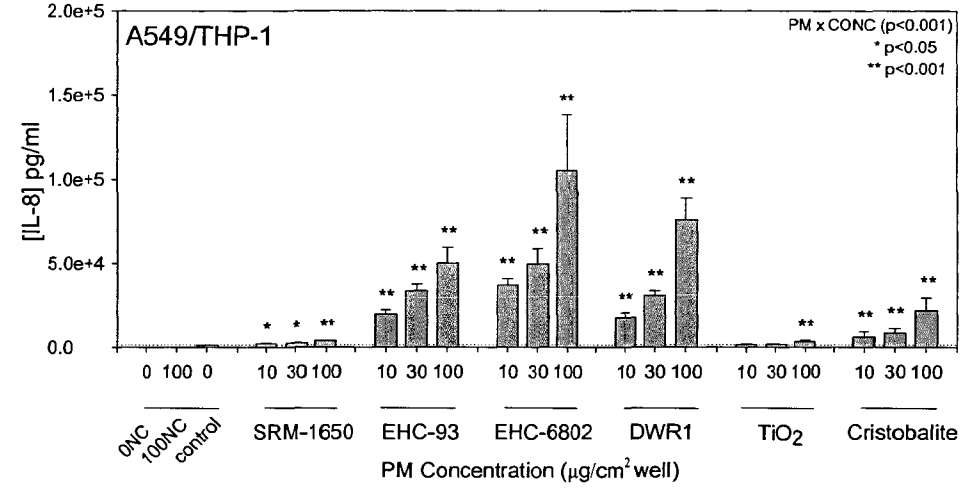
A549/THP-1
PM x CONC (p<0.001)
* p<0.05
** p<0.001
[IL-8] pg/ml
2.0e+5
1.5e+5
1.0e+5
5.0e+4
0.0
0 100 0
10 30 100
SRM-1650
EHC-93
EHC-6802
DWR1
TiO2
Cristobalite
0NC
100NC
control
PM Concentration (µg/cm² well)

B

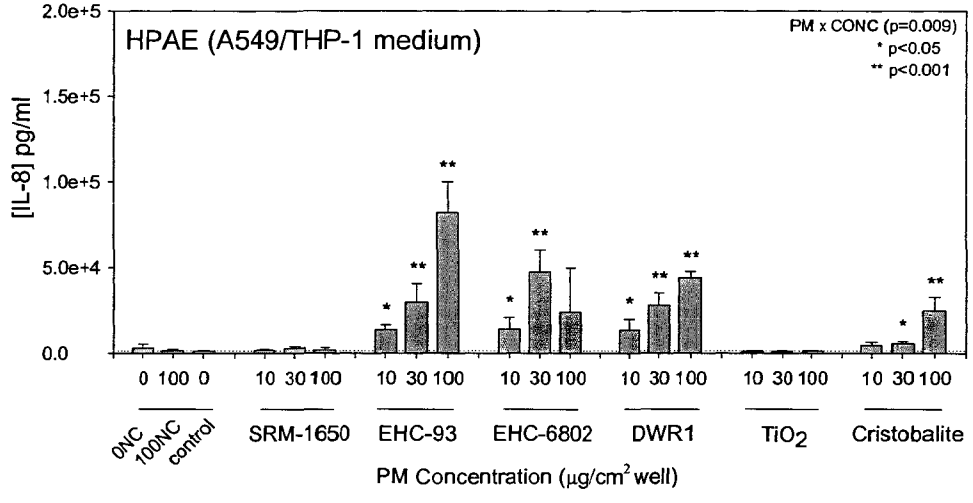
HPAE (A549/THP-1 medium)
PM x CONC (p=0.009)
* p<0.05
** p<0.001
[IL-8] pg/ml
2.0e+5
1.5e+5
1.0e+5
5.0e+4
0.0
0 100 0
10 30 100
SRM-1650
EHC-93
EHC-6802
DWR1
TiO2
Cristobalite
0NC
100NC
control
PM Concentration (µg/cm² well)

Figure 2.24. Interleukin (IL)-8 levels in cell culture supernatants of A549/THP-1 co-cultures exposed for 24 hrs to particle preparations (A), as well as HPAE endothelial cells incubated with co-culture-conditioned media (B). Levels of the chemokine were determined by Bio-Plex assay. For HPAE cells, the IL-8 levels produced are presented as the difference of IL-8 in the cell supernatants minus the potential contribution from A549/THP-1 co-culture production within the conditioned media. Values are presented as mean ± standard error (n=3). PM x CONC interaction was obtained for IL-8 levels in co-culture supernatants and in supernatants from HPAE cells incubated with co-culture-conditioned media, by 2-way ANOVA. Asterisks above bars represent effects significantly different from control.

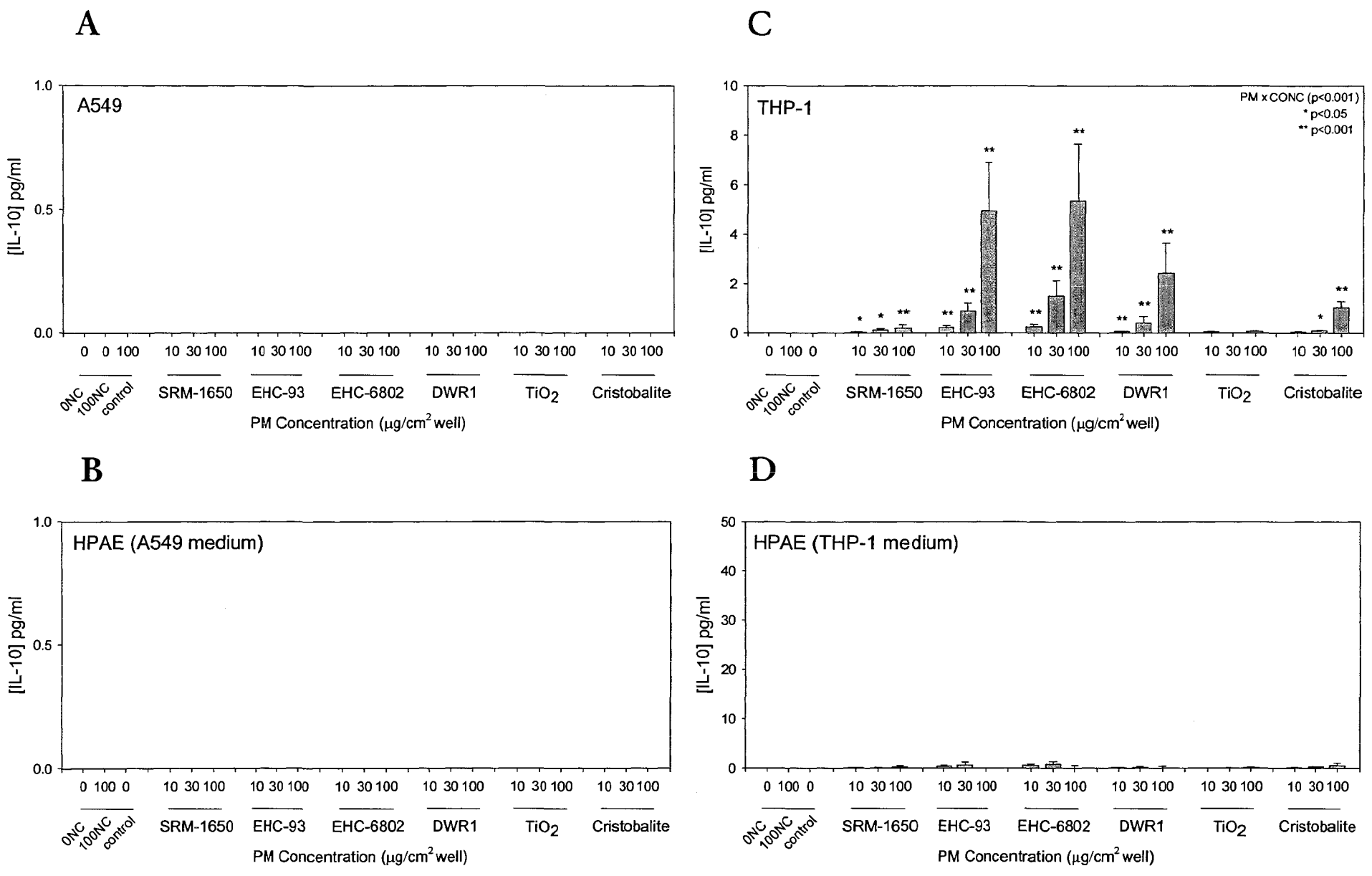
A
A549
[IL-10] pg/ml
1.0
0.5
0.0
0 0 100
10 30 100
0NC
100NC
control
SRM-1650
EHC-93
EHC-6802
DWR1
TiO2
Cristobalite
PM Concentration (µg/cm2 well)
C
THP-1
PM x CONC (p<0.001)
* p<0.05
** p<0.001
10
8
6
4
2
0
0 100 0
B
HPAE (A549 medium)
D
HPAE (THP-1 medium)
50
40
30
20

Figure 2.25. Interleukin (IL)-10 levels in cell culture supernatants of A549 epithelial cells (A), THP-1 macrophage cells (C) exposed for 24 hrs to particle preparations, as well as HPAE endothelial cells incubated with A549- or THP-1-conditioned media (B, D). Levels of the cytokine were determined by Bio-Plex assay. For HPAE cells, the IL-10 levels produced are presented as the difference of IL-10 in the cell supernatants minus the potential contribution from A549 or THP-1 mono-culture production within the conditioned media. Values are presented as mean ± standard error (n=3). IL-10 was not detected in supernatants of A549 cells. Differences in IL-10 levels in supernatants of HPAE cells incubated with A549- or THP-1-conditioned media were not statistically significant. PM x CONC interaction was obtained for IL-10 levels in supernatants of THP-1 cells (2-way ANOVA). Asterisks above bars represent effects significantly different from control, where PM x CONC interaction was observed.

A

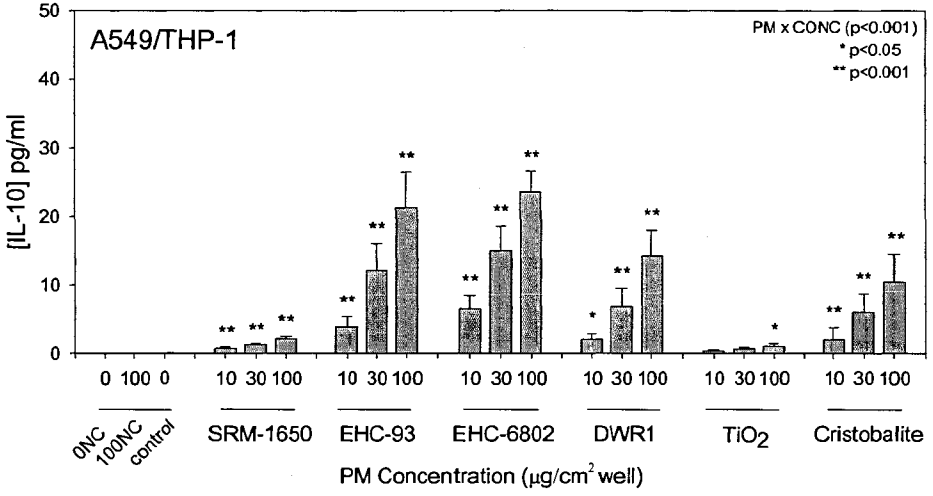
A549/THP-1
PM x CONC (p<0.001)
* p<0.05
** p<0.001
[IL-10] pg/ml
0 10 20 30 40 50
0 100 0
10 30 100
0NC
100NC
control
SRM-1650
EHC-93
EHC-6802
DWR1
TiO2
Cristobalite
PM Concentration (µg/cm2 well)

B

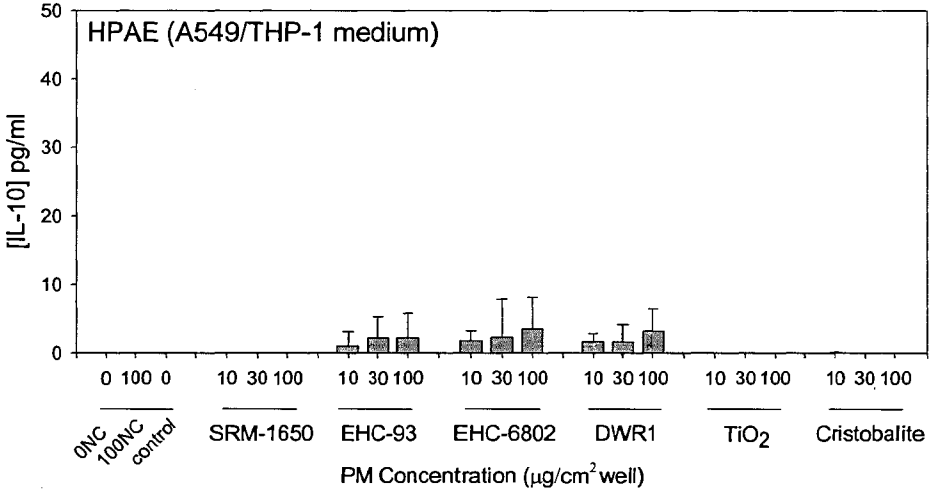
HPAE (A549/THP-1 medium)
[IL-10] pg/ml
0 10 20 30 40 50
0 100 0
10 30 100
0NC
100NC
control
SRM-1650
EHC-93
EHC-6802
DWR1
TiO2
Cristobalite
PM Concentration (µg/cm2 well)

Figure 2.26. Interleukin (IL)-10 levels in cell culture supernatants of A549/THP-1 co-cultures exposed for 24 hrs to particle preparations (A), as well as HPAE endothelial cells incubated with co-culture-conditioned media (B). Levels of the cytokine were determined by Bio-Plex assay. For HPAE cells, the IL-10 levels produced are presented as the difference of IL-10 in the cell supernatants minus the potential contribution from A549/THP-1 co-culture production within the conditioned media. Values are presented as mean ± standard error (n=3). PM x CONC interaction was obtained for IL-10 levels in co-culture supernatants. Asterisks above bars represent effects significantly different from control, where PM x CONC interaction was observed. PM main effect was obtained for IL-10 levels in supernatants from HPAE cells incubated with co-culture-conditioned media, by 2-way ANOVA.

The pattern of particle response was similar to that observed in THP-1 cells (Figures 2.27C, 2.28A). Only very small amount of GM-CSF was detectable in supernatants of HPAE cells incubated with A549 CM for 24 hrs (Figure 2.27B). The production of GM-CSF by HPAE cells incubated with THP-1 CM was markedly higher when compared to THP-1 cells directly exposed to particles, with comparable pattern of particle effects. (Figure 2.27D). HPAE cells incubated with co-culture CM from cells exposed to particles also released more GM-CSF into culture supernatants in comparison to co-cultures directly exposed to particles, with a similar pattern of particle response (Figure 2.28B). This overall amount was also higher in comparison to HPAE cells incubated with THP-1 CM (Figures 2.27D, 2.28B).

Monocyte Chemoattractant Protein 1

The production of MCP-1 chemokine in A549 cells was significantly higher in response to particles, in comparison to the control, with highest increase in MCP-1 observed in cells exposed to SRM-1650 diesel particles and mineral dust Cristobalite (Figure 2.29A). Overall, THP-1 cells produced less MCP-1 in comparison to A549 cells, with more variability in the responses. In THP-1 cells, responses to EHC-93 and EHC-6802 were significantly different from the rest of the particles. Furthermore, all concentrations showed significantly increased response in MCP-1 production in the cells, in comparison to controls (Figure 2.29C). A549/THP-1 co-cultures were highly responsive to urban particles, DWR1 and Cristobalite with over 10-fold and 30-fold difference compared to A549 and THP-1 cells respectively, exposed to the urban particles and DWR. The differences in MCP-1 levels between the mono-culture and co-culture responses to mineral dust TiO_2 were not substantial (Figures 2.29A, 2.29C, 2.30A). In HPAE cells exposed to A549 CM, the MCP-1 response was comparable in pattern of particle response and magnitude of the response to that from A549 cells exposed directly to particles (Figures 2.29A, 2.29B). Conditioned media from THP-1 cells exposed to particles increased the production of the chemokine in HPAE cells to very high levels, with over 20,000 pg/ml of MCP-1 detectable in response to CM from the highest concentration of EHC-6802 in comparison to 300 pg/ml detected in THP-1 cells in response to the direct particle treatment (Figures 2.29C, 2.29D). The highest response was observed with the urban particles, followed by DWR1, Cristobalite,

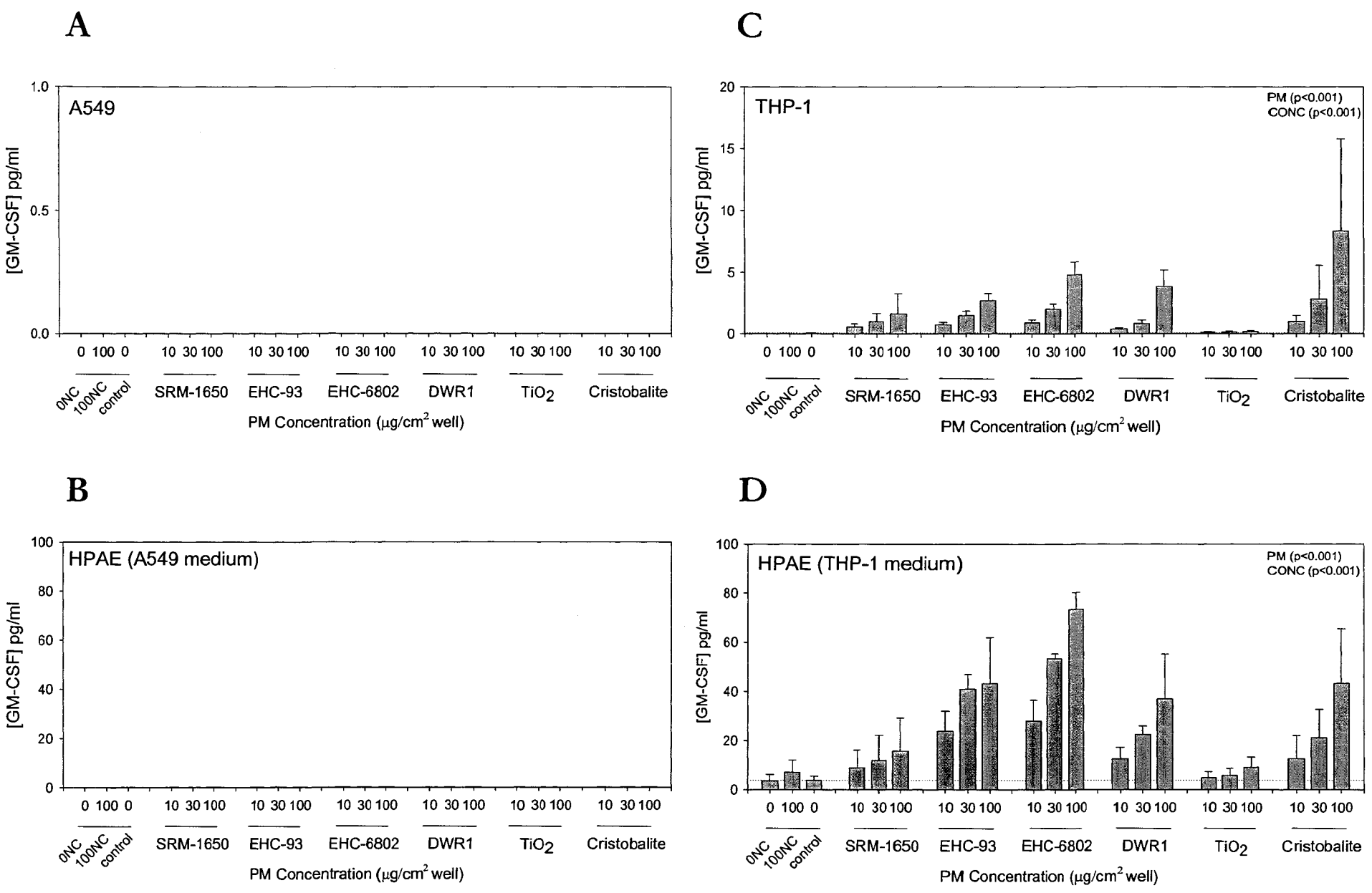
A
A549
[GM-CSF] pg/ml
1.0
0.5
0.0
0 100 0
10 30 100
0NC
100NC
control
SRM-1650
EHC-93
EHC-6802
DWR1
TiO2
Cristobalite
PM Concentration (μg/cm2 well)
C
THP-1
PM (p<0.001)
CONC (p<0.001)
20
15
10
5
0
B
HPAE (A549 medium)
100
80
60
40
20
0
D
HPAE (THP-1 medium)

Figure 2.27. Granulocyte-Macrophage Colony-Stimulating Factor (GM-CSF) levels in cell culture supernatants of A549 epithelial cells (A), THP-1 macrophage cells (C) exposed for 24 hrs to particle preparations, as well as HPAE endothelial cells incubated with A549- or THP-1-conditioned media (B, D). Levels of the chemokine were determined by Bio-Plex assay. For HPAE cells, the GM-CSF levels produced are presented as the difference of GM-CSF in the cell supernatants minus the potential contribution from A549 or THP-1 mono-culture production within the conditioned media. Values are presented as mean ± standard error (n=3). GM-CSF was not present in supernatants of A549 cells. Differences in GM-CSF levels in supernatants of HPAE cells incubated with A549-conditioned media were not statistically significant. Main effects were observed for GM-CSF levels in supernatants of THP-1 cells and HPAE cells incubated with THP-1-conditioned media (2-way ANOVA).

A

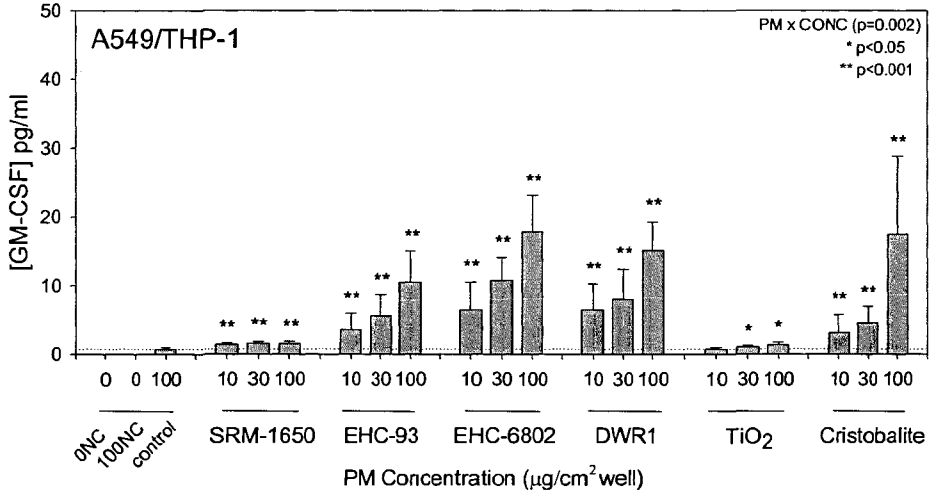
A549/THP-1
PM x CONC (p=0.002)
* p<0.05
** p<0.001
[GM-CSF] pg/ml
0 10 20 30 40 50
0 0 100 10 30 100 10 30 100 10 30 100 10 30 100 10 30 100 10 30 100
0NC
100NC
control
SRM-1650
EHC-93
EHC-6802
DWR1
TiO2
Cristobalite
PM Concentration (µg/cm2 well)

B

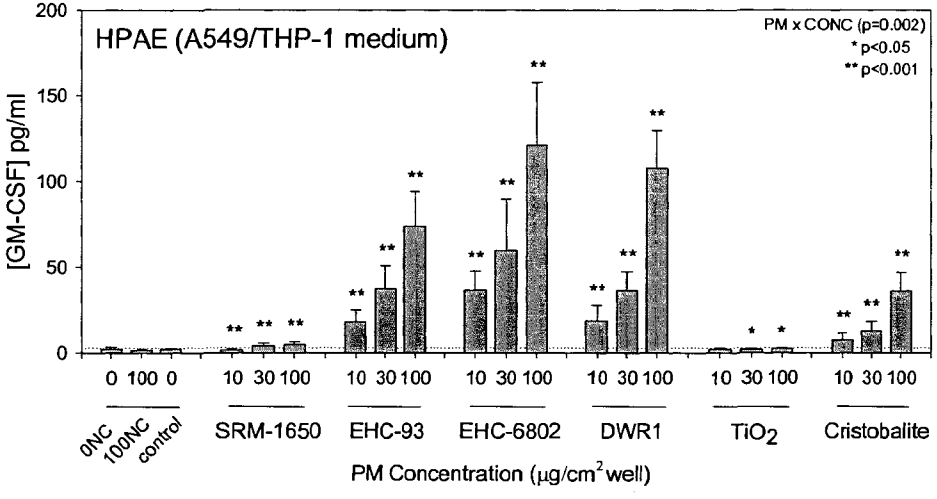
HPAE (A549/THP-1 medium)
PM x CONC (p=0.002)
* p<0.05
** p<0.001
[GM-CSF] pg/ml
0 50 100 150 200
0 100 0 10 30 100 10 30 100 10 30 100 10 30 100 10 30 100 10 30 100
0NC
100NC
control
SRM-1650
EHC-93
EHC-6802
DWR1
TiO2
Cristobalite
PM Concentration (µg/cm2 well)

Figure 2.28. Granulocyte-Macrophage Colony-Stimulating Factor (GM-CSF) levels in cell culture supernatants of A549/THP-1 co-cultures exposed for 24 hrs to particle preparations (A), as well as HPAE endothelial cells incubated with co-culture-conditioned media (B). Levels of the chemokine were determined by Bio-Plex assay. For HPAE cells, the GM-CSF levels produced are presented as the difference of GM-CSF in the cell supernatants minus the potential contribution from A549/THP-1 co-culture production within the conditioned media. Values are presented as mean ± standard error (n=3). PM x CONC interaction was obtained for GM-CSF levels in co-culture supernatants and supernatants from HPAE cells incubated with co-culture-conditioned media, by 2-way ANOVA. Asterisks above bars represent effects significantly different from control.

A

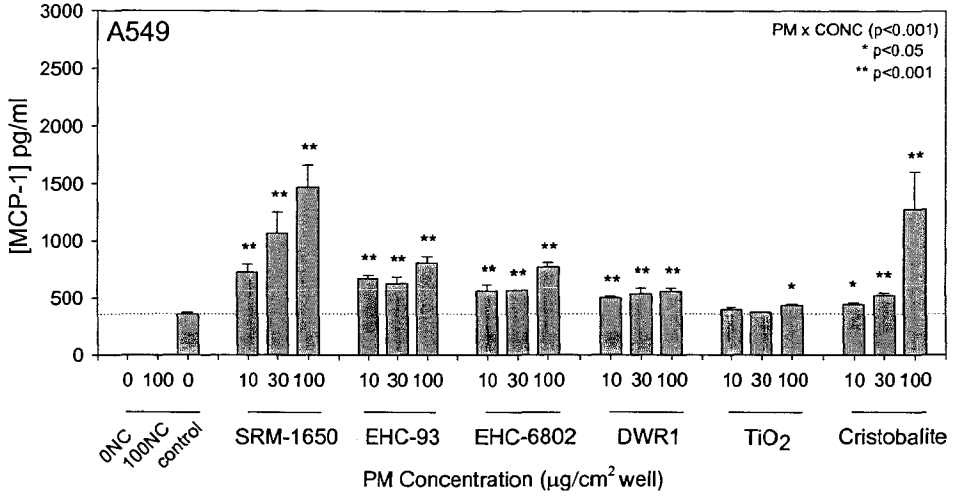
A549
PM x CONC (p<0.001)
* p<0.05
** p<0.001
[MCP-1] pg/ml
3000
2500
2000
1500
1000
500
0
0 100 0
10 30 100
0NC
100NC
control
SRM-1650
EHC-93
EHC-6802
DWR1
TiO2
Cristobalite
PM Concentration (µg/cm2 well)

C

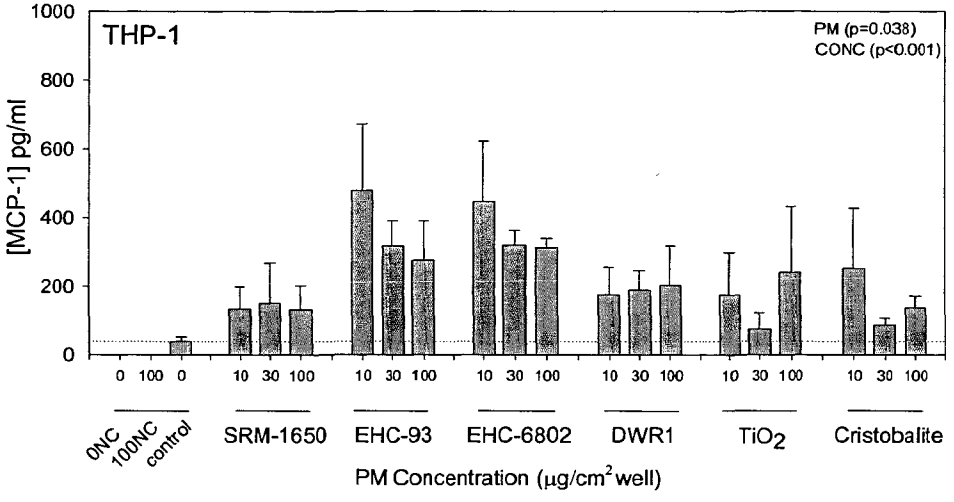
THP-1
PM (p=0.038)
CONC (p<0.001)
[MCP-1] pg/ml
1000
800
600
400
200
0
0 100 0
10 30 100
0NC
100NC
control
SRM-1650
EHC-93
EHC-6802
DWR1
TiO2
Cristobalite
PM Concentration (µg/cm2 well)

B

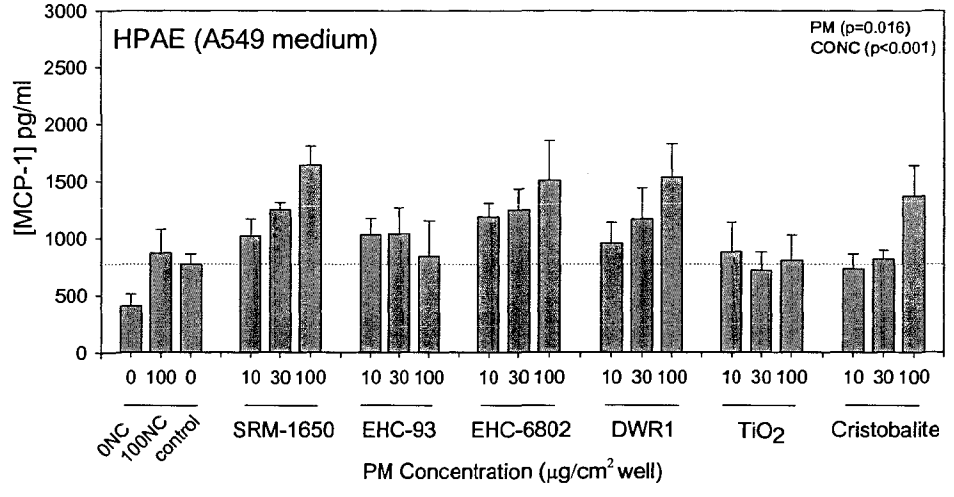
HPAE (A549 medium)
PM (p=0.016)
CONC (p<0.001)
[MCP-1] pg/ml
3000
2500
2000
1500
1000
500
0
0 100 0
10 30 100
0NC
100NC
control
SRM-1650
EHC-93
EHC-6802
DWR1
TiO2
Cristobalite
PM Concentration (µg/cm2 well)

D

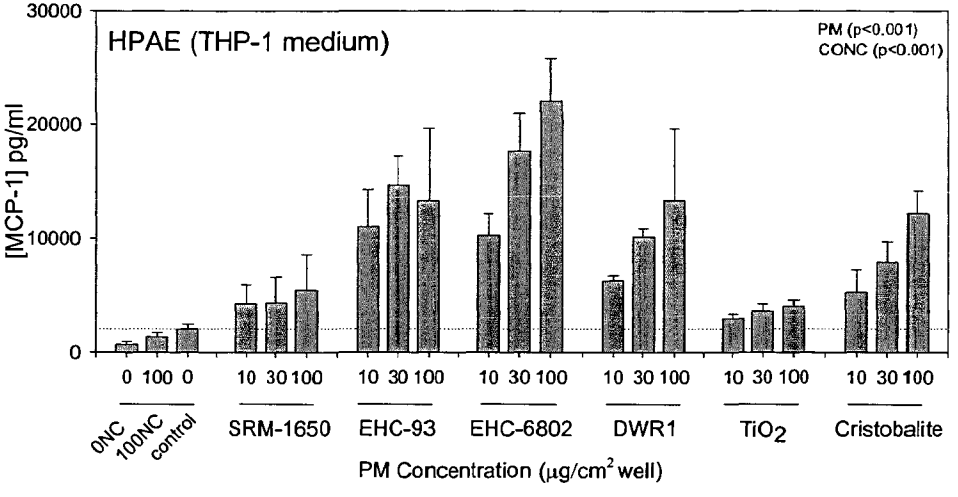
HPAE (THP-1 medium)
PM (p<0.001)
CONC (p<0.001)
[MCP-1] pg/ml
30000
20000
10000
0
0 100 0
10 30 100
0NC
100NC
control
SRM-1650
EHC-93
EHC-6802
DWR1
TiO2
Cristobalite
PM Concentration (µg/cm2 well)

Figure 2.29. Monocyte Chemoattractant Protein (MCP)-1 levels in cell culture supernatants of A549 epithelial cells (A), THP-1 macrophage cells (C) exposed for 24 hrs to particle preparations, as well as HPAE endothelial cells incubated with A549- or THP-1-conditioned media (B, D). Levels of the chemokine were determined by Bio-Plex assay. For HPAE cells, the MCP-1 levels produced are presented as the difference of MCP-1 in the cell supernatants minus the potential contribution from A549 or THP-1 mono-culture production within the conditioned media. Values are presented as mean ± standard error (n=3). PM x CONC interaction was obtained for MCP-1 levels in A549 cell supernatants. Asterisks above bars represent effects significantly different from control, where PM x CONC interaction was observed. Main effects were observed for MCP-1 levels in supernatants of THP-1 cells and HPAE cells incubated with A549- or THP-1-conditioned media (2-way ANOVA).

A

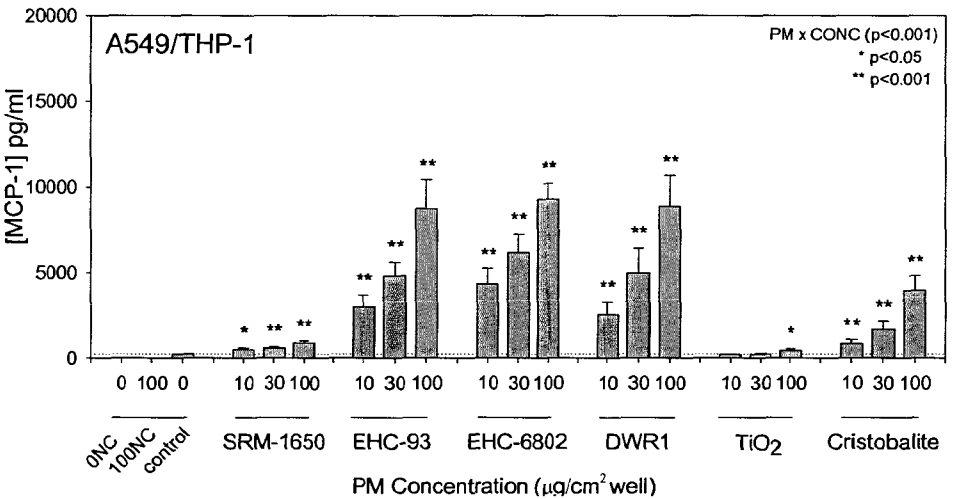
A549/THP-1
PM x CONC (p<0.001)
* p<0.05
** p<0.001
[MCP-1] pg/ml
20000
15000
10000
5000
0
0 100 0
10 30 100
10 30 100
10 30 100
10 30 100
10 30 100
10 30 100
0NC
100NC
control
SRM-1650
EHC-93
EHC-6802
DWR1
TiO2
Cristobalite
PM Concentration (μg/cm2 well)

B

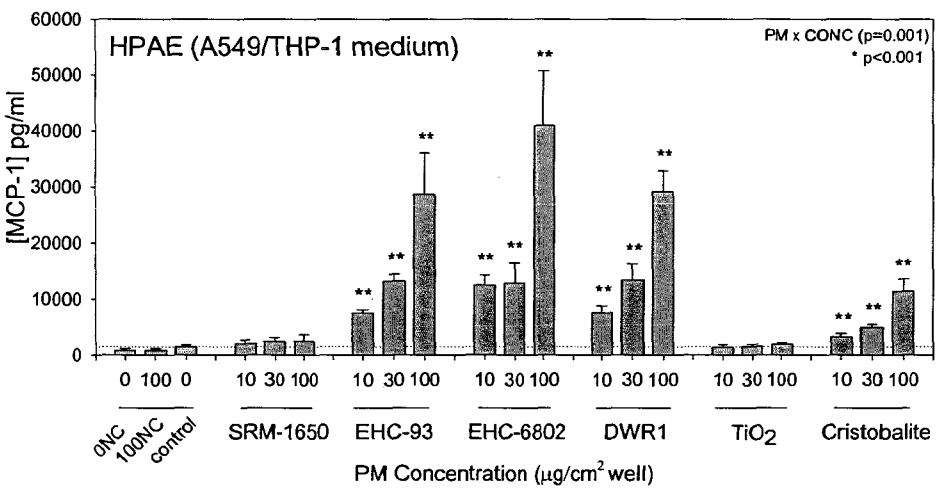
HPAE (A549/THP-1 medium)
PM x CONC (p=0.001)
* p<0.001
[MCP-1] pg/ml
60000
50000
40000
30000
20000
10000
0
0 100 0
10 30 100
10 30 100
10 30 100
10 30 100
10 30 100
10 30 100
0NC
100NC
control
SRM-1650
EHC-93
EHC-6802
DWR1
TiO2
Cristobalite
PM Concentration (μg/cm2 well)

Figure 2.30. Monocyte Chemoattractant Protein (MCP)-1 levels in cell culture supernatants of A549/THP-1 co-cultures exposed for 24 hrs to particle preparations (A), as well as HPAE endothelial cells incubated with co-culture-conditioned media (B). Levels of the chemokine were determined by Bio-Plex assay. For HPAE cells, the MCP-1 levels produced are presented as the difference of MCP-1 in the cell supernatants minus the potential contribution from A549/THP-1 co-culture production within the conditioned media. Values are presented as mean ± standard error (n=3). PM x CONC interaction was obtained for MCP-1 levels in co-culture supernatants and supernatants from HPAE cells incubated with co-culture-conditioned media, by 2-way ANOVA. Asterisks above bars represent effects significantly different from control.

SRM-1650 and TiO_2 particles, with significant PM and CONC main effects ($P<0.001$). When HPAE cells were incubated with co-culture CM, the overall MCP-1 production increased to even higher levels (~2-fold) in comparison to those detected in HPAE cells incubated in CM from THP-1 cells from urban particles and DWR1 exposures (Figures 2.29D, 2.30B). The levels of the chemokine were also higher (>3-fold) in comparison to MCP-1 levels detected in A549/THP-1 co-culture exposures to all particles (Figures 2.30A, 2.30B). The pattern of particle potency was also very similar between HPAE cell exposures to THP-1- and-co-culture CM, as well as co-cultures directly exposed to particles.

Tumor Necrosis Factor α

TNF-α was undetectable in A549 cell supernatants from particle-treated and control cells (Figure 2.31A). THP-1 cells produced high levels of TNF-α in response to EHC-93, EHC-6802 and DWR1 particle exposures, with over 1,000 pg/ml of TNF-α detectable in THP-1 cells exposed to the highest concentration of EHC-6802. The measures were statistically significant with PM and CONC main effects ($P<0.001$) (Figure 2.31C). In A549/THP-1 cells, the pattern of particle effects was similar to that observed with a number of cytokines measured in the cells, with the urban dust and DWR1 showing the strongest potency of TNF-α induction in comparison to control levels, followed by Cristobalite, SRM-1650 and TiO_2 particles (Figure 2.32A). Interestingly, the TNF-α levels induced in A549/THP-1 co-cultures by the urban dusts and DWR1 were >2-fold lower than the levels detected in supernatants of THP-1 cells exposed to the same particles (Figures 2.31C, 2.32A). HPAE cells incubated with A549 CM for 24 hrs produced only a very small amount of TNF-α (Figure 2.31B). Somewhat higher levels of TNF-α were detected in the HPAE control supernatants, as well as in the HPAE supernatants after incubations with THP-1- and co-culture CM, with overall high variability in the particle-exposure media (Figures 2.31D, 2.32B).

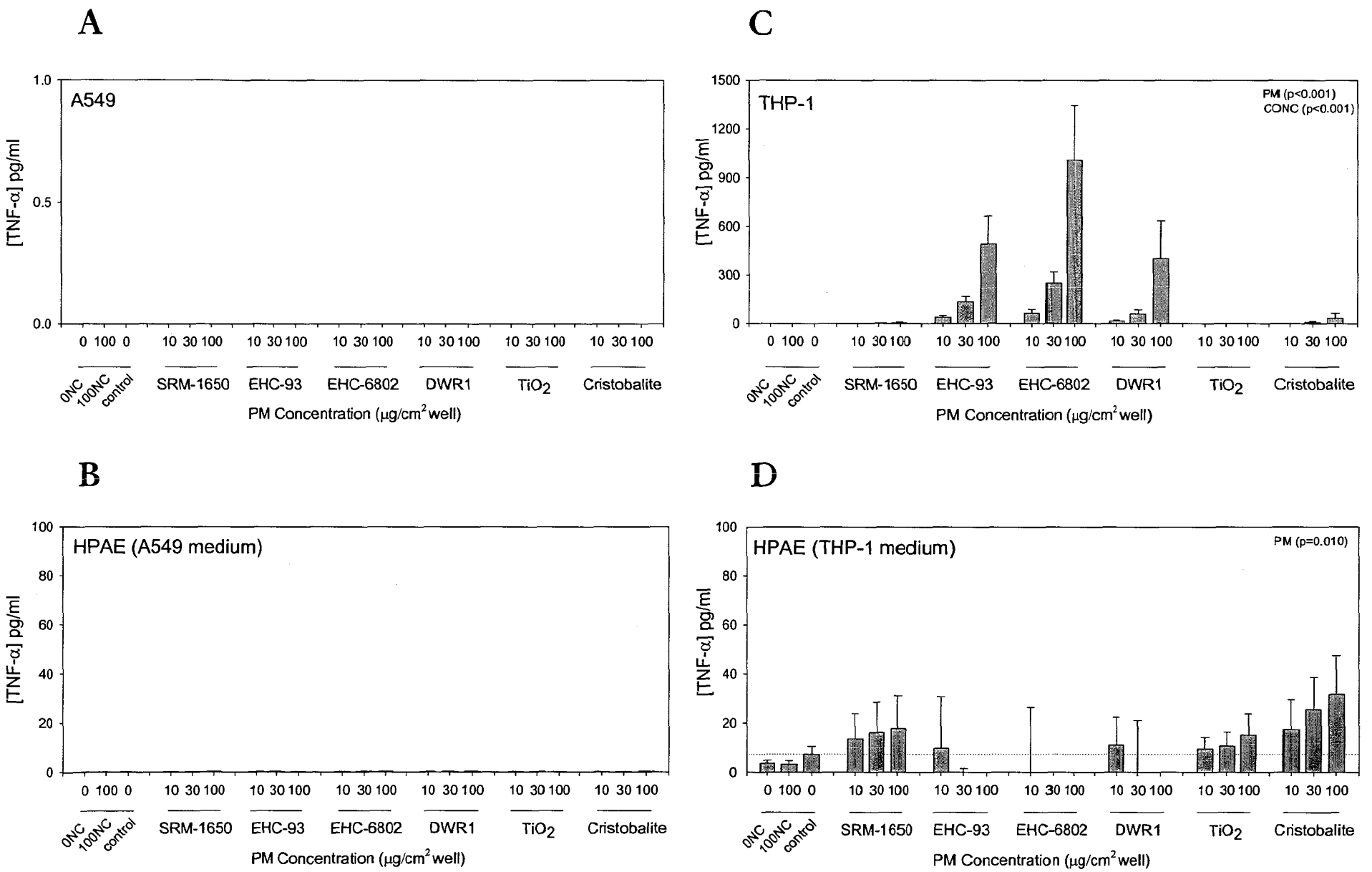
A
A549
[TNF-α] pg/ml
1.0
0.5
0.0
0 100 0
10 30 100
0NC
100NC
control
SRM-1650
EHC-93
EHC-6802
DWR1
TiO2
Cristobalite
PM Concentration (μg/cm2 well)
C
THP-1
PM (p<0.001)
CONC (p<0.001)
1500
1200
900
600
300
0
B
HPAE (A549 medium)
100
80
60
40
20
0
D
HPAE (THP-1 medium)
PM (p=0.010)

Figure 2.31. Tumor Necrosis Factor (TNF)-α levels in cell culture supernatants of A549 epithelial cells (A), THP-1 macrophage cells (C) exposed for 24 hrs to particle preparations, as well as HPAE endothelial cells incubated with A549- or THP-1-conditioned media (B, D). Levels of the cytokine were determined by Bio-Plex assay. For HPAE cells, the TNF-α levels produced are presented as the difference of TNF-α in the cell supernatants minus the potential contribution from A549 or THP-1 mono-culture production within the conditioned media. Values are presented as mean ± standard error (n=3). TNF-α was undetected in A549 cell supernatants. Differences in TNF-α levels in supernatants of HPAE cells incubated with A549-conditioned media were not statistically significant. Main effects were obtained by 2-way ANOVA for the TNF-α levels in supernatants of THP-1 cells and supernatants from HPAE cells incubated with THP-1 conditioned media.

A

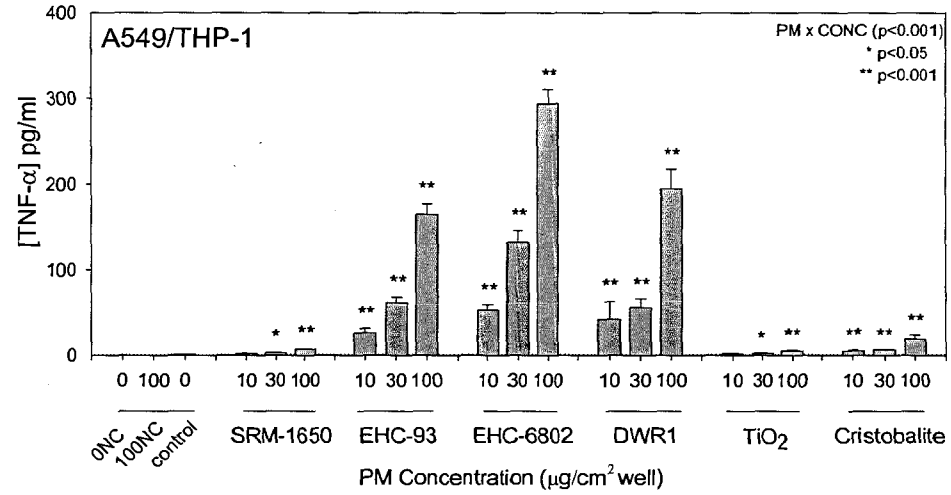
A549/THP-1
PM x CONC (p<0.001)
* p<0.05
** p<0.001
[TNF-α] pg/ml
400
300
200
100
0
0 100 0
10 30 100
10 30 100
10 30 100
10 30 100
10 30 100
10 30 100
0NC
100NC
control
SRM-1650
EHC-93
EHC-6802
DWR1
TiO2
Cristobalite
PM Concentration (μg/cm² well)

B

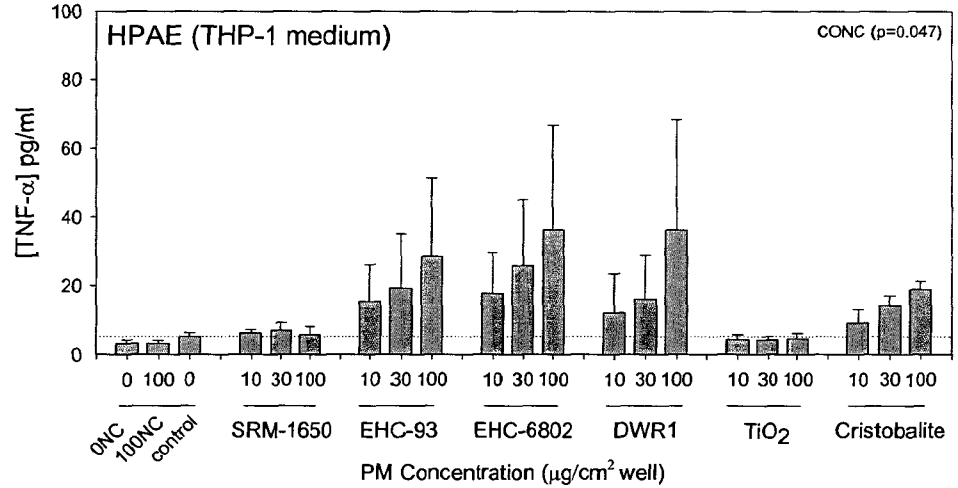
HPAE (THP-1 medium)
CONC (p=0.047)
[TNF-α] pg/ml
100
80
60
40
20
0
0 100 0
10 30 100
10 30 100
10 30 100
10 30 100
10 30 100
10 30 100
0NC
100NC
control
SRM-1650
EHC-93
EHC-6802
DWR1
TiO2
Cristobalite
PM Concentration (μg/cm² well)

Figure 2.32. Tumor Necrosis Factor (TNF)-α levels in cell culture supernatants of A549/THP-1 co-cultures exposed for 24 hrs to particle preparations (A), as well as HPAE endothelial cells incubated with co-culture-conditioned media (B). Levels of the cytokine were determined by Bio-Plex assay. For HPAE cells, the TNF-α levels produced are presented as the difference of TNF-α in the cell supernatants minus the potential contribution from A549/THP-1 co-culture production within the conditioned media. Values are presented as mean ± standard error (n=3). PM x CONC interaction was obtained for TNF-α levels in co-culture supernatants. Asterisks above bars represent effects significantly different from control, where PM x CONC interaction was observed. CONC main effect was determined by 2-way ANOVA for TNF-α levels in supernatants from HPAE cells incubated with co-culture-conditioned media.

11.3.5 Endotoxin Content of Particles

The endotoxin content of EHC-93, EHC-6802 and DWR1 particles was comparable (18 - 21 EU/mg of particle). Endotoxin was not detected in diesel particle preparation (SRM-1650), the mineral dusts (TiO_2, CRI) and the particle preparation buffer. For reference, soluble fraction of EHC-93 contained ~15 % (2.9 EU/mg) of the total EHC-93 content. (Table 2.3).

Table 2.3. Endotoxin content of particle preparations

Particle	Endotoxin Content (EU/mg particle/ml buffer)
DWR1	18.00 ± 0.88
EHC-93	20.01 ± 0.30
EHC-93*sol*	2.90 ± 0.20
EHC-6802	20.82 ± 2.03
SRM-1650	n.d.
TiO_2	n.d.
Cristobalite	n.d.
Particle Buffer	n.d.

n.d.. – not detected

11.3.6 Effects of Particles in Mice

The urban particle EHC-6802, fine particle mixture DWR1 and diesel particle SRM-1650 were chosen to represent the overall range of effects seen in the profiles of the variety of endpoints measured in the *in vitro* co-culture study experiments. The effects of these particles were examined *in vivo* upon their intra-tracheal instillation into the lungs of BALB/*c* mice. A number of endpoints were assessed in bronchoalveolar lavage and blood plasma of the animals upon their exposure to the particles for 2 and 24 hrs. A panel of biochemical endpoints (LDH, total protein) and cell differential counts in BAL (total cells, neutrophils, macrophages, band cells lymphocytes, eosinophils, monocytes, basophils and multinucleated giant cells) were assessed as an index of cytotoxicity (Figures 2.33 - 2.36). Adhesion factors ICAM-1, VCAM-1 and E-selectin were measured in BAL of the animals as factors involved in endothelial activation (Figure 2.37). The extent of pulmonary inflammation was determined from the measurements of a cytokines/chemokines profile in BAL (IL-1α, IL-1β, IL-5, IL-6, IL-10, GM-CSF, KC, MIP-1α, RANTES, TNF-α) (Figures 2.38 - 2.41). Systemic inflammatory effects were assessed by the

measurement of the blood plasma profile of cytokines/chemokines (IL-1α, IL-1β, IL-5, IL-6, IL-10, GM-CSF, KC, MIP-1α, RANTES and TNF-α) (Figures 2.42 - 2.46). The statistical significance of all measured responses was summarized in Tables A-12 to A-14.

11.3.7 Cytotoxicity in Mice

No statistically significant changes in LDH levels in BAL fluid were detected after 2 or 24 h exposure of mice to particle preparations (Figure 2.33A, 2.33B). A significant overall dose-dependent increase in total protein in BAL was observed upon 2 h intratracheal instillation of particles in mice, in comparison to control animals, although in animals exposed to particles for 24 hrs the differences in total protein were not statistically significant (Figures 2.33C, 2.33D). Macrophage clearance of particles from lungs was manifested by statistically significant dose-dependent reduction in BAL macrophage counts in animals exposed to particles for 24 hrs in comparison to control mice (Figure 2.34B). A trend of reduction in macrophage counts was observable in mice exposed to particles for 2 hrs, although without statistical significance (Figure 2.34A). Examination of neutrophil counts in BAL fluid showed that the number of neutrophils was significantly higher in animals exposed for 2 hrs to EHC-6802 and DWR1 in comparison to those exposed to diesel SRM-1650 particles. In addition, overall dose effect was observed in comparison to control mice (Figure 2.34C). After a 24 h instillation of particles, statistically significant differences in EHC-6802 and SRM-1650 exposures were observed. Additionally, the overall dose effect was also observed in particle-treated mice in comparison to control mice (Figure 2.34D). Band cells were undetectable in BAL of SRM-1650 exposed mice and in mice exposed to low dose of DWR1 for 2 hrs. A significantly increased band cell count was detected in mice exposed to EHC-6802 for 2 hrs. An overall dose effect was also observed (Figure 2.35A). After the 24 h exposure, band cells were detectable in BAL of mice exposed to every particle, showing a significant difference in BAL band cell numbers between SRM-1650 treated mice, and the mice exposed to EHC-6802 or DWR1 particles. An overall significant dose-dependent increase in the BAL lymphocyte numbers was observed in all animals exposed to particle for 2 hrs (Figure 2.35C). After 24 hrs, the number of lymphocytes did not significantly differ between the various treatments (Figure 2.35D). No significant differences in total BAL cell counts were observed in any of the particle instillations after 2 or 24 hrs (Figure 2.36A, 2.36B).

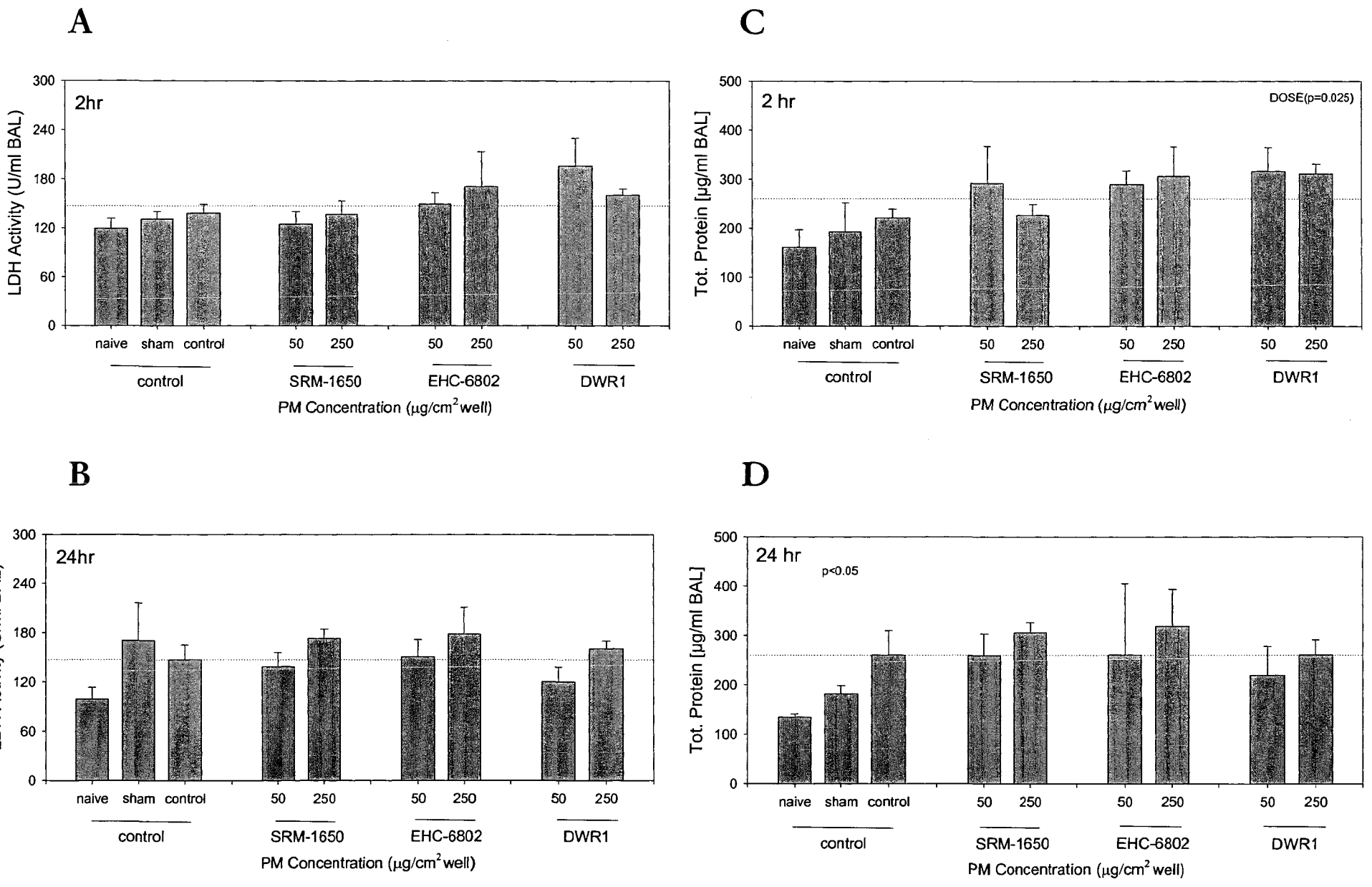
A
2hr
LDH Activity (U/ml BAL)
300
240
180
120
60
0
naive sham control 50 250 50 250 50 250
control
SRM-1650
EHC-6802
DWR1
PM Concentration (μg/cm² well)
C
2 hr
DOSE(p=0.025)
Tot. Protein [μg/ml BAL]
500
400
300
200
100
0
naive sham control 50 250 50 250 50 250
control
SRM-1650
EHC-6802
DWR1
PM Concentration (μg/cm² well)
B
24hr
LDH Activity (U/ml BAL)
300
240
180
120
60
0
naive sham control 50 250 50 250 50 250
control
SRM-1650
EHC-6802
DWR1
PM Concentration (μg/cm² well)
D
24 hr
p<0.05
Tot. Protein [μg/ml BAL]
500
400
300
200
100
0
naive sham control 50 250 50 250 50 250
control
SRM-1650
EHC-6802
DWR1
PM Concentration (μg/cm² well)

Figure 2.33. Lactate Dehydrogenase (LDH) (A, B) and total protein (C, D) levels in BAL of BALB/*c* mice exposed to particulate matter for 2 and 24 hrs by intratracheal instillation. LDH levels were measured colorimetrically by a Cytotox 96 assay. Total protein was determined colorimetrically from BAL samples, by Coomassie Assay. Values are presented as mean ± standard error (n=~5). LDH data were not statistically significant. DOSE main effect was observed for total protein detected in the 2 h time point BAL samples by 2-way ANOVA. Total protein levels showed trends without statistical significance for the 24 h time point. Statistically significant difference in total protein in BAL control samples at 24 hrs was detected by 1-way ANOVA ($P < 0.05$).

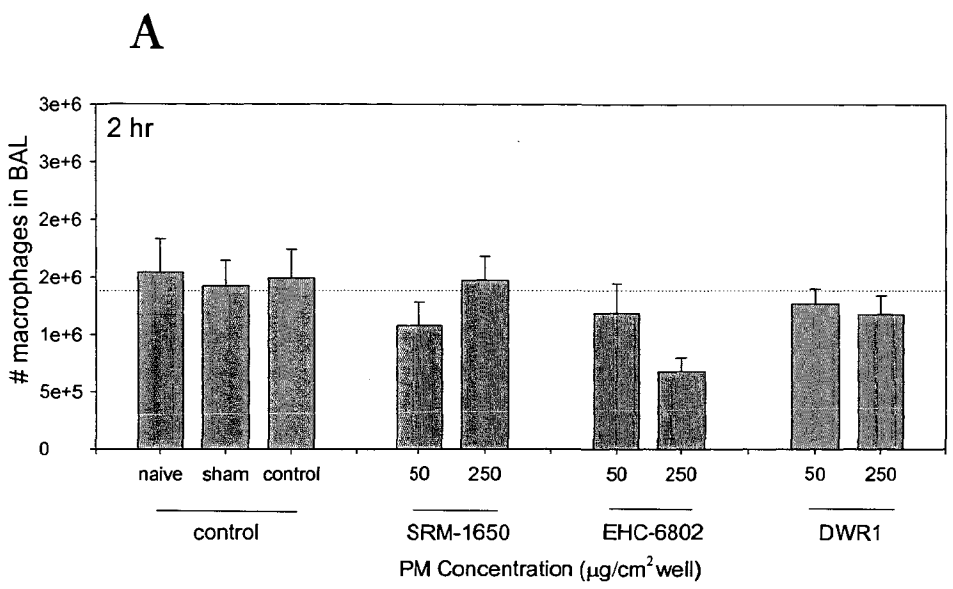
A
2 hr
macrophages in BAL
3e+6
3e+6
2e+6
2e+6
1e+6
5e+5
0
naive sham control 50 250 50 250 50 250
control
SRM-1650
EHC-6802
DWR1
PM Concentration (μg/cm² well)

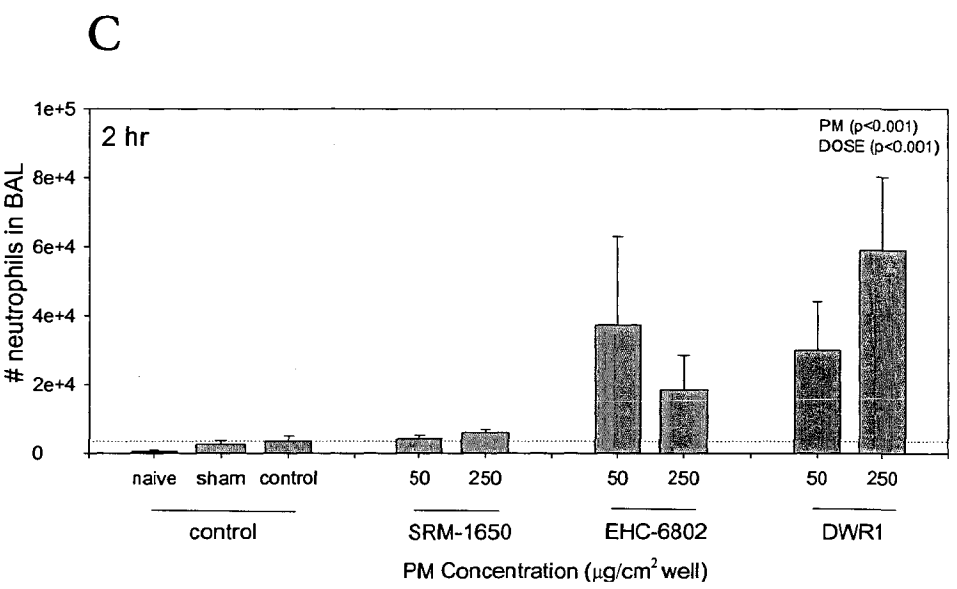
C
2 hr
PM (p<0.001)
DOSE (p<0.001)
neutrophils in BAL
1e+5
8e+4
6e+4
4e+4
2e+4
0
naive sham control 50 250 50 250 50 250
control
SRM-1650
EHC-6802
DWR1
PM Concentration (μg/cm² well)

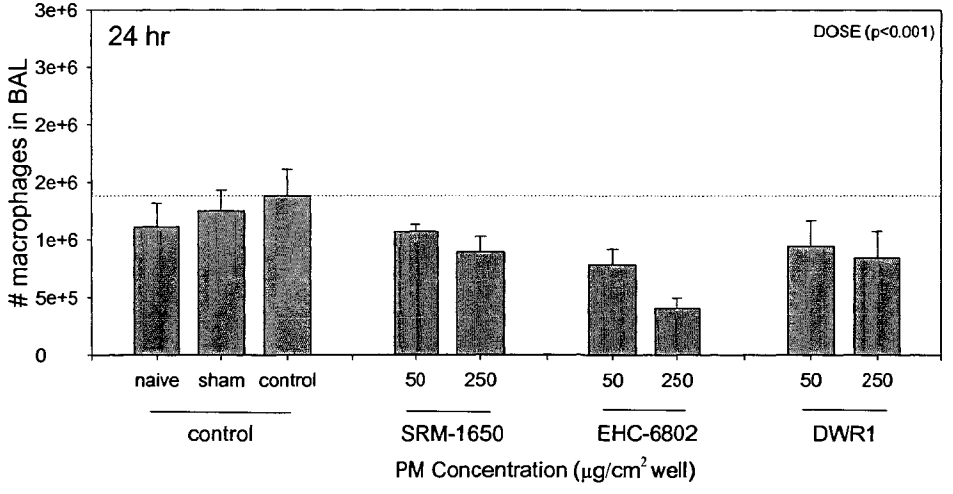
B
24 hr
DOSE (p<0.001)
macrophages in BAL
3e+6
3e+6
2e+6
2e+6
1e+6
5e+5
0
naive sham control 50 250 50 250 50 250
control
SRM-1650
EHC-6802
DWR1
PM Concentration (μg/cm² well)

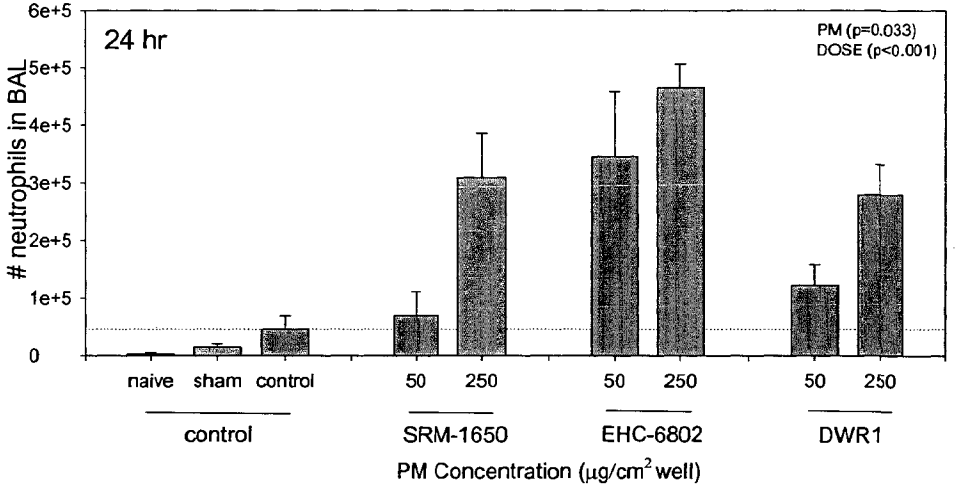
D
24 hr
PM (p=0.033)
DOSE (p<0.001)
neutrophils in BAL
6e+5
5e+5
4e+5
3e+5
2e+5
1e+5
0
naive sham control 50 250 50 250 50 250
control
SRM-1650
EHC-6802
DWR1
PM Concentration (μg/cm² well)

Figure 2.34. Macrophage (A, B) and neutrophil (C, D) cell counts in bronchoalveolar lavage (BAL) fluid of BALB/*c* mice exposed to particulate matter for 2 and 24 hrs by intratracheal instillation. Cell counts were determined from cytospin preparations of BAL. Values are presented as mean ± standard error (n= ~5). Macrophage counts at the 2 h time points were not statistically significant. DOSE main effect was observed for 24 h macrophage counts. PM and DOSE main effects were obtained for neutrophil cell counts by 2-way ANOVA .

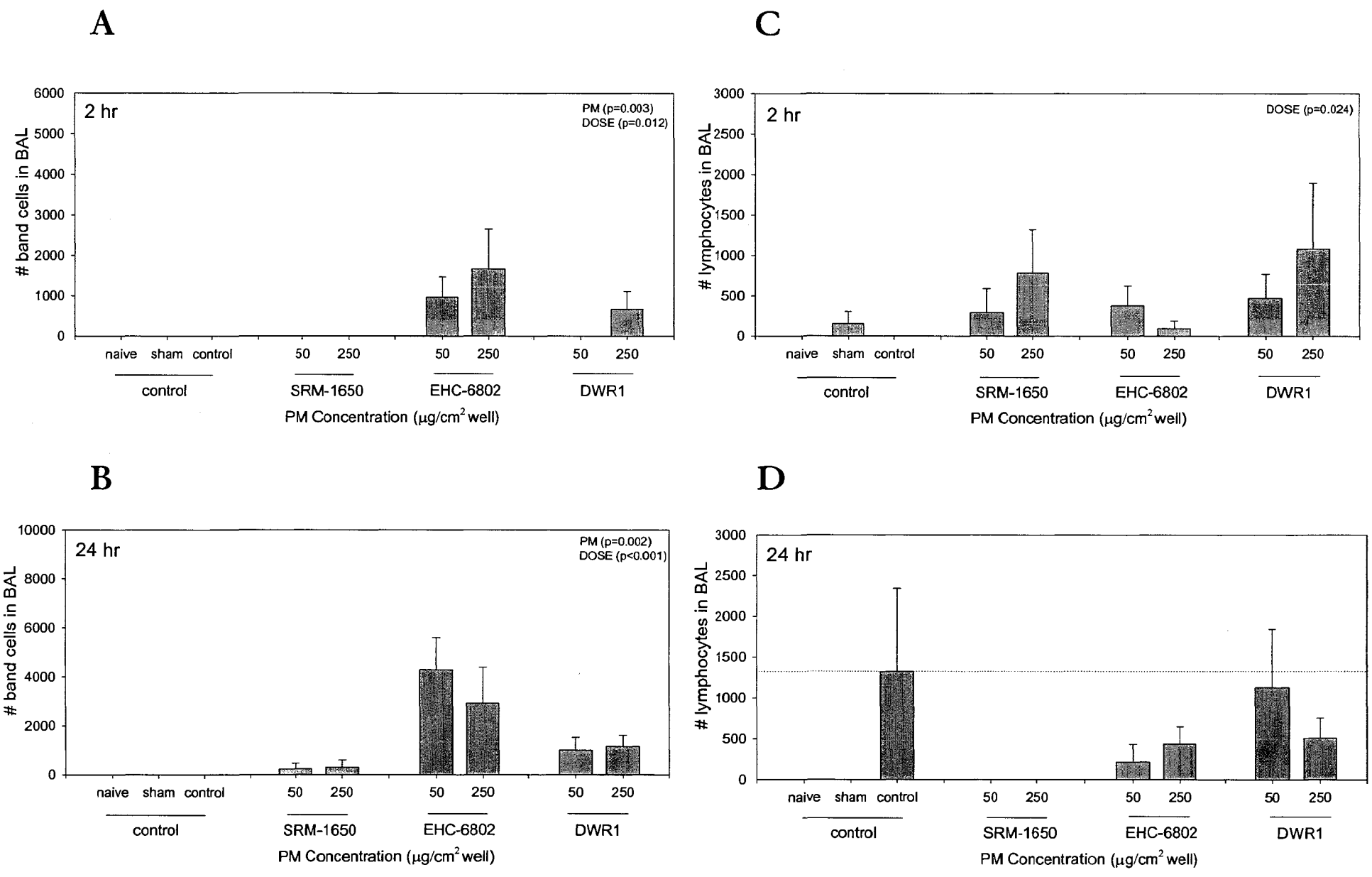
A
2 hr
PM (p=0.003)
DOSE (p=0.012)
band cells in BAL
6000
5000
4000
3000
2000
1000
0
naive sham control 50 250 50 250 50 250
control
SRM-1650
EHC-6802
DWR1
PM Concentration (μg/cm² well)
C
2 hr
DOSE (p=0.024)
lymphocytes in BAL
3000
2500
2000
1500
1000
500
0
naive sham control 50 250 50 250 50 250
control
SRM-1650
EHC-6802
DWR1
PM Concentration (μg/cm² well)
B
24 hr
PM (p=0.002)
DOSE (p<0.001)
band cells in BAL
10000
8000
6000
4000
2000
0
naive sham control 50 250 50 250 50 250
control
SRM-1650
EHC-6802
DWR1
PM Concentration (μg/cm² well)
D
24 hr
lymphocytes in BAL
3000
2500
2000
1500
1000
500
0
naive sham control 50 250 50 250 50 250
control
SRM-1650
EHC-6802
DWR1
PM Concentration (μg/cm² well)

Figure 2.35. Band cells (A, B) and lymphocyte (C, D) counts in bronchoalveolar lavage (BAL) fluid of BALB/*c* mice exposed to particulate matter for 2 and 24 hrs by intratracheal instillation. Cell counts were determined from cytospin preparations of BAL. Values are presented as mean ± standard error (n= ~5). PM and DOSE main effects were obtained for band cell counts. DOSE main effect was observed for 2 h lymphocyte counts by 2-way ANOVA. Lymphocyte counts at the 24 h time points were not statistically significant.

A

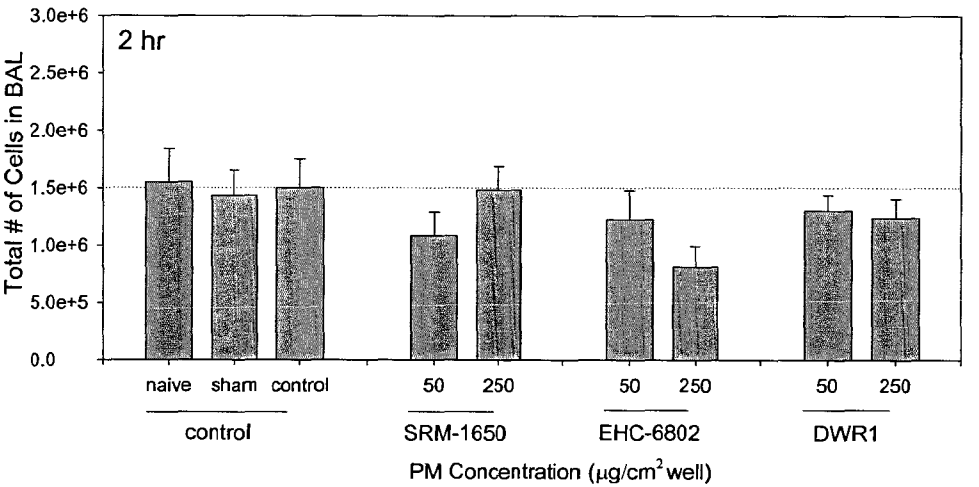
2 hr
Total # of Cells in BAL
3.0e+6
2.5e+6
2.0e+6
1.5e+6
1.0e+6
5.0e+5
0.0
naive
sham
control
50
250
50
250
50
250
control
SRM-1650
EHC-6802
DWR1
PM Concentration (μg/cm² well)

B

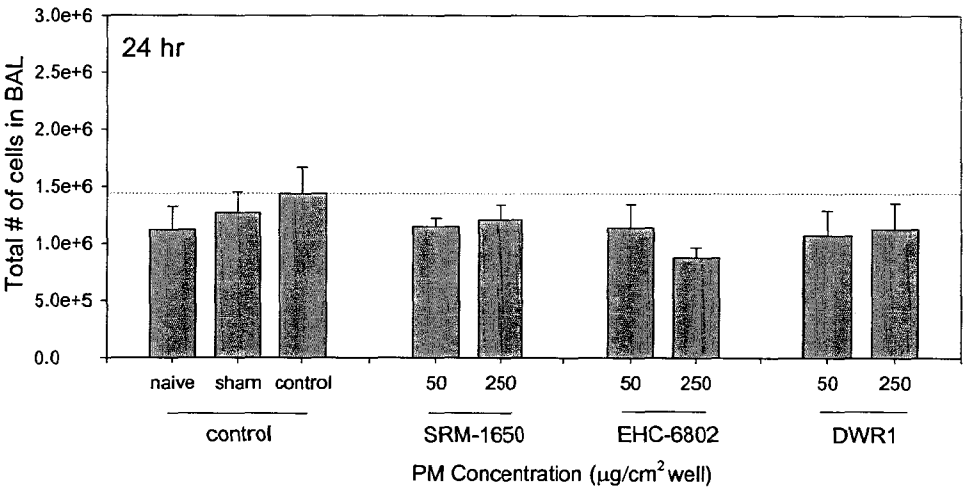
24 hr
Total # of cells in BAL
3.0e+6
2.5e+6
2.0e+6
1.5e+6
1.0e+6
5.0e+5
0.0
naive
sham
control
50
250
50
250
50
250
control
SRM-1650
EHC-6802
DWR1
PM Concentration (μg/cm² well)

Figure 2.36. Total cell counts in bronchoalveolar lavage (BAL) fluid of BALB/*c* mice exposed to particulate matter for 2 hrs (A) and 24 hrs (B) by intratracheal instillation. Cell counts were determined from cytospin preparations of BAL. Values are presented as mean ± standard error (n = ~5). Total cell counts were not statistically significant by 2-way ANOVA.

Adhesion Factors

ICAM-1 was detected in BAL fluid of mice 2 hrs after particle instillation, although no significant changes in ICAM-1 were observed (Figure 2.37A). In mice exposed to particles for 24 hrs, a significant dose effect was observed showing overall increased levels of ICAM-1 in BAL in particle treated mice in comparison to control mice (Figure 2.37B). The levels of the adhesion factor VCAM-1 in mice exposed to EHC-6802 or DWR1 particles for 2 hrs were significantly elevated compared to VCAM-1 levels in mice exposed to SRM-1650. Overall, the levels of VCAM-1 were higher in mice exposed to the high dose of the particles in comparison to control mice (Figure 2.37C). In mice exposed to particles for 24 hrs, VCAM-1 levels for the various treatments were not statistically significant (Figure 2.37D). E-selectin was not detected in BAL fluid from mice after 2 or 24 h instillations of particles.

11.3.8 Pulmonary Inflammation

Interleukin 1α and 1β

Exposure of the mice to particle preparations for 2 hrs resulted in significant particle type- and dose-dependent changes in IL-1α levels in BAL of the treated mice. Animals exposed to EHC-6802 and DWR1 particles displayed BAL IL-1α levels which were higher than those detected in mice exposed to SRM-1650 particles (Figure 2.38A). IL-1α levels significantly increased in mice exposed to EHC-6802 for 24 hrs in comparison to SRM-1650 and DWR1 particles. A significant overall particle dose effect was observed in comparison to control mice (Figure 2.38B). IL-1β was not detected in the BAL fluid samples from mice exposed to particles or vehicle controls for both time points.

Interleukin 5

IL-5 cytokine levels were significantly elevated in BAL of mice exposed to EHC-6802 and DWR1 particles in comparison to diesel-exposed mice in 2 h exposures (Figure 2.38C). The effect was not sustained over time, as mice exposed to the particles did not show statistically significant differences in IL-5 levels in BAL fluid (Figure 2.38D).

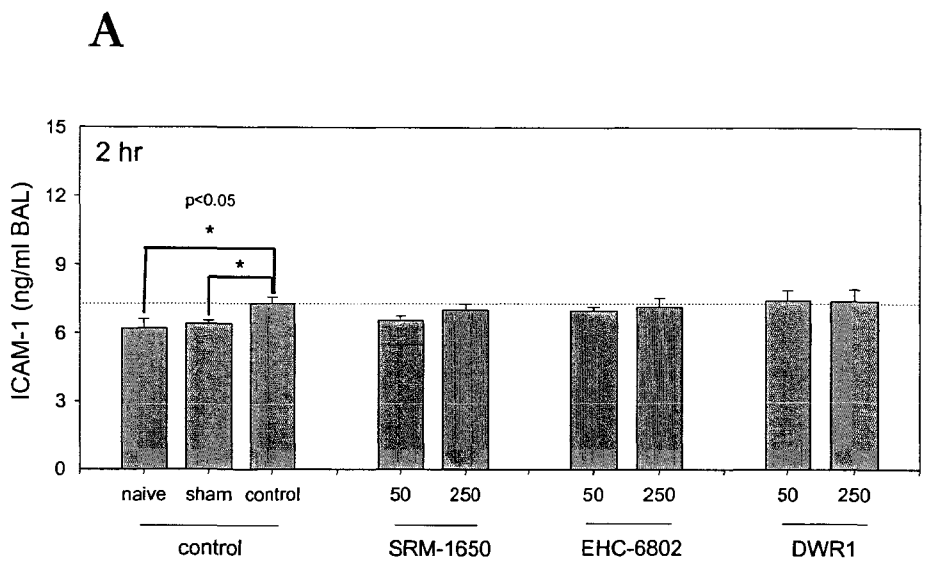
A
2 hr
ICAM-1 (ng/ml BAL)
p<0.05
naive
sham
control
50
250
control
SRM-1650
EHC-6802
DWR1

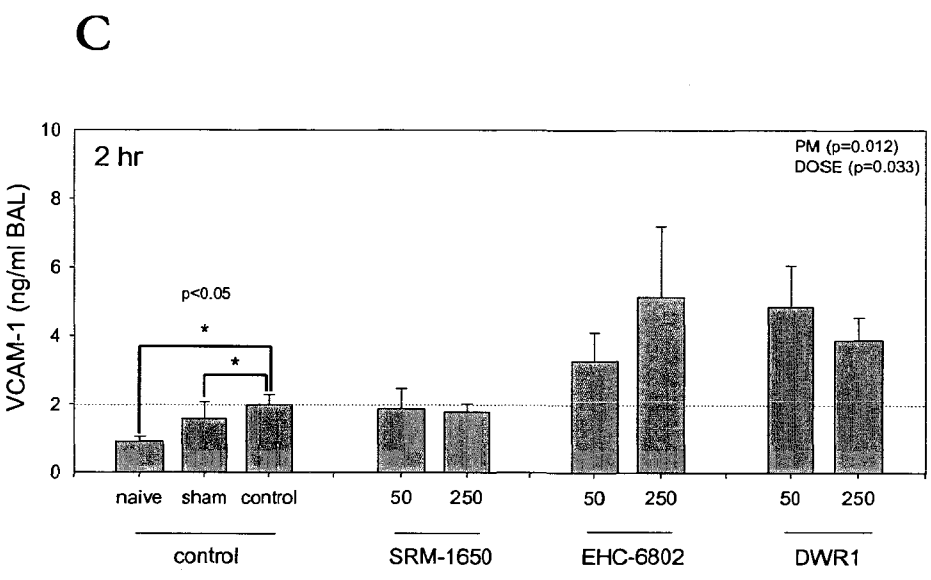
C
2 hr
PM (p=0.012)
DOSE (p=0.033)
VCAM-1 (ng/ml BAL)
p<0.05
naive
sham
control
50
250
control
SRM-1650
EHC-6802
DWR1

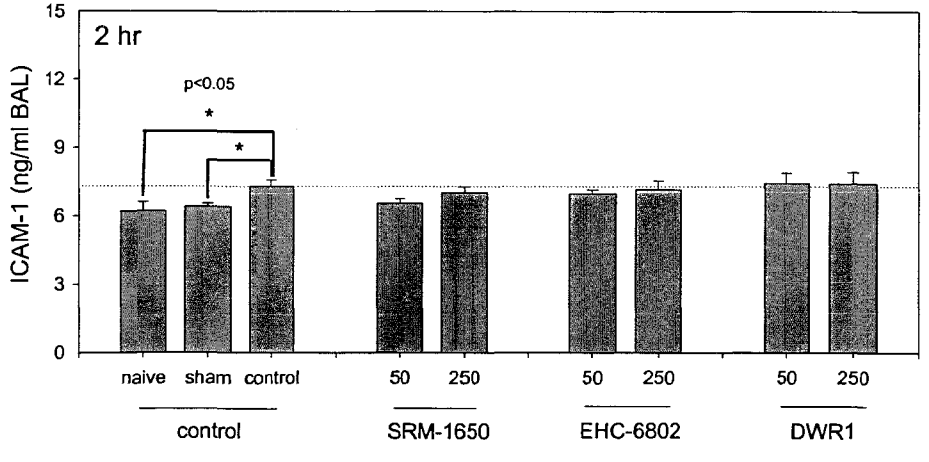
B
2 hr
ICAM-1 (ng/ml BAL)
p<0.05
naive
sham
control
50
250
control
SRM-1650
EHC-6802
DWR1

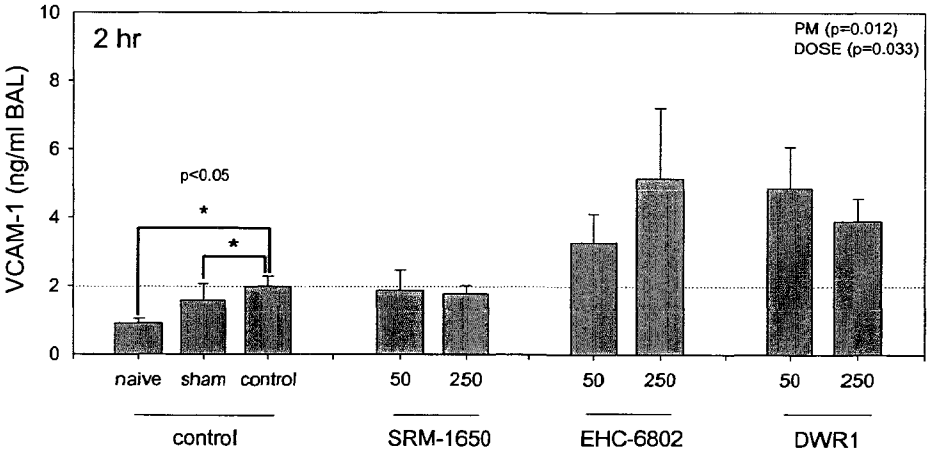
D
2 hr
PM (p=0.012)
DOSE (p=0.033)
VCAM-1 (ng/ml BAL)
p<0.05
naive
sham
control
50
250
control
SRM-1650
EHC-6802
DWR1

Figure 2.37. Intercellular Adhesion Molecule (ICAM)-1 (A, B) and Vascular Cell Adhesion Molecule (VCAM)-1 (C, D) levels in bronchoalveolar lavage fluid (BAL) of BALB/*c* mice exposed to particulate matter for 2 and 24 h by intratracheal instillation. Levels of the adhesion factors were determined by Bio-Plex assay. Values are presented as mean ± standard error (n= ~5). ICAM-1 levels were not statistically significant at the 2 h time point. DOSE main effect was observed for ICAM-1 at 24 h time point. PM and DOSE main effects were obtained for VCAM-1 BAL levels at 2 hrs by 2-way ANOVA. VCAM-1 levels were not statistically significant at the 24 h time point. Statistically significant differences ICAM-1 levels at 2 hrs and VCAM-1 levels at 2 and 24 hrs were detected in BAL control samples by 1-way ANOVA ($P < 0.05$).

Interleukin 6

IL-6 levels were significantly higher in BAL of mice exposed to EHC-6802, or DWR1 particles for 2 hrs in comparison to diesel-exposed mice. In 24 h exposures of mice, the levels of EHC-6802 were still elevated in comparison to diesel-treated animals, however, ~5-fold lower in magnitude, in comparison to the BAL levels detected in the 2 h exposure. The DWR1 levels have substantially decreased after 24 hrs, and were no longer significantly different form diesel-exposed animals (Figures 2.39A, 2.39B).

Interleukin 10

IL-10 cytokine was detectable in BAL of all animals at both time points. In mice exposed for 2 hrs to the particles, an overall main effect was detectable for low dose exposures in comparison to control animals ($p=0.025$). No significant differences in the BAL levels of the cytokine remained between the various treatments in mice exposed to particles for 24 hrs (Figures 2.39C, 2.39D).

Granulocyte-Macrophage Colony-Stimulating Factor

Significantly elevated levels of GM-CSF were measured in BAL of mice exposed to EHC-6802 particles, with overall significant particle dose effect also observed in 2 h exposures. GM-CSF levels in mice exposed to 50 μg and 250 μg doses of EHC-6802 were ~8-fold and 30-fold elevated in comparison to control mice (Figure 2.40A). After 24 hrs, GM-CSF levels in EHC-6802-exposed mice were no longer significant and have overall decreased ~3-fold in comparison to those measured in 2 h exposures, , although still showing a trend of treatment-dependent increase (Figure 2.40B).

Keratinocyte-derived Chemokine

Statistically significant elevations in KC were measured BAL of mice exposed to all three particles. The effects of particles on BAL KC levels were significantly different from control in mice exposed to both doses of EHC-6802 and DWR1 and in mice exposed to 250 μg dose of SRM-1650. EHC-6802 was most potent in stimulating KC release, followed by DWR1 and diesel particles (Figure 2.40C). After 24 hrs, the levels of KC from all treatments have markedly declined, with no statistically significant differences between particle exposures remaining. An overall

significant high dose main effect only remained in 24 h exposures in comparison to control mice (Figure 2.40D).

Macrophage Inflammatory Protein 1α

MIP-1α chemokine was measured in BAL fluid from mice 2 hrs after intratracheal instillation of the particles. Significantly elevated levels of the chemokine were detectable in mice exposed to EHC-6802 and DWR1 particles. Interestingly, DWR1 was more potent in comparison to EHC-6802 in stimulating MIP-1α release into BAL in the 2 h exposure. A clear dose response was observed in DWR1-treated animals, while EHC-6802 animals did not show a defined dose response (Figure 2.41A). Interestingly, 24 hrs upon instillation of the particles into mice, MIP-1α BAL levels in EHC-6802-exposed mice were significantly elevated in comparison to the diesel – exposed animals, with an overall particle dose effect in comparison to control mice. The levels of MIP-1α in DWR1 treated mice have substantially declined 24 hrs upon particle instillation and were no longer significant (Figure 2.41B).

Tumor Necrosis Factor α

An acute significant elevation of TNF-α was detected in BAL fluid from mice exposed to EHC-6802 and DWR1 particles for 2 hrs, with 4,000 – 6,000 pg/ml of the cytokine measured in the BAL samples from 250 μg dose exposures of these particles. A trend of increased TNF-α was observed in high dose diesel-exposed animals, although without statistical significance due to high variability in the measurement (Figure 2.41C). When BAL samples from mice exposed to particles for 24 hrs were assessed for the presence of TNF-α, significant elevations with EHC-6802 and DWR1 were still detectable, although at much lower magnitude in comparison to 2 hr exposures, with only <70 pg/ml detected in BAL samples from 250 μg dose exposures of EHC-6802. TNF-α levels in BAL of DWR1-exposed mice substantially declined, with no clear dose response remaining in 24 h exposures in comparison to 2 h exposures. TNF-α levels in BALof mice exposed for 24 hrs to the high dose of SRM-1650 were significantly elevated in comparison to controls, although the magnitude of the BAL TNF-α levels was much lower in comparison to EHC-6802. EHC-6802 was the most potent particle, followed by DWR1 and SRM-1650 (Figure 2.41D).

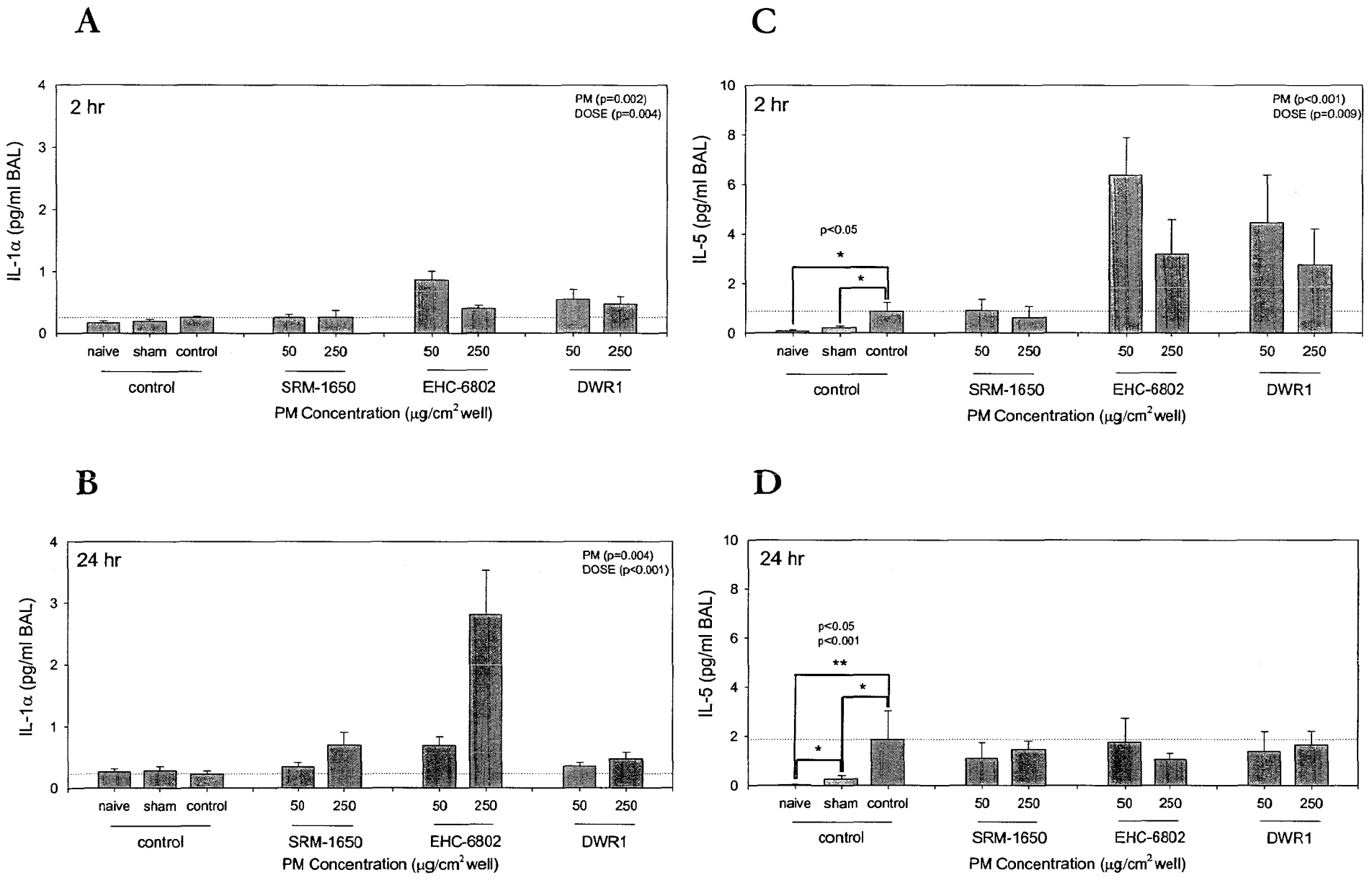
A
2 hr
PM (p=0.002)
DOSE (p=0.004)
IL-1α (pg/ml BAL)
naive sham control 50 250 50 250 50 250
control
SRM-1650
EHC-6802
DWR1
PM Concentration (μg/cm² well)
C
2 hr
PM (p<0.001)
DOSE (p=0.009)
IL-5 (pg/ml BAL)
p<0.05
naive sham control 50 250 50 250 50 250
control
SRM-1650
EHC-6802
DWR1
PM Concentration (μg/cm² well)
B
24 hr
PM (p=0.004)
DOSE (p<0.001)
IL-1α (pg/ml BAL)
naive sham control 50 250 50 250 50 250
control
SRM-1650
EHC-6802
DWR1
PM Concentration (μg/cm² well)
D
24 hr
p<0.05
p<0.001
IL-5 (pg/ml BAL)
naive sham control 50 250 50 250 50 250
control
SRM-1650
EHC-6802
DWR1
PM Concentration (μg/cm² well)

Figure 2.38. Interleukin (IL)-1α (A, B) and IL-5 (C, D) levels in bronchoalveolar lavage (BAL) fluid of BALB/*c* mice exposed to particulate matter for 2 and 24 hrs by intratracheal instillation. Cytokine levels in BAL were determined by Bio-Plex assay. Values are presented as mean ± standard error (n = ~5). PM and DOSE main effects were obtained for IL-1α at both time points and for IL-5 at 2 hrs by 2-way ANOVA (not shown). IL-5 levels were not statistically significant at the 24 h time point. Statistically significant differences in IL-5 levels in BAL control samples at 2 and 24 hrs were detected by 1-way ANOVA (*P <0.05; **P <0.001).

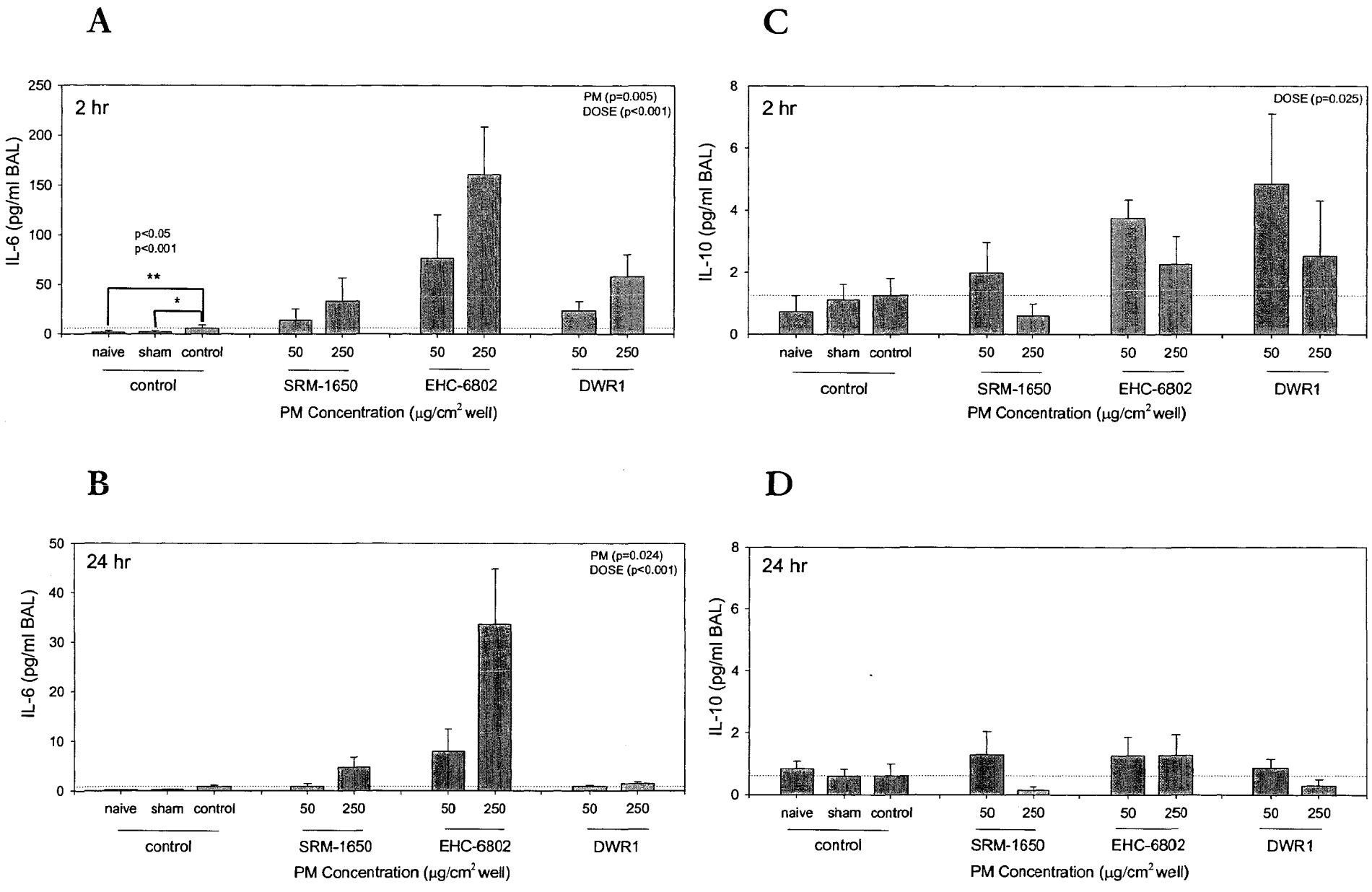
A
2 hr
PM (p=0.005)
DOSE (p<0.001)
IL-6 (pg/ml BAL)
250
200
150
100
50
0
p<0.05
p<0.001
**
*
naive sham control
50 250 50 250 50 250
control
SRM-1650
EHC-6802
DWR1
PM Concentration (μg/cm² well)
C
2 hr
DOSE (p=0.025)
IL-10 (pg/ml BAL)
8
6
4
2
0
naive sham control
50 250 50 250 50 250
control
SRM-1650
EHC-6802
DWR1
PM Concentration (μg/cm² well)
B
24 hr
PM (p=0.024)
DOSE (p<0.001)
IL-6 (pg/ml BAL)
50
40
30
20
10
0
naive sham control
50 250 50 250 50 250
control
SRM-1650
EHC-6802
DWR1
PM Concentration (μg/cm² well)
D
24 hr
IL-10 (pg/ml BAL)
8
6
4
2
0
naive sham control
50 250 50 250 50 250
control
SRM-1650
EHC-6802
DWR1
PM Concentration (μg/cm² well)

Figure 2.39. Interleukin (IL)-6 (A, B) and IL-10 (C, D) levels in bronchoalveolar lavage (BAL) fluid of BALB/*c* mice exposed to particulate matter for 2 and 24 hrs by intratracheal instillation. Cytokine levels in BAL were determined by Bio-Plex assay. Values are presented as mean ± standard error (n=~5). PM and DOSE main effects were obtained for IL-6 levels at both time points. DOSE main effect was observed for IL-10 at 2 hrs by 2-way ANOVA. IL-10 levels at 24 hrs were not statistically significant. Statistically significant difference in IL-6 in BAL control samples at 2 hrs was detected by 1-way ANOVA (*$P < 0.05$; **$P < 0.001$).

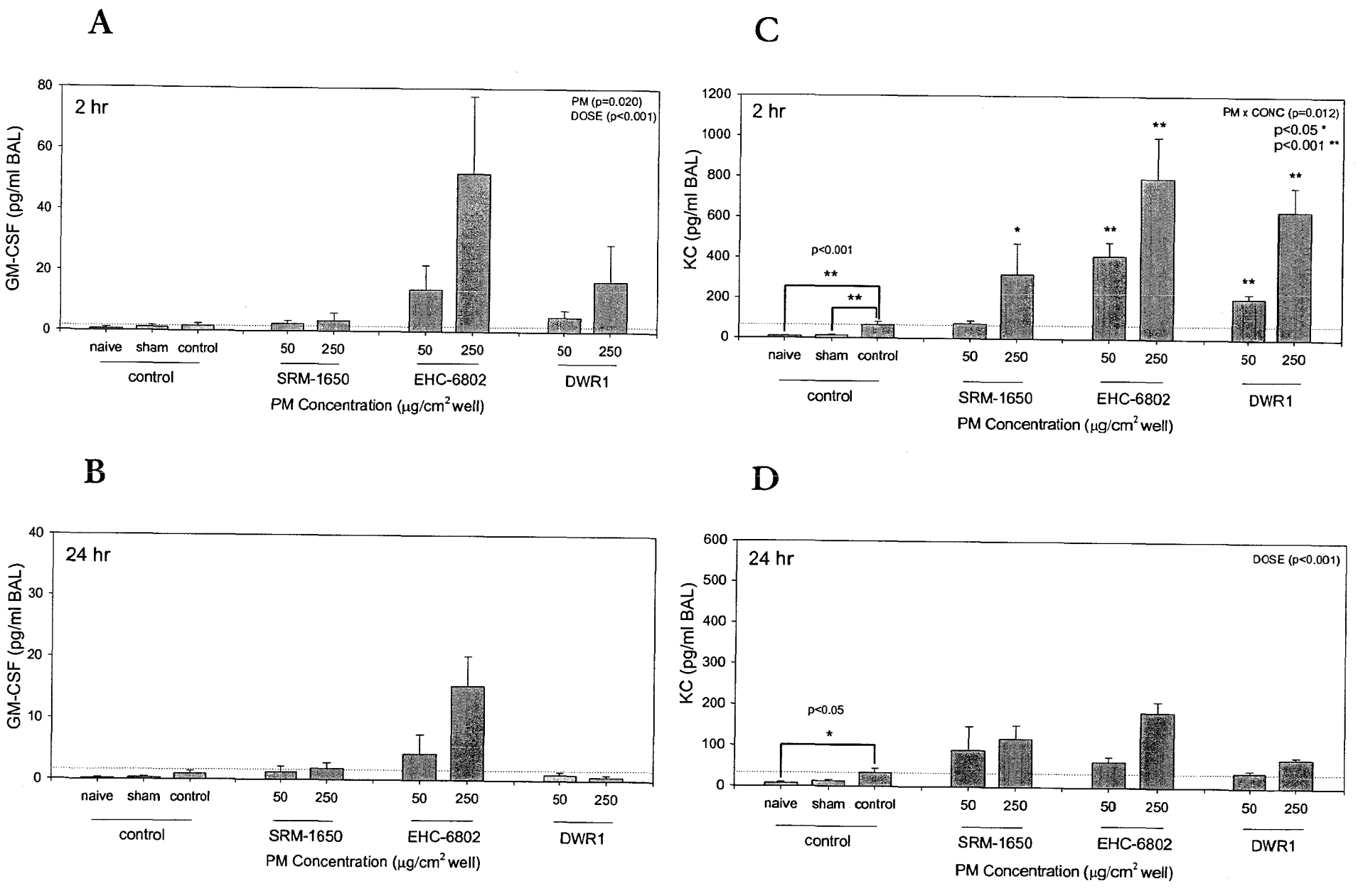
A
2 hr
PM (p=0.020)
DOSE (p<0.001)
GM-CSF (pg/ml BAL)
80
60
40
20
0
naive sham control
50 250
50 250
50 250
control
SRM-1650
EHC-6802
DWR1
PM Concentration (μg/cm² well)
C
2 hr
PM x CONC (p=0.012)
p<0.05 *
p<0.001 **
KC (pg/ml BAL)
1200
1000
800
600
400
200
0
p<0.001
**
**
*
**
**
**
**
naive sham control
50 250
50 250
50 250
control
SRM-1650
EHC-6802
DWR1
PM Concentration (μg/cm² well)
B
24 hr
GM-CSF (pg/ml BAL)
40
30
20
10
0
naive sham control
50 250
50 250
50 250
control
SRM-1650
EHC-6802
DWR1
PM Concentration (μg/cm² well)
D
24 hr
DOSE (p<0.001)
KC (pg/ml BAL)
600
500
400
300
200
100
0
p<0.05
*
naive sham control
50 250
50 250
50 250
control
SRM-1650
EHC-6802
DWR1
PM Concentration (μg/cm² well)

Figure 2.40. Granulocyte-Macrophage Colony-Stimulating Factor (GM-CSF) (A, B) and Keratinocyte-derived Chemokine (KC) (C, D) levels in bronchoalveolar lavage (BAL) fluid of BALB/*c* mice exposed to particulate matter for 2 and 24 hrs by intratracheal instillation. Chemokine levels in BAL were determined by Bio-Plex assay. Values are presented as mean ± standard error (n= ~5). PM and DOSE main effects were obtained for GM-CSF levels in BAL at 2 h time point. GM-CSF levels were statistically insignificant at 24 hrs. Dose main effect was observed for KC at 24 hrs. PM x DOSE interaction was seen for KC at 2 h time point. Asterisks above bars represent dose effects significantly different from control, where PM x CONC interaction was observed (2-way ANOVA). Statistically significant differences KC in BAL control samples at 2 and 24 hrs were detected by 1-way ANOVA (*$P < 0.05$; **$P < 0.001$).

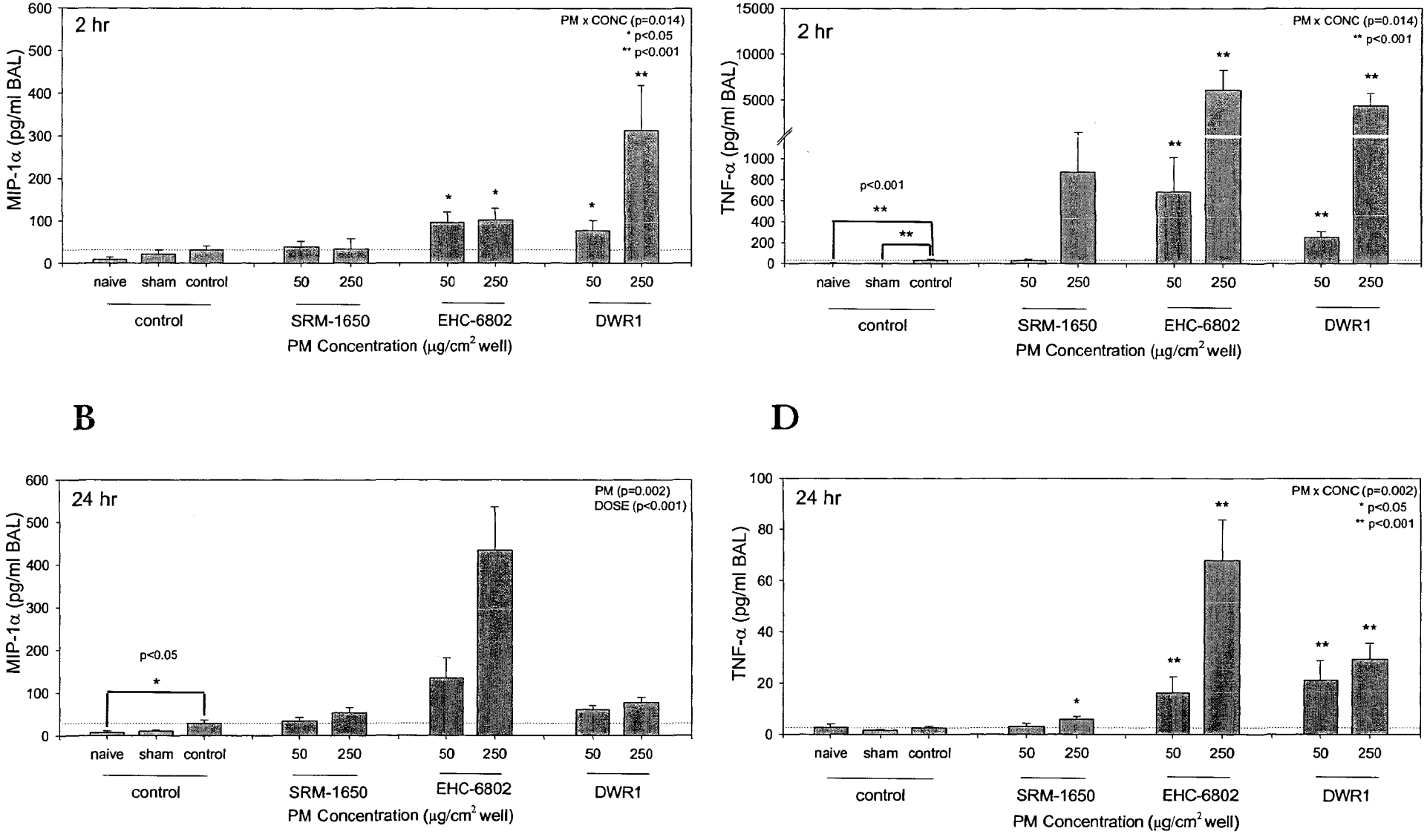
A
2 hr
PM x CONC (p=0.014)
* p<0.05
** p<0.001
MIP-1α (pg/ml BAL)
600
500
400
300
200
100
0
naive sham control
50 250 50 250 50 250
control
SRM-1650
EHC-6802
DWR1
PM Concentration (μg/cm² well)
C
2 hr
PM x CONC (p=0.014)
** p<0.001
TNF-α (pg/ml BAL)
15000
10000
5000
1000
800
600
400
200
0
p<0.001
**
**
naive sham control
50 250 50 250 50 250
control
SRM-1650
EHC-6802
DWR1
PM Concentration (μg/cm² well)
B
24 hr
PM (p=0.002)
DOSE (p<0.001)
MIP-1α (pg/ml BAL)
600
500
400
300
200
100
0
p<0.05
*
naive sham control
50 250 50 250 50 250
control
SRM-1650
EHC-6802
DWR1
PM Concentration (μg/cm² well)
D
24 hr
PM x CONC (p=0.002)
* p<0.05
** p<0.001
TNF-α (pg/ml BAL)
100
80
60
40
20
0
naive sham control
50 250 50 250 50 250
control
SRM-1650
EHC-6802
DWR1
PM Concentration (μg/cm² well)

Figure 2.41. Macrophage Inflammatory Protein (MIP)-1α (A, B) and Tumor Necrosis Factor (TNF)-α (C, D) levels in bronchoalveolar lavage (BAL) fluid of BALB/*c* mice exposed to particulate matter for 2 and 24 hrs by intratracheal instillation. Cytokine and chemokine levels in BAL were determined by Bio-Plex assay. Values are presented as mean ± standard error (n=~5). PM and DOSE main effects were observed for BAL MIP-1α levels at 24 hrs. PM x DOSE interaction was seen for MIP-1α levels at 2 hrs and TNF-α levels at both time points. Asterisks above bars represent dose effects significantly different from control (2-way ANOVA). Statistically significant differences in MIP-1α in BAL controls at 24 hrs and TNF-α in BAL controls at 2 hrs were detected by 1-way ANOVA (*$P < 0.05$; **$P < 0.001$).

11.3.9 Systemic Inflammation

The cytokines IL-1α, IL-1β, IL-5, IL-6, IL-10 and TNF-α were all present in the blood plasma samples from mice exposed to particles and in control mice at both time points, however, no statistically significant differences were obtained between the various treatments for all of these cytokines, with high variability in the various measurements observed (Figures 2.42 - 2.44B).

Granulocyte-Macrophage Colony-Stimulating Factor

The chemokine GM-CSF was detected in blood plasma of all animals at both time points. In mice exposed for 2 hrs to the particles, an overall main effect was observed for the exposure to both, low and high doses in comparison to control mice ($p=0.003$). No significant differences in plasma GM-CSF levels remained between the various treatments in mice exposed to particles for 24 hrs (Figures 2.44C, 2.44D).

Keratinocyte-derived Chemokine

Cytokine analysis of blood plasma taken from mice intratracheally exposed to particles for 2 hrs showed the presence of KC in the samples. KC levels were overall elevated in plasma from particle-treated mice in comparison to control mice, with particle dose main effect ($p=0.033$), without significant differences between the various particle treatments. No significant differences in plasma KC levels were observed in mice exposed to particles for 24 hrs (Figures 2.45A, 2.45B).

Macrophage Inflammatory Protein 1α

MIP-1α chemokine was overall elevated in blood plasma of mice exposed to particles in comparison to control mice, with significant particle dose effect ($p<0.001$). The 2 h exposures did not reveal any significant differences between the effects of particles on MIP-1α plasma levels in the treated mice (Figure 2.45C). No changes were observed in plasma levels of the chemokine upon 24 h exposure of mice to particles preparations (Figure 2.45D).

Regulated upon Activation Normal T cell Expressed and Secreted

When mice were exposed to DWR1 particles for 2 hrs by intratracheal instillation, plasma levels of RANTES were found to be elevated in mice in comparison to mice exposed to SRM-1650 or EHC-6802 particle preparations, without a defined dose response (Figure 2.46A). In 24 h exposures of animals to particles, the DWR-induced effect on RANTES levels was no longer significant. An overall 50 μg dose effect was observed in 24 h exposure blood plasma samples, in comparison to control mice (Figure 2.46B).

11.3.10 Correlation of PM-Induced BAL Neutrophilia with *In Vitro* Co-culture Model Responses

The parametric test Pearson Product Moment Correlation was used to examine the association of BAL neutrophil counts at 2 and 24 h time points with the *in vitro* endpoints measured in mono- and co-cultures of A549 and THP-1 cells directly exposed to particles for 24hrs. The analysis was also conducted with HPAE cells exposed for 24 hrs to CM from the mono- and co-cultures of A549 and THP-1 cells. When considering all assays of the cytotoxicity, endothelial activation and inflammation responses of mono-cultures to particles EHC-6802, DWR1 and SRM-1650, only, big ET-1, VEGF and ICAM-1 levels in THP-1 cell supernatants and ET-1 levels in supernatants of A549 cells were significantly correlated with BAL neutrophil counts at 2 hr time point ($p < 0.05$) (Table 2.4). The number of correlated endpoints increased from 4 to 12, when relationships between the mono-culture endpoints and BAL neutrophil counts at 24 h time point were compared. From the cytotoxicity assays, cell viability of A549 cells, as measured by Alamar Blue assay was highly negatively correlated with 24 h BAL neutrophil counts (R=-0.871). The AhR assay was significantly, positively correlated with BAL neutrophil counts (R=0.691). From the assays of factors of endothelial activation, big ET-1, ICAM-1 levels in THP-1 cell supernatants and VEGF levels in A549 cell supernatants were highly positively correlated with BAL neutrophil counts at the 24 h time point of exposure. The ET-1 levels in A549 cell media did not correlate well with BAL neutrophil counts at 24 h time point. From the inflammation subset of assays, all cytokines measured in THP-1 cells were significantly correlated with 24 h BAL neutrophil counts. Overall, the number of endpoints from co-culture exposures correlated with BAL neutrophil

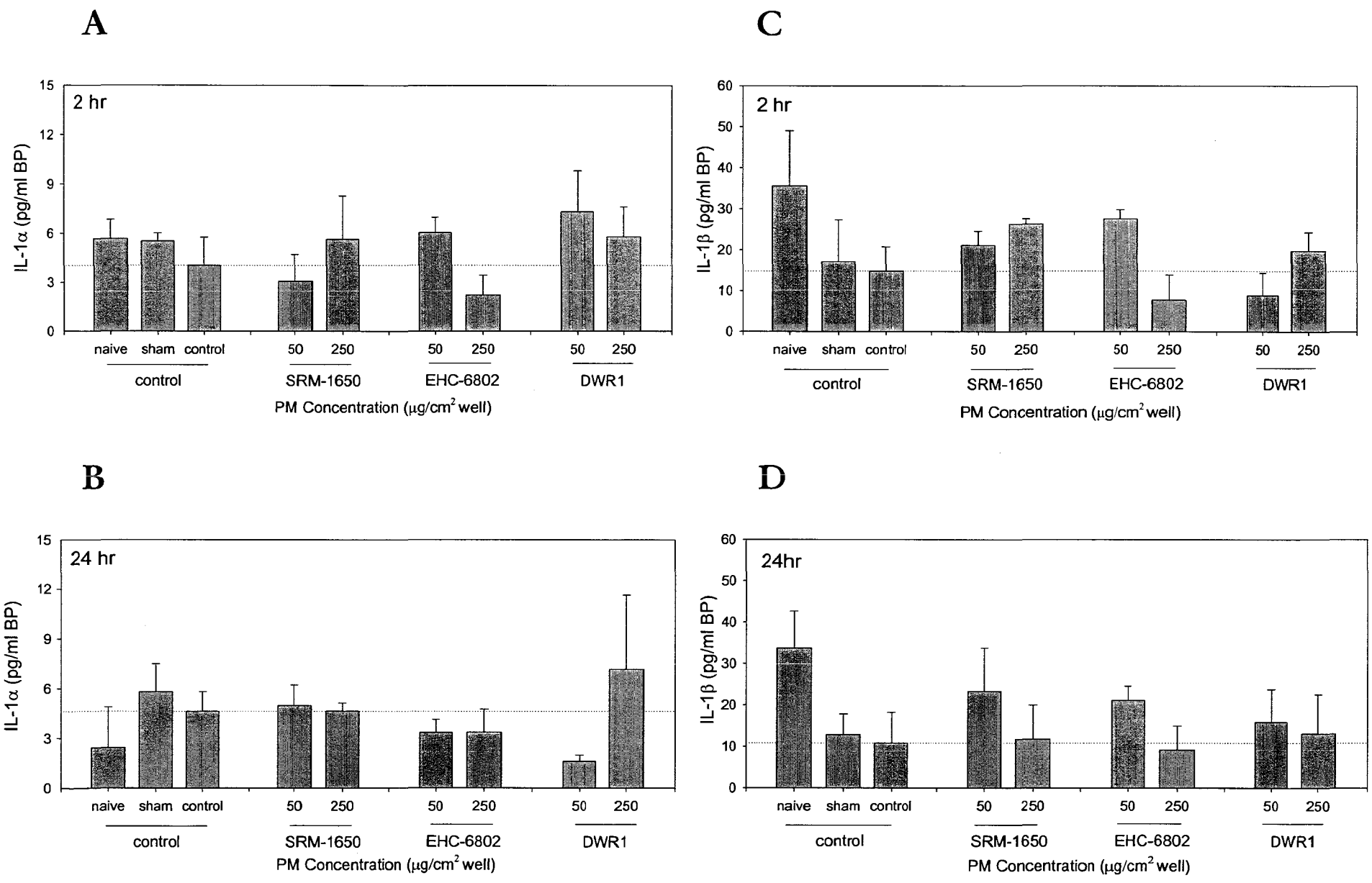
A
2 hr
IL-1α (pg/ml BP)
15
12
9
6
3
0
naive
sham
control
50
250
50
250
50
250
control
SRM-1650
EHC-6802
DWR1
PM Concentration (μg/cm² well)
C
2 hr
IL-1β (pg/ml BP)
60
50
40
30
20
10
0
naive
sham
control
50
250
50
250
50
250
control
SRM-1650
EHC-6802
DWR1
PM Concentration (μg/cm² well)
B
24 hr
IL-1α (pg/ml BP)
15
12
9
6
3
0
naive
sham
control
50
250
50
250
50
250
control
SRM-1650
EHC-6802
DWR1
PM Concentration (μg/cm² well)
D
24hr
IL-1β (pg/ml BP)
60
50
40
30
20
10
0
naive
sham
control
50
250
50
250
50
250
control
SRM-1650
EHC-6802
DWR1
PM Concentration (μg/cm² well)

Figure 2.42. Interleukin (IL)-1α (A, B) and IL-1β (C, D) levels in blood plasma from BALB/*c* mice exposed to particulate matter for 2 and 24 hrs by intratracheal instillation. Cytokine levels in plasma were determined by Bio-Plex assay. Values are presented as mean ± standard error (n = ~5). IL-1α and IL-1β did not show statistical significance by 2-way ANOVA.

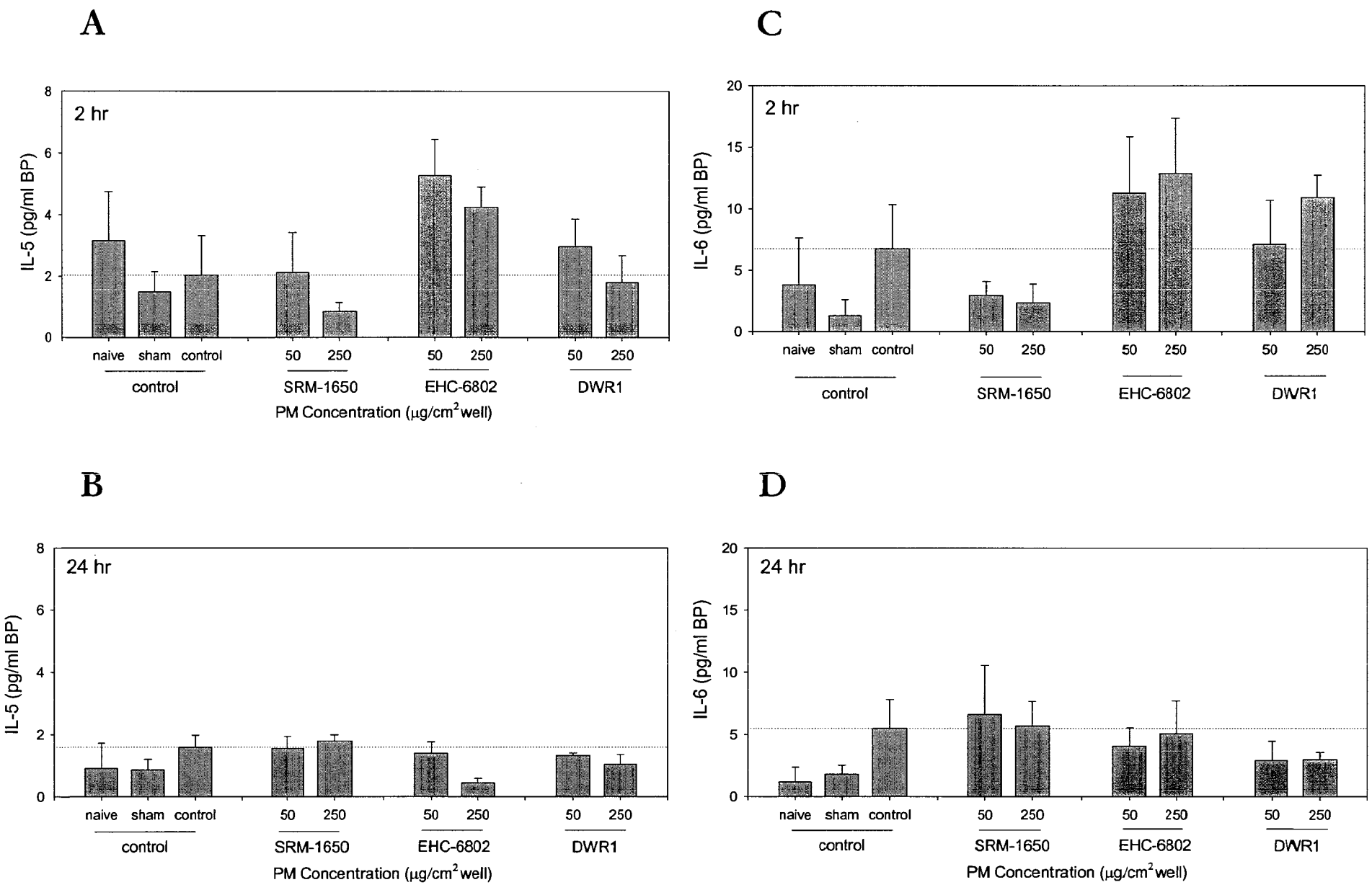
A
2 hr
IL-5 (pg/ml BP)
naive sham control 50 250 50 250 50 250
control
SRM-1650
EHC-6802
DWR1
PM Concentration (μg/cm²well)
C
2 hr
IL-6 (pg/ml BP)
naive sham control 50 250 50 250 50 250
control
SRM-1650
EHC-6802
DWR1
B
24 hr
IL-5 (pg/ml BP)
naive sham control 50 250 50 250 50 250
control
SRM-1650
EHC-6802
DWR1
PM Concentration (μg/cm²well)
D
24 hr
IL-6 (pg/ml BP)
naive sham control 50 250 50 250 50 250
control
SRM-1650
EHC-6802
DWR1
PM Concentration (μg/cm²well)

Figure 2.43. Interleukin (IL)-5 (A, B) and IL-6 (C, D) levels in blood plasma from BALB/*c* mice exposed to particulate matter for 2 and 24 hrs by intratracheal instillation. Cytokine levels in plasma were determined by Bio-Plex assay. Values are presented as mean ± standard error (n = ~5). IL-5 and IL-6 did not show statistical significance by 2-way ANOVA.

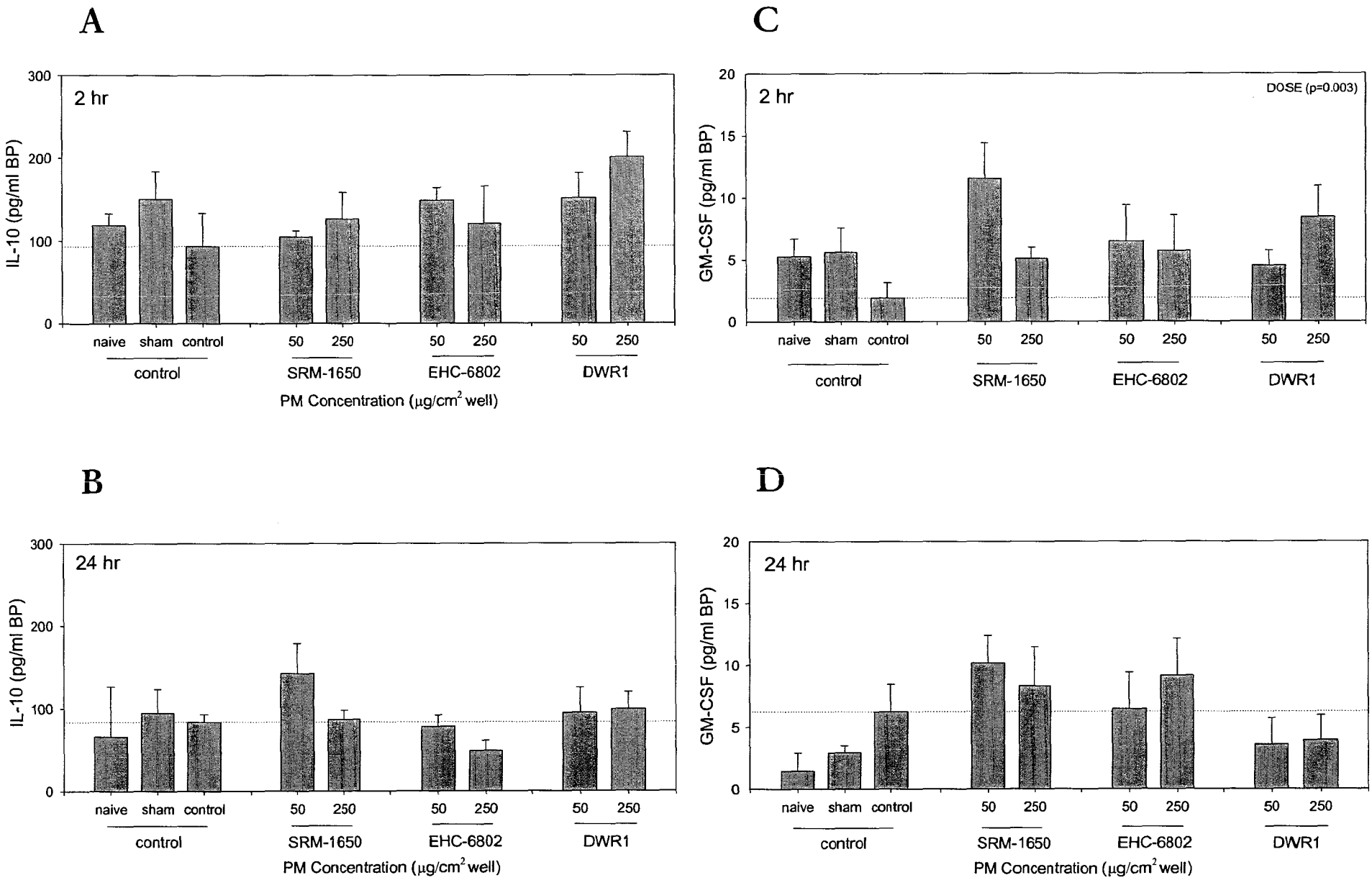
A
2 hr
IL-10 (pg/ml BP)
300
200
100
0
naive sham control
50 250
50 250
50 250
control
SRM-1650
EHC-6802
DWR1
PM Concentration (μg/cm² well)
C
2 hr
DOSE (p=0.003)
GM-CSF (pg/ml BP)
20
15
10
5
0
naive sham control
50 250
50 250
50 250
control
SRM-1650
EHC-6802
DWR1
B
24 hr
IL-10 (pg/ml BP)
300
200
100
0
naive sham control
50 250
50 250
50 250
control
SRM-1650
EHC-6802
DWR1
PM Concentration (μg/cm² well)
D
24 hr
GM-CSF (pg/ml BP)
20
15
10
5
0
naive sham control
50 250
50 250
50 250
control
SRM-1650
EHC-6802
DWR1
PM Concentration (μg/cm² well)

Figure 2.44. Interleukin (IL)-10 (A, B) and Granulocyte-Macrophage Colony-Stimulating Factor (GM-CSF) (C, D) levels in blood plasma from BALB/*c* mice exposed to particulate matter for 2 and 24 hrs by intratracheal instillation. Cytokine/chemokine levels in plasma were determined by Bio-Plex assay. Values are presented as mean ± standard error (n=~5). IL-10 at both time points and GM-CSF at the 24 h time point did not show statistical significance. DOSE main effect was obtained for plasma levels of GM-CSF at 2 hrs (2-way ANOVA).

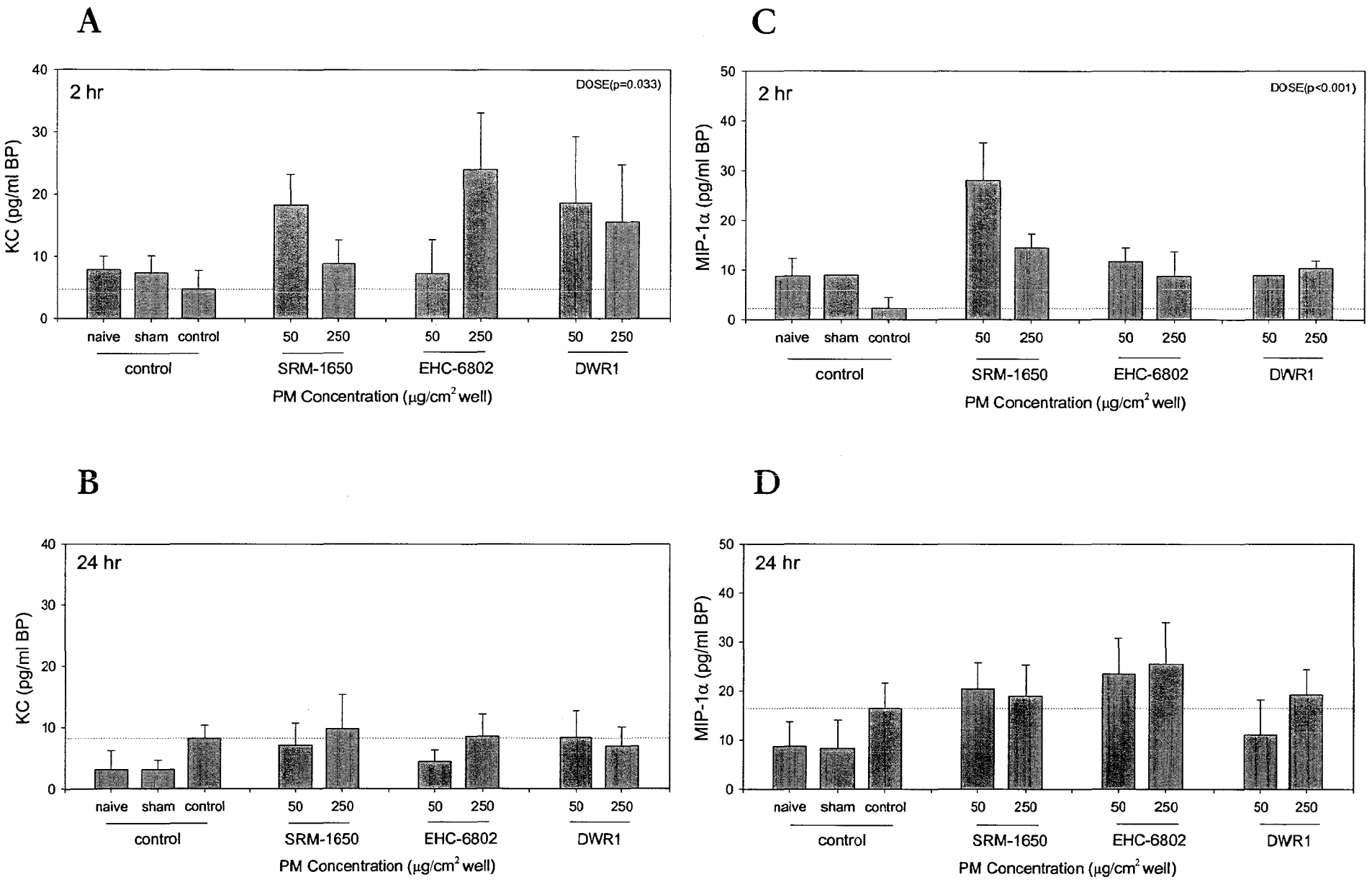
A
2 hr
DOSE(p=0.033)
KC (pg/ml BP)
0
10
20
30
40
naive
sham
control
50
250
50
250
50
250
control
SRM-1650
EHC-6802
DWR1
PM Concentration (μg/cm² well)
C
2 hr
DOSE(p<0.001)
MIP-1α (pg/ml BP)
0
10
20
30
40
50
naive
sham
control
50
250
50
250
50
250
control
SRM-1650
EHC-6802
DWR1
PM Concentration (μg/cm² well)
B
24 hr
KC (pg/ml BP)
0
10
20
30
40
naive
sham
control
50
250
50
250
50
250
control
SRM-1650
EHC-6802
DWR1
PM Concentration (μg/cm² well)
D
24 hr
MIP-1α (pg/ml BP)
0
10
20
30
40
50
naive
sham
control
50
250
50
250
50
250
control
SRM-1650
EHC-6802
DWR1
PM Concentration (μg/cm² well)

Figure 2.45. Keratinocyte-derived Chemokine (KC) (A, B) and Macrophage Inflammatory Protein (MIP)-1α (C, D) levels in blood plasma from BALB/c mice exposed to particulate matter for 2 and 24 hrs by intratracheal instillation. Cytokine/chemokine levels in plasma were determined by Bio-Plex assay. Values are presented as mean ± standard error (n= ~5). DOSE main effects were observed for KC and MIP-1α plasma levels at the 2 h time point by 2-way ANOVA. Plasma levels of KC and MIP-1α were not statistically significant at the 24 h time point.

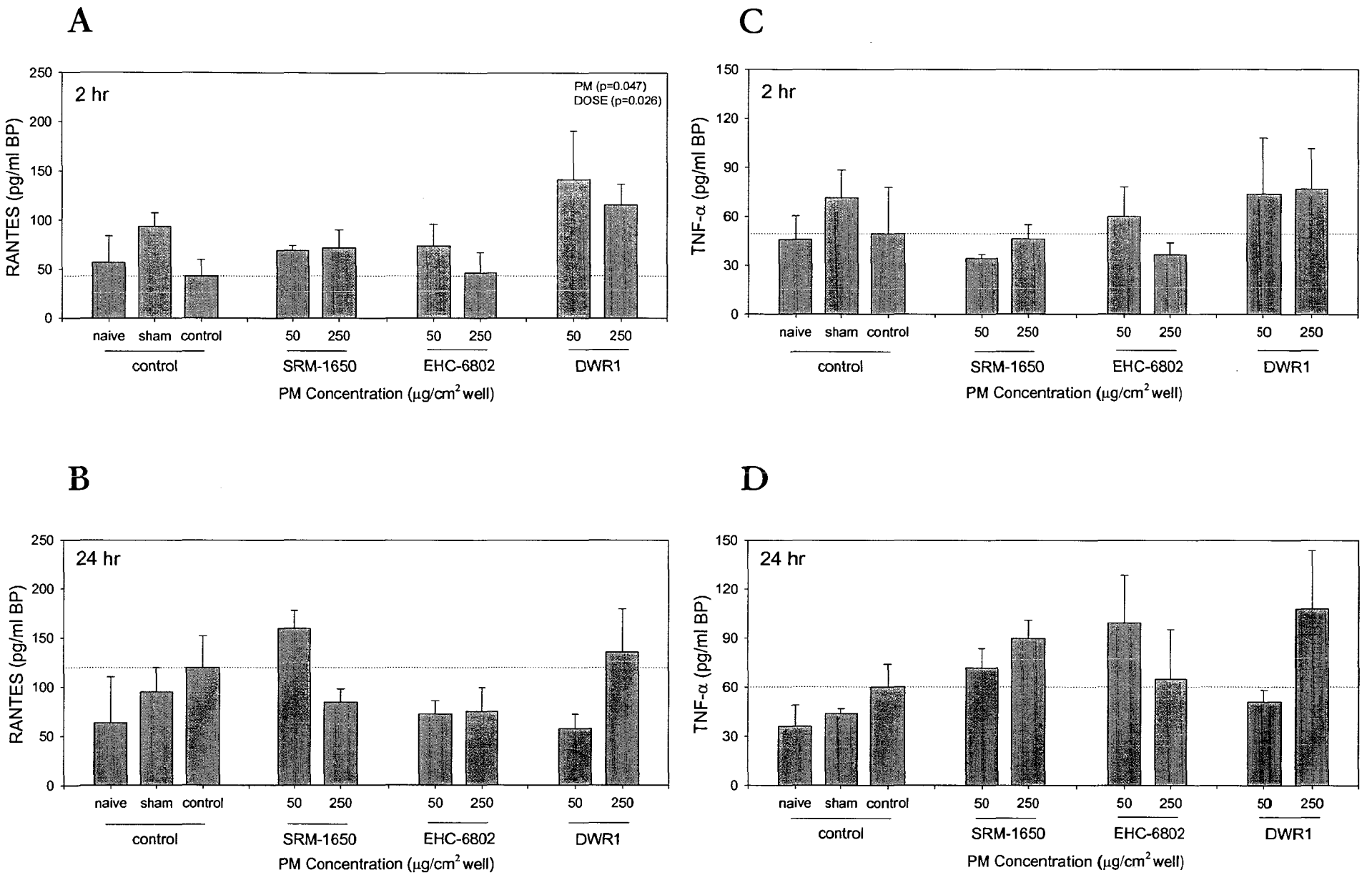
A
2 hr
PM (p=0.047)
DOSE (p=0.026)
RANTES (pg/ml BP)
250
200
150
100
50
0
naive sham control 50 250 50 250 50 250
control
SRM-1650
EHC-6802
DWR1
PM Concentration (μg/cm² well)
C
2 hr
TNF-α (pg/ml BP)
150
120
90
60
30
0
naive sham control 50 250 50 250 50 250
control
SRM-1650
EHC-6802
DWR1
PM Concentration (μg/cm² well)
B
24 hr
RANTES (pg/ml BP)
250
200
150
100
50
0
naive sham control 50 250 50 250 50 250
control
SRM-1650
EHC-6802
DWR1
PM Concentration (μg/cm² well)
D
24 hr
TNF-α (pg/ml BP)
150
120
90
60
30
0
naive sham control 50 250 50 250 50 250
control
SRM-1650
EHC-6802
DWR1
PM Concentration (μg/cm² well)

Figure 2.46. Regulated upon Activation Normal T cell Expressed and Secreted (RANTES) (A, B) and Tumor Necrosis Factor (TNF)-α (C, D) levels in blood plasma from BALB/*c* mice exposed to particulate matter for 2 and 24 hrs by intratracheal instillation. Cytokine/chemokine levels in plasma were determined by Bio-Plex assay. Values are presented as mean ± standard error (n=~5). PM and DOSE main effects were observed for RANTES plasma levels at the 2 h time point by 2-way ANOVA. Plasma levels of TNF-α at the 2 h time point, and RANTES and TNF-α at both time points were not statistically significant.

Table 2.4. Pearson Product Moment Correlation of BALB/*c* BAL neutrophil counts (2hr and 24hr timepoint) with *in vitro* measures of biological responses of mono-cultures and co-cultures of cells to a set of particles (EHC-6802, DWR1 and SRM-1650).

Subset	Endpoint[1]	2 hr TP		24 hr TP	
		Correl. Coeff.[2]	P value	Correl. Coeff.[2]	P value
Mono-Culture					
Cytotoxicity	Alamar Blue (A)	-0.127	0.745	**-0.871**	0.002
	Alamar Blue (T)	-0.396	0.291	0.349	0.357
	AhR Assay (H)	-0.094	0.810	**0.691**	0.039
Endothelial Activation	big ET-1 (A)	-0.390	0.299	0.003	0.993
	big ET-1 (T)	**0.836**	0.005	**0.758**	0.018
	ET-1 (A)	**0.787**	0.012	0.399	0.287
	ET-1 (T)	-0.140	0.720	-0.637	0.065
	VEGF (A)	0.378	0.315	**0.832**	0.005
	VEGF (T)	**0.708**	0.033	0.476	0.196
	ICAM-1 (T)	**0.672**	0.048	**0.822**	0.006
	VCAM-1 (T)	0.428	0.251	0.124	0.751
Inflammation	IL-1β (T)	0.460	0.213	**0.935**	0.0002
	IL-6 (A)	-0.280	0.466	0.248	0.520
	IL-6 (T)	0.396	0.291	**0.839**	0.004
	IL-8 (A)	-0.304	0.427	0.215	0.578
	IL-8 (T)	0.445	0.230	**0.857**	0.003
	IL-10 (T)	0.447	0.227	**0.821**	0.007
	GM-CSF (T)	0.614	0.078	**0.887**	0.001
	MCP-1 (A)	-0.165	0.672	0.399	0.287
	MCP-1 (T)	0.630	0.069	**0.849**	0.004
	TNF-α (T)	0.404	0.281	**0.801**	0.010
Co-culture					
Cytotoxicity	Alamar Blue (C)	0.388	0.302	-0.006	0.988
Endothelial Activation	big ET-1 (C)	0.200	0.606	**0.730**	0.026
	ET-1 (C)	**0.785**	0.012	0.195	0.616
	VEGF (C)	**0.868**	0.00239	**0.733**	0.025
	ICAM-1 (C)	**0.916**	0.0005	**0.699**	0.036
Inflammation	IL-1β (C)	**0.775**	0.0142	**0.813**	0.008
	IL-6 (C)	**0.846**	0.004	**0.749**	0.020
	IL-8 (C)	**0.687**	0.041	**0.816**	0.007
	IL-10 (C)	0.656	0.055	**0.873**	0.002
	GM-CSF (C)	**0.772**	0.015	**0.800**	0.010
	MCP-1 (C)	**0.824**	0.006	**0.781**	0.013
	TNF-α (C)	0.639	0.064	**0.831**	0.006

1 A – A549 cells; T – THP-1 cells; H – H1L1 cells, C – A549 and THP-1 cells co-culture
2 Statistically significant correlation coefficients are shown in bold ($p<0.050$)

counts was similar between the two time points, although the profile of the correlated assays differed. ET-1, VEGF and ICAM-1 measurements from co-culture supernatants were highly positively correlated with 2 h neutrophil counts in BAL fluid. The strengths of these relationships decreased when the 24 h BAL neutrophil count was considered, with ET-1 correlation changing most substantially. VEGF and ICAM-1 remained significantly correlated with 24 h BAL neutrophil counts along with big ET-1. From the measures of inflammatory mediators, IL-1β, IL-6, IL-8, GM-CSF and MCP-1 in co-culture supernatants were positively correlated with 2 h BAL neutrophil counts. When the co-culture inflammatory measures were compared to neutrophil counts in BALB/*c* BAL fluid from the 24 h time point, all measured cytokines showed statistically significant correlations with $R>0.74$. Overall, an increase in the number of endpoints significantly correlated with BAL neutrophil counts was observed with 24 h BAL neutrophil counts in comparison to the 2 h counts and the co-culture responses to particles correlated well with neutrophil counts from both timepoints. From all mono-culture and co-culture measures, ICAM-1 levels in co-culture supernatants of A549 and THP-1 cells showed the strongest association with BAL neutrophil counts at the 2 h time point ($R=0.916$).

The strengths of the relationships between indirect biological responses to particles *in vitro* and overall particle response *in vivo* were examined by correlating the assay measurements taken from exposures of HPAE endothelial cells to CM from PM-exposed mono- and co-cultures of A549 and THP-1 with BAL neutrophil counts at 2 and 24 h time points. Similarly, as observed in direct particle exposures of epithelial and macrophage cell mono-cultures, the number of endpoints measured in HPAE cells incubated with these mono-culture CM with significant correlation ($p<0.05$) with BAL neutrophil counts had increased over time from 2 to 11 endpoints (Table 2.5). Only ET-1 and IL-6 levels in supernatants of HPAE cells, incubated with THP-1 CM were significantly correlated with 2 h BAL neutrophil counts. When compared to the BAL neutrophil counts at the 24 h time point, cytokine levels of GM-CSF and MCP-1 along with IL-6 from supernatants of HPAE cells exposed to THP-1 CM, as well as IL-6 and MCP-1 levels from HPAE cell supernatants incubated with A549 CM were significantly correlated. From the factors of endothelial activation, only ET-1 levels in supernatants from HPAE cells incubated with THP-1 CM showed a significant association with 2 h BAL neutrophil counts ($R=701$). In contrast, ET-1, ICAM-1, VCAM-1 and E-selectin in supernatants of HPAE endothelial cells incubated with

THP-1 CM along with ICAM-1 and VCAM-1 in supernatants of HPAE cells incubated with A549 CM were highly positively correlated with 24 h BAL neutrophil counts. From all endpoints, the only high negative correlation coefficient was shown for the VCAM-1 content in supernatants of HPAE cells incubated with A549 CM and 24 h BAL neutrophil counts (R=-0.865). A comparison of correlations of BAL neutrophil counts and endothelial cells incubated with co-culture CM revealed a similar picture to that with co-cultures exposed directly to particles, with a similar number of *in vitro* endpoints which were highly correlated with *in vivo* neutrophil counts between the two time points. The levels of the three adhesion factors ICAM-1, VCAM-1 and E-selectin in HPAE cells incubated in co-culture CM were significantly correlated with BAL neutrophil counts at both time points, with higher correlation coefficients observed with the 24 h time point. Cytotoxicity measure Alamar Blue was not significantly correlated with BAL neutrophil counts at either time point, as observed previously with endothelial cells incubated with mono-culture CM and with co-cultures directly exposed to particles. A comparison of inflammatory mediators measured in supernatants of HPAE cells incubated with co-culture CM showed some differences in profile of cytokines correlated with BAL neutrophil counts from the two time points. IL-1β, IL-6, IL-8, IL-10, GM-CSF, TNF-α were significantly correlated with 2 h BAL neutrophil counts and IL-10, GM-CSF, MCP-1 and TNF-α only remained significantly correlated with 24 h BAL neutrophil counts. From all endpoints, IL-8 levels detected in HPAE cells incubated with co-culture CM showed the highest degree of similarity to 2 h BAL neutrophil counts (R=0.939). The association had decreased and became statistically insignificant when 24 h BAL neutrophil counts were considered.

11.3.11 Association of PM-Induced BAL Neutrophilia with Other Responses in Mice

The summary of the correlations of BAL neutrophil counts with the *in vivo* endpoints measured in BALB/c mice exposed to particles EHC-6802, DWR1 and SRM-1650 at 2 and 24 h time points is presented in Table 2.6. From the measures representing the cytotoxic response of animals to particles, total protein and lymphocyte counts showed a significant correlation with neutrophil counts at 2 hrs (R=0.726, R=0.701 respectively). After 24 hrs, the strength of these associations had decreased and became statistically insignificant. After 24 hrs, counts of macrophages, band

Table 2.5. Pearson Product Moment Correlation of BALB/*c* BAL neutrophil counts (2hr and 24hr timepoint) with *in vitro* measures of biological responses of HPAE cells treated with conditioned media from mono-cultured and co-cultured cells exposed to particles (EHC-6802, DWR1 and SRM-1650).

Subset	Endpoint[1]	2 hr TP		24 hr TP	
		Correl. Coeff.[2]	P value	Correl. Coeff.[2]	P value
HPAE Cells Exposed to Mono-Culture Media					
Cytotoxicity	Alamar Blue (H_A)	-0.569	0.110	-0.614	0.079
	Alamar Blue (H_T)	-0.244	0.527	-0.638	0.064
Endothelial Activation	big ET-1 (H_A)	0.403	0.283	0.445	0.230
	big ET-1 (H_T)	-0.186	0.633	0.124	0.751
	ET-1 (H_A)	0.292	0.446	0.400	0.286
	ET-1 (H_T)	**0.701**	0.035	**0.854**	0.003
	ICAM-1 (H_A)	0.465	0.208	**0.813**	0.008
	ICAM-1 (H_T)	0.616	0.077	**0.826**	0.006
	VCAM-1 (H_A)	-0.263	0.495	**-0.865**	0.003
	VCAM-1 (H_T)	0.592	0.093	**0.832**	0.005
	E-Selectin (H_T)	0.640	0.063	**0.870**	0.002
Inflammation	IL-6 (H_A)	0.610	0.081	**0.743**	0.022
	IL-6 (H_T)	**0.824**	0.006	**0.870**	0.002
	IL-8 (H_A)	0.076	0.846	0.631	0.068
	IL-8 (H_T)	0.601	0.087	0.096	0.806
	GM-CSF (H_T)	0.569	0.110	**0.906**	0.0008
	MCP-1 (H_A)	0.494	0.176	**0.807**	0.008
	MCP-1 (H_T)	0.653	0.057	**0.883**	0.002
	TNF-α (H_T)	-0.699	0.036	-0.349	0.358
HPAE Cells Exposed to Co-Culture Media					
Cytotoxicity	Alamar Blue (H_C)	-0.655	0.055	-0.560	0.117
Endothelial Activation	big ET-1 (H_C)	-0.234	0.545	-0.425	0.255
	ET-1 (H_C)	0.240	0.535	0.566	0.112
	ICAM-1 (H_C)	**0.719**	0.029	**0.786**	0.012
	VCAM-1 (H_C)	**0.687**	0.041	**0.811**	0.008
	E-Selectin (H_C)	**0.759**	0.018	**0.778**	0.014
Inflammation	IL-1β (H_C)	**0.896**	0.001	0.586	0.098
	IL-6 (H_C)	**0.690**	0.040	0.537	0.136
	IL-8 (H_C)	**0.939**	0.0002	0.606	0.084
	IL-10 (H_C)	**0.807**	0.008	**0.770**	0.015
	GM-CSF (H_C)	**0.751**	0.020	**0.788**	0.012
	MCP-1 (H_C)	0.637	0.065	**0.770**	0.015
	TNF-α (H_C)	**0.814**	0.008	**0.782**	0.013

1 H_A – HPAE cells in A549 media; H_T – HPAE cells in THP-1 media; H_C – HPAE cells in media from A549/THP-1 Co-cultures
2 Statistically significant correlation coeficients are shown in bold ($p<0.050$)

cells and total cell count, as well as BAL LDH levels were significantly associated with neutrophil counts ($p < 0.05$), with BAL macrophage counts showing a 93.1% similarity to neutrophil counts.

Counts of macrophage counts and total cell count were negatively correlated with neutrophil counts. The adhesion factor ICAM-1, representing a measure of endothelial activation, became highly correlated with neutrophil counts 24 hrs after intratracheal exposure of mice to particles (R=0.922). No changes in VCAM-1 were found at both time points. Measurements of cytokines/chemokines in BAL fluid were taken to represent an index of inflammatory response in the lungs. A number of these have shown an increase in correlation with neutrophil counts over time, with IL-1α, IL-6, GM-CSF, KC, MIP-1α and TNF-α showing above 70 % similarity with neutrophil counts 24 hrs after exposure of mice to particles. At 2 hrs, IL-1α, IL-5 and MIP-1α were significantly associated with BAL neutrophil counts, with BAL MIP-1α showing the strongest association with neutrophil counts (R=0.905). From all BAL cytokines with statistically significant correlation coefficients, MIP-1α and IL-5 showed a marked decrease in correlation with neutrophil counts when the two time points were considered. The IL-5 association with neutrophil counts became statistically insignificant after 24 hrs, in contrast to a significant 69.6 % similarity after 2 hrs. To obtain a measure of a degree of systemic inflammation, levels of cytokines and chemokines in blood stream of the mice exposed to particles were determined at both 2 and 24 h time points. The correlation analysis revealed that from these analytes only IL-10, RANTES and TNF-α were significantly correlated with BAL neutrophil counts 2 hrs after exposure. From these, plasma IL-10 levels were most highly associated with BAL neutrophil counts, with a ositive correlation (R=0.96). After 24 hrs, the cytokine/chemokine profile has markedly changed, with plasma IL-10 becoming negatively correlated with BAL neutrophil counts, with a loss of statistical significance for the correlation. Additionally, at 24 hrs, plasma levels of MIP-1α were positively associated with BAL neutrophil counts ((R=0.729), while IL-5 levels and BAL neutrophil counts showed a negative association (R= -0.667) of borderline statistical significance (p=0.0498) (Table 2.6). Overall the analysis showed that a number of endpoints were significantly correlated with BAL neutrophil counts at both time points and that the number of the significantly correlated endpoints with 24 h BAL neutrophil counts was higher (12 versus 8) in comparison to those correlated with 2 h neutrophil counts.

Table 2.6. Pearson Product Moment Correlation of BAL neutrophil counts with other *in vivo* measures of biological responses to a set of particles (EHC-6802, DWR1 and SRM-1650) in BALB/*c* mice.

Subset	Endpoint	2 hr TP		24 hr TP	
		Correl. Coeff.[3]	P value	Correl. Coeff.[3]	P value
Cytotoxicity [1]	LDH	0.569	0.110	**0.722**	0.028
	Total protein	**0.726**	0.027	0.658	0.054
	Total cells	-0.322	0.398	**-0.776**	0.014
	Macrophages	-0.352	0.354	**-0.931**	0.0003
	Band Cells	0.472	0.200	**0.770**	0.015
	Lymphocytes	**0.701**	0.035	-0.626	0.071
Endothelial Activation [1]	ICAM-1	0.332	0.382	**0.922**	0.0004
	VCAM-1	0.646	0.060	0.645	0.061
Pulmonary Inflammation[1]	IL-1α	**0.715**	0.030	**0.791**	0.011
	IL-5	**0.696**	0.037	-0.428	0.251
	IL-6	0.398	0.289	**0.771**	0.015
	IL-10	0.641	0.063	0.180	0.642
	GM-CSF	0.325	0.393	**0.742**	0.022
	KC	0.646	0.060	**0.796**	0.010
	MIP-1α	**0.905**	0.0008	**0.788**	0.012
	TNF-α	0.506	0.164	**0.776**	0.014
Systemic Inflammation[2]	IL-1α	0.549	0.126	-0.0769	0.844
	IL-1β	0.127	0.744	-0.0691	0.860
	IL-5	0.350	0.356	-0.667	0.0498
	IL-6	0.643	0.062	-0.298	0.437
	IL-10	**0.960**	0.00004	-0.530	0.142
	GM-CSF	0.397	0.290	0.207	0.593
	KC	0.348	0.358	-0.155	0.691
	MIP-1α	0.055	0.888	**0.729**	0.026
	RANTES	**0.705**	0.034	-0.526	0.146
	TNF-α	**0.785**	0.012	0.552	0.124

1 Endpoints within the subsets were measured in BAL of BALB/*c* mice exposed to PM
2 Endpoints within the subset were measured in blood plasma of BALB/*c* mice exposed to PM
3 Statistically significant correlation coefficients are shown in bold ($p<0.050$)

11.3.12 Control Effects

In this *in vivo* experiment, three types of controls were utilized; Naïve, sham and vehicle control. The naïve control represented mice that were housed in the same facility and maintained in the identical way as the experimental animals but otherwise left untreated. Sham animals were utilized to control for the procedure. They were anaesthesized at the appropriate time intervals, with the MicroSprayer aerosolizer placed into their trachea, without delivery of particles. The vehicle controls represented mice that were exposed to the particle vehicle solution only, (50 μl of 0.9 % saline with 0.005 % Tween-80) delivered by intratracheal instillation with the MicroSprayer aerosolizer. Analysis of control data for the *in vivo* study shows statistically significant differences between the controls for some of the analyzed endpoints (Table A-15). In comparison to vehicle controls, sham and naïve control animals showed significantly lower BAL levels of adhesion factors ICAM-1 and VCAM-1 in the 2 h exposures and VCAM-1 in the 24 h exposures. Significantly increased total protein content was measured in BAL samples from mice exposed to the vehicle solution for 24 hrs in comparison to naïve control mice. Differences in the BAL levels of some pro-inflammatory cytokines/chemokines were also observed between the various controls. For the 2 h exposures, significantly elevated levels of IL-5, IL-6, KC and TNF-α were detected in BAL samples of vehicle-exposed mice, in comparison to naïve or sham control mice. For the 24 h exposures, significantly increased amount of chemokines KC and MIP-1α were detected in BAL samples from vehicle-treated mice in comparison to naïve animals only. Furthermore, IL-5 levels were also elevated in BAL samples of mice exposed to vehicle solution for 24 hrs in comparison to both sham and naïve animals. In addition, the sham and naïve animal BAL samples were also significantly different in IL-5 levels upon the 24 h exposure, with higher IL-5 levels detected in samples from sham control mice.

DISCUSSION

The current study was conducted with the goals of (1) assessing the utility of the *in vitro* co-culture design for elucidations of biological effects of particles, with respect to their varied physicochemical properties, and (2) assessing the potential of the *in vitro* co-culture assay system for simulating the complexity of the biological effects observed in response to a pulmonary challenge of animals with particles. The study revealed synergistic interaction of epithelial cells and macrophages grown in co-culture, with significant modulations of the profile of pro-inflammatory cytokines (mostly IL-1β, IL-6, IL-8, MCP-1 and TNF-α), and other factors such as ICAM-1, and VEGF released by the cells in response to particle exposures. Cellular mediators from PM-exposed mono-cultures and co-cultures of epithelial cells and macrophages can distinctly influence the endothelium, as manifested by differential production of cellular factors including cytokines (mostly IL-6, IL-8, GM-CSF, MCP-1) and adhesion factors (ICAM-1, VCAM-1 and E-selectin) by the endothelial cells, when they were treated with the conditioned media from the PM-exposed cells. Exposure of BALB/*c* mice to EHC-6802, DWR1 and SRM-1650 particles by instillation resulted in BAL neutrophilia, accompanied by elevated BAL cytokines (mostly IL-6, KC, MIP-1α, TNF-α), without marked changes in biochemical markers, thus consistent with mild, acute pulmonary inflammation 2 and 24 hrs post-exposure, with more pronounced inflammatory state measured at 2 hrs post-exposure. Overall, the PM_{10} and $PM_{2.5}$ urban particles were most potent both *in vitro* and *in vivo*. Cristobalite displayed moderate potency (only assessed *in vitro*) in inducing cellular mediator productions from exposed cells. A statistical comparison of the *in vitro* co-culture responses with neutrophil counts in BAL of mice exposed to PM demonstrated that the assessment of the production of inflammatory cytokines and adhesion factors in a human co-culture model consisting of direct PM exposure of A549/THP-1 co-cultures and indirect co-culture conditioned media exposure of HPAE cells correlates well with the *in vivo* murine pulmonary neutrophilic response to particles.

A549 alveolar epithelial cells and THP-1 macrophages were cultured together to simulate an alveolar layer of cells with a close presence of inflammatory cells. The response of the co-cultures was evaluated in comparison to mono-cultures of the two cell types, upon 24 h exposures to particles. Direct exposure of cells to particles resulted in a decrease in cell viability, mostly apparent

in A549 and THP-1 cells exposed to EHC-93 and Cristobalite. Direct exposure to low and medium concentrations of particles appeared to induce bi-phasic effects in the metabolic activity of A549/THP-1 co-cultures, although the magnitude of the responses was low. The reason for the observation is not known at the present. Since the responses were different from those observed with mono-cultures exposed to particles, the data suggest that the cell interactions may affect their biological activity. Low dose stimulations of cellular metabolic activity have been previously described in response to toxicants such as heavy metals. The increased activity coincided with the production of stress proteins, suggesting that this may represent a cellular adaptive response (Damelin *et al.*, 2000). There does not, however, appear to be much research done on the role of cell-cell interaction in cellular adaptation to stress. The possibility that the bi-phasic effects observed in A549/THP-1 co-cultures exposed to particles could represent an adaptive response requires further examination. Concentration-dependent decrease in cell viability was also observed in endothelial cells treated with CM from A549 and THP-1 mono- and co-cultures exposed to particles. Small decreases in total protein were also observed in A549 cells in response to EHC-93 and Cristobalite and in THP-1 cells exposed to the highest concentration of Cristobalite, as well as in HPAE cells treated with CM from co-cultures exposed to particles. The data are suggestive of cytotoxicity induced by particles. The cells, however, were rinsed with PBS before the total protein analysis was conducted, and some loss of cells was observed with the procedure. Thus it is difficult to determine the degree of cytotoxic effect of particles on the basis of the total protein analysis.

In order to ensure that the content of cell metabolites present in the CM at the 70:30 ratio (CM: fresh medium) would not be high enough to independently influence endothelial cell behavior, comparisons of cell density between A549 and THP-1cells and co-cultures during the experimental conditions and during cell maintenance were compared. The comparison showed that the cell density during the experimental conditions was below and/or comparable to the cell density at which the cultures were initially maintained, therefore an influence of CM-cell metabolites on the endothelial cells was unlikely.

Cytokine profiling showed cell type-specific, differential production between the mono-cultures. Additionally, modulation of the overall cytokine profile was observed when the two cell types were grown together. In general, A549 cells responded to particles by low-level production of IL-6 and high-level productions of IL-8 and MCP-1 chemokines. THP-1 cells produced small amounts of

IL-6, IL-10 and GM-CSF; moderate amounts of IL-1β and MCP-1, and high amounts of IL-8 and TNF-α in response to a number of the particles. For both cell lines, the basal production of cytokines were generally low, thus the presence of particles resulted in concentration-dependent elevations of cytokine release. Most of the effects were seen in response to urban particles EHC-93, EHC-6802 and DWR1 exposures, although diesel particles (SRM-1650) and crystalline silica (Cristobalite) induced significant release of MCP-1 and IL-8 chemokines from A549 mono-cultures only. A trend of increase in IL-6 was also seen in A549 cell culture supernatants in response to SRM-1650 exposure, although not statistically significant.

Of interest was an observation of difference in cytokine profile of the A549 cells in the first study (see Chapter 1), and the current study. In the first study, A549 cells showed comparable baseline production of IL-8, a ~2 fold higher levels of MCP-1, high production of IL-6 (<400 pg/ml) and very low levels of GM-CSF in comparison to very low production of IL-6 and no release of GM-CSF in the current study. Additionally, difference in response to particles was also observed, with A549 cells in the first study showing a higher degree of response to mineral, and PM_{10} particle exposures, and less response to DWR1 in cytokine release. The reason for the difference is not known. The cells were cultured in different media; M199 medium was used in the first experiment and RPMI-1640 medium in the current study. In both studies, the media were supplemented with 2 mM L-glutamine and 10 % FBS. The adaptation of the cells to RPMI-1640 medium was necessary, as it was the most appropriate versatile medium capable of supporting epithelial, macrophage and endothelial cells, thus eliminating the possibility of potential confounding effects of the use of distinct media for each cell type. There are slight differences between the media formulations, such as the presence of a range of vitamins in RPMI-1640, and the presence of nucleotides and cholesterol in the M-199 medium. The subtle compositional difference, however, may not be sufficient to explain the observed difference, in light of FBS supplementation in both studies. One study has reported culture media-dependent differences in prolactin and growth hormone production by rat anterior pituitary cells (glandular epithelial cells) when they were cultured in M199 versus RPMI-1640 media, suggesting that media culture conditions can influence the degree of expression of constitutive phenotypes in the cells (Cronin *et al.*, 1987). In both studies, the cells were exposed to particles on the basis of PM mass/surface area of the well, therefore, comparable masses of particles were present in the wells between the two studies.

Concentration of the particles between the two studies, however, was different, as 100 μl of media were present in the 96-well in comparison to 1 ml of media present in the 24-well. Therefore the concentration of the soluble factors in the 96-well (first study), was ~1.5 fold higher than in the 24-well, although, it remains to be determined whether this difference could account for differential production of cytokines.

In general, three patterns of cytokine production were observed in co-cultures. Firstly, IL-β, and TNF-α were lower in co-cultures, compared to the levels produced by THP-1 mono-cultures, suggesting that the presence of factors produced by the epithelial cells in the medium resulted in the attenuation of the production of the described macrophage cytokine/chemokine products. Secondly, the epithelial-macrophage cell interaction resulted in synergistically increased production of IL-6, IL-10, GM-CSF and MCP-1 inflammatory mediators. Thirdly, co-culture of A549 and THP-1 cells did not appear to alter IL-8 levels in the culture supernatants, which were comparable to the THP-1 mono-culture. These results are in agreement with a number of studies that have demonstrated synergistic increases of cytokine levels via lung macrophage-epithelial interactions (Fujii *et al.*, 2002; Tao and Kobzik, 2002, Ishii *et al.*, 2004).

Fujii *et al.* (2002) showed that exposures of primary human bronchial epithelial cells (HBEC) and AM co-cultures to 100 μg/ml of EHC-93 for 24 hrs resulted in elevated mRNA and protein levels of IL-1β, IL-6, IL-8, GM-CSF and TNF-α inflammatory cytokines. GM-CSF and IL-6 were augmented synergistically. Furthermore, instillation of supernatants from AM/HBEC co-cultures into lungs of rabbits shortened the transit time of polymorphonuclear leukocytes through the bone marrow and increased the number of circulating band cells. The authors stated that the synergistic production of GM-CSF and IL-6 by co-cultures suggests that cell-cell interactions may contribute to the systemic response to PM_{10} exposures, as these mediators stimulate the bone marrow to produce and mobilize monocytes (Fujii *et al.*, 2002). Ishii and colleagues (2004) examined the cytokine interactions between mono-cultures of primary human AM, A549 alveolar epithelial cells, and HBEC. The authors showed that supernatants containing TNF-α and IL-1β cytokines released by AM exposed to 100 μg/ml of EHC-93 for 24 hrs, could increase the gene expression of a number of cytokines (TNF-α, IL-1β and IL-8, among others), as well as ICAM-1 and VEGF mRNA in A549 cells upon 3 h treatment with the AM supernatants. Pre-incubation of

the AM supernatants with antibodies against IL-1β and TNF-α significantly reduced the mRNA expressions of the above inflammatory mediators, including VEGF and ICAM-1. The responses were also shown to be NFκB and AP-1 mediated. Comparable results were obtained with HBEC cells treated with supernatants from PM-exposed macrophages, with some differences in the relative importance of the two blocking antibodies, suggesting potentially distinct cytokine regulations between the lower and upper airways. Because the antibodies did not completely block the above-described mRNA gene expressions, the authors suggested that other mediators present in the EHC-93-stimulated AM supernatant also likely play a role in these cytokine cascades (Ishii *et al.*, 2004). In agreement, the current study shows that THP-1 cells exposed to particles are the likely initial source of TNF-α and IL-1β in the co-culture, as the cytokines were produced by THP-1 mono-cultures but not A549 mono-cultures in response to PM.

The current study also extends these findings by showing that levels of IL-1β and TNF-α in supernatants of PM-exposed co-cultures were decreased in comparison to those of PM-exposed THP-1 mono-cultures, specifically in exposures to EHC-93, EHC-6802 and DWR1 particles. In contrast, Fujii *et al.* (2002) did not demonstrate a decrease in IL-1β and TNF-α levels in AM/HBEC co-cultures, although a trend of decrease could be observed in their study for TNF-α in comparison to AM mono-culture. The reason for the disparity may be due to the different cell types used in the study, ie. bronchial epithelial cells versus alveolar epithelial cells, or primary cells versus cell lines, as different cell types may have distinct cytokine expression profiles. For example, Mono Mac 6 and THP-1 human macrophage cell lines show differential productions of IL-6 and IL-8 peptide in co-cultures with A549 cells, upon 24 h exposures to crystalline and amorphous silica, as well as hematite particles. Interestingly, the macrophages also show marked difference in their susceptibility to mineral-induced cytotoxicity, with THP-1 cells showing significantly greater plasma membrane damage (LDH release) than Mono Mac 6 cells (Wottrich *et al.*, 2004). As shown previously, in addition to these cytokines, augmented productions of IL-10, IL-6, GM-CSF and MCP-1, along with decreased IL-1β and TNF-α were observed in the A549/THP-1 co-cultures. This response is suggestive of IL-6 mediated feedback mechanism which results in attenuation of excessive TNF-α production by blockage of IL-1β signaling via elevation of IL-1 receptor antagonist (IL-1ra). IL-6 is a multifunctional cytokine that has been shown to exert both pro- and anti-inflammatory effects. The pro-inflammatory functions of IL-6 include roles in elaboration of

the acute phase response and in B cells proliferation (Dube *et al.*, 2004). Through the IL-1ra-associated mechanism, IL-6 is thought to mediate the switch from the early neutrophilic inflammatory response to a sustained monocytic response. The transition from the recruitment of leukocytes associated with innate immunity (preceded by early activation of IL-1β and TNF-α) to mononuclear leukocytes important in acquired immunity is crucial to a resolution of inflammation and return to tissue homeostasis (Hurst *et al.*, 2001). Through this mechanism, IL-6 can also induce expression of chemokines (IL-8 and MCP-1) and adhesion molecules (ICAM-1 and VCAM-1) (Hurst *et al.*, 2001). IL-10 is a Th2-type anti-inflammatory cytokine produced by T cells, monocytes and macrophages. It is a potent inhibitor of a number of pro-inflammatory cytokines including IL-1, IL-8, TNF-α among others (Standiford *et al.*, 1999).

The increased levels of IL-8 and MCP-1 in A549 cell culture supernatants in response to diesel particles or silica exposures are in agreement with the literature. The studies show increased production of the chemokines in cell cultures and in animals, governed by either TNF-α- and ROS-dependent, or TNF-α independent mechanisms, based on the physicochemical properties of the particles (Steerenberg *et al.*, 1998, Barrett *et al.*, 1999, Hetland *et al.*, 2001; Saber *et al.*, 2006).

Circulating cytokines activate the vascular endothelium, which is manifested by elevation of von Willebrand factor involved in hemostasis, adhesion molecules ICAM-1, VCAM-1 and E-selectin. Stimulation with pro-inflammatory cytokines leads to up-regulation of ICAM-1 and VCAM-1 on the endothelium (van Eeden *et al.*, 2005). Elevated expression of these factors in subjects with coronary heart disease correlates with particulate air pollution (Rückerl *et al.*, 2006). The adhesion factors are involved in cell-cell interactions of leukocytes with the endothelium and airway mucosa. The process involves a "loose adhesion" event of rolling of leukocytes on the endothelial surface mediated by selectins such as E-selectin expressed on activated endothelium; firm adhesion mediated by binding of integrins CD11a/CD18 and CD11b/CD18 of the leukocyte to ICAM-1 on endothelial cells, and transmigration via intercellular junctions into the subendothelial space mediated by VCAM-1 (Huo and Ley, 2001).

In the current study, exposure of THP-1 macrophages to EHC-93, EHC-6802 and DWR1 particles induced marked elevation in ICAM-1, as well as low secretion of VCAM-1. Neither basal, nor PM-induced production of the adhesion factors could be detected in A549 cells.

ICAM-1 and VCAM-1 were detected in A549/THP-1 co-cultures, although at levels below those observed in THP-1 cells treated with particles, suggesting the presence of factors in the co-culture media capable of reducing ICAM-1 production. The absence of A549 cell production of ICAM-1 is in contrast to that observed by Brown *et al.* (2007), who showed increased ICAM-1 expression in A549 cells, upon their treatments with conditioned medium (CM) from PM_{10}-exposed human primary monocytes. A549 cells do not express ICAM-1 mRNA constitutively, but show significant induction of mRNA and protein in response to a treatment with inflammatory cytokines including TNF-α and IL-1β, as well as with LPS (Fakler *et al.*, 2000). Inhibition of IL-1β and TNF-α with antibodies against these peptides results in 79 % and 32 % inhibition of ICAM-1 expression respectively, in A549 cells treated with bronchial lavage from patients with asthma (Tillie-Leblond *et al.*, 1999). Thus the lack of these cytokines in culture media from PM-treated or control cells may explain the absence of secreted ICAM-1. Besides endothelial cells and epithelial cells, fibroblasts, lymphocytes and monocytes/macrophages also show basal expression of ICAM-1 (Hubbard *et al.*, 2001). Pulmonary macrophages from mice exposed intratracheally to silica show increased expression of ICAM-1, suggesting that macrophages may also participate in silica-induced influx of neutrophils into the alveoli, with its expression mediated via ROS and TNF-α (Hubbard *et al.*, 2001). While endothelial expression of ICAM-1 mediates the interaction between leukocytes and the endothelium, in monocytes/macrophages ICAM-1 plays a role in antigen presentation and interaction with cell types other than endothelial cells (Ruetten *et al.*, 1999). Interestingly, a recent study showed that a pre-treatment of HBEC cells with anti-ICAM-1 antibody, or cross-linking of ICAM-1 on HBEC cells did not reduce the elevated expression of cytokines in AM/HBEC co-cultures in response to a 24 h exposure to EHC-93 particles. Based on the findings, the authors suggested that β2-integrin/ICAM-1 interaction between AM and lung epithelial cells may not contribute to AM production of cytokines (Ishii *et al.*, 2005). As the current study suggests, however, significantly increased production of ICAM-1, VCAM-1 and E-selectin, in addition to a variety of cytokines can be observed by HPAE cells treated with CM from THP-1 cells and A549/THP-1 co-cultures exposed to particles for 24 hrs, suggesting that in addition to lung epithelial cells and AM, pulmonary endothelial cells may play a critical role in the amplification of the lung inflammatory events induced by particles, as well as expression of adhesion factors involved in the recruitment of circulating leukocytes into tissues.

VEGF is a multifunctional protein that plays a role as a growth and survival factor for vascular endothelial cells, as well as promotes their migration and alters their pattern of gene expression. In addition, VEGF induces vascular permeability with consequent influx of blood plasma constituents such as fibrinogen into the extravascular space, a process required for angiogenesis (Brown *et al.*, 1997). Furthermore, VEGF stimulates an NFκB-mediated expression of adhesion molecules ICAM-1, VCAM-1 and E-selectin on vascular endothelial cells (Kim *et al.*, 2001). In the lungs, type II pneumocytes and AM are the principal source of VEGF. VEGF exerts its function by binding specific receptors on endothelial cells, resulting in activation of signaling cascades (Lahm *et al.*, 2007). VEGF has been shown to stimulate migration of circulating monocytes and promote accumulation of macrophages in developing atherosclerotic plaques (Matsumoto and Mugishima, 2006). In the current study, small concentration-dependent increases in VEGF levels were observed in A549 cells upon exposure to particles, while in THP-1 cells, VEGF levels were increased above baseline in response to the PM_{10} and DWR1 particles. We have previously demonstrated elevated secretion of VEGF by A549 cells exposed to EHC-93, its insoluble fraction and Cristobalite, as well as its inhibition by the soluble fraction of EHC-93 (Chauhan *et al.*, 2005). In human lungs, VEGF transcript is found primarily in alveolar epithelial cells, where it functions as a specific mitogen for endothelial cells, as well as it is required for the maintenance of the alveolar structures and protection from alveolar septal cell apoptosis. VEGF also plays a critical role in angiogenesis (Koyama *et al.*, 2002). Additionally, VEGF has been shown to induce the production of ET-1 in human umbilical vein endothelial cells (HUVEC), and enhance ET-1 mRNA expression in bovine aortic endothelial cells (Matsuura *et al.*, 1998; Lee *et al.*, 2007).

The role of ET-1 has been extensively studied in the context of PM_{10}-associated adverse health effects, in relation to its physiological function as a potent vasoconstrictor. Elevations of ET-1 have been detected in animals exposed to urban air particles (Bouthillier *et al.*, 1998; Vincent *et al.*, 2001), as well as in humans (Calderón-Garcidueñas *et al.*, 2007). As stated previously, ET-1 also appears to play a role as a proinflammatory mediator, in light of its ability to prime neutrophils, promote chemotaxis and proliferation of monocytes and fibroblasts and stimulate monocytes to produce a variety of cytokines such as IL-1α, IL-6, IL-8, TNF-α and transforming growth factor-β. Elevated levels of ET-1 have also been observed in patients with pulmonary hypertension and idiopathic pulmonary fibrosis (Teder and Noble, 2000). Additionally, highest levels of ET-1 are

found in lungs in comparison to other tissues. ET-1 is secreted by endothelial cells, epithelial cells, alveolar macrophages, fibroblasts and polymorphonuclear leukocytes (Teder and Noble, 2000). In the current study, ET-1 peptide and its precursor big ET-1 remained mostly unchanged in A549 cells, THP-1 macrophages and in co-cultures, although THP-1 cells displayed a small elevation in low magnitude production of big ET-1, in response to EHC-93, EHC-6802 and DWR1 particles.

Inflammatory mediators such as cytokines, adhesion molecules, or growth factors produced by epithelial cells and macrophages in response to their encounter with urban air particles could be envisioned to stimulate the vascular endothelium and thus enhance PM-associated inflammatory events in the lung, as well as provide a potential for triggering systemic exacerbations of pre-existing diseases. Therefore, to examine whether mediators produced by epithelial and macrophage mono- and co-cultures are capable of influencing the pulmonary vascular endothelium, primary human pulmonary artery endothelial cells (HPAE) were treated with CM from mono- and co-cultures exposed to the particles. The study showed that endothelial cells responded to treatments with mono- and co-culture CM by significant productions of inflammatory cytokines and other soluble mediators. HPAE cells produced moderate amount of IL-6, IL-8 and MCP-1 basally. Treatment of HPAE cells with CM from mono-cultures exposed to particles resulted in elevated release of mostly IL-6, IL-8 and MCP-1, GM-CSF and TNF-α in response to THP-1 CM only, with highest magnitude production of MCP-1 and IL-8 in response to THP-1 CM. Overall, the cells responded more strongly to macrophage CM in comparison to epithelial CM, showing that the soluble mediator profile from macrophages may be more significant in stimulating endothelial cells than that from epithelia. In general, endothelial cells showed highest responses to CM from cells exposed to PM_{10} and $PM_{2.5}$ particles. This matched the observations with cytokine productions from epithelial cells and macrophages directly exposed to particles. The result suggests that endothelial cells, epithelial and macrophage cells respond similarly to the common stressor via the inflammatory mediators produced by the A549 and THP-1 cells in response to urban particles. Incubation of endothelial cells with media from A549/THP-1 co-cultures exposed to particles resulted in an HPAE cytokine profile more comparable to that seen with HPAE cells treated with THP-1 CM, suggesting that in general, soluble mediators produced by macrophage cells are more potent stimulants of endothelial cells than those made by epithelia. Most significantly, production of GM-CSF cytokine and MCP-1 chemokine by HPAE

cells was markedly elevated in a synergistic manner, in response to a 24 h treatment with A549/THP-1 CM. The CM from co-cultures exposed to EHC-93, EHC-6802 and DWR1 produced the most significant effects.

The inflammatory mediators GM-CSF and MCP-1 play a prominent role in the context of endothelial dysfunction. MCP-1 is a potent chemoattractant for leukocytes (Mills *et al.*, 1999), while GM-CSF is a chemotactic survival factor for circulating leukocytes (Mire-Sluis and Thorpe, 1998), thus the cytokines are capable of amplifying the inflammatory state associated with endothelial dysfunction by homing T-lymphocytes and monocytes into the subendothelial space. Highly inflammogenic oxidized low-density lipoprotein associated with atherogenesis induces release of GM-CSF, MCP-1 and IL-8 in umbilical vein endothelial cells (de Castellarnau *et al.*, 2007). Additionally, elevated expression of soluble VCAM-1, E-selectin, IL-6 and MCP-1 is produced by saphenous vein endothelial cells isolated from coronary bypass patients with diabetes in comparison to non-diabetic subjects, suggesting a link between proinflammatory state in diabetic endothelial cells and endothelial dysfunction in diabetic disease (Lehle *et al.*, 2007). Finally, cultured human pulmonary microvascular endothelial cells show increased expression of GM-CSF mRNA upon treatment with IL-1β, TNF-α or LPS for over 72 hrs, implying a potential role for the cytokine in endothelial dysfunction associated with pulmonary disorders such as acute respiratory distress syndrome (Burg *et al.*, 2002). Thus, IL-1β and TNF-α present in the co-culture medium were likely promoters of the elevated GM-CSF and MCP-1 in endothelial cells, with macrophages being their source, since A549 cells did not produce IL-1β and TNF-α. Nevertheless, A549 epithelial cells appear to play a role in the process, as the production of GM-CSF and MCP-1 by endothelial cells in response to CM from co-culture was higher than that observed in response to CM from the macrophages.

The lungs are the site of clearance and the primary source of circulating ET-1 (Dupuis *et al.*, 1996). Previous study with A549 type II epithelial cells exposed to EHC-93 particles for 24 hrs showed that the cells did not produce increased levels of ET-1, suggesting that alveolar epithelial cells may not be the source of elevated plasma levels of ET-1 in animals exposed to EHC-93 (Chauhan *et al.*, 2005). The current study confirmed this, and further showed that cell-cell interactions in A549/THP-1 co-culture exposed to EHC-93 did not lead to elevated production of ET-1. A549

cells exposed to EHC-93, however, display elevations in IL-8 and VEGF (Chauhan *et al.*, 2005), and as the current study shows, THP-1 cells and A549/THP-1 co-cultures also produce VEGF and IL-8, among a variety of other inflammatory mediators. VEGF and IL-8 have been shown to enhance the production of ET-1 by bronchial epithelial cells and endothelial cells (Endo *et al.*, 1992; Matsuura *et al.*, 1998; Lee *et al.*, 2007).

Thus, these soluble mediators could in turn act on endothelial cells to induce increased production of ET-1, and its release into circulation. HPAE endothelial cells showed moderate basal production of big ET-1 and ET-1 peptide. Treatment of HPAE cells with CM from particle-exposed A549 cells, THP-1 cells, or A549/THP-1 co-cultures did not affect the big ET-1 levels, as well as ET-1 levels were un-altered by treatments with A549 and co-culture conditioned media. Small, significant elevation in ET-1 was observed when endothelial cells were treated with CM from macrophages exposed to the urban particles EHC-93 and EHC-6802 and $PM_{2.5}$ particle DWR1 in comparison to HPAE cells treated with CM from THP-1 cells exposed to diesel particles and mineral particles. It is not possible to determine from this study, whether IL-8 and VEGF were responsible for the observed increased levels of ET-1. Addition of neutralizing antibodies against IL-8 and VEGF to the conditioned medium prior to incubation with HPAE cells could be used to determine their potential involvement. Furthermore, a significant difference in ET-1 levels in HPAE cells treated with CM from A549/THP-1 co-cultures exposed to the urban particles was not found, due to high variability in the measurements, although the data suggest a potential trend of increase, which will require further investigation.

HPAE cells produced basal levels of ICAM-1 and VCAM-1 but not E-selectin. Treatment with CM from A549 cells exposed to particles did not alter basal levels of the adhesion factors in HPAE cells. Treatment with CM from THP-1 cells exposed to EHC-93, EHC-6802, DWR1 and Cristobalite resulted in increased production of ICAM-1, VCAM-1 and E-selectin by HPAE cells. E-selectin synthesis was induced *de novo* by the factors contained within the CM. *De novo* synthesis of E-selectin has been observed in response to a number of stimuli including TNF-α, IL-1β, interferon-γ, or endotoxin (Leeuwenberg *et al.*, 1990). Incubation of the HPAE cells with the CM from co-cultures exposed to particles produced levels of adhesion factors comparable to those obtained with THP-1 CM. Enhanced endothelial expression of adhesion factors and monocytic cell adhesion were recently demonstrated in HUVEC cells exposed directly to Mexico City PM_{10}

and and $PM_{2.5}$ particles. ICAM-1, PECAM-1, VCAM-1, E-selectin and P-selectin expressions were induced by PM_{10}, while $PM_{2.5}$ only induced E-selectin, P-selectin and ICAM-1 (Montiel-Dávalos *et al.*, 2007). As shown by Alfaro-Moreno *et al.* (2007), endotoxin content of PM_{10} appeared to play a significant role in the activation of endothelial cells, as evidenced by increased E-selectin expression and enhanced adhesion of U937 monocytes to the HUVEC monolayer exposed directly for 6 hrs to Mexico City PM_{10} or the insoluble fraction of the particles, but not the soluble fraction, as detected by fluorescence microscopy and flow cytometry. A treatment with polymyxin B partially inhibited (72 %) E-selectin expression by HUVEC cells, suggesting that, other factors likely participated in the activation of the endothelium. The Mexico City particles contained 56 EU/mg, with 70 % contained within the insoluble fraction and 30 % in the water-soluble fraction (Alfaro-Moreno *et al.*, 2007). In the current study, urban air particles were in general the most potent inducers of inflammatory mediators and other soluble factors including adhesion molecules in cells directly exposed to the particles, as well as in endothelial cells exposed to CM from the direct cell exposures. Analysis of endotoxin in the particles showed that EHC-93, EHC-6802 and DWR-1 contained 18 - 21 EU/mg of endotoxin, about 35 % of the content of Mexico City particles, which is comparable to the endotoxin content seen in the water-soluble fraction of the Mexico City PM_{10} (17 EU/mg) which did not modify E-selectin expression in HUVEC cells, in their study. Furthermore, while Alfaro-Moreno *et al.* (2007) exposed endothelial cells directly to whole particles, in the current study, the HPAE cells did not encounter whole particles, as they were exposed to conditioned media, which were centrifuged to exclude the pellet (insoluble fraction of particles). Our analysis of endotoxin content in EHC-93 and its subfractions indicated that the water-soluble fraction of EHC-93 contained 2.9 EU/mg of endotoxin, ~15 % of the total EHC-93 content and since the HPAE cells were exposed to 70:30 ratio of CM/fresh media the HPAE cells encountered only a small fraction of the endotoxin content measured by Alfaro-Moreno *et al.* (2007) in their soluble fraction of Mexico City PM_{10}. The data suggest that endotoxin did not significantly contribute to the stimulation of endothelial cells observed when they were treated with CM from mono- and co-cultures of A549 and THP-1 cells exposed to urban particles. Additionally, the significant activation of endothelial cells as observed by their marked production of inflammatory factors was likely mediated by soluble cell factors present within the media, which were products of epithelial and macrophage cells' encounter with particulate matter. Soluble components of the particles such as transition metals or water-soluble organic compounds could

also contribute to the stimulation of the endothelial cells, however, the fact that CM from cells exposed to Cristobalite also significantly induce the production of inflammatory factors, as well as adhesion molecules suggests that they play a less important role in the activation of endothelial cells. Thus the findings support a view that the inflammatory mediators produced by pulmonary epithelial and AM cells upon their encounter with inhaled particles could be sufficient to activate the vascular endothelium.

The results from the AhR assay showed that EHC-6802 diesel particles had the highest content of AhR agonists such as PAHs, followed by EHC-93 and EHC-6802 urban particles. DWR1 fine particle mixture induced ~5 fold lower AhR activity than SRM-1650 particles. The assay was performed with whole particles only, thus the actual content of AhR agonists in the CM was unknown. Organic compounds such as PAHs are lipophilic and in general, strongly hydrophobic (Castelli *et al.*, 2002), however, their presence in trace quantities in the CM could be envisioned, potentially associated with lipid components of the media and serum, such as lipoproteins. Nevertheless, the study results show that CM from cells exposed to SRM-1650 particles did not bring about marked stimulation of endothelial cells, thus the organic compounds were unlikely modulators of HPAE endothelial activation in this model. Additionally, PAHs, while highly cytotoxic (Xia *et al.*, 2004) and mutagenic (Rosenkranz, 1995), can also induce significant suppression of lung immunity in rats, characterized by inhibition of alveolar macrophage and natural killer cell-mediated production of cytokines including TNF-α and IL-1 (Kong *et al.*, 1994).

Differential induction of endothelial cells was observed with CM from epithelial and/or macrophage cells exposed to Cristobalite in comparison to TiO_2. CM from Cristobalite-exposed cells caused elevated secretion of a number of cytokines and adhesion factors by HPAE cells, while effects on HPAE cells, of CM from TiO_2-exposed A549 and THP-1 cells were generally lacking. The data suggest that other factors that govern the differential toxicities of the two minerals should also be considered.

Overall, the data provide evidence that cell-cell interactions may play a critical role in the modulation of inflammatory processes initiated by encounter of epithelial cells and macrophages of the respiratory tract with specific inhaled pollutant particles. Furthermore, the joint production of inflammatory mediators and other effector molecules by the interacting cells can in turn

stimulate endothelial cells to produce more cytokines and to express molecules necessary for recruitment of leukocytes from circulation.

Thus *in vitro* co-culture models show a great potential for their utility in studies aimed at gaining a better understanding of intercellular communications and their role in mechanisms that govern the adverse biological effects of air pollution particles. In addition, their potential to more closely model the *in vivo* scenario warrants their use in particle toxicity screening studies. As they still only represent *in vitro* models of *in vivo* conditions, their utility needs to be validated by comparisons to effects *in vivo*, in animal models.

For this purpose, a subset of the particles utilized in the co-culture study, SRM-1650, EHC-6802 and DWR1 were intratracheally instilled into BALB/*c* mice for 2 and 24 hrs, after which a variety of toxicity and inflammation endpoints were analyzed in the BAL and blood of the animals. Overall, temporal and magnitudinal differences in the biological responses to diesel and urban PM were observed. As demonstrated by the previous study (see Chapter 1), acute neutrophil influx into the lungs was the most prominent feature of the response to particle exposures. Overall, the influx of neutrophils was more substantial after 24 hrs. This finding is in line with the study by Gerlofs-Nijland and colleagues (2005), who showed significantly elevated BAL neutrophil counts in spontaneously hypertensive rats exposed to EHC-93 and road tunnel PM, after 24 hrs, in comparison to 4 h. BAL neutrophil counts were elevated 2 hrs upon instillation in response to EHC-6802 and DWR1. SRM-1650 produced a more delayed response, with significant induction of BAL neutrophil influx, with counts comparable to those seen with the DWR1 particles, with clear dose-response. EHC-6802 particles were highest inducers of neutrophilia at both doses of particles, suggesting its greater potency in comparison to diesel and $PM_{2.5}$ particle DWR1. In line with the previous study (see Chapter 1), the neutrophilic response was accompanied by decrease in AM apparent after 24 hrs. This was in line with findings by Happo *et al.* (2007) who reported decreased macrophage numbers at their 12 h time point in C57Bl/6J mice exposed to size-fractionated PM samples, and EHC-93. Small elevations of band cells were also observed in the BAL from mice at 2 and 24 h, predominantly in response to EHC-6802 particles, although without temporal effects on their magnitude. A small, dose-dependent elevation of lymphocytes was also observed at the 2 h time point, but not at 24 hrs. The overall pattern of cellular effects

was consistent with low acute inflammatory response to a challenge with urban particulate matter, in line with other studies (Happo *et al.*, 2007; Gerlofs-Nijland *et al.*, 2005).

Analysis of adhesion factors in BAL revealed a general dose-dependent elevation of ICAM-1 at the 24 h time point and increased levels of VCAM-1 at 2 hrs in mice exposed to EHC-6802 and DWR-1 particles, in comparison to SRM-1650 exposure, while E-selectin was not detected. Increased expression of ICAM-1 in the lungs, mainly by AM plays a role, in the recruitment of neutrophils from the circulation into the lung parenchyma, as well as it may represent a resident macrophage-derived signal for migration of neutrophils, as has been suggested by studies with mice intratracheally exposed to silica (Hubbard *et al.*, 2001). Enhanced lung expression of ICAM-1 was also demonstrated in mice exposed to DEP, after a primary challenge with endotoxin (Takano *et al.*, 2002). In agreement, augmented production of ICAM-1 was observed with THP-1 macrophages exposed to urban particles and silica *in vitro* in the current study, however, no change in ICAM-1 was seen in the cells exposed to SRM-1650 particles. The reasons behind the difference are presently not known. Since THP-1 cells were consistently less sensitive to SRM-1650 *in vitro*, as evidenced by a lack of significant changes in their production of inflammatory mediators in response to diesel exposure, the disparity may point to cell type-specific difference in response to diesel particles, as THP-1 are a peripheral blood derived monocyte/macrophage cell line. The assessment of cytokine/chemokine levels in BAL upon particle instillations showed a particle-type and dose-associated differences in the various cytokine responses, which also varied with time. In general, cytokine response to particle exposures was rapid, with substantial dose-dependent elevation of TNF-α (>5,000 pg/ml, 250 μg dose of PM) in response to EHC-6802 and DWR1. SRM-1650 particles also showed a trend of increase in TNF-α at the high dose, although not significant. KC, MIP-1α and IL-6 were moderately elevated at 2 h time point, and IL-1α, IL-5, IL-10 and GM-CSF were also significantly elevated, but produced at lower quantities. After 24 hrs, the cytokine responses were significantly attenuated, with TNF-α decreased about 100 fold in comparison to the 2 hr time point. MIP-1α was the most sensitive cytokine detected at the highest levels in BAL at the 24 h time point, with IL-6, KC and TNF-α observed at moderate levels in BAL. In general, EHC-6802 and DWR1 particles were highly inflammogenic 2 hrs upon exposure, with EHC-6802 particles showing a sustained potency in their ability to induce elevated cytokines in the lungs, after 24 hrs, with the strongest effect observed at the high dose of the particle (250

μg). Interestingly, data also showed that the inflammogenic potency of DWR1 was high at the 2 hr time point, with the particle showing less potency after 24 hrs, which was mostly apparent in its effect on TNF-α levels. Overall, the cytokine responses between the current study and the previous *in vivo* study that included EHC particles and DWR1 are in agreement. Similarly, Happo *et al.* (2007) showed time-dependent, increased levels of BAL IL-6, TNF-α and KC in their study with C57Bl/6J mice exposed intratracheally to size-fractionated urban particles collected from a number of European cities, which were also comparable in magnitude and PM-class dependent response, to the current study.

Cytokine levels in blood plasma were assessed to determine potential systemic impacts of the acute inflammatory response localized to the lungs. The analysis revealed small, but significant dose-dependent increase in plasma levels of GM-CSF, MIP-1α, KC and RANTES cytokines detectable at the 2 hr time point, with most of the cytokine effects becoming non-significant at the 24 h time point, with the exception of RANTES, which showed a small, low dose-dependent main effect ($p=0.009$). In light of the small magnitude of effects detected in plasma of the animals, and the high variability of the measurements, these observations warrant further investigation.

Finally, significant variability was observed between the naïve, sham and vehicle animal controls for a number of endpoints in the *in vivo* study. This finding does not confound the analysis of particle effects in mice, as the statistical analysis was conducted in comparison to vehicle control measurements, which were consistently higher, or comparable to the sham or naïve controls for all the analytes. This shows that vehicle treatment, as well as the surgical procedure itself, may affect the levels of adhesion factors, pro-inflammatory cytokines/chemokines and total protein content detectable in BAL. Thus it is critical to include a comprehensive set of controls in animal studies to identify potential confounding factors that could affect the interpretation of the findings.

Validation of the panel of *in vitro* assays in the BALB/*c* mouse model was performed by using the Pearson correlation test to compare the *in vitro* cellular responses to the EHC-6802, DWR1 and SRM-1650 subset of particles with neutrophil counts in BAL of mice exposed to the same set of particles. The validation analysis revealed that the majority of endpoints measured in co-cultures of A549 and THP-1 macrophages were significantly correlated with BAL neutrophil responses to particles at both 2 and 24 h time points. In contrast, mono-cultures of the cells showed few

significant correlations with the 2 h BAL neutrophil counts but a greater number of correlations with the 24 h neutrophil counts, with majority attributed to the THP-1 cytokine responses. The best correlation for A549 epithelial cells was achieved with Alamar Blue assay, which showed a significant negative association with 24 h BAL neutrophil counts ($r=-0.871$, $p<0.05$). Other *in vitro* assay endpoints, including VEGF and ICAM-1 were also strongly associated with BAL neutrophil counts. Overall, the highest correlation was observed between the *in vitro* measurement of IL-1β in THP-1 cells, with the 24 h BAL neutrophil counts ($r=0.935$, $p<0.001$), and between the *in vitro* ICAM-1 response measured in A549/THP-1 co-cultures, with the 2 h BAL neutrophil counts ($r=0.916$, $p<0.001$). The data suggest that the activated THP-1 macrophage cells represent a good model system for the assessment of biological effects of particles *in vitro*, with strong predictive ability for the *in vivo* inflammatory neutrophilic response to a particle challenge in mice. The A549/THP-1 co-culture model also correlates well with BAL neutrophil counts, with the added advantage of correlating with both early (2 h) and later (24 h) BAL responses to particles in the *in vivo* mouse model, thus showing association with temporal change in neutrophil responses in animals exposed to particles.

A validation of the indirect effects of particles *in vitro* on the endothelial cells with the BAL neutrophilic response *in vivo* showed that the responses of vascular endothelial cells *in vitro* can also be of great use for gauging the BAL neutrophilic response in animals exposed intratracheally to urban air particles. Endothelial cell responses to CM from mono-cultures also showed high correlation with 24 h BAL neutrophil counts, but not the 2 h neutrophil estimates. Additionally, the endothelial cell responses to CM from co-cultures showed a good predictability of PM-induced BAL neutrophilia at both 2 and 24 h time points. In general, the data revealed that in combination with the direct exposure of epithelial cells and macrophages, especially their co-culture, the assessment of the production of inflammatory cytokines and adhesion factors by the HPAE cells correlates well with the *in vivo* murine pulmonary neutrophilic response to particles.

Similarly, the Pearson linear correlation test was employed to examine the relationships between various inflammatory, biochemical, and cell differential endpoints with neutrophil counts in BAL. The analysis showed that more endpoints were significantly correlated with neutrophil counts at the 24 time point than at the 2 hr time point (12 vs. 8). At the 2 h time point, MIP-1α was highly correlated with the 2 h BAL neutrophil count ($r=0.905$, $p<0.001$). The IL-10 cytokine in the blood

plasma of the animals 2 h after exposure showed the highest correlation with 2h BAL neutrophil count, however, the assay measurements were not significant, although showing potential increasing trend. As stated previously, the blood cytokine measurements showed high variability, thus further investigation would require an increased number of animals and/or an improved plasma extraction technique could be used to decrease data variability. At the 24 h timepoint, cytotoxicity assays, as defined by biochemical and cell differential measurements showed a stronger level of correlation in comparison to the 2 h time point, with the 24 h BAL macrophage counts showing a strong negative correlation with 24 h BAL neutrophil counts ($r=-0.931$, $p<0.001$). Additionally, a higher number of cytokines were highly associated with 24 h BAL neutrophil counts, including TNF-α. Finally, the adhesion factor 24 h BAL ICAM-1 measurements were strongly associated with 24 h BAL neutrophil counts in mice exposed to the particles ($r=0.922$, $p<0.001$). These associations pinpoint to potentially significant relationships between biochemical and cellular measures of cytotoxicity (neutrophil and alveolar macrophage counts), measures of acute lung inflammation (MIP-1α, KC, TNF-α) and markers of immune cell recruitment necessary for the amplification of an immune response (ICAM-1), in response to a pulmonary challenge of animals with air pollution particles. The mechanisms governing the observed associations will need to be examined in detail, in the future.

CONCLUSION & FINAL COMMENTS

The biological effects of air pollution particles including a range of PM_{10}, $PM_{2.5}$ particles and mineral dusts were investigated at the level of various endpoints of cytotoxicity and inflammation. The focus of this thesis was to systematically evaluate the usefulness of the endpoints for their ability to differentiate between the various particles on the basis of their toxic potencies in cells, and to validate the capacity of the *in vitro* screening approach to predict the toxicity of the particles instilled into the lungs of experimental animals. Likewise, an *in vitro* human cell interaction model was developed for the investigation of the biological effects of particles, to determine if the added degree of biological complexity would make it a better *in vitro* tool for simulating the particle toxicity *in vivo*, in comparison to the mono-culture systems.

As was made apparent by this work, a focussed panel of *in vitro* assays can provide a tool with good predictive ability of a fundamental measure of biological impact of inhaled or instilled air pollution particles in experimental animals, namely neutrophilia. The study shows that a combination of classical endpoint assays of cytotoxicity and cytokine biomarkers of inflammation can facilitate screens of particles with relevance to their *in vivo* impact. The initial choice of the particles for screening, however, has an impact on the sensitivity of the *in vitro* model. Specifically, the model may distinguish between the toxic potencies of different classes of particles, such as urban air particles versus minerals, but its performance is improved when only a panel of urban particles is evaluated. This suggests that if the purpose is to evaluate relative toxicity of urban particles, the inclusion of particles with highly distinct physicochemical properties, such as the minerals, will change the efficacy of the model. At the same time, the choice of the *in vivo* benchmark of biological impact is of great importance, as it needs to be reflective of the biological impact of the particles. The high correlation of BAL neutrophil counts with a number of proinflammatory cytokines, as well as several cellular and biochemical benchmarks in BAL shows that neutrophilia is a good benchmark of acute lung inflammatory effects of particles. As neutrophils are recruited from the circulation, it also provides a systemic benchmark of the activation of innate immunity. Thus, strengths of associations of systemically measured endpoints with neutrophilia induced by different particles may provide additional insight into the extrapulmonary effects of inhaled/instilled particles.

The current model also has some limitations. Although intratracheal instillation is widely used in studies as a more simple, rapid and cost-effective alternative to inhalation, there are some differences in the distribution, clearance and retention of the materials when administered by the two techniques. Thus it is also recommended to conduct a particle inhalation study, when possible. Despite the differences between the techniques, the majority of pulmonary toxicity studies indicate qualitatively comparable results for endpoints such as inflammation, fibrosis, or allergic sensitization between the two techniques (Driscoll *et al.*, 2000). The second aspect is that the employment of *in vitro* approaches generally utilizing monolayers of cells represents an over-simplification of the complexities of *in vivo* biological responses, which may impact the interpretation of the findings from *in vitro* assays in relation to their ability to accurately reflect *in vivo* toxicity results. Along the same line, the use of continuous cell lines in the studies as surrogates for normal cells found *in vivo*, presents an additional degree of uncertainty. Therefore, the utility of primary cells harvested from animals, or obtained from human subjects is recommended, alongside the established cell lines, to compare the observed responses. Cell lines, with their virtually infinite potential to proliferate are significantly different from terminally differentiated or senescent primary cells. Nevertheless, cell lines share a number of morphological, functional and biochemical features with their primary cell-counterparts. These features, along with their ease of use and low cost make cell lines ideal for high throughput toxicity screening of xenobiotics, or for controlled mechanistic studies.

As demonstrated by this thesis, re-creation of epithelial-macrophage interactions *in vitro* results in amplified, particle-dependent differential productions of a number of inflammatory cytokines, and other molecules such as growth factors or adhesion molecules, with properties that may be relevant to the particle-associated health effects observed *in vivo*. Furthermore, the ability of particle-induced mediators to activate endothelial cells with a concomitant expression of adhesion molecules and release of cytokines and chemokines, indicates that the effects of particles on cells other than the initial target cells of atmospheric pollutants, namely airway epithelial cells and macrophages, need to be included in the investigations of pathogenic effects of particles. Therefore, co-culture models which can enable cellular crosstalk provide a markedly improved exposure system, with an added level of physiological complexity, and can be utilized both for studying the mechanisms of particle effects, as well as for toxicity screening of particles with different compositions.

The usefulness and the physiological relevance of the co-culture system can be additionally improved by re-creating a more accurate model of specific pulmonary micro-environments. In response to an inflammatory stimulus, leukocytes will migrate from the bloodstream across the endothelium in an apical-to-basolateral direction into the tissues, followed by crossing the airway epithelium in the basolateral-to-apical direction, to enter the lumen of the lung (Liu *et al.*, 1996).

For example, to simulate the pulmonary micro-environments and the encounter of alveolar macrophages and airway epithelial cells with urban air particles, airway epithelial cells can be co-cultured in a regular well with alveolar macrophages and exposed to a variety of particles. In a second well, lung microvascular endothelial cells can be cultured on top of a transwell insert, with epithelial cells cultured on the opposite side of the insert. The conditioned media from the particle-exposed cells (without particles) will be added into the basolateral (bottom compartment), while fluorescently labelled neutrophils in fresh media will be added to the apical compartment (upper compartment), on top of the endothelial cells. The model would thus recreate the physiological basolateral-to-apical polarization. The rate of transmigration of the neutrophils across the bilayer of cells and the basement membrane formed between the cells could be assessed in response to chemotactic stimuli in the CM from PM-exposed macrophage/epithelial cell co-cultures. The fluorescence in both compartments would be quantified and related to the total input. The ability of the various particles to promote chemotaxis of neutrophils could thus be examined. The proper formation of confluent cell layers can be assessed by immunocytochemical staining of the bilayers for markers expressed at cellular junctions, or measurements of transepithelial electric resistance across the bilayer. A multitude of endpoints including inflammatory mediator production, adhesion factor expression, or the release of factors such as VEGF and ET-1 could be assessed. Additionally, the mechanisms of leukocyte transmigration in response to CM from PM-exposed cells can be studied by pre-incubations of CM with antibodies for neutralizing specific mediators present in the CM, prior to its addition to the basolateral compartment of the second well, or the use of metal chelators and antioxidant compounds to block metal-dependent activity and oxidative stress (Figure 2-47). The model could also be employed in the same manner for the study of allergic mechanisms in relation to particle exposures, by using eosinophils instead of neutrophils. Finally, by co-culturing fibroblasts with airway epithelial cells and alveolar macrophages, the mechanisms that govern PM-induced airway wall remodeling could be explored, by simulating the presence of connective tissue underlying the airway epithelium.

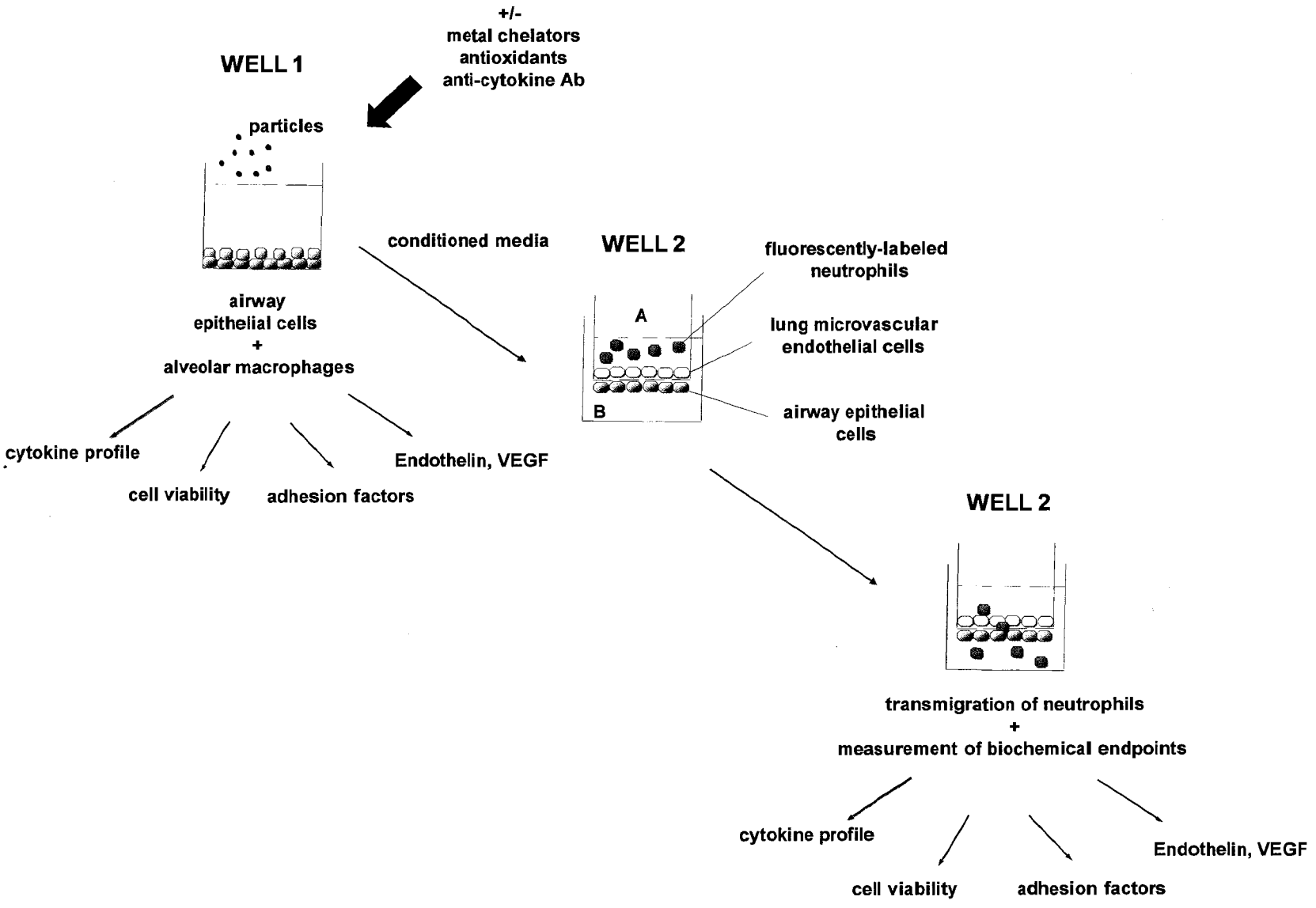
+/-
metal chelators
antioxidants
anti-cytokine Ab
WELL 1
particles
airway
epithelial cells
+
alveolar macrophages
conditioned media
cytokine profile
cell viability
adhesion factors
Endothelin, VEGF
WELL 2
A
B
fluorescently-labeled
neutrophils
lung microvascular
endothelial cells
airway epithelial
cells
WELL 2
transmigration of neutrophils
+
measurement of biochemical endpoints
cytokine profile
cell viability
adhesion factors
Endothelin, VEGF

Figure 2.47. Schematic for a proposed *in vitro* co-culture cell model for the study of air pollution particle-mediated inflammatory, allergic or pro-fibrotic events. Alveolar macrophages and airway epithelial cells can be co-cultured (well 1) and exposed to particulate matter (PM), in the presence or absence of neutralizing antibodies (Ab), antioxidants, or chelators. Lung endothelial and epithelial cells are cultured in a transwell insert in a physiological basolateral-to-apical polarization (well 2), and exposed in a basolateral compartment (B) to conditioned media from well 1. Fluorescently labelled neutrophils are added to the apical compartment (A). Chemotaxis of the neutrophils across the cell bilayer is quantified. Multiple endpoints (cytokines, adhesion factors, VEGF, ET-1 are measured in wells 1 and 2. The model could also be utilized to examine allergic, or pro-fibrotic mechanisms in relation to particle exposures, using the relevant cell types.

As the thesis also shows, differential biological responses observed in both studies by the assessment of a number of *in vitro* and *in vivo* endpoints are particle-type dependent, and appear to be related to the specific compositional differences and properties of the individual particles. As pointed out by Mage (1983) in response to the US Environmental Protection Agency decision to adopt mass, concentration PM standards independent of the toxicity of their constituents, the chemical composition of the air pollution particles determines their toxic potency. Thus the same concentration of the particles will not be indicative of the same health effects due to the compositional differences between the particles. Similarly, low concentration of a potent mix of particles will likely be more hazardous than a high concentration of inert particles.

"A particle is not a *partide* is not a PARTICLE" (Mage, 2002).

The findings stress the importance of developing new study designs that will enable the linking of potential health effects with the physicochemical properties of the specific particles. The use of recently developed "omics" scientific technologies for the studies of an entire genome, and thousands of proteins and metabolites, in combination with a high throughput screening of *in vitro* toxic potencies of air pollution particles across cell types and species could be employed to generate a vast biochemical database of information. With the use of multivariate statistical methodologies and data mining tools, key endpoints and pathways impacted by specific particles could be identified. The approach will also require a development of improved descriptors of toxic potency that can also take into account complex non-linear biological responses (eg. bi-phasic), which are at times observed and remain largely unexplored.

More research is also needed to determine and validate variables such as particle dose metrics, time points, exposure duration, cell culture conditions, or choice of relevant cell types, to facilitate easier comparisons of findings between studies, to develop standardized experimental approaches, as well as to better characterize the physicochemical properties of the specific particles under study.

A few recent studies have illustrated the utility of the approach for relating biological effects obtained from measurements of toxicity endpoints in cell culture, or in animals with specific components of PM_{10} and $PM_{2.5}$ particles, including transition metals, secondary aerosols, organic

chemicals and biogenic components. The studies utilized multivariate statistical approaches including multiple linear regressions, or principal component analysis (Steerenberg *et al.*, 2006; Rosas Pérez *et al.*, 2007; Alfaro-Moreno *et al.* 2007).

With the rapid emergence of nanotechnologies, which promise to provide societal benefits, but are also likely to carry unforseen risks to human health and the biosphere, an improved understanding of biological impacts of atmospheric pollutants is needed, to establish policies that will effectively mitigate pollution on the basis of the chemical and physical properties of the particles responsible for the health effects.

In conclusion, the current work represents an original contribution to the research on the health effects of urban air pollution particles. The study is an extensive and comprehensive toxicity screening evaluation of particulate matter, examining the effects of multiple types of particles in different cell types, utilizing a large panel of endpoints to assess various cellular functions. The work provides an original mechanistically-based model for the validation of *in vitro* toxicity and inflammation assays, enabling their comparison to critical *in vivo* endpoints, and illustrating a proof of concept for the utility of alternative (non-animal) methods in toxicology screening, with high relevance to the *in vivo* health effects. The model could also provide an alternative testing strategy for health effects of chemical substances such as cosmetics, therapeutics, or industrial and household chemicals, thus it is also relevant to other research fields. Finally, an original human *in vitro* co-culture model was also developed in this study, which provided evidence for the cell interaction-induced modulation of cytotoxic and inflammatory cellular responses to particulate matter. By validating the human *in vitro* co-culture model with respect to the *in vivo* particle exposure of mice, and by contrasting with a study of the cell types in isolation, it was shown that the human cell co-culture provides a more accurate model of the *in situ* milieu. Therefore, cell interactions should be highly considered in the development of an *in vitro* screening strategy for the biological effects of air pollution particles. The mechanisms governing the observed cell interaction responses to specific particle exposures will require further investigation.

CONTRIBUTIONS OF COLLABORATORS

I would like to to express my gratitude to the following people, whose efforts were instrumental in completing my studies. I could not have completed my project without their help;

Dr. Sabit Cakmak for his expert help, troubleshooting and advice with statistical analyses, and Andrew Williams, for helping with my numerous statistical queries.

Animal Resources Division (Health Canada, Ottawa) staff led by Douglas Parks who were responsible for the experimental animal handling, and Svetlana Popovic and Kevin Kittle from the ARD, who expertly performed the IT particle deliveries in mice.

Patrick Goegan, Erica Blais, Devi Ganesh and Marc Bourbeau for performing the laborious necropsies and sample collections during the animal studies (2006, 2007).

Marcelle Phaneuf for her flawless coordination of the animal studies, animal protocol submissions, sample handling, and assistance with cell cultures.

Lorraine Casavant for tirelessly conducting the BAL cell differential analysis for both animal studies.

Miriam Dubreuil, Dr. Vinita Chauhan, Yunus Siddiqui and Marcelle Phaneuf for lengthy cytospin cell processing.

Lorraine Casavant and Dr. Mohamed Abdel Salam for their assistance with BAL and plasma sample post-processing.

Dr. Vinita Chauhan for her experimental collaboration and co-authorship of two manuscripts published in 2004 and 2005, and Patrick Goegan for his experimental work in the 2004 manuscript.

Yunus Siddiqui for his assistance with AhR assay, and for performing the endotoxin analysis of particle preparations.

Dr. Michael S. Denison (University of California, Davis, CA) for generously providing the H1L1.1c2 cells.

Dr. Jeffrey R. Brook (Environment Canada, Toronto, ON) for kindly providing the Trans-Canada Collection $PM_{2.5}$ particles.

Dr. Hiroshi Mukae and his team at the Second Department of Internal Medicine, Nagasaki University, as well as Dr. Kozo Ohkusu-Tsukada and his lab team, in the Immunology Divison of the Graduate School of Biomedical Sciences, Nagasaki University for the opportunity to conduct research in their laboratories and learn new techniques, in turn providing me with a highly rewarding and satisfying experience.

APPENDIX

Table A-1. Summary of statistical analyses for *in vitro* cytotoxicity assays (Chapter 1).

Endpoint	Cells	Main Effects[a]	Comparisons[b]	p
Alamar Blue	A549	PM x CONC		**<0.001**
	J774A.1	PM x CONC		**0.049**
WST-1	A549	PM x CONC		**<0.001**
	J774A.1	PM		<0.001
			DWR1 vs. SRM-1649	<0.001
			DWR1 vs. EHC-2000	<0.001
			SRM-1648 vs. SRM-1649	<0.001
			DWR1 vs. EHC-98	<0.001
			EHC-93 vs. SRM-1649	<0.001
			CRI vs. SRM-1649	<0.001
			DWR1 vs. TiO_2	<0.001
			SRM-1648 vs. EHC-2000	<0.001
			EHC-93 vs. EHC-2000	0.002
	J774A.1	CONC		<0.001
			20 vs. 160	<0.001
			10 vs. 160	<0.001
			40 vs. 160	<0.001
			20 vs. 0	<0.001
			80 vs. 160	<0.001
			10 vs. 0	<0.001
			40 vs. 0	<0.001
			20 vs. 80	<0.001
			0 vs. 160	<0.001
			10 vs. 80	<0.001
			40 vs. 80	<0.001
LDH	A549	PM x CONC		**<0.001**
	J774A.1	PM x CONC		**<0.001**
ATP	A549	PM		<0.001
			DWR1 vs. SRM-1649	<0.001
			DWR1 vs. CRI	<0.001
			DWR1 vs. SRM-1648	<0.001
			EHC-93 vs. SRM-1649	<0.001
			EHC-93 vs. CRI	<0.001
			EHC-93 vs. SRM-1648	<0.001
			DWR1 vs. TiO_2	0.001
			DWR1 vs. EHC-2000	0.002
			EHC-98 vs. SRM-1649	0.003
			EHC-98 vs. CRI	0.005
			EHC-98 vs. SRM-1648	0.011
			DWR1 vs. EHC-98	0.012
			EHC-2000 vs. SRM-1649	0.021
			TiO_2 vs. SRM-1649	0.026
			EHC-2000 vs. SRM-1649	0.031
			TiO_2 vs. CRI	0.039
	A549	CONC		<0.001
			10 vs. 160	<0.001
			20 vs. 160	<0.001
			10 vs. 80	<0.001
			40 vs. 160	<0.001

Endpoint	Cells	Main Effects[a]	Comparisons[b]	p
			10 vs. 0	<0.001
			20 vs. 80	<0.001
			0 vs. 160	<0.001
			10 vs. 40	<0.001
			20 vs. 0	0.004
			80 vs. 160	0.006
			20 vs. 40	0.032
	J774A.1	PM		<0.001
			TiO_2 vs. SRM-1649	<0.001
			DWR1 vs. SRM-1649	<0.001
			EHC-98 vs. SRM-1649	<0.001
			EHC-2000 vs. SRM-1649	0.003
			TiO_2 vs. SRM-1648	0.003
			DWR1 vs. SRM-1648	0.004
			EHC-98 vs. SRM-1648	0.006
			EHC-2000 vs. SRM-1648	0.016
			EHC-93 vs. SRM-1649	0.024
			CRI vs. SRM-1649	0.033
	J774A.1	CONC		<0.001
			20 vs. 160	<0.001
			40 vs. 160	<0.001
			10 vs. 160	<0.001
			80 vs. 160	<0.001
			20 vs. 0	<0.001
			0 vs. 160	<0.001
			40 vs. 0	0.001
			10 vs. 0	0.006
			20 vs. 80	0.007
			40 vs. 80	0.021
BrDU ELISA	A549	PM		0.004
			EHC-93 vs. TiO_2	<0.001
			EHC-93 vs. EHC-2000	0.004
			CRI vs. TiO_2	0.005
			EHC-93 vs. SRM-1649	0.005
			SRM-1648 vs. TiO_2	0.011
			EHC-93 vs. EHC-98	0.015
			DWR1 vs. TiO_2	0.020
			CRI vs. EHC-2000	0.039
	A549	CONC		<0.001
			10 vs. 160	<0.001
			10 vs. 80	<0.001
			40 vs. 160	<0.001
			40 vs. 80	<0.001
			10 vs. 20	0.002
			10 vs. 0	0.006
			0 vs. 160	0.009
			40 vs. 20	0.023
			20 vs. 160	0.030
			0 vs. 80	0.036
	J774A.1	PM		<0.001
			DWR1 vs. TiO_2	<0.001

Endpoint	Cells	Main Effects[a]	Comparisons[b]	p
			CRI vs. TiO_2	<0.001
			DWR1 vs. SRM-1649	<0.001
			CRI vs. SRM-1649	<0.001
			DWR1 vs. SRM-1648	<0.001
			CRI vs. SRM-1649	<0.001
			DWR1 vs. EHC-2000	<0.001
			CRI vs. EHC-2000	<0.001
			EHC-93 vs. TiO_2	0.002
			DWR1 vs. EHC-98	0.003
			CRI vs. EHC-98	0.003
			EHC-93 vs. SRM-1649	0.006
			EHC-93 vs. TiO_2	0.020
			DWR1 vs. EHC-93	0.031
			CRI vs. EHC-93	0.033
			EHC-93 vs. SRM-1648	0.041
	J774A.1	CONC		<0.001
			10 vs. 160	<0.001
			0 vs. 160	<0.001
			10 vs. 80	<0.001
			0 vs. 80	<0.001
			20 vs. 160	<0.001
			10 vs. 40	<0.001
			40 vs. 160	<0.001
Total Protein	A549	PM		<0.001
			DWR1 vs. TiO_2	<0.001
			EHC-2000 vs. TiO_2	<0.001
			SRM-1649 vs. TiO_2	<0.001
			DWR1 vs. CRI	<0.001
			SRM-1648 vs. TiO_2	<0.001
			EHC-98 vs. TiO_2	0.002
			DWR1 vs. EHC-93	0.003
			DWR1 vs. SRM-1648	0.004
			EHC-2000 vs. EHC-93	0.005
			EHC-2000 vs. SRM-1648	0.008
			SRM-1648 vs. TiO_2	0.008
			SRM-1649 vs. CRI	0.013
			EHC-93 vs. TiO_2	0.014
			DWR1 vs. EHC-98	0.019
			EHC-2000 vs. EHC-98	0.032
	A549	CONC		<0.001
			0 vs. 160	<0.001
			10 vs. 160	<0.001
			20 vs. 160	<0.001
			0 vs. 80	<0.001
			40 vs. 160	<0.001
			10 vs. 80	<0.001
			20 vs. 80	<0.001
			0 vs. 40	0.002
			80 vs. 160	0.006
			40 vs. 80	0.031

Endpoint	Cells	Main Effects[a]	Comparisons[b]	p
	J774A.1	PM		<0.001
			DWR1 vs. SRM-1649	<0.001
			EHC-98 vs. SRM-1649	<0.001
			EHC-2000 vs. SRM-1649	<0.001
			DWR1 vs. CRI	<0.001
			DWR1 vs. EHC-93	0.001
			EHC-98 vs. CRI	0.002
			EHC-98 vs. EHC-93	0.005
			DWR1 vs. TiO_2	0.007
			DWR1 vs. SRM-1648	0.007
			EHC-2000 vs. CRI	0.011
			EHC-2000 vs. EHC-93	0.020
			EHC-98 vs. TiO_2	0.025
			EHC-98 vs. SRM-1648	0.027
	J774A.1	CONC		<0.001
			20 vs. 160	<0.001
			10 vs. 160	<0.001
			40 vs. 160	<0.001
			0 vs. 160	<0.001
			80 vs. 160	0.001
AhR Assay	H1L1.1c2	PM x CONC		**<0.001**

[a]For all assays where interactions were observed by two-way ANOVA, only the p value for PM x CONC interaction is listed (main effects are not shown). P values for interactions are shown in bold.

[b]For all assays where interactions were not observed, main effects and comparisons (Holm-Sidak method) are listed.

Table A-2. Summary of statistical analyses for *in vitro* cytokine/chemokine assays (Chapter 1).

Endpoint	Cells	Main Effects[a]	Comparisons[b]	p
IL-1α	J774A.1	PM		<0.001
			EHC-2000 vs. CRI	<0.001
			EHC-2000 vs. DWR1	<0.001
			EHC-98 vs. CRI	<0.001
			EHC-2000 vs. TiO_2	0.001
			SRM-1648 vs. CRI	0.002
			EHC-98 vs. DWR1	0.004
			EHC-2000 vs. SRM-1649	0.005
			SRM-1648 vs. DWR1	0.015
			EHC-98 vs. TiO_2	0.017
			EHC-93 vs. CRI	0.022
			EHC-2000 vs EHC-93	0.023
			EHC-98 vs. SRM-1649	0.049
		CONC		<0.001
			160 vs. 0	<0.001
			40 vs. 0	<0.001
			160 vs. 10	<0.001
			40 vs. 10	0.002
			10 vs. 0	0.004
IL-1β	J774A.1	PM		<0.001
			EHC-2000 vs. TiO_2	<0.001
			EHC-2000 vs. CRI	0.002
			EHC-98 vs. TiO_2	0.002
			SRM-1648 vs. TiO_2	0.004
			EHC-2000 vs. DWR1	0.005
			EHC-2000 vs. SRM-1649	0.017
			EHC-98 vs. CRI	<0.017
			SRM-1648 vs. CRI	0.027
			EHC-2000 vs EHC-93	0.031
			EHC-98 vs. DWR1	0.039
		CONC		<0.001
			160 vs. 0	<0.001
			40 vs. 10	<0.001
			160 vs. 10	0.003
			40 vs. 10	0.007
			10 vs. 0	0.030
IL-6	A549	CONC		<0.001
			160 vs. 0	<0.001
			160 vs. 10	0.001
			40 vs. 0	0.005
	J774A.1	PM x CONC		**<0.001**
IL-8	A549	PM		<0.001
			TiO_2 vs. DWR1	<0.001
			CRI vs. DWR1	<0.001
			SRM-1649 vs. DWR1	<0.001
			EHC-98 vs. DWR1	<0.001
			TiO_2 vs. EHC-98	0.003
			EHC-93 vs. DWR1	0.005

Endpoint	Cells	Main Effects[a]	Comparisons[b]	p
			EHC-2000 vs. DWR1	0.005
			CRI vs. EHC-2000	0.011
			CRI vs. EHC-93	0.012
			SRM-1649 vs. EHC-2000	0.021
			SRM-1649 vs. EHC-93	0.022
			TiO_2 vs. SRM-1648	0.041
IL-8	A549	CONC		<0.001
			160 vs. 0	<0.001
			40 vs. 0	<0.001
			160 vs. 10	<0.001
			10 vs. 0	<0.001
			40 vs. 10	<0.001
			160 vs. 40	0.002
IL-10	J774A.1	PM		<0.001
			CRI vs. EHC-98	<0.001
			CRI vs. SRM-1649	<0.001
			DWR1 vs. EHC-98	0.001
			DWR1 vs. SRM-1649	0.003
			CRI vs. EHC-93	0.011
			EHC-2000 vs. EHC-98	0.012
			CRI vs. TiO_2	0.014
			EHC-2000 vs. SRM-1649	0.022
			CRI vs. SRM-1648	0.034
			SRM-1648 vs. EHC-98	0.035
	J774A.1	CONC	0 vs. 160	<0.001
			10 vs. 160	<0.001
			40 vs. 160	<0.001
			0 vs. 40	0.012
GM-CSF	A549	CONC		<0.001
			160 vs. 10	<0.001
			160 vs. 0	<0.001
			160 vs. 40	<0.001
			40 vs. 10	0.005
	J774A.1	PM x CONC		**0.035**
MCP-1	A549	PM x CONC		**0.013**
RANTES	J774A.1	PM x CONC		**<0.001**
TNF-α	J774A.1	PM x CONC		**<0.001**

[a]For all assays where interactions were observed by two-way ANOVA, only the p value for PM x CONC interaction is listed (main effects are not shown). P values for interactions are shown in bold.

[b]For all assays where interactions were not observed, main effects and comparisons (Holm-Sidak method) are listed.

Table A-3. Summary of statistical analyses for *in vivo* biochemical endpoints and cell differential counts (Chapter 1).

Endpoint	Source	Main Effects[a]	Comparisons[b]	p
8-Isoprostane	Blood plasma	DOSE		<0.001
			100 vs. 0	<0.001
			50 vs. 0	0.005
			250 vs. 0	0.012
			100 vs. 250	0.034
LDH	BAL	PM		0.009
			CRI vs. DWR1	<0.001
			CRI vs. EHC-2000	0.011
			SRM-1649 vs. DWR1	0.020
		DOSE		0.041
			250 vs. 0	0.007
			250 vs. 100	0.021
Total Protein	BAL	DOSE		<0.001
			250 vs. 0	<0.001
			250 vs. 50	<0.001
			250 vs. 100	<0.001
			100 vs. 0	0.039
Total Cells	BAL			n.s.
Neutrophils	BAL	PM x DOSE		**0.004**
Macrophages	BAL	PM		0.034
			DWR1 vs. CRI	0.014
			TiO_2 vs. CRI	0.021
			DWR1 vs. SRM-1649	0.025
			TiO_2 vs. SRM-1649	0.036
		DOSE		<0.001
			0 vs. 250	<0.001
			0 vs. 100	<0.001
			0 vs. 50	<0.001
Band Cells	BAL	DOSE		<0.001
			50 vs. 0	<0.001
			250 vs. 0	<0.001
			100 vs. 0	0.006
Lymphocytes	BAL	DOSE		<0.001
			50 vs. 0	<0.001
			250 vs. 0	<0.001
			100 vs. 0	0.006

[a]For all assays where interactions were observed by two-way ANOVA, only the p value for PM x DOSE interaction is listed (main effects are not shown). P values for interactions are shown in bold. N.S. indicates not statistically significant data.

[b]For all assays where interactions were not observed, main effects and comparisons (Holm-Sidak method) are listed.

Table A-4. Summary of statistical analyses for *in vivo* cytokine/chemokine assays (Chapter 1).

Endpoint	Source	Main Effects[a]	Comparisons[b]	p
IL-1α	BAL	PM		<0.001
			CRI vs. TiO_2	<0.001
			EHC-2000 vs. TiO_2	<0.001
			CRI vs. DWR1	<0.001
			EHC-2000 vs. DWR1	<0.001
			SRM-1649 vs. TiO_2	0.001
			SRM-1649 vs. DWR1	0.028
			CRI vs. SRM-1649	0.044
		DOSE		<0.001
			250 vs. 0	<0.001
			100 vs. 0	<0.001
			50 vs. 0	<0.001
			250 vs. 50	<0.001
			250 vs. 100	0.011
			100 vs. 50	0.040
IL-1β	BAL	PM		<0.001
			CRI vs. TiO_2	<0.001
			CRI vs. DWR1	<0.001
			EHC-2000 vs. TiO_2	<0.001
			EHC-2000 vs. DWR1	<0.001
			SRM-1649 vs. TiO_2	0.003
			SRM1649 vs. DWR1	0.012
		DOSE		<0.001
			250 vs. 0	<0.001
			100 vs. 0	<0.001
			50 vs. 0	<0.001
			250 vs. 50	<0.001
			250 vs. 100	<0.001
			100 vs. 50	0.050
IL-5	BAL	DOSE		0.001
			250 vs. 0	<0.001
			250 vs. 50	0.003
			100 vs. 0	0.017
IL-6	BAL	PM x DOSE		**0.001**
IL-10				n.s.
KC	BAL	PM x DOSE		**0.029**
MIP-1α	BAL	PM x DOSE		**0.001**
RANTES	BAL:	DOSE		<0.001
			250 vs. 0	<0.001
			100 vs. 0	<0.001
			250 vs. 50	<0.001
			50 vs. 0	0.004
			250 vs. 100	0.016
			100 vs. 50	0.048

Endpoint	Source	Main Effects[a]	Comparisons[b]	p
TNF-α	BAL	PM		0.001
			EHC-2000 vs. TiO_2	<0.001
			CRI vs. TiO_2	<0.001
			SRM-1649 vs. TiO_2	0.006
			DWR1 vs. TiO_2	0.008
		DOSE		<0.001
			250 vs. 0	<0.001
			100 vs. 0	<0.001
			50 vs. 0	<0.001
			250 vs. 50	0.002

[a]For all assays where interactions were observed by two-way ANOVA, only the p value for PM x DOSE interaction is listed (main effects are not shown). P values for interactions are shown in bold. N.S. indicates not statistically significant data.

[b]For all assays where interactions were not observed, main effects and comparisons (Holm-Sidak method) are listed.

Table A-5. Particle potency estimates for *in vitro* cytotoxicity assays (Chapter 1).

Cytotoxicity *in vitro*	Ranked Particles[a]	Potency Estimate	Scaled Potency Estimate[b]
Alamar Blue (A549)			
	TiO_2	-1.34E-03	1.00
	SRM-1649	-1.30E-03	0.97
	SRM-1648	-1.28E-03	0.96
	EHC-2000	-9.94E-04	0.74
	EHC-98	-8.64E-04	0.64
	EHC-93	-7.09E-04	0.53
	DWR1	-5.50E-04	0.41
	CRI	-4.68E-04	0.35
Alamar Blue (J774A.1)			
	EHC-93	-1.35E-03	1.00
	SRM-1648	-1.18E-03	0.88
	CRI	-1.17E-03	0.87
	SRM-1649	-1.12E-03	0.83
	TiO_2	-7.59E-04	0.56
	EHC-2000	-6.19E-04	0.46
	EHC-98	-5.14E-04	0.38
	DWR1	-1.54E-04	0.11
WST-1 (A549)			
	TiO_2	7.23E-04	1.00
	EHC-98	4.40E-04	0.609
	EHC-93	4.38E-04	0.605
	EHC-2000	4.16E-04	0.58
	CRI	7.19E-05	0.10
	SRM-1648	-2.65E-04	-0.37
	SRM-1649	-3.77E-04	-0.52
	DWR1	-9.07E-04	-1.25
WST-1 (J774A.1)			
	EHC-93	-1.82E-03	1.00
	SRM-1648	-1.10E-03	0.61
	EHC-98	-9.41E-04	0.52
	SRM-1649	-9.34E-04	0.51
	TiO_2	-9.18E-04	0.50
	CRI	-8.39E-04	0.46
	EHC-2000	-7.68E-04	0.42
	DWR1	-1.39E-04	0.08
ATP (A549)			
	SRM-1649	-1.12E-03	1.00
	SRM-1648	-9.84E-04	0.88
	CRI	-9.73E-04	0.87
	TiO_2	-8.02E-04	0.71
	EHC-98	-4.17E-04	0.37
	EHC-2000	-3.60E-04	0.32
	EHC-93	-2.42E-04	0.22
	DWR1	-1.86E-04	0.17

Cytotoxicity *in vitro*	Ranked Particles[a]	Potency Estimate	Scaled Potency Estimate[b]
ATP (J774A.1)			
	SRM-1648	-1.36E-03	1.00
	SRM-1649	-1.32E-03	0.97
	EHC-93	-1.18E-03	0.86
	CRI	-8.25E-04	0.60
	EHC-2000	-5.25E-04	0.38
	EHC-98	-3.51E-04	0.26
	DWR1	-1.49E-04	0.11
	TiO_2	-1.28E-04	0.09
BrDU ELISA (A549)			
	TiO_2	-1.04E-03	1.00
	SRM-1649	-1.04E-03	0.995
	EHC-2000	-7.52E-04	0.72
	SRM-1648	-7.21E-04	0.69
	DWR1	-3.21E-04	0.31
	EHC-93	-2.57E-04	0.25
	EHC-98	3.47E-05	-0.03
	CRI	7.82E-05	-0.08
BrDU ELISA (J774A.1)			
	SRM-1649	-4.23E-03	1.00
	TiO_2	-3.74E-03	0.88
	SRM-1648	-3.12E-03	0.74
	EHC-93	-2.99E-03	0.71
	EHC-2000	-2.86E-03	0.68
	EHC-98	-2.36E-03	0.56
	CRI	-1.93E-03	0.46
	DWR1	-3.89E-04	0.09
LDH (A549)			
	SRM-1649	2.02E-03	1.00
	SRM-1648	1.85E-03	0.91
	TiO_2	1.76E-03	0.87
	EHC-93	1.70E-03	0.84
	CRI	1.45E-03	0.72
	EHC-98	1.36E-03	0.67
	EHC-2000	1.28E-03	0.64
	DWR1	-2.07E-04	-0.10
LDH (J774A.1)			
	EHC-93	8.15E-03	1.00
	SRM-1649	5.24E-03	0.64
	EHC-2000	4.19E-03	0.51
	SRM-1648	3.97E-03	0.49
	EHC-98	3.35E-03	0.41
	CRI	2.62E-03	0.32
	TiO_2	1.19E-05	0.001
	DWR1	-2.24E-03	-0.27

Cytotoxicity *in vitro*	Ranked Particles[a]	Potency Estimate	Scaled Potency Estimate[b]
Total Protein (A549)			
	TiO_2	-1.02E-03	1.00
	SRM-1649	-8.26E-04	0.81
	SRM-1648	-7.94E-04	0.78
	CRI	-7.18E-04	0.70
	EHC-93	-5.77E-04	0.56
	EHC-98	-4.32E-04	0.42
	EHC-2000	-2.84E-04	0.28
	DWR1	-2.04E-04	0.20
Total Protein (J774A.1)			
	EHC-93	-1.27E-03	1.00
	SRM-1649	-9.25E-04	0.73
	CRI	-7.70E-04	0.61
	SRM-1648	-4.92E-04	0.39
	EHC-2000	-2.54E-04	0.20
	TiO_2	-1.88E-04	0.15
	EHC-98	-9.66E-05	0.08
	DWR1	1.74E-04	-0.14
AhR Assay (H1L1)			
	SRM-1648	8.20E-01	1.00
	SRM-1649	7.95E-01	0.97
	EHC-2000	7.69E-01	0.94
	EHC-98	7.66E-01	0.93
	EHC-93	7.34E-01	0.89
	DWR1	4.72E-01	0.58
	CRI	-8.87E-02	-0.11
	TiO_2	-1.23E-01	-0.15

[a]Most potent particles in each assay are shown in bold
[b]Potency estimate is scaled relative to most potent particle

Table A-6. Particle potency estimates for *in vitro* cytokine/chemokine assays (Chapter 1).

Cytokines *in vitro*	Ranked Particles[a]	Potency Estimate	Scaled Potency Estimate[b]
IL-1α (J774A.1)			
	EHC-2000	4.10E-01	1.00
	EHC-98	3.10E-01	0.76
	SRM-1648	2.03E-01	0.49
	EHC-93	1.00E-01	0.24
	SRM-1649	7.36E-02	0.18
	DWR1	5.61E-02	0.14
	TiO_2	4.16E-02	0.10
	CRI	1.78E-02	0.04
IL-1β (J774A.1)			
	EHC-2000	2.60E-01	1.00
	EHC-98	2.06E-01	0.79
	SRM-1648	1.63E-01	0.63
	SRM-1649	9.11E-02	0.35
	EHC-93	8.23E-02	0.316
	DWR1	8.20E-02	0.315
	CRI	4.89E-02	0.19
	TiO_2	4.55E-02	0.17
IL-6 (A549)			
	TiO_2	2.56E-01	1.00
	SRM-1649	2.35E-01	0.92
	SRM-1648	1.97E-01	0.77
	CRI	1.86E-01	0.73
	EHC-98	1.48E-01	0.58
	EHC-2000	1.34E-01	0.52
	EHC-93	1.14E-01	0.44
	DWR1	3.49E-02	0.14
IL-6 (J774A.1)			
	EHC-2000	1.18E+00	1.00
	EHC-98	1.04E+00	0.88
	SRM-1649	8.53E-01	0.72
	SRM-1648	7.67E-01	0.65
	EHC-93	5.16E-01	0.44
	DWR1	3.71E-01	0.31
	TiO_2	1.17E-01	0.10
	CRI	5.41E-02	0.05
IL-8 (A549)			
	TiO_2	3.09E-01	1.00
	CRI	2.73E-01	0.88
	SRM-1649	2.35E-01	0.76
	SRM-1648	2.17E-01	0.70
	EHC-98	2.10E-01	0.68
	EHC-2000	1.67E-01	0.54
	EHC-93	1.64E-01	0.53
	DWR1	7.59E-02	0.25

Cytokines *in vitro*	Ranked Particles[a]	Potency Estimate	Scaled Potency Estimate[b]
IL-10 (J774A.1)			
	SRM-1649	-1.31E-01	1.00
	EHC-98	-1.29E-01	0.99
	EHC-93	-9.11E-02	0.70
	TiO_2	-5.95E-02	0.45
	SRM-1648	-5.74E-02	0.44
	EHC-2000	-3.79E-02	0.29
	DWR1	-2.23E-02	0.17
	CRI	1.25E-03	-0.01
GM-CSF (A549)			
	SRM-1649	1.63E-01	1.00
	SRM-1648	1.28E-01	0.79
	TiO_2	8.61E-02	0.53
	CRI	7.98E-02	0.49
	EHC-2000	5.90E-02	0.36
	EHC-98	3.61E-02	0.22
	EHC-93	-3.13E-03	-0.02
	DWR1	-2.29E-02	-0.14
GM-CSF (J774A.1)			
	EHC-2000	2.45E-01	1.00
	EHC-98	2.18E-01	0.89
	SRM-1648	1.01E-01	0.41
	EHC-93	6.10E-02	0.25
	SRM-1649	4.69E-02	0.19
	DWR1	3.40E-02	0.14
	TiO_2	1.52E-02	0.06
	CRI	-2.08E-02	-0.08
MCP-1 (A549)			
	CRI	1.23E-01	1.00
	SRM-1648	1.12E-01	0.912
	EHC-98	1.12E-01	0.909
	EHC-93	8.12E-02	0.66
	TiO_2	7.18E-02	0.58
	EHC-2000	6.66E-02	0.54
	SRM-1649	5.69E-02	0.46
	DWR1	-2.18E-03	-0.02
RANTES (J774A.1)			
	EHC-2000	2.12E-01	1.00
	EHC-98	1.88E-01	0.89
	SRM-1648	1.55E-01	0.73
	EHC-93	6.18E-02	0.29
	DWR1	6.03E-02	0.28
	SRM-1649	3.76E-02	0.18
	TiO_2	3.42E-02	0.16
	CRI	1.81E-02	0.09

Cytokines *in vitro*	Ranked Particles[a]	Potency Estimate	Scaled Potency Estimate[b]
TNF-α (J774A.1)			
	EHC-98	1.16E+00	1.00
	EHC-2000	1.15E+00	0.99
	SRM-1648	1.03E+00	0.89
	SRM-1649	8.17E-01	0.71
	EHC-93	6.41E-01	0.55
	TiO_2	4.66E-01	0.403
	DWR1	4.62E-01	0.399
	CRI	1.33E-01	0.11

[a]Most potent particles in each assay are shown in bold
[b]Potency estimate is scaled relative to most potent particle

Table A-7. Particle potency estimates for *in vivo* biochemical endpoints and BAL cell counts (Chapter 1).

Cytokines *in vitro*	Ranked Particles[a]	Potency Estimate	Scaled Potency Estimate[b]
LDH			
	SRM-1649	2.00E-01	1.00
	CRI	1.20E-01	0.60
	EHC-2000	3.04E-02	0.15
	TiO_2	1.67E-02	0.08
	DWR1	-3.47E-02	-0.17
8-Isoprostane			
	EHC-2000	2.22E-01	1.00
	TiO_2	1.86E-01	0.84
	CRI	1.81E-01	0.81
	SRM-1649	1.28E-01	0.58
	DWR1	1.02E-01	0.46
Total Protein			
	SRM-1649	1.30E-01	1.00
	CRI	1.13E-01	0.87
	EHC-2000	1.10E-01	0.85
	DWR1	6.30E-02	0.49
	TiO2	4.85E-02	0.37
Total Cell Count			
	SRM-1649	-8.96E-02	1.00
	DWR1	-5.63E-02	0.63
	EHC-2000	-5.43E-02	0.61
	TiO_2	-4.35E-02	0.49
	CRI	-3.06E-02	0.34
Neutrophils			
	CRI	6.23E-01	1.00
	EHC-2000	5.87E-01	0.942
	SRM-1649	5.85E-01	0.939
	TiO_2	4.78E-01	0.77
	DWR1	4.53E-01	0.73
Macrophages			
	SRM-1649	-2.44E-01	1.00
	CRI	-2.14E-01	0.88
	EHC-2000	-2.02E-01	0.83
	TiO_2	-1.35E-01	0.56
	DWR1	-1.14E-01	0.47
Band Cells			
	EHC-2000	1.77E-01	1.00
	CRI	8.70E-02	0.49
	SRM-1649	8.08E-02	0.46
	TiO_2	-4.80E-02	-0.27
	DWR1	-3.94E-01	-2.22
Lymphocytes			
	SRM-1649	1.29E+00	1.00
	TiO_2	1.17E+00	0.91
	EHC-2000	1.15E+00	0.90
	CRI	1.08E+00	0.84
	DWR1	9.77E-01	0.76

[a]Most potent particles in each assay are shown in bold
[b]Potency estimate is scaled relative to most potent particle

Table A-8. Particle potency estimates for *in vivo* cytokine/chemokine assays (Chapter 1).

Cytokines *in vitro*	Ranked Particles[a]	Potency Estimate	Scaled Potency Estimate[b]
IL-1α			
	CRI	6.91E-01	1.00
	EHC-2000	6.27E-01	0.91
	SRM-1649	5.30E-01	0.77
	TiO_2	4.43E-01	0.64
	DWR1	3.62E-01	0.52
IL-1β			
	CRI	5.72E-01	1.00
	EHC-2000	5.63E-01	0.99
	SRM-1649	4.99E-01	0.87
	TiO_2	4.45E-01	0.78
	DWR1	3.47E-01	0.61
IL-5			
	EHC-2000	1.78E-01	1.00
	SRM-1649	1.36E-01	0.77
	DWR1	1.13E-01	0.64
	TiO_2	1.03E-01	0.58
	CRI	-1.50E-02	-0.08
IL-6			
	SRM-1649	1.96E+00	1.00
	EHC-2000	1.86E+00	0.95
	CRI	1.63E+00	0.83
	TiO_2	1.58E+00	0.80
	DWR1	1.41E+00	0.72
IL-10			
	TiO_2	1.24E-01	1.00
	DWR1	1.23E-01	0.99
	CRI	9.85E-02	0.79
	EHC-2000	6.57E-02	0.53
	SRM-1649	-8.67E-03	-0.07
KC			
	CRI	4.55E-01	1.00
	SRM-1649	4.43E-01	0.98
	EHC-2000	4.01E-01	0.88
	TiO_2	2.33E-01	0.51
	DWR1	1.95E-01	0.43
MIP-1α			
	SRM-1649	5.28E-01	1.00
	EHC-2000	5.20E-01	0.99
	CRI	4.82E-01	0.91
	DWR1	2.84E-01	0.54
	TiO_2	2.07E-01	0.39

Cytokines *in vitro*	Ranked Particles[a]	Potency Estimate	Scaled Potency Estimate[b]
RANTES			
	EHC-2000	4.28E-01	1.00
	SRM-1649	3.99E-01	0.93
	CRI	2.80E-01	0.66
	TiO_2	2.48E-01	0.58
	DWR1	2.33E-01	0.55
TNF-α			
	EHC-2000	4.95E-01	1.00
	CRI	4.50E-01	0.91
	DWR1	3.98E-01	0.80
	SRM-1649	3.84E-01	0.78
	TiO_2	2.90E-01	0.59

[a]Most potent particles in each assay are shown in bold
[b]Potency estimate is scaled relative to most potent particle

Table A-9. Summary of statistical analyses for *in vitro* co-culture study endpoints of the cytotoxicity subset (Chapter 2).

Endpoint	Cells	Treatment	Main Effects[a]	Comparisons[b]	p
Alamar Blue	A549	PM	CONC		0.028
				100 vs 0	0.009
				10 vs 0	0.039
	THP-1	PM	PM		0.032
				EHC-6802 vs CRI	0.002
				EHC-93 vs CRI	0.007
				DWR1 vs CRI	0.016
				SRM-1650 vs CRI	0.036
	A549/THP-1	PM	PM x CONC		**0.032**
	HPAE	A549 media	CONC		0.031
				100 vs 0	0.009
				30 vs 0	0.030
	HPAE	THP-1 media	CONC		0.029
				100 vs 0	0.019
				30 vs 0	0.021
	HPAE	A549/THP-1 media	CONC		0.001
				30 vs 0	<0.001
				10 vs 0	0.002
Total Protein	A549	PM	PM		0.002
				SRM-1650 vs CRI	<0.001
				DWR1 vs CRI	0.002
				SRM-1650 vs EHC-93	0.003
				DWR1 vs EHC-93	0.005
			CONC		0.030
				10 vs 100	0.006
				10 vs 30	0.019
				10 vs 0	0.038
	THP-1	PM	PM x CONC		**0.035**
	A549/THP-1	PM			n.s.
	HPAE	A549 media			n.s.
	HPAE	THP-1 media			n.s.
	HPAE	A549/THP-1 media	CONC		0.011
				30 vs 0	0.002
				30 vs 10	0.012
AhR Assay	H1L1.1c2		PM x CONC		**<0.001**

[a]For all assays where interactions were observed by two-way ANOVA, only the p value for PM x CONC interaction is listed (main effects are not shown). P values for interactions are shown in bold. N.S. indicates not statistically significant data. N.D. indicates not detected.

[b]For all assays where interactions were not observed, main effects and comparisons (Holm-Sidak method) are listed.

Table A-10. Summary of statistical analyses for *in vitro* co-culture study endpoints of the endothelial activation subset (Chapter 2).

Endpoint	Cells	Treatment	Main Effects[a]	Comparisons[b]	p
ICAM-1	A549	PM			n.d.
	THP-1	PM	PM x CONC		**0.023**
	A549/THP-1	PM	PM x CONC		**0.003**
	HPAE	A549 media			n.s.
	HPAE	THP-1 media	PM		<0.001
				EHC-6802 vs SRM-1650	<0.001
				EHC-6802 vs TiO_2	<0.001
				EHC-93 vs SRM-1650	<0.001
				EHC-93 vs TiO_2	<0.001
				EHC-6802 vs CRI	0.015
				DWR1 vs SRM-1650	0.019
				DWR1 vs TiO_2	0.022
				EHC-6802 vs DWR1	0.026
				CRI vs SRM-1650	0.032
				CRI vs TiO_2	0.036
			CONC		<0.001
				100 vs 0	<0.001
				30 vs 0	<0.001
				10 vs 0	<0.001
				100 vs 10	0.047
	HPAE	A549/THP-1 media	PM x CONC		**0.006**
VCAM-1	A549	PM			n.d.
	THP-1	PM	PM x CONC		**<0.001**
	A549/THP-1	PM			n.d.
	HPAE	A549 media			n.s
	HPAE	THP-1 media	PM		<0.001
				EHC-6802 vs TiO_2	<0.001
				EHC-6802 vs SRM-1650	0.001
				CRI vs TiO_2	0.002
				EHC-93 vs TiO_2	0.004
				DWR1 vs TiO_2	0.009
			CONC		<0.001
				100 vs 0	<0.001
				30 vs 0	<0.001
				10 vs 0	0.001
				30 vs 10	0.028
				100 vs 10	0.040
	HPAE	A549/THP-1 media	PM x CONC		**0.012**
E-Selectin	A549	PM			n.d.
	THP-1	PM			n.d.
	A549/THP-1	PM			n.d.
	HPAE	A549 media			n.d
	HPAE	THP-1 media	PM x CONC		**0.029**

Endpoint	Cells	Treatment	Main Effects[a]	Comparisons[b]	p
E-Selectin	HPAE	A549/THP-1 media	PM		<0.001
				DWR1 vs TiO_2	<0.001
				DWR1 vs SRM-1650	<0.001
				EHC-93 vs TiO_2	<0.001
				EHC-6802 vs TiO_2	<0.001
				EHC-93 vs SRM-1650	0.002
				EHC-6802 vs SRM-1650	0.003
				DWR1 vs CRI	0.024
				CRI vs TiO_2	0.042
			CONC		<0.001
				100 vs 0	<0.001
				30 vs 0	<0.001
				10 vs 0	0.002
				100 vs 10	0.007
big ET-1	A549	PM			n.s.
	THP-1	PM	PM		<0.001
				EHC-93 vs SRM-1650	<0.001
				EHC-93 vs TiO_2	0.001
				EHC-6802 vs SRM-1650	0.002
				EHC-6802 vs TiO_2	0.007
				EHC-93 vs CRI	0.010
				DWR1 vs EHC-6802	0.041
				EHC-6802 vs CRI	0.041
			CONC		<0.001
				10 vs 0	<0.001
				30 vs 0	0.004
				100 vs 0	0.006
	A549/THP-1	PM			n.s.
	HPAE	A549 media			n.s.
	HPAE	THP-1 media			n.s.
	HPAE	A549/THP-1 media			n.s.
ET-1	A549	PM			n.s.
	THP-1	PM			n.s.
	A549/THP-1	PM			n.s.
	HPAE	A549 media			n.s.
	HPAE	THP-1 media	PM		<0.001
				EHC-6802 vs CRI	<0.001
				EHC-6802 vs TiO_2	<0.001
				EHC-6802 vs SRM-1650	<0.001
				EHC-93 vs CRI	0.011
				DWR1 vs CRI	0.015
				EHC-93 vs TiO_2	0.020
				DWR1vs TiO_2	0.028
				EHC-93 vs SRM-1650	0.029
				DWR1 vs SRM-1650	0.042
			CONC		<0.001
				100 vs 0	<0.001
				30 vs 0	<0.001
				10 vs 0	0.001
				100 vs 10	0.011
				30 vs 10	0.027
				100 vs 30	0.050

Endpoint	Cells	Treatment	Main Effects[a]	Comparisons[b]	p
ET-1	HPAE	A549/THP-1 media			n.s.
VEGF	A549	PM	CONC		<0.001
				100 vs 0	<0.001
				30 vs 0	<0.001
				100 vs 10	<0.001
				10 vs 0	<0.001
				100 vs 30	0.007
	THP-1	PM	PM		<0.001
				EHC-6802 vs SRM-1650	<0.001
				DWR1 vs SRM-1650	<0.001
				EHC-6802 vs CRI	0.001
				EHC-93 vs SRM-1650	0.002
				DWR1 vs CRI	0.004
				TiO_2 vs SRM-1650	0.022
				EHC-93 vs CRI	0.028
	A549/THP-1	PM	PM x CONC		**0.019**
	HPAE	A549 media			n.d.
	HPAE	THP-1 media			n.d.
	HPAE	A549/THP-1 media			n.d.

[a]For all assays where interactions were observed by two-way ANOVA, only the p value for PM x CONC interaction is listed (main effects are not shown). P values for interactions are shown in bold. N.S. indicates not statistically significant data. N.D. indicates not detected.

[b]For all assays where interactions were not observed, main effects and comparisons (Holm-Sidak method) are listed.

Table A-11. Summary of statistical analyses for *in vitro* co-culture study endpoints of the inflammation subset (Chapter 2).

Endpoint	Cells	Treatment	Main Effects[a]	Comparisons[b]	p
IL-1β	A549	PM			n.d.
	THP-1	PM	PM		0.002
				EHC-6802 vs TiO_2	<0.001
				EHC-93 vs TiO_2	0.001
				EHC-6802 vs SRM-1650	0.002
				EHC-93 vs SRM-1650	0.006
				CRI vs TiO_2	0.021
				DWR1 vs TiO_2	0.049
			CONC		<0.001
				100 vs 0	<0.001
				30 vs 0	<0.001
				10 vs 0	<0.001
				100 vs 10	0.049
	A549/THP-1	PM	PM		<0.001
				EHC-6802 vs TiO_2	<0.001
				EHC-6802 vs SRM-1650	<0.001
				CRI vs TiO_2	<0.001
				EHC-93 vs TiO_2	<0.001
				DWR1 vs TiO_2	<0.001
				CRI vs SRM-1650	<0.001
				EHC-93 vs SRM-1650	0.001
				DWR1 vs SRM-1650	0.002
			CONC		<0.001
				100 vs 0	<0.001
				30 vs 0	<0.001
				10 vs 0	<0.001
				100 vs 10	<0.001
				30 vs 10	0.014
				100 vs 30	0.023
	HPAE	A549 media			n.s.
	HPAE	THP-1 media			n.s.
	HPAE	A549/THP-1 media			n.s.
IL-6	A549	PM	CONC		<0.001
				100 vs 0	<0.001
				30 vs 0	0.024
				100 vs 10	0.040
	THP-1	PM	PM		<0.001
				EHC-6802 vs TiO_2	<0.001
				EHC-6802 vs SRM-1650	<0.001
				EHC-93 vs TiO_2	<0.001
				EHC-93 vs SRM-1650	<0.001
				EHC-6802 vs CRI	0.003
				DWR1 vs TiO_2	0.007
				EHC-93 vs CRi	0.016
				DWR1 vs SRM-1650	0.020
			CONC		<0.001
				100 vs 0	<0.001
				30 vs 0	<0.001
				10 vs 0	<0.001

Endpoint	Cells	Treatment	Main Effects[a]	Comparisons[b]	p
IL-6	A549/THP-1	PM	PM x CONC		**0.001**
	HPAE	A549 media			n.s.
	HPAE	THP-1 media	CONC		<0.001
				30 vs 0	<0.001
				100 vs 0	<0.001
				10 vs 0	<0.001
	HPAE	A549/THP-1			n.s.
IL-8	A549	PM	PM x CONC		**<0.001**
	THP-1	PM	PM		0.005
				EHC-6802 vs TiO_2	<0.001
				EHC-6802 vs SRM-1650	0.001
				EHC-6802 vs CRI	0.003
			CONC		<0.001
				100 vs 0	<0.001
				30 vs 0	<0.001
				10 vs 0	<0.001
	A549/THP-1	PM	PM x CONC		**<0.001**
	HPAE	A549 media			n.s.
	HPAE	THP-1 media	CONC		0.022
				30 vs 0	0.014
				100 vs 0	0.017
	HPAE	A549/THP-1 media	PM x CONC		**0.009**
IL-10	A549	PM			n.d.
	THP-1	PM	PM x CONC		**<0.001**
	A549/THP-1	PM	PM x CONC		**<0.001**
	HPAE	A549 media			n.d.
	HPAE	THP-1 media			n.s.
IL-10	HPAE	A549/THP-1 media	PM		<0.001
				DWR1 vs SRM-1650	0.001
				DWR1 vs CRI	0.003
				EHC-6802 vs SRM-1650	0.004
				EHC-6802 vs CRI	0.004
				EHC-93 vs SRM-1650	0.005
				EHC-93 vs CRI	0.006
				DWR1 vs TiO_2	0.013
				EHC-6802 vs TiO_2	0.027
				EHC-93 vs TiO_2	0.039
GM-CSF	A549	PM			n.d.
	THP-1	PM	PM		<0.001
				EHC-6802 vs TiO_2	<0.001
				EHC-93 vs TiO_2	<0.001
				EHC-6802 vs SRM-1650	0.002
				EHC-93 vs SRM-1650	0.006
				DWR1 vs TiO_2	0.016
				CRI vs TiO_2	0.020
			CONC		<0.001
				100 vs 0	<0.001
				30 vs 0	<0.001
				10 vs 0	<0.001
				100 vs 10	0.031

Endpoint	Cells	Treatment	Main Effects[a]	Comparisons[b]	p
GM-CSF	A549/THP-1	PM	PM x CONC		**0.002**
	HPAE	A549 media			n.s.
	HPAE	THP-1 media	PM		<0.00
				EHC-6802 vs TiO_2	<0.00
				EHC-6802 vs SRM-1650	<0.001
				EHC-93 vs TiO2	0.001
				EHC-93 vs SRM-1650	0.002
				DWR1 vs TiO_2	0.03
				DWR1 vs SRM-1650	0.036
				CRI vs vs TiO_2	0.03
				CRI vs SRM-1650	0.044
				EHC-6802 vs CRI	0.049
			CONC		<0.001
				100 vs 0	<0.001
				30 vs 0	<0.001
				10 vs 0	<0.001
				100 vs 10	0.032
	HPAE	A549/THP-1 media	PM x CONC		**0.002**
MCP-1	A549	PM	PM x CONC		**<0.001**
	THP-1	PM	PM		0.038
				EHC-6802 vs TiO_2	0.009
				EHC-93 vs TiO_2	0.018
				EHC-6802 vs SRM-1650	0.020
				EHC-93 vs SRM-1650	0.038
				EHC-6802 vs CRI	0.044
			CONC		<0.001
				10 vs 0	<0.001
				100 vs 0	<0.001
				30 vs 0	<0.001
MCP-1	A549/THP-1	PM	PM x CONC		**<0.001**
	HPAE	A549 media	PM		0.016
				SRM-1650 vs TiO_2	0.004
				EHC-6802 vs TiO_2	0.004
				DWR1 vs TiO_2	0.021
				SRM-1650 vs CRI	0.033
				EHC-6802 vs CRI	0.037
			CONC		<0.001
				100 vs 0	<0.001
				30 vs 0	0.005
				10 vs 0	0.016
	HPAE	THP-1 media	PM		<0.001
				EHC-6802 vs TiO_2	<0.001
				EHC-6802 vs SRM-1650	<0.001
				EHC-93 vs TiO_2	<0.001
				EHC-93 vs SRM-1650	0.001
				DWR1 vs TiO_2	0.013
				CRI vs TiO_2	0.018
				DWR1 vs SRM-1650	0.021
				EHC-6802 vs CRI	0.025
				CRI vs SRM-1650	0.029

Endpoint	Cells	Treatment	Main Effects[a]	Comparisons[b]	p
MCP-1			CONC		<0.001
				100 vs 0	<0.001
				30 vs 0	<0.001
				10 vs 0	<0.001
	HPAE	A549/THP-1 media	PM x CONC		**0.001**
TNF-α	A549	PM			n.d.
	THP-1	PM	PM		<0.001
				EHC-6802 vs SRM-1650	<0.001
				EHC-6802 vs SRM-1650	<0.001
				EHC-93 vs TiO_2	<0.001
				EHC-93 vs TiO_2	<0.001
				EHC-6802 vs CRI	<0.001
				EHC-93 vs CRI	0.001
				DWR1 vs SRM-1650	0.004
				DWR1 vs TiO_2	0.023
			CONC		<0.001
				100 vs 0	<0.001
				30 vs 0	<0.001
				10 vs 0	<0.001
	A549/THP-1	PM	PM x CONC		**<0.001**
	HPAE	A549 media			n.s.
	HPAE	THP-1 media	PM		0.010
				CRI vs EHC-6802	0.001
				CRI vs EHC-93	0.006
				SRM-1650 vs EHC-6802	0.015
				TiO_2 vs EHC-6802	0.023
				CRI vs DWR1	0.042
	HPAE	A549/THP-1 media	CONC		0.047
				100 vs 0	0.009

[a]For all assays where interactions were observed by two-way ANOVA, only the p value for PM x CONC interaction is listed (main effects are not shown). P values for interactions are shown in bold. N.S. indicates not statistically significant data. N.D. indicates not detected.

[b]For all assays where interactions were not observed, main effects and comparisons (Holm-Sidak method) are listed.

Table A-12. Summary of statistical analyses for *in vivo* biochemical endpoints and cell differential counts measured in BALB/*c* bronchoalveolar lavage (BAL) (Chapter 2).

Endpoint	Source	Main Effects[a]	Comparisons[b]	p
LDH (2 hr)	BAL			n.s.
LDH (24 hr)	BAL			n.s.
Total Protein (2 hr)	BAL	DOSE		0.025
			0 vs. 50	0.013
			0 vs. 250	0.035
Total Protein (24 hr)	BAL			n.s.
Total Cells (2 hr)	BAL			n.s.
Total Cells (24 hr)	BAL			n.s.
Neutrophils (2 hr)	BAL	PM		<0.001
			DWR1 vs. SRM-1650	<0.001
			EHC-6802 vs. SRM-1650	0.015
		DOSE		0.001
			250 vs. 0	<0.001
			50 vs. 0	<0.001
Neutrophils (24 hr)	BAL	PM		0.033
			EHC-6802 vs. SRM-1650	0.011
		DOSE		<0.001
			250 vs. 0	0.017
			250 vs. 50	0.025
			50 vs. 0	0.050
Macrophages (2 hr)	BAL			n.s.
Macrophages (24 hr)		DOSE		<0.001
			0 vs. 250	<0.001
			0 vs. 50	0.011
Band Cells (2hr)	BAL	PM		0.003
			EHC-6802 vs. SRM-1650	<0.001
			EHC-6802 vs. DWR1	0.019
		DOSE		0.012
			250 vs. 0	0.003
Band Cells (24hr)	BAL	PM		0.002
			EHC-6802 vs. SRM-1650	<0.001
			DWR1 vs. SRM-1650	0.039
		DOSE		<0.001
			50 vs. 0	<0.001
			250 vs. 0	<0.001
Lymphocytes (2hr)	BAL	DOSE		0.024
			250 vs. 0	0.016
			50 vs. 0	0.025
Lymphocytes (24hr)	BAL			n.s.

[a]For all assays where interactions were observed by two-way ANOVA, only the p value for PM x DOSE interaction is listed (main effects are not shown). P values for interactions are shown in bold. N.S. indicates not statistically significant data.

[b]For all assays where interactions were not observed, main effects and comparisons (Holm-Sidak method) are listed.

Table A-13. Summary of statistical analyses for *in vivo* cytokine/chemokine assays and adhesion factors measured in BALB/*c* bronchoalveolar lavage (BAL) (Chapter 2).

Endpoint	Source	Main Effects[a]	Comparisons[b]	p
IL-1α (2hr)	BAL	PM		0.002
			EHC-6802 vs. SRM-1650	<0.001
			DWR1 vs. SRM-1650	0.015
		DOSE		<0.001
			50 vs. 0	<0.001
			50 vs. 250	0.047
IL-1α (24hr)	BAL	PM		0.004
			EHC-6802 vs. DWR1	0.003
			EHC-6802 vs. SRM-1650	0.006
		DOSE		<0.001
			250 vs. 0	<0.001
			50 vs. 0	0.001
			250 vs. 50	0.043
IL-1β (2hr)	BAL			n.d.
IL-1β (24hr)	BAL			n.d.
IL-5 (2 hr)	BAL	PM		<0.001
			EH-6802 vs. SRM-1650	<0.001
			DWR1 vs. SRM-1650	0.013
		DOSE		0.009
			50 vs. 0	0.002
IL-5 (24 hr)	BAL			n.s.
IL-6 (2hr)	BAL	PM		0.005
			EHC-6802 vs. SRM-1650	0.002
			DWR1 vs. SRM-1650	0.026
		DOSE		<0.001
			250 vs. 0	<0.001
			50 vs. 0	<0.001
IL-6 (24hr)	BAL	PM		0.024
			EHC-6802 vs. SRM-1650	0.014
			EHC-6802 vs. DWR1	0.022
		DOSE		<0.001
			250 vs. 0	0.017
			250 vs. 50	0.005
IL-10 (2 hr)	BAL	DOSE		0.025
			50 vs. 0	0.010
			50 vs. 250	0.034
IL-10 (24 hr)	BAL			n.s.
GM-CSF (2 hr)	BAL	PM		0.020
			EHC-6802 vs. SRM-1650	0.005
		DOSE		<0.001
			250 vs. 0	<0.001
			50 vs. 0	0.001
GM-CSF (24 hr)	BAL			n.s.

Endpoint	Source	Main Effects[a]	Comparisons[b]	p
KC (2 hr)	BAL	PM x DOSE		**0.012**
KC (24 hr)	BAL	DOSE		<0.001
			250 vs. 0	<0.001
			250 vs. 50	<0.001
MIP-1α (2 hr)	BAL	PM x DOSE		**0.014**
MIP-1α (24 hr)	BAL	PM		0.002
			EHC-6802 vs. SRM-1650	<0.001
			DWR1 vs. SRM-1650	0.049
		DOSE		<0.001
			250 vs. 0	<0.001
			50 vs. 0	<0.001
			250 vs. 50	0.013
RANTES (2 hr)	BAL			n.d.
RANTES (24 hr)	BAL			n.d.
TNF-α (2 hr)	BAL	PM x DOSE		**0.002**
TNF-α (24 hr)	BAL	PM x DOSE		**0.009**
ICAM-1 (2 hr)	BAL			n.s.
ICAM-1 (24 hr)	BAL	DOSE		<0.001
			0 vs. 250	<0.001
			50 vs. 250	<0.001
			0 vs. 50	<0.001
VCAM-1 (2hr)	BAL	PM		0.012
			DWR1 vs. SRM-1650	0.004
			EHC-6802 vs. SRM-1650	0.039
		DOSE		0.033
			250 vs. 0	0.013
VCAM-1 (24 hr)	BAL			n.s.
E-Selectin (2hr)	BAL			n.d.
E-Selectin (24 hr)	BAL			n.d.

[a]For all assays where interactions were observed by two-way ANOVA, only the p value for PM x DOSE interaction is listed (main effects are not shown). P values for interactions are shown in bold. N.S. indicates not statistically significant data. N.D. indicates not detected.

[b]For all assays where interactions were not observed, main effects and comparisons (Holm-Sidak method) are listed.

Table A-14. Summary of statistical analyses for *in vivo* cytokine/chemokine assays and adhesion factors measured in BALB/*c* blood plasma (BP) (Chapter2).

Endpoint	Source	Main Effects	Comparisons[a]	p
IL-1α (2hr)	BP			n.s.
IL-1α (24hr)	BP			n.s.
IL-1β (2hr)	BP			n.s.
IL-1β (24hr)	BP			n.s.
IL-5 (2 hr)	BP			n.s.
IL-5 (24 hr)				n.s.
IL-6 (2hr)	BP			n.s.
IL-6 (24hr)	BP			n.s.
IL-10 (2 hr)	BP			n.s.
IL-10 (24 hr)	BP			n.s.
GM-CSF (2 hr)	BP	DOSE		0.003
			50 vs. 0	0.001
			250 vs. 0	0.008
GM-CSF (24 hr)	BP			n.s.
KC (2 hr)	BP	DOSE		0.033
			250 vs. 0	0.017
			50 vs. 0	0.043
KC (24 hr)	BP			n.s.
MIP-1α (2 hr)	BP	DOSE		<0.001
			50 vs. 0	<0.001
			250 vs. 0	<0.001
MIP-1α (24 hr)	BP			n.s.
RANTES (2 hr)	BP	PM		0.047
			DWR1 vs. EHC-6802	0.022
			DWR1 vs. SRM-1650	0.049
		DOSE		0.026
			50 vs. 0	0.009
RANTES (24 hr)	BP			n.s.
TNF-α (2 hr)	BP			n.s.
TNF-α (24 hr)	BP			n.s.

[a] For all assays where interactions were not observed, main effects and comparisons (Holm-Sidak method) are listed. N.S. indicates not statistically significant data.

Table A-15. Summary of statistically significant differences in controls from endpoints measured *in vivo* in BALB/*c* mice (Chapter 2).

Endpoint	Source	Comparisons[a]	p
ICAM-1 (2hr)	BAL	control vs naïve	0.017
		control vs sham	0.048
VCAM-1(2hr)	BAL	control vs naïve	0.007
VCAM-1 (24hr)	BAL	control vs naïve	0.004
		control vs sham	0.027
Total Protein (24hr)	BAL	control vs naïve	0.014
IL-5 (2hr)	BAL	control vs naïve	0.002
		control vs sham	0.019
IL-5 (24hr)	BAL	control vs naïve	<0.001
		sham vs naïve	0.003
		control vs sham	0.030
IL-6 (2hr)	BAL	control vs naïve	<0.001
		control vs sham	0.029
KC (2hr)	BAL	control vs naïve	<0.001
		control vs sham	<0.001
KC (24hr)	BAL	control vs naïve	0.006
MIP-1α (24hr)	BAL	control vs naïve	0.015
TNF-α (24hr)	BAL	control vs naïve	<0.001
		control vs sham	<0.001

[a] Only statistically significant comparisons are listed, as found by Holm-Sidak multiple comparisons procedure in a one-way ANOVA, or by Dunn's multiple comparisons test in a Kruskal-Wallis ANOVA on Ranks, with overall significance level = 0.05.

REFERENCES

Adamson, I.Y., and Bowden, D.H. (1974). The type 2 cell as progenitor of alveolar epithelial regeneration. A cytodynamic study in mice after exposure to oxygen. Lab Invest. *30*, 35-42.

Adamson, I.Y., Prieditis, H., Hedgecock, C, and Vincent, R. (2000). Zinc is the toxic factor in the lung response to an atmospheric particulate sample. Toxicol. Appl. Pharmacol. *166*, 111-119.

Albert, C.M., Ma, J, Rifai, N., Stampfer, M.J., and Ridker, P.M. (2002). Prospective study of C-reactive protein, homocysteine, and plasma lipid levels as predictors of sudden cardiac death. Circulation. *105*, 2595-2599.

Alfaro-Moreno, E., Martínez, L., Garcia-Cuellar, C., Bonner, J.C., Murray, J.C., Rosas, I., Rosales, S.P., and Osornio-Vargas, A.R. (2002). Biologic effects induced *in vitro* by PM10 from three different zones of Mexico City. Environ. Health Perspect. *110*, 715-20.

Alfaro-Moreno, E., López-Marure, R., Montiel-Dávalos, A., Symonds P., Osornio-Vargas A.R., Rosas I., and Clifford Murray J. (2007). E-Selectin expression in human endothelial cells exposed to PM10: the role of endotoxin and insoluble fraction. Environ. Res. *103*, 221-228.

Alfaro-Moreno, E., Ponce-de-León, S., Osornio-Vargas, A.R., García-Cuellar, C., Martínez, L., and Rosas, I. (2007). Potential toxic effects associated to metals and endotoxin present in PM10: an ancillary study using multivariate analysis. Inhal. Toxicol. *19 Suppl. 1*, 49-53.

Arrieta, D.E., Ontiveros, C.C., Li, W.W., Garcia, J.H., Denison, M.S., McDonald, JD, Burchiel, S.W., and Washburn, B.S. (2003). Aryl hydrocarbon receptor-mediated activity of particulate organic matter from the Paso del Norte airshed along the U.S.-Mexico border. Environ. Health Perspect. *111*, 1299-1305.

ATCC, The Global Bioresource Center™.
http://www.atcc.org/common/catalog/numSearch/numResults.cfm?collection=ce&atccNum=CRL-2598 (October 25, 2007)

Baeza-Squiban, A., Bonvallot, V., Boland, S., and Marano, F. (1999). Airborne particles evoke an inflammatory response in human airway epithelium. Activation of transcription factors. Cell Biol. Toxicol. *15*, 375-380.

Bai, N., Khazaei, M., van Eeden, S.F., and Laher I. (2007). The pharmacology of particulate matter air pollution-induced cardiovascular dysfunction. Pharmacol. Ther. *113*, 16-29.

Balduzzi, M., Diociaiuti, M., De Berardis, B., Paradisi, S., and Paoletti, L. (2004). *In vitro* effects on macrophages induced by noncytotoxic doses of silica particles possibly relevant to ambient exposure. Environ. Res. *96*, 62-71.

Bals, R., and Hiemstra, P.S. (2004). Innate immunity in the lung: how epithelial cells fight against respiratory pathogens. Eur. Respir. J. *23*, 327-333.

Barbarin, V., Xing, Z., Delos, M., Lison, D., and Huaux, F. (2005). Pulmonary overexpression of IL-10 augments lung fibrosis and Th2 responses induced by silica particles. Am. J. Physiol. Lung Cell. Mol. Physiol. *288*, L841-L848.

Barrett, E.G., Johnston, C., Oberdörster, G., Finkelstein, J.N. (1999). Silica-induced chemokine expression in alveolar type II cells is mediated by TNF-alpha-induced oxidant stress. Am. J. Physiol. *276*, L979-L988.

Becher, R., Hetland, R.B., Refsnes, M., Dahl, J.E., Dahlman, H.J., and Schwarze, P.E. (2001). Rat lung inflammatory responses after *in vivo* and *in vitro* exposure to various stone particles. Inhal. Toxicol. *13*, 789-805.

Becker, S., Fenton, M.J., and Soukup, J.M. (2002). Involvement of microbial components and toll-like receptors 2 and 4 in cytokine responses to air pollution particles. Am. J. Respir. Cell Mol. Biol. *27*, 611-618.

Becker, S., Soukup, J.M., Sioutas, C., and Cassee, F.R. (2003). Response of human alveolar macrophages to ultrafine, fine, and coarse urban air pollution particles. Exp. Lung Res. *29*, 29-44.

Beeson, W.L., Abbey, D.E., and Knutsen, S.F. (1998). Long-term concentrations of ambient air pollutants and incident lung cancer in California adults: results from the AHSMOG study.Adventist Health Study on Smog. Environ. Health Perspect. *106*, 813-823.

Bentley, C., Bejta, F., De Pascale, C., Avella, M., Wheeler-Jones, C.P., Botham, K.M., and Lawson C. (2007). Dietary fats induce human monocyte activation *in vitro*. Biochem. Soc. Trans. *35*, 464-465.

Berridge, M.V., Herst, P.M., and Tan, A.S. (2005). Tetrazolium dyes as tools in cell biology: new insights into their cellular reduction. Biotechnol. Annu. Rev. *11*, 127-152.

BéruBé, K., Balharry, D., Sexton, K., Koshy, L., Jones, T. (2007). Combustion-derived nanoparticles: mechanisms of pulmonary toxicity. Clin. Exp. Pharmacol. Physiol. *34*, 1044-1050.

Bonvallot, V., Baeza-Squiban, A., Baulig, A., Brulant, S., Boland, S., Muzeau, F., Barouki, R., and Marano, F. (2001). Organic compounds from diesel exhaust particles elicit a proinflammatory response in human airway epithelial cells and induce cytochrome p450 1A1 expression. Am. J. Respir. Cell. Mol. Biol. *25*, 515-521.

Borm, P.J.A., Schins, R.P.F., and Albrecht, C. (2004). Inhaled particles and lung cancer. Part B: paradigms and risk assessment. Int. J. Cancer *110*, 3–14.

Bouthillier, L., Vincent, R., Goegan, P., Adamson, I.Y., Bjarnason, S., Stewart, M., Guenette, J., Potvin, M., and Kumarathasan, P. (1998). Acute effects of inhaled urban particles and ozone: lung morphology, macrophage activity, and plasma endothelin-1. Am. J. Pathol. *153*, 1873-1884.

Brain, J.D., Knudson, D.E., Sorokin, S.P., and Davis, M.A. (1976). Pulmonary distribution of particles given by intratracheal instillation or by aerosol inhalation. Environ. Res. *11*, 13-33.

Brook, R.D., Brook, J.R., Urch, B., Vincent, R., Rajagopalan, S., and Silverman, F. (2002). Inhalation of fine particulate air pollution and ozone causes acute arterial vasoconstriction in healthy adults. Circulation. *105*, 1534-1536.

Brown, L.F., Detmar, M., Claffey, K., Nagy, J.A., Feng, D., Dvorak, A.M., Dvorak, H.F. (1997). Vascular permeability factor/vascular endothelial growth factor: a multifunctional angiogenic cytokine. EXS. *79*, 233-269.

Brown, D.M., Stone, V., Findlay, P., MacNee, W., and Donaldson, K. (2000). Increased inflammation and intracellular calcium caused by ultrafine carbon black is independent of transition metals or other soluble components. Occup. Environ. Med. *57*, 685-691.

Brown, D.M., Donaldson, K., and Stone V. (2004). Effects of PM10 in human peripheral blood monocytes and J774 macrophages. Respir. Res. *21*, 5:29.

Brown, D.M., Hutchison, L., Donaldson, K., and Stone, V. (2007). The effects of PM10 particles and oxidative stress on macrophages and lung epithelial cells: modulating effects of calcium-signaling antagonists. Am. J. Physiol. Lung Cell. Mol. Physiol. *292*, L1444-L1451.

Brunekreef, B., Holgate S.T. (2002). Air pollution and health. Lancet. *360*, 1233-42.

Brunekreef, B., and Forsberg, B. (2005). Epidemiological evidence of effects of coarse airborne particles on health. Eur. Respir. J. 26, 309-318.

Burg, J., Krump-Konvalinkova, V., Bittinger, F., and Kirkpatrick, C.J. (2002). GM-CSF expression by human lung microvascular endothelial cells: *in vitro* and *in vivo* findings. Am. J. Physiol. Lung Cell. Mol. Physiol. *283*, L460-L467.

Burnett, R.T., Brook, J., Dann, T., Delocla, C., Philips, O., Cakmak, S., Vincent, R., Goldberg, M.S., and Krewski, D. (2000). Association between particulate- and gas-phase components of urban air pollution and daily mortality in eight Canadian cities. Inhal Toxicol. *12 Suppl. 4*, 15-39.

Calderón-Garcidueñas, L., Maronpot, R.R., Torres-Jardon, R., Henríquez-Roldán C, Schoonhoven R, Acuña-Ayala H, Villarreal- Calderón A, Nakamura J, Fernando R, Reed W, Azzarelli B, et al. (2003). DNA damage in nasal and brain tissues of canines exposed to air pollutants is associated with evidence of chronic brain inflammation and neurodegeneration. Toxicol. Pathol. *31*, 524-538.

Calderón-Garcidueñas, L., Vincent, R., Mora-Tiscareño, A., Franco-Lira, M., Henríquez-Roldán, C., Barragán-Mejía, G., Garrido-García, L., Camacho-Reyes, L., Valencia-Salazar, G., Paredes, R., et al. (2007). Elevated plasma endothelin-1 and pulmonary arterial pressure in children exposed to air pollution. Environ. Health Perspect. *115*, 1248-1253.

Castelli, F., Librando, V., and Sarpietro, M.G. (2002). Calorimetric approach of the interaction and absorption of polycyclic aromatic hydrocarbons with model membranes. Environ. Sci. Technol. *36*, 2717-2723.

Cerri, C., Chimenti, D., Conti, I., Neri, T., Paggiaro, P., and Celi, A. (2006). Monocyte/ macrophage-derived microparticles up-regulate inflammatory mediator synthesis by human airway epithelial cells. J. Immunol. *177*, 1975-1980.

Chevalier, G., and Collet, A. J. (1972). *In vivo* incorporation of choline- ^{3}H, leucine-^{3}H and galactose-^{3}H in alveolar type II pneumocytes in relation to surfactant synthesis: a quantitative radioautographic study in mouse by electron microscopy. Anat. Rec. *174*, 289-310.

Chatterjee, S., Hadi, A. S., and Price., B. (2000). Regression Analysis by Example. (New York: John Wiley and Sons, Inc.).

Chauhan, V., Breznan, D., Goegan, P., Nadeau, D., Karthikeyan, S., Brook, J.R., and Vincent, R. (2004). Effects of ambient air particles on nitric oxide production in macrophage cell lines. Cell Biol. Toxicol. *20*, 221-239.

Chauhan, V., Breznan, D., Thomson, E., Karthikeyan, S., and Vincent, R. (2005). Effects of ambient air particles on the endothelin system in human pulmonary epithelial cells (A549). Cell Biol. Toxicol. *21*, 191-205.

Chen, F., Kuhn, D.C., Gaydos, L.J., and Demers, L.M. (1996). Induction of nitric oxide and nitric oxide synthase mRNA by silica and lipopolysaccharide in PMA-primed THP-1 cells. APMIS. *104*, 176-182.

Churg, A., and Wright, J.L. (2003). Bronchiolitis caused by occupational and ambient atmospheric particles. Semin. Respir. Crit. Care Med. *24*, 577-584.

Clancy, L., Goodman, P., Sinclair, H., and Dockery, D.W. (2002). Effect of air-pollution control on death rates in Dublin, Ireland: an intervention study. Lancet. *360*, 1210-1214.

Clarke, R.W., Coull, B., Reinisch, U., Catalano, P., Killingsworth, C.R., Koutrakis, P., Kavouras, I., Murthy, G.G., Lawrence, J., Lovett, E., et al. (2000). Inhaled concentrated ambient particles are associated with hematologic and bronchoalveolar lavage changes in canines. Environ. Health Perspect. *108*, 1179-1187.

Conover, W. J., Iman, R. L. (1981). Rank transformations as a bridge between parametric and nonparametric statistics. American Statistician. *35*, 124-129.

Cormack, D.H., and Ham, A.W. (1987). Ham's Histology (Philadelphia: Lippincott Williams & Wilkins).

Costa, D.L., and Dreher, K.L. (1997). Bioavailable transition metals in particulate matter mediate cardiopulmonary injury in healthy and compromised animal models. Environ. Health Perspect. *105 Suppl. 5*, 1053-1060.

Cronin, M.J., Weiss, J., Rogol, A.D., Baertschi, A.J. (1987). Response of anterior pituitary cells to culture media. Endocr. Res. *13*, 85-95.

Cruz, C.M., Rinna, A., Forman, H.J., Ventura, A.L., Persechini, P.M., and Ojcius, D.M. (2007). ATP activates a reactive oxygen species-dependent oxidative stress response and secretion of proinflammatory cytokines in macrophages. J Biol. Chem. *282*, 2871-2879.

Gunha, F.Q., Moncada, S., and Liew, F.Y. (1992). Interleukin-10 (IL-10) inhibits the induction of nitric oxide synthase by interferon-gamma in murine macrophages. Biochem. Biophys. Res. Commun. *182*, 1155-1159.

Dai, J., Xie, C., Vincent, R., and Churg, A. (2003). Air pollution particles produce airway wall remodeling in rat tracheal explants. Am. J. Respir. Cell. Mol. Biol. *29*, 352-358.

Damelin, L.H., Vokes, S., Whitcutt, J.M., Damelin, S.B., and Alexander, J.J. (2000). Hormesis: a stress response in cells exposed to low levels of heavy metals. Hum.. Exp. Toxicol. *19*, 420-430.

Daniel, C., and Wood, F. (1980). Fitting Equations to Data (New York: Wiley & Sons, Inc.).

de Castellarnau, C., Bancellsm C., Benítez, S., Reina, M., Ordóñez-Llanos, J., and Sánchez-Quesada, J.L. (2007). Atherogenic and inflammatory profile of human arterial endothelial cells (HUVEC) in response to LDL subfractions. Clin. Chim. Acta. *376*, 233-236.

de Fries, R., and Mitsuhashi, M. (1995). Quantification of mitogen induced human lymphocyte proliferation: comparison of alamarBlue assay to 3H-thymidine incorporation assay. J. Clin. Lab Anal. *9*, 89-95.

Devlin, R.B., Frampton, M.L., and Ghio, A.J. (2005). *In vitro* studies: what is their role in toxicology? Exp. Toxicol. Pathol. *57 Suppl. 1*, 183-188.

Dick, CA, Singh, P, Daniels, M, Evansky, P, Becker, S, and Gilmour, MI. (2003). Murine pulmonary inflammatory responses following instillation of size-fractionated ambient particulate matter. J. Toxicol. Environ. Health A. *66*, 2193-2207.

DiPietro, L.A., Burdick, M., Low, Q.E., Kunkel, S.L., and Strieter, R.M. (1998). MIP-1alpha as a critical macrophage chemoattractant in murine wound repair. J. Clin. Invest. *101*, 1693-1698.

Dockery, D.W., Pope, C.A. 3rd, Xu, X., Spengler, J.D., Ware, J.H., Fay, M.E., Ferris, B.G. Jr, And Speizer, F.E. (1993). An association between air pollution and mortality in six U.S. cities. N. Engl. J. Med. *329*, 1753-1759.

Don Porto Carero, A, Hoet, PH, Verschaeve, L, Schoeters, G, and Nemery, B. (2001). Genotoxic effects of carbon black particles, diesel exhaust particles, and urban air particulates and their extracts on a human alveolar epithelial cell line (A549) and a human monocytic cell line (THP-1). Environ. Mol. Mutagen. *37*, 155-163.

Donaldson, K., Beswick, P.H., and Gilmour, P.S. (1996). Free radical activity associated with the surface of particles: a unifying factor in determining biological activity? Toxicol. Lett. *88*, 293-298.

Dong, W., Lewtas, J., and Luster, M.I. (1996). Role of endotoxin in tumor necrosis factor alpha expression from alveolar macrophages treated with urban air particles. Exp. Lung Res. *22*, 577-92.

Dreher, K.L. (2000). Particulate matter physicochemistry and toxicology: in search of causality - a critical perspective. Inhal. Toxicol. *12*, 45–57.

Driscoll, K.E., Hassenbein, D.G., Carter, J., Poynter, J., Asquith, T.N., Grant, R.A., Whitten, J., Purdon, M.P., and Takigiku, R. (1993). Macrophage inflammatory proteins 1 and 2: expression by rat alveolar macrophages, fibroblasts, and epithelial cells and in rat lung after mineral dust exposure. Am. J. Respir. Cell. Mol. Biol. *8*, 311-318.

Driscoll, K.E., Costa, D.L., Hatch, G., Henderson, R., Oberdörster, G., Salem, H., and Schlesinger, R.B. (2000). Intratracheal instillation as an exposure technique for the evaluation of respiratory tract toxicity: uses and limitations. Toxicol. Sci. *55*, 24-35.

Dube, P.H., Handley, S.A., Lewis, J., and Miller, V.L. (2004). Protective role of interleukin-6 during Yersinia enterocolitica infection is mediated through the modulation of inflammatory cytokines. Infect. Immun. *72*, 3561-3570.

Dupuis, J., Stewart, D.J., Cernacek, P., and Gosselin, G. (1996). Human pulmonary circulation is an important site for both clearance and production of endothelin-1. Circulation. *94*, 1578-1584.

Elbekai, R.H., Korashy, H.M., Wills, K., Gharavi, N., and El-Kadi, A.O. (2004). Benzo[a]pyrene, 3-methylcholanthrene and beta-naphthoflavone induce oxidative stress in hepatoma hepa 1c1c7 Cells by an AHR-dependent pathway. Free Radic Res. *38*, 1191-1200.

Elder, A., Gelein, R., Finkelstein, J., Phipps, R., Frampton, M., Utell, M., Kittelson, D.B., Watts, W.F., Hopke, P., Jeong, C.H., et al. (2004). On-road exposure to highway aerosols. 2. Exposures of aged, compromised rats. Inhal. Toxicol. *16 Suppl. 1*, 41-53.

Endo, T., Uchida, Y., Matsumoto, H., Suzuki, N., Nomura, A., Hirata F., and Hasegawa, S. (1992). Regulation of endothelin-1 synthesis in cultured guinea pig airway epithelial cells by various cytokines. Biochem. Biophys. Res. Commun. *186*, 1594-1599.

Fakler, C.R., Wu, B., McMicken, H.W., Geske, R.S., and Welty, S.E. (2000) Molecular mechanisms of lipopolysaccharide induced ICAM-1 expression in A549 cells. Inflamm. Res. *49*, 63-72.

Fehrenbach, H. (2001). Alveolar epithelial type II cell: defender of the alveolus revisited. Respir. Res. *2*, 33-46.

Frampton, M.W., Ghio, A.J., Samet, J.M., Carson, J.L., Carter, J.D., and Devlin, R.B. (1999). Effects of aqueous extracts of PM(10) filters from the Utah valley on human airway epithelial cells. Am. J. Physiol. *277*, L960-L967.

Fubini, B., Aust, A.E., Bolton, R.E., Borm, P.J.A., Bruch, J., Ciapetti, G., Donaldson, K., Elias, Z., Gold, J., Jaurand, M.C., et al. (1998). Non-animal test for evaluating the toxicity of solid materials. ATLA. *26*, 579-617.

Fubini, B., and Hubbard, A. (2003). Reactive oxygen species (ROS) and reactive nitrogen species (RNS) generation by silica in inflammation and fibrosis. Free Radic. Biol. Med. *34*, 1507-1516.

Fujii, T., Hayashi, S., Hogg, J.C., Vincent, R., and van Eeden, S.F. (2001). Particulate matter induces cytokine expression in human bronchial epithelial cells. Am. J. Respir. Cell. Mol. Biol. *25*, 265-271.

Fujii, T., Hayashi, S., Hogg, J.C., Mukae, H., Suwa, T., Goto, Y., Vincent, R., and van Eeden S.F. (2002). Interaction of alveolar macrophages and airway epithelial cells following exposure to particulate matter produces mediators that stimulate the bone marrow. Am. J. Respir. Cell. Mol. Biol. *27*, 34-41.

Galatius-Jensen, S., Wroblewski, H., Emmeluth, C., Bie, P., Haunso, S., and Kastrup, J. (1996). Plasma endothelin in congestive heart failure: a predictor of cardiac death? J. Card. Fail. 2, 71-76.

Ganesh, D. (2006). Effect of superoxide dismutase mimetic, *AEOL 10150* on the regulation of the endothelinergic system in lungs & heart of rats exposed to air pollutants. M.Sc. Thesis (Ottawa, University of Ottawa Press).

Gardiner, K., Trethowan, N.W., Harrington, J.M., Rossiter, C.E., and Calvert, I.A.. (1993). Respiratory health effects of carbon black: a survey of European carbon black workers. Br. J. Ind. Med. *50*, 1082-1096.

Garrison, P.M., Tullis, K., Aarts, J.M., Brouwer, A., Giesy, J.P., and Denison, M.S. (1996). Species-specific recombinant cell lines as bioassay systems for the detection of 2,3,7,8-tetrachlorodibenzo-p-dioxin-like chemicals. Fundam. Appl. Toxicol. *30*, 194-203.

Gavett, S.H., Madison, S.L., Dreher, K.L., Winsett, D.W., McGee, J.K., and Costa, D.L. (1997). Metal and sulfate composition of residual oil fly ash determines airway hyperreactivity and lung injury in rats. Environ. Res. *72*, 162-172.

Gehr, P., Blank, F., and Rothen-Rutishauser, B.M. (2006). Fate of inhaled particles after interaction with the lung surface. Paediatr. Respir. Rev. *7 Suppl. 1*, S73-S75.

Gerlofs-Nijland, M.E., Dormans, J.A., Bloemen, H.J., Leseman, D.L., John, A., Boere, F., Kelly, F.J., Mudway, I.S., Jimenez A.A., Donaldson K., et al. Toxicity of coarse and fine particulate matter from sites with contrasting traffic profiles. Inhal. Toxicol. *19*, 1055-1069.

Giard, D.J., Aaronson, S.A., Todaro, G.J., Arnstein, P., Kersey, J.H., Dosik, H., and Parks, W.P. (1973). *In vitro* cultivation of human tumors: establishment of cell lines derived from a series of solid tumors. J. Natl. Cancer Inst. *51*, 1417-1423.

Gilmour, P.S., Brown, D.M., Lindsay, T.G., Beswick, P.H., MacNee, W., and Donaldson, K. Adverse health effects of PM10 particles: involvement of iron in generation of hydroxyl radical. Occup. Environ. Med. *53*, 817-822.

Goegan P., Vincent, R., Kumarathasan, P., and Brook, J. (1998). Sequential *in vitro* effects of airborne particles in lung macrophages and reporter CAT-gene cell lines. Toxicol. *In Vitro. 12*, 25-37.

Gold, D.R., Litonjua, A., Schwartz, J., Lovett, E., Larson, A., Nearing, B., Allen, G., Verrier, M., Cherry, R., and Verrier, R. (2000). Ambient pollution and heart rate variability. Circulation. 2000 Mar 21;101(11):1267-73.

Goldberg, M.S., Burnett, R.T., Bailar, J.C. 3rd, Tamblyn, R., Ernst, P., Flegel, K., Brook, J., Bonvalot, Y., Singh, R., Valois, M.F., and Vincent, R. (2001). Identification of persons with cardiorespiratory conditions who are at risk of dying from the acute effects of ambient air particles. Environ. Health Perspect. *109 Suppl. 4*, 487-494.

Gonzalez, R.J., and Tarloff, J.B. (2001). Evaluation of hepatic subcellular fractions for Alamar blue and MTT reductase activity. Toxicol. *In Vitro. 15*, 257-259.

Goto, Y., Ishii, H., Hogg, J.C., Shih, C.H., Yatera, K., Vincent, R., and van Eeden, S.F. (2004). Particulate matter air pollution stimulates monocyte release from the bone marrow. Am. J. Respir. Crit. Care Med. *170*, 891-897.

Green, T.R., Fisher, J., Stone, M., Wroblewski, B.M., and Ingham, E. (1998). Polyethylene particles of a 'critical size' are necessary for the induction of cytokines by macrophages *in vitro*. Biomaterials. *19*, 2297-2302.

Gurgueira, S.A., Lawrence, J., Coull, B., Murthy, G.G., and Gonzalez-Flecha, B. (2002). Rapid increases in the steady-state concentration of reactive oxygen species in the lungs and heart after particulate air pollution inhalation. Environ. Health Perspect. *110*, 749-755.

Han, D., Nagy, S.R., and Denison, M.S. (2002). Recombinant cell lines for the detection of dioxins and Ah receptor ligands - not all assays are created equal. Organohalogen Compounds. *58*, 421-424.

Happo, M.S., Salonen, R.O., Halinen, A.I., Jalava, P.I., Pennanen, A.S., Kosma, V.M., Sillanpaa, M., Hillamo, R., Brunekreef, B., Katsouyanni, K., et al. (2007). Dose and time dependency of inflammatory responses in the mouse lung to urban air coarse, fine, and ultrafine particles from six European cities. Inhal. Toxicol. *19*, 227-246.

Harrison, R.M., and Yin, J. (2000). Particulate matter in the atmosphere: which particle properties are important for its effects on health? Sci. Total Environ. *249*, 85-101.

Hashimoto, S., Gon, Y., Matsumoto, K., Maruoka, S., Takeshita, I., Hayashi, S., Asai, Y., Jibiki, I., Machino, T., and Horie, T. (2000). Selective inhibitor of p38 mitogen-activated protein kinase inhibits lipopolysaccharide-induced interleukin-8 expression in human pulmonary vascular endothelial cells. J. Pharmacol. Exp. Ther. *293*, 370-375.

Hetland, R.B., Refsnes, M, Myran, T., Johansen, B.V., Uthus, N, and Schwarze, P.E. (2000). Mineral and/or metal content as critical determinants of particle-induced release of IL-6 and IL-8 from A549 cells. J. Toxicol. Environ. Health A. *60*, 47-65.

Hetland, R.B., Myhre, O., Lag, M., Hongve, D., Schwarze, P.E., and Refsnes, M. (2001). Importance of soluble metals and reactive oxygen species for cytokine release induced by mineral particles. Toxicology. *165*, 133-144.

Hocking, R.R. (1976) "The Analysis and Selection of Variables in Linear Regression" Biometrics *32*, 1-50.

Hoek, G., Fischer, P., Van Den Brandt, P., Goldbohm, S., and Brunekreef, B. (2001). Estimation of long-term average exposure to outdoor air pollution for a cohort study on mortality. J. Exp. Anal. Environ. Epidemiol. *11*, 459-469.

Holgate, S.T., Peters-Golden, M., Panettieri, R.A., and Henderson, W.R. Jr. (2003). Roles of cysteinyl leukotrienes in airway inflammation, smooth muscle function, and remodeling. J Allergy Clin Immunol. *111 Suppl 1*, S18-S36.

Huang, S.L., Cheng, W.L., Lee, C.T., Huang, H.C., and Chan, C.C. (2002). Contribution of endotoxin in macrophage cytokine response to ambient particles *in vitro*. J. Toxicol. Environ. Health A. *65*, 1261-1272.

Hubbard, A.K., Thibodeau, M., and Giardina, C. (2001). Cellular and molecular mechanisms regulating silica-induced adhesion molecule expression in mice. J. Environ. Pathol. Toxicol. Oncol. *20 Suppl. 1*, 45-51.

Huo, Y., and Ley, K. (2001). Adhesion molecules and atherogenesis. Acta Physiol. Scand. *173*, 35-43.

Hurst, S.M., Wilkinson, T.S., McLoughlin, R.M., Jones, S., Horiuchi, S., Yamamoto, N., Rose-John, S., Fuller, G.M., Topley, N., and Jones, S.A. (2001). Il-6 and its soluble receptor orchestrate a temporal switch in the pattern of leukocyte recruitment seen during acute inflammation. Immunity. *14*, 705-714.

IARC (International Agency for Research on Cancer). (1989). Diesel engine exhaust. IARC Monogr. Eval. Carcinog. Risks Hum. *46*, 41.

Imrich, A., Ning, Y.Y., Koziel, H., Coull, B., and Kobzik, L. (1999). Lipopolysaccharide priming amplifies lung macrophage tumor necrosis factor production in response to air particles. Toxicol. Appl. Pharmacol. *159*, 117-124.

Inoue, A., Yanagisawa, M., Kimura, S., Kasuya, Y., Miyauchi, T., Goto, K., Masaki, T. (1989). The human endothelin family: three structurally and pharmacologically distinct isopeptides predicted by three separate genes. Proc. Natl. Acad. Sci. U S A. *86*, 2863-2867.

Inoue, K., Takano, H., Yanagisawa, R., Ichinose, T., Shimada, A., and Yoshikawa, T. (2005). Pulmonary exposure to diesel exhaust particles induces airway inflammation and cytokine expression in NC/Nga mice. Arch. Toxicol. *79*, 595-599.

Ishii, H., Fujii, T., Hogg, J.C., Hayashi, S., Mukae, H., Vincent, R., and van Eeden, S.F. (2004). Contribution of IL-1 beta and TNF-alpha to the initiation of the peripheral lung response to atmospheric particulates (PM10). Am. J. Physiol. Lung Cell. Mol. Physiol. *287*, L176-L183.

Ishii, H., Hayashi, S., Hogg, J.C., Fujii, T., Goto, Y., Sakamoto, N., Mukae, H, Vincent, R., and van Eeden, S.F. (2005). Alveolar macrophage-epithelial cell interaction following exposure to atmospheric particles induces the release of mediators involved in monocyte mobilization and recruitment. Respir. Res. *1*, 76:87.

Janssen, Y.M., Marsh, J.P., Driscoll, K.E., Borm, P.J., Oberdörster, G., and Mossman, B.T. (1994). Increased expression of manganese-containing superoxide dismutase in rat lungs after inhalation of inflammatory and fibrogenic minerals. Free Radic. Biol. Med. *16*, 315-322.

Jiménez, L.A., Drost, E.M., Gilmour, P.S., Rahman, I., Antonicelli, F., Ritchie, H., MacNee, W., and Donaldson, K. (2002). PM(10)-exposed macrophages stimulate a proinflammatory response in lung epithelial cells via TNF-alpha. Am. J. Physiol. Lung Cell. Mol. Physiol. *282*, L237-L248.

Johannessen, L.N., Nilsen, A.M., and Lovik, M. (2005). The mycotoxins citrinin and gliotoxin differentially affect production of the pro-inflammatory cytokines tumour necrosis factor-alpha and interleukin-6, and the anti-inflammatory cytokine interleukin-10. Clin. Exp. Allergy. *35*, 782-789.

Kennedy, T., Ghio A.J., Reed, W., Samet, J., Zagorski, J., Quay, J., Carter, J., Dailey, L., Hoidal, J.R., and Devlin, R.B. (1998). Copper-dependent inflammation and nuclear factor-kappaB activation by particulate air pollution. Am. J. Respir. Cell. Mol. Biol. *19*, 366-378.

Kim, I., Moon, S.O., Kim, S.H., Kim, H.J., Koh, Y.S., and Koh, G.Y. (2001). Vascular endothelial growth factor expression of intercellular adhesion molecule 1 (ICAM-1), vascular cell adhesion molecule 1 (VCAM-1), and E-selectin through nuclear factor-kappa B activation in endothelial cells. J. Biol. Chem. *276*, 7614-7620.

Kobzik, L., Goldsmith, C.A., Ning, Y.Y., Qin, G., Morgan, B., Imrich, A., Lawrence, J., Murthy, G.G., and Catalano, P.J. (2001). Effects of combined ozone and air pollution particle exposure in mice. Res. Rep. Health Eff. Inst. *106*, 5-38.

Kodavanti, U.P., Schladweiler, M.C., Ledbetter, A.D., Hauser, R., Christiani, D.C., Samet, J.M., McGee, J., Richards, J.H., and Costa, D.L. (202). Pulmonary and systemic effects of zinc-containing emission particles in three rat strains: multiple exposure scenarios. Toxicol. Sci. *70*, 73-85.

Kong, L.Y., Luster, M.I., Dixon, D., O'Grady, J., and Rosenthal, GJ. (1994). Inhibition of lung immunity after intratracheal instillation of benzo[a]pyrene. Am. J. Respir. Crit. Care Med. *150*, 1123-1129.

Koyama S., Sato E., Tsukadaira A., Haniuda M., Numanami H., Kurai M., Nagai S., and Izumi T. (2002). Vascular endothelial growth factor mRNA and protein expression in airway epithelial cell lines *in vitro*. Eur Respir J. *20*, 1449-1456.

Krewski, D., Burnett, R., Goldberg, M.S., Hoover, K., Siemiatycki, J., Jerrett, M., Abrahamowicz, M., and White, W.H. (2000). Reanalysis of the Harvard Six Cities study and the American Cancer Society study of particulate air pollution and mortality. Health. Eff. Inst. Special Rep., 1-97.

Kreyling, W.G., Semmler, M., Erbe, F., Mayer, P., Takenaka, S., Schulz, H., Oberdörster, G., and Ziesenis A. (2002). Translocation of ultrafine insoluble iridium particles from lung epithelium to extrapulmonary organs is size dependent but very low. J. Toxicol. Environ. Health A. *65*, 1513-30.

Kuhn, D.C., Griffith, J.W., Stauffer, J.L., Riling, S., Demers, L.M. (1993). Characterization of alveolar macrophage eicosanoid production in a non-human primate model of mineral dust exposure. Prostaglandins. *46*, 207-220.

Kulkarni, N., Pierse, N., Rushton, L., and Grigg, J. (2006). Carbon in airway macrophages and lung function in children. N. Engl. J. Med. *355*, 21-30.

Kumarathasan, P., Blais, E., Goegan, P., Yagminas, A., Guénette, J., Adamson, I.Y., Crapo, J.D., Mason, R.J., and Vincent, R. (2005). 90-day repeated inhalation exposure of surfactant Protein-C/tumor necrosis factor-alpha, (SP-C/TNF-alpha) transgenic mice to air pollutants. Int. J. Toxicol. *24*, 59-67.

Lahm, T., Crisostomo, P.R., Markel, T.A., Wang, M., Lillemoe, K.D., and Meldrum, D.R. (2007). The critical role of vascular endothelial growth factor in pulmonary vascular remodeling after lung injury. Shock. *28*, 4-14.

Lay, J.C., Bennett, W.D., Kim, C.S., Devlin, R.B., and Bromberg, P.A. (1998). Retention and intracellular distribution of instilled iron oxide particles in human alveolar macrophages. Am. J. Respir. Cell. Mol. Biol. *18*, 687-695.

Lee, K.J., Kim, M.K., Park, Y.H., Seol, H.J., Lim, J.E., Lee, J.N., and Oh, M.J. 2007. Vascular endothelial growth factor induces endothelin-1 production via matrix metalloproteinase-2 rather than endothelin-converting enzyme-1. Hypertens. Pregnancy. *26*, 189-199.

Leeuwenberg, J.F., von Asmuth, E.J., Jeunhomme, T.M., and Buurman, W.A. (1990). IFN-gamma regulates the expression of the adhesion molecule ELAM-1 and IL-6 production by human endothelial cells *in vitro*. J. Immunol. *145*, 2110-2114.

Lehle, K., Preuner, J.G., Vogt, A., Rupprecht, L., Keyser, A., Kobuch, R., Schmid, C., and Birnbaum, D.E. (2007). Endothelial cell dysfunction after coronary artery bypass grafting with extracorporeal circulation in patients with type 2 diabetes mellitus. Eur. J. Cardiothorac. Surg. *32*, 611-6.

Levin, E.R. (1995). Endothelins. N. Engl. J. Med. *333*, 356-363.

Li, X.Y., Gilmour, P.S., Donaldson, K., and MacNee, W. (1996). Free radical activity and pro-inflammatory effects of particulate air pollution (PM10) *in vivo* and *in vitro*. Thorax. *51*, 1216-1222.

Li, N., Wang, M., Oberley, T.D., Sempf, J.M., and Nel, A.E. (2002). Comparison of the pro-oxidative and proinflammatory effects of organic diesel exhaust particle chemicals in bronchial epithelial cells and macrophages. J. Immunol. *169*, 4531-4541.

Libby, P. (2002). Inflammation in atherosclerosis. Nature. *420*, 868-874.

Lieber, M., Smith, B., Szakal, A., Nelson-Rees, W., and Todaro, G. (1976). A continuous tumor-cell line from a human lung carcinoma with properties of type II alveolar epithelial cells. Int. J. Cancer. *17*, 62-70.

Lippmann, M., and Schlesinger, R.B. (2000). Toxicological bases for the setting of health-related air pollution standards. Annu. Rev. Public Health. *21*, 309-333.

Liu, L., Mul, F.P., Kuijpers, T.W., Lutter, R., Roos, D., and Knol, E.F. (1996). Neutrophil transmigration across monolayers of endothelial cells and airway epithelial cells is regulated by different mechanisms. Ann. N. Y. Acad. Sci. *796*, 21-29.

López, E., Figueroa, S., Oset-Gasque, M.J., and González, M.P. (2003). Apoptosis and necrosis: two distinct events induced by cadmium in cortical neurons in culture. Br. J. Pharmacol. *138*, 901-911.

Luscher, T.F., and Barton, M. (2000). Endothelins and endothelin receptor antagonists: therapeutic considerations for a novel class of cardiovascular drugs. Circulation. *102*, 2434-2440.

MacLean, J.A., Xia, W., Pinto, C.E., Zhao, L., Liu, H.W., and Kradin, R.L. (1996). Sequestration of inhaled particulate antigens by lung phagocytes. A mechanism for the effective inhibition of pulmonary cell-mediated immunity. Am. J. Pathol. *148*, 657-666.

Mage, D.T. (1983). Public health aspects of air quality surveilance. Public Health Rev. *XI*, 5-54.

Mage, D.T. (2002). A particle is not a *partide* is not a PARTICLE. J. Expo. Anal. Environ. Epidemiol. *12*, 93-95.

Mallows, C.L. (1973). Some comments on Cp. Technometrics. *15*, 661-675.

Martin, T.R., and Frevert, C.W. (2005). Innate immunity in the lungs. Proc. Am. Thorac. Soc. *2*, 403-411.

Matsumoto, T., and Mugishima, H. (2006). Signal transduction via vascular endothelial growth factor (VEGF) receptors and their roles in atherogenesis. J. Atheroscler. Thromb. *13*, 130-135.

Matsushima, K., and Oppenheim, J.J. (1989). Interleukin 8 and MCAF: novel inflammatory cytokines inducible by IL 1 and TNF. Cytokine. *1*, 2-13.

Matsuura, A, Yamochi, W, Hirata, K, Kawashima, S, and Yokoyama, M. (1998). Stimulatory interaction between vascular endothelial growth factor and endothelin-1 on each gene expression. Hypertension. *32*, 89-95.

Means, T., Golenbock, K., D. T., and Fenton, M.J. (2000). The biology of Toll-like receptors. Cytokine Growth Factor Rev. *11*, 219-232.

Mills, P.R., Davies, R.J., and Devalia, J.L. (1999). Airway epithelial cells, cytokines, and pollutants. Am. J. Respir. Crit. Care Med. *160*, S38-S43.

Mire-Sluis, A., and Thorpe, R. (1998). Cytokines (San Diego: Academic Press).

Miyabara, Y., Yanagisawa, R., Shimojo, N., Takano, H., Lim, H.B., Ichinose, T., and Sagai, M. (1998). Murine strain differences in airway inflammation caused by diesel exhaust particles. Eur. Respir. J. 11, 291-298.

Mögel, M., Krüger, E., Krug, H.F., and Seidel, A. (1998). A new co-culture-system of bronchial epithelial and endothelial cells as a model for studying ozone effects on airway tissue. Toxicol. Lett. *96-97*, 25-32.

Montiel-Dávalos, A., Alfaro-Moreno, E., and López-Marure, R. (2007). PM2.5 and PM10 induce the expression of adhesion molecules and the adhesion of monocytic cells to human umbilical vein endothelial cells. Inhal Toxicol. *19 Suppl. 1*, 91-98.

Mukae H., Hogg J.C., English D., Vincent R., and van Eeden S.F. (2000). Phagocytosis of particulate air pollutants by human alveolar macrophages stimulates the bone marrow. Am. J. Physiol. Lung Cell. Mol. Physiol. *279*, L924-31.

Nadeau, D., Fouquette-Couture, L., Paradis, D., Khorami, J., Lane, D. and Dunnigan, J. (1987). Cytotoxicity of respirable dusts from industrial minerals: comparison of two naturally occurring and two man-made silicates. Drug. Chem. Toxicol. *10*, 49-86.

Nardone, L.L., and Andrews, S.B. (1979). Cell line A549 as a model of the type II pneumocyte. Phospholipid biosynthesis from native and organometallic precursors. Biochim. Biophys. Acta. *573*, 276-295.

Nebert, D.W., Roe, A.L., Dieter, M.Z., Solis, W.A., Yang, Y., and Dalton, T.P. (2000). Role of the aromatic hydrocarbon receptor and [Ah] gene battery in the oxidative stress response, cell cycle control, and apoptosis. Biochem. Pharmacol. *59*, 65-85.

Nemmar, A, Vanbilloen, H, Hoylaerts, MF, Hoet, PH, Verbruggen, A, and Nemery, B. (2001). Passage of intratracheally instilled ultrafine particles from the lung into the systemic circulation in hamster. Am. J. Respir. Crit. Care Med. *164*, 1665-1668.

Nemmar, A., Hoylaerts, M.F., Hoet, P.H., Vermylen, J., and Nemery, B. (2003). Size effect of intratracheally instilled particles on pulmonary inflammation and vascular thrombosis. Toxicol. Appl. Pharmacol. *186*, 38-45.

Ning, Y., Tao, F., Qin, G., Imrich, A., Goldsmith, C.A., Yang, Z., and Kobzik, L. (2004). Particle-epithelial interaction: effect of priming and bystander neutrophils on interleukin-8 release. Am. J. Respir. Cell. Mol. Biol. *30*, 744-750.

Oberdörster, G., Ferin, J., Gelein, R., Soderholm, S.C., and Finkelstein, J. (1992). Role of the alveolar macrophage in lung injury: studies with ultrafine particles. Environ. Health Perspect. *97*, 193-199.

Oberdörster, G., Ferin, J., and Lehnert, B.E. (1994). Correlation between particle size, *in vivo* particle persistence, and lung injury. Environ. Health Perspect. *102 Suppl. 5*, 173-179.

Oberdörster, G. (1996). Significance of particle parameters in the evaluation of exposure-dose-response relationships of inhaled particles. Inhal. Toxicol. *8 Suppl.*, 73-89.

Oberdörster, G., Sharp, Z., Atudorei, V., Elder, A., Gelein, R., Lunts, A., Kreyling, W., and Cox, C. (2002). Extrapulmonary translocation of ultrafine carbon particles following whole-body inhalation exposure of rats. J. Toxicol. Environ. Health A. *65*, 1531-1543.

Obot, C.J., Morandi, M.T., Hamilton, R.F., and Holian, A. (2004). A comparison of murine and human alveolar macrophage responses to urban particulate matter. Inhal. Toxicol. *16*, 69-76.

O'Brien, J., Wilson, I., Orton, T., and Pognan, F. (2000). Investigation of the Alamar Blue (resazurin) fluorescent dye for the assessment of mammalian cell cytotoxicity. Eur. J. Biochem. *267*, 5421-5426.

Ohtsuka, Y., Brunson, K.J., Jedlicka, A.E., Mitzner, W., Clarke, R.W., Zhang, L.Y., Eleff, S.M., and Kleeberger, S.R. (2000). Genetic linkage analysis of susceptibility to particle exposure in mice. Am. J. Respir. Cell. Mol. Biol. *22*, 574-581.

Osornio-Vargas, A.R., Bonner, J.C., Alfaro-Moreno, E., Martínez, L., García-Cuellar, C., Ponce-de-León Rosales, S., Miranda, J., and Rosas, I. (2003). Proinflammatory and cytotoxic effects of Mexico City air pollution particulate matter *in vitro* are dependent on particle size and composition. Environ. Health Perspect. *111*, 1289-1293.

Ostro, B., Feng, W.Y., Broadwin, R., Green, S., and Lipsett, M. (2007). The effects of components of fine particulate air pollution on mortality in california: results from CALFINE. Environ. Health Perspect. *115*, 13-19.

Ovrevik, J., Myran, T., Refsnes, M., Låg, M., Becher, R., Hetland, R.B., and Schwarze, P.E. (2005). Mineral particles of varying composition induce differential chemokine release from epithelial lung cells: importance of physico-chemical characteristics. Ann. Occup. Hyg. *49*, 219-31.

Pare, PD, Wiggs, BR, James, A, Hogg, JC, Bosken, C. (1991). The comparative mechanics and morphology of airways in asthma and in chronic obstructive pulmonary disease. Am. Rev. Respir. Dis. *143*, 1189-1193.

Park, S., Lee, Y.K., Jung, M., Kim, K.H., Chung, N., Ahn, E.K., Lim, Y., and Lee, K.H. (2007). Cellular toxicity of various inhalable metal nanoparticles on human alveolar epithelial cells. Inhal. Toxicol. *19 Suppl. 1*, 59-65.

PennCentury™, Manufacturer of Microsprayer Aerosolizers.
http://www.penncentury.com/products/index.php/ (October 20, 2007)

Peters, A., Döring, A., Wichmann, H.E., and Koenig, W. (1997). Increased plasma viscosity during an air pollution episode: a link to mortality? Lancet. *349*, 1582-1587.

Peters, A., Frohlich, M., Doring, A., Immervoll, T., Wichmann, H.E., Hutchinson, W.L., Pepys, M.B., and Koenig, W. (2001). Particulate air pollution is associated with an acute phase response in men; results from the MONICA-Augsburg Study. Eur. Heart J. *22*, 1198-1204.

Pinkerton, K.E., Green, F.H., Saiki, C., Vallyathan, V., Plopper, C.G., Gopal, V., Hung, D., Bahne, E.B., Lin, S.S., Menache, M.G., and Schenker, M.B. (2000). Distribution of particulate matter and tissue remodeling in the human lung. Environ. Health Perspect. *108*, 1063-1069.

Pope, C.A. 3rd, Thun, M.J., Namboodiri, M.M., Dockery, D.W., Evans, J.S., Speizer, F.E., and Heath, C.W. Jr. (1995). Particulate air pollution as a predictor of mortality in a prospective study of U.S. adults. Am. J. Respir. Crit. Care Med. *151*, 669-674.

Pope, C.A. 3rd, Verrier, R.L., Lovett, E.G., Larson, A.C., Raizenne, M.E., Kanner, R.E., Schwartz, J., Villegas, G.M., Gold, D.R., and Dockery, D.W. (1999). Heart rate variability associated with particulate air pollution. Am. Heart J. *138*, 890-899.

Pope, C.A. 3rd, Burnett, R.T., Thun, M.J., Calle, E.E., Krewski, D., Ito, K., and Thurston, G.D. (2002). Lung cancer, cardiopulmonary mortality, and long-term exposure to fine particulate air pollution. JAMA. *287*, 1132-1141.

Pozzi, R., De Berardis, B., Paoletti, L., and Guastadisegni, C. (2003). Inflammatory mediators induced by coarse (PM2.5-10) and fine (PM2.5) urban air particles in RAW 264.7 cells. Toxicology. *183*, 243-254.

Ralph, P., and Nakoinz, I. (1975). Phagocytosis and cytolysis by a macrophage tumour and its cloned cell line. Nature. *257*, 393-394.

Ralph, P., Moore, M.A., and Nilsson, K. (1976). Lysozyme synthesis by established human and murine histiocytic lymphoma cell lines. J. Exp. Med. *143*, 1528-1533.

Ralph, P., and Nakoinz, I. (1977). Direct toxic effects of immunopotentiators on monocytic, myelomonocytic, and histiocytic or macrophage tumor cells in culture. Cancer Res. *37*, 546-550.

Robb, S.J., Robb-Gaspers, L.D., Scaduto, R.C. Jr., Thomas, A.P., and Connor, J.R. 1999). Influence of calcium and iron on cell death and mitochondrial function in oxidatively stressed astrocytes. J. Neurosci. Res. *55*, 674-686.

Rosas Pérez, I., Serrano, J., Alfaro-Moreno, E., Baumgardner, D., García-Cuellar, C., Martín Del Campo, J.M., Raga, G.B., Castillejos, M., Colín, R.D., and Osornio Vargas, A.R. (2007). Relations between PM10 composition and cell toxicity: a multivariate and graphical approach. Chemosphere. *67*, 1218-1228.

Rosenkranz, H.S. (1995). Mutagenic nitroarenes, diesel emissions, particulate-induced mutations and cancer: an essay on cancer-causation by a moving target. Mutat. Res. *367*, 65-72.

Ross, R. (1986). Endothelium, monocytes, platelets, and atherosclerosis. Monogr. Atheroscler. *14*, 169-172.

Routledge, H.C., and Ayres, J.G. (2005). Air pollution and the heart. Occup. Med. (Lond). *55*, 439-447.

Rückerl, R., Ibald-Mulli, A., Koenig, W., Schneider, A., Woelke, G., Cyrys, J., Heinrich, J., Marder, V., Frampton, M., Wichmann, H.E., et al. (2006). Air pollution and markers of inflammation and coagulation in patients with coronary heart disease. Am. J. Respir. Crit. Care Med. *173*, 432-441.

Rückerl, R., Phipps, R.P., Schneider, A., Frampton, M., Cyrys, J., Oberdörster, G., Wichmann, H.E., and Peters, A. (2007). Ultrafine particles and platelet activation in patients with coronary heart disease--results from a prospective panel study. Part. Fibre Toxicol. *4*, 1.

Ruetten, H., Thiemermann, C., and Perretti, M. (1999). Upregulation of ICAM-1 expression on J774.2 macrophages by endotoxin involves activation of NF-kappaB but not protein tyrosine kinase: comparison to induction of iNOS. Mediators Inflamm. *8*, 77-84.

Saber, A.T., Jacobsen, N.R., Bornholdt, J., Kjaer, S.L., Dybdahl, M., Risom, L., Loft, S, Vogel, U, and Wallin, H. (2006). Cytokine expression in mice exposed to diesel exhaust particles by inhalation. Role of tumor necrosis factor. Part. Fibre Toxicol. *20*, 3:4.

Sagai, M., Saito, H., Ichinose, T., Kodama, M., and Mori, Y. (1993). Biological effects of diesel exhaust particles. I. *In vitro* production of superoxide and *in vivo* toxicity in mouse. Free Radic. Biol. Med. *14*, 37-47.

Schins, R.P., and Knaapen, A.M. (2007). Genotoxicity of poorly soluble particles. Inhal. Toxicol. *19 Suppl. 1*, 189-198.

Schikowski, T., Sugiri, D., Ranft, U., Gehring, U., Heinrich, J., Wichmann, H.E., and Kramer, U. (2005). Long-term air pollution exposure and living close to busy roads are associated with COPD in women. Respir. Res. *6*, 152.

Schlesinger, R.B. (1995). Deposition and clearance of inhaled particles. In Concepts in Inhalation Toxicology, R. O. McClellan, and R. F. Henderson, eds. (Washington: Taylor and Francis), pp. 191–224.

Schlesinger R.B., Ben-Jebria, A., Dahl, A.R., Snipes, M.B., and Ultman, J. (1997). Chapter 12: Disposition of Inhaled Toxicants. In Handbook of Human Toxicology, E.J. Massaro, ed. (New York: CRC Press), pp. 493-550.

Schlesinger, R.B., Kunzli, N., Hidy, G.M., Gotschi, T., and Jerrett, M. (2006). The health relevance of ambient particulate matter characteristics: coherence of toxicological and epidemiological inferences. Inhal. Toxicol. *18*, 95-125.

Schlesinger, R.B. (2007). The health impact of common inorganic components of fine particulate matter (PM2.5) in ambient air: a critical review. Inhal. Toxicol. *19*, 811-832.

Seagrave, J., McDonald, J.D., Gigliotti, A.P., Nikula, K.J., Seilkop, S.K., Gurevich, M., and Mauderly, J.L. (2002). Mutagenicity and *in vivo* toxicity of combined particulate and semivolatile organic fractions of gasoline and diesel engine emissions. Toxicol. Sci. *70*, 212-226.

Seagrave, J., Mauderly, J.L., Seilkop, S.K. (2003). *In vitro* relative toxicity screening of combined particulate and semivolatile organic fractions of gasoline and diesel engine emissions. J. Toxicol. Environ. Health A. *66*, 1113-1132.

Seaman, J. W., Walls, S. C., Wide, S.E. and Jaeger, R.G.(1994) Caveat emptor: rank transform methods and interactions. Trends Ecol. Evol. *9*, 261-263.

Seaton, A., MacNee, W., Donaldson, K., and Godden, D. (1995). Particulate air pollution and acute health effects. Lancet. *345*, 176-178.

Seidel, S.D., Winters, G.M., Rogers, W.J., Ziccardi, M.H., Li, V., Keser, B., and Denison, M.S. (2001). Activation of the Ah receptor signaling pathway by prostaglandins. J. Biochem. Mol. Toxicol. *15*, 187-196.

Sevastyanova, O., Binkova, B., Topinka, J., Sram, R.J., Kalina, I., Popov, T., Novakova, Z., and Farmer, P.B. (2007). *In vitro* genotoxicity of PAH mixtures and organic extract from urban air particles part II: human cell lines. Mutat. Res. *620*, 123-134.

Shapiro, D.L., Nardone, L.L., Rooney, S.A., Motoyama, E.K., and Munoz, J.L. (1978). Phospholipid biosynthesis and secretion by a cell line (A549) which resembles type II aleveolar epithelial cells. Biochim. Biophys. Acta. *530*, 197-207.

Shima, M. (2007). Air pollution and serum C-reactive protein concentration in children. J. Epidemiol. *17*, 169-176.

Simpson, J.C., Niven, R.M., Pickering, C.A., Oldham, L.A., Fletcher, A.M., and Francis, H.C. (1999). Comparative personal exposures to organic dusts and endotoxin. Ann. Occup. Hyg. 43, 107-115.

Singh, S., Shi, T., Duffin, R., Albrecht, C., van Berlo, D., Hohr, D., Fubini, B., Martra, G., Fenoglio, I., Borm, P.J., et al. (2007). Endocytosis, oxidative stress and IL-8 expression in human lung epithelial cells upon treatment with fine and ultrafine TiO2: role of the specific surface area and of surface methylation of the particles. Toxicol. Appl. Pharmacol. *222*, 141-151.

Souza, M.B., Saldiva, P.H., Pope, C.A. 3rd, and Capelozzi, V.L. (1998). Respiratory changes due to long-term exposure to urban levels of air pollution: a histopathologic study in humans. Chest. *113*, 1312-1318.

Standiford, T.J., Mehrad, B., Tsai, W.C., and Moore, T.A. (1999). Pulmonary host defenses: the role of cytokines in mediating lung inflammation. Medscape General Medicine. *1*, http://www.medscape.com/viewarticle/408743/ (July 16, 2007).

Steerenberg, P.A., Zonnenberg, J.A., Dormans, J.A., Joon, P.N., Wouters, I.M., van Bree, L., Scheepers, P.T., and Van Loveren, H. (1998). Diesel exhaust particles induced release of interleukin 6 and 8 by (primed) human bronchial epithelial cells (BEAS 2B) *in vitro*. Exp. Lung Res. *24*, 85-100.

Steerenberg, P.A., van Amelsvoort, L., Lovik, M., Hetland, R.B., Alberg, T., Halatek, T., Bloemen, H.J., Rydzynski, K., Swaen, G., Schwarze, P., et al. (2006). Relation between sources of particulate air pollution and biological effect parameters in samples from four European cities: an exploratory study. Inhal. Toxicol. *18*, 333-346.

Steinebach, O.M., and Wolterbeek, H.T. (1993). Effects of zinc on rat hepatoma HTC cells and primary cultured rat hepatocytes. Toxicol. Appl. Pharmacol. *118*, 245-254.

Steinvil, A., Kordova-Biezuner, L., Shapira, I., Berliner, S., and Rogowski, O. (2007). Short-term exposure to air pollution and inflammation-sensitive biomarkers. Environ. Res. *106*, 51-61.

Stenfors, N., Nordenhäll, C., Salvi, S.S., Mudway, I., Söderberg, M., Blomberg, A., Helleday, R., Levin, J.O., Holgate, S.T., Kelly, F.J., et al. (2004). Different airway inflammatory responses in asthmatic and healthy humans exposed to diesel. Eur. Respir. J. *23*, 82-86.

Stringer, B., Imrich, A., and Kobzik, L. (1996). Lung epithelial cell (A549) interaction with unopsonized environmental particulates: quantitation of particle-specific binding and IL-8 production. Exp. Lung Res. *22*, 495-508.

Stříž, I., Wang, Y.M., Teschler, H., Sorg, C., Costabel, U. (1993). Phenotypic markers of alveolar macrophage maturation in pulmonary sarcoidosis. Lung. *171*, 293-303.

Stříž, I., Slavčev, A., Kalanin, J., Jarešová, M., and Rennard, S.I. (2001). Cell-cell contacts with epithelial cells modulate the phenotype of human macrophages. Inflammation. *25*, 241-246.

Su, G. L., Simmons, R. L., and Wang, S. C. (1995). Lipopolysaccharide binding protein participation in cellular activation by LPS. Crit. Rev. Immunol. *15*, 201–214.

Sutherland, E.R., and Martin, R.J. (2003). Airway inflammation in chronic obstructive pulmonary disease: comparisons with asthma. J. Allergy Clin. Immunol. *112*, 819-827.

Suwa, T., Hogg, J.C., Quinlan, K.B., Ohgami, A., Vincent, R., and van Eeden, S.F. (2002). Particulate air pollution induces progression of atherosclerosis. J. Am. Coll. Cardiol. *39*, 935-942.

Takano, H., Yoshikawa, T., Ichinose, T., Miyabara, Y., Imaoka, K., and Sagai, M. (1997). Diesel exhaust particles enhance antigen-induced airway inflammation and local cytokine expression in mice. Am. J. Respir. Crit. Care Med. *156*, 36-42.

Takano, H., Yanagisawa, R., Ichinose, T., Sadakane, K., Yoshino, S., Yoshikawa, T., and Morita, M. (2002). Diesel exhaust particles enhance lung injury related to bacterial endotoxin through expression of proinflammatory cytokines, chemokines, and intercellular adhesion molecule-1. Am. J. Respir. Crit. Care Med. *165*, 1329-1335.

Takizawa, H. (1998). Airway epithelial cells as regulators of airway inflammation. Int. J. Mol. Med. *1*, 367-378.

Tan, W.C., Qiu, D., Liam, B.L., Ng, T.P., Lee, S.H., van Eeden, S.F., D'Yachkova, Y., and Hogg, J.C. (2000). The human bone marrow response to acute air pollution caused by forest fires. Am. J. Respir. Crit. Care Med. *161*, 1213-1217.

Tao, F., and Kobzik, L. (2002). Lung macrophage-epithelial cell interactions amplify particle-mediated cytokine release. Am. J. Respir. Cell. Mol. Biol. *26*, 499-505.

Teder, P., and Noble, P.W. (2000). A cytokine reborn? Endothelin-1 in pulmonary inflammation and fibrosis. Am. J. Respir. Cell. Mol. Biol. *23*, 7-10.

Terashima, T., Wiggs, B., English, D., Hogg, J.C., and van Eeden, S.F. (1997). Phagocytosis of small carbon particles (PM10) by alveolar macrophages stimulates the release of polymorphonuclear leukocytes from bone marrow. Am. J. Respir. Crit. Care Med. *155*, 441-447.

Thomas, E.D., Ramberg, R.E., Sale, G.E., Sparkes, R.S., and Golde, D.W. (1976). Direct evidence for a bone marrow origin of the alveolar macrophage in man. Science. *192*, 1016-1018.

Thomson, E., Goegan, P., Kumarathasan, P., Vincent, R. (2004). Air pollutants increase gene expression of the vasoconstrictor endothelin-1 in the lungs. Biochim. Biophys. Acta. *1689*, 75-82.

Thomson, E., Kumarathasan, P., Goegan, P., Aubin, R.A., and Vincent, R. (2005). Differential regulation of the lung endothelin system by urban particulate matter and ozone. Toxicol. Sci. *88*, 103-113.

Thomson, E., Kumarathasan, P., and Vincent, R. (2006). Pulmonary expression of preproET-1 and preproET-3 mRNAs is altered reciprocally in rats after inhalation of air pollutants. Exp. Biol. Med. (Maywood). *231*, 979-984.

Thomson, E.M., Kumarathasan, P., Calderón-Garcidueñas, L., and Vincent, R. (2007). Air pollution alters brain and pituitary endothelin-1 and inducible nitric oxide synthase gene expression. Environ. Res. *105*, 224-233.

Tillie-Leblond, I., Pugin, J., Marquette, C.H., Lamblin, C., Saulnier, F., Brichet, A., Wallaert, B., Tonnel, A.B., and Gosset, P. (1999). Balance between proinflammatory cytokines and their inhibitors in bronchial lavage from patients with status asthmaticus. Am. J. Respir. Crit. Care Med. *159*, 487-494.

Timblin, C., Berube, K., Churg, A., Driscoll, K., Gordon, T., Hemenway, D., Walsh, E., Cummins, A.B., Vacek, P., and Mossman, B. (1998). Ambient particulate matter causes activation of the c-jun kinase/stress-activated protein kinase cascade and DNA synthesis in lung epithelial cells. Cancer Res. *58*, 4543-4547.

Trigg, C.J., Manolitsas, N.D., Wang, J., Calderón, M.A., McAulay, A., Jordan, S.E., Herdman, M.J., Jhalli, N., Duddle, J.M., Hamilton, S.A., et al. (1994). Placebo-controlled immunopathologic study of four months of inhaled corticosteroids in asthma. Am. J. Respir. Crit. Care Med. *150*, 17-22.

Tsuchiya, S., Yamabe, M., Yamaguchi, Y., Kobayashi, Y., Konno, T., Tada, K. (1980). Establishment and characterization of a human acute monocytic leukemia cell line (THP-1). Int. J. Cancer. *26*, 171-176.

Tsuchiya, S., Kobayashi., Y, Goto, Y., Okumura, H., Nakae, S., Konno, T., and Tada, K. (1982). Induction of maturation in cultured human monocytic leukemia cells by a phorbol diester. Cancer Res. *42*, 1530-1536.

Tsuji, H., Venditti Jr., F.J., Manders, E.S., Evans, J.C., Larson, M.G., Feldman, C.L., and Levy, D., (1996). Determinants of heart rate variability. J. Am. Coll. Cardiol. *28*, 1539– 1546.

Ulrich, M.M., Alink, G.M., Kumarathasan, P., Vincent, R., Boere, A.J., and Cassee, F.R.. (2002). Health effects and time course of particulate matter on the cardiopulmonary system in rats with lung inflammation. J. Toxicol. Environ. Health A. *65*, 1571-1595.

Urch, B., Brook, J.R., Wasserstein, D., Brook, R.D., Rajagopalan, S., Corey, P., Silverman, F. (2004). Relative contributions of PM2.5 chemical constituents to acute arterial vasoconstriction in humans. Inhal. Toxicol. *16*, 345-352.

van Eeden, SF, Tan, WC, Suwa, T, Mukae, H, Terashima, T, Fujii, T, Qui, D, Vincent, R, and Hogg, JC. (2001). Cytokines involved in the systemic inflammatory response induced by exposure to particulate matter air pollutants (PM(10)). Am. J. Respir. Crit. Care Med. *164*, 826-830.

van Eeden, S.F., Yeung, A., Quinlam, K., and Hogg, J.C. (2005). Systemic response to ambient particulate matter: relevance to chronic obstructive pulmonary disease. Proc. Am. Thorac. Soc. 2, 61-67.

van Zijverden, M., and Granum, B. (2000). Adjuvant activity of particulate pollutants in different mouse models. Toxicology. *152*, 69-77.

Vincent, R., Vu, D., Hatch, G., Poon, R., Dreher, K., Guénette, J., Bjarnason, S., Potvin, M., Norwood, J., and McMullen, E. (1996). Sensitivity of lungs of aging Fischer 344 rats to ozone: assessment by bronchoalveolar lavage. Am. J. Physiol. Lung Cell. Mol. Physiol. *271*, L555-L565.

Vincent, R., Bjarnason, S.G., Adamson, I.Y., Hedgecock, C., Kumarathasan, P., Guenette, J., Potvin, M., Goegan, P., and Bouthillier, L. (1997a). Acute pulmonary toxicity of urban particulate matter and ozone. Am. J. Pathol. *151*, 1563-1570.

Vincent, R., Goegan, P., Johnson, G., Brook, J.R., Kumarathasan, P., Bouthillier, L., and Burnett, R.T. (1997b). Regulation of promoter-CAT stress genes in HepG2 cells by suspensions of particles from ambient air. Fundam. Appl. Toxicol. *39*, 18-32.

Vincent, R, Kumarathasan, P, Goegan, P, Bjarnason, SG, Guenette, J, Berube, D, Adamson, IY, Desjardins, S, Burnett, RT, Miller, FJ, Battistini, B. (2001). Inhalation toxicology of urban ambient particulate matter: acute cardiovascular effects in rats. Res. Rep. Health Eff. Inst. *104*, 5-62.

von Klot, S., Peters, A., Aalto, P., Bellander, T., Berglind, N., D'Ippoliti, D., Elosua, R., Hormann, A., Kulmala, M., Lanki, T., et al. (2005). Health Effects of Particles on Susceptible Subpopulations (HEAPSS) Study Group. Ambient air pollution is associated with increased risk of hospital cardiac readmissions of myocardial infarction survivors in five European cities. Circulation. *112*, 3073-3079.

Wichmann, H.E., Mueller, W., Allhoff, P., Beckmann, M., Bocter, N., Csicsaky, M.J., Jung, M., Molik, B., and Schoeneberg, G. (1989). Health effects during a smog episode in West Germany in 1985. Environ. Health Perspect. *79*, 89-99.

Wiebert, P., Sanchez-Crespo, A., Seitz, J., Falk, R., Philipson, K., Kreyling, W.G., Möller, W., Sommerer, K, Larsson, S., and Svartengren, M. (2006). Negligible clearance of ultrafine particles retained in healthy and affected human lungs. Eur. Respir. J. *28*, 286-290.

Wilson, W.E., and Suh, H.H. (1997). Fine particles and coarse particles: concentration relationships relevant to epidemiologic studies. J. Air Waste Manag. Assoc. *12*, 1238-1249.

Wilson, M.R., Lightbody, J.H., Donaldson, K., Sales, J., and Stone, V. (2002). Interactions between ultrafine particles and transition metals *in vivo* and *in vitro*. Toxicol. Appl. Pharmacol. *184*, 172-9.

Wottrich, R., Diabate, S., and Krug H.F. (2004). Biological effects of ultrafine model particles in human macrophages and epithelial cells in mono- and co-culture. Int. J. Hyg. Environ. Health. *207*, 353-361.

Xia, T., Korge, P., Weiss, J.N., Li, N., Venkatesen, M.I., Sioutas, C., and Nel, A. (2004). Quinones and aromatic chemical compounds in particulate matter induce mitochondrial dysfunction: implications for ultrafine particle toxicity. Environ. Health Perspect. *112*, 1347-1358.

Xia, T., Kovochich, M., Brant, J., Hotze, M., Sempf, J., Oberley, T., Sioutas, C., Yeh, J.I., Wiesner M.R., and Nel A.E. (2006). Comparison of the abilities of ambient and manufactured nanoparticles to induce cellular toxicity according to an oxidative stress paradigm. Nano Lett. *6*, 1794-1807.

Xia, T., Kovochich, M., and Nel, A.E. (2007). Impairment of mitochondrial function by particulate matter (PM) and their toxic components: implications for PM-induced cardiovascular and lung disease. Front. Biosci. *12*, 1238-1246.

Yamawaki, H., and Iwai, N. (2006). Mechanisms underlying nano-sized air-pollution-mediated progression of atherosclerosis: carbon black causes cytotoxic injury/inflammation and inhibits cell growth in vascular endothelial cells. Circ. J. *70*, 129-140.

Yin, X.J., Ma, J.Y., Antonini, J.M., Castranova, V., and Ma, J.K. (2004). Roles of reactive oxygen species and heme oxygenase-1 in modulation of alveolar macrophage-mediated pulmonary immune responses to *Listeria monocytogenes* by diesel exhaust particles. Toxicol. Sci. *82*, 143-153.

Yuen, I.S., Hartsky, M.A., Snajdr, S.I., and Warheit, D.B. (1996). Time course of chemotactic factor generation and neutrophil recruitment in the lungs of dust-exposed rats. Am. J. Respir. Cell. Mol. Biol. 15, 268-274.

Zalata, A.A., Lammertijn, N., Christophe, A., and Comhaire, F.H. (1998). The correlates and alleged biochemical background of the resazurin reduction test in semen. Int. J. Androl. *21*, 289-294.

Zhou, H., and Kobzik, L. (2007). Effect of concentrated ambient particles on macrophage phagocytosis and killing of *Streptococcus pneumoniae*. Am. J. Respir. Cell. Mol. Biol. *36*, 460-465.

Dalibor Breznan

Education

2002 – present	PhD: Biochemistry candidate University of Ottawa & Health Canada Ottawa, Ontario, Canada Supervisor: Dr. R. Vincent Project Title: Toxicology of Urban Particulate Matter: *In Vitro* and *In Vivo* Bioassays
1999 - 2001	MSc: Biochemistry University of Ottawa Heart Institute Ottawa, Ontario, Canada Supervisor: Dr. D.L. Sparks Dissertation Title: The High Density Lipoprotein Metabolism by the Kidney.
1993 - 1998	BSc: Biology / Biotechnology (Magna Cum Laude) Carleton University Ottawa, Ontario, Canada Supervisor: Dr. N. Chaly Dissertation Title: An Analysis of Apoptotic Nuclear Events in Heat-treated Mouse Splenocytes and in Differentiating Rat L6E9 Muscle Cells.

Employment

05/2003 – 08/2003	Summer Research Fellow Nagasaki University, Second Department of Internal Medicine, Japan
05/1995 – 05/2003	Avian Care Technician Wild Bird Care Centre, Ottawa
01/2002 – 05/2002	Research Technician Health Canada, Inhalation Toxicology and Aerobiology Section
09/1998 – 05/1999	Teaching Assistant Department of Biology, Carleton University Biochemistry and Cell Biology courses

09/1996 - 05/1997 Research Assistant
Department of Biology, Carleton University
Cell Biology laboratory

Awards and Memberships

- (2007-2009) NSERC-JSPS Postdoctoral Fellowship
- (2004-2006) OGSST Scholarship
- (2003) NSERC-JSPS Summer Fellowship in Japan
- (2002-2006) Research Excellence Award (tuition waver), University of Ottawa
- (2000) Best Student Poster in MSc Category Award, University of Ottawa
- (1998) JIAS Canada National Academic Scholarship
- (1997) Dean's Honour List Scholar, Carleton University

- member of the American Physiology Society (APS), (2003-2007)
- member of the Carleton University Biology Society (CUBS), (1996-1998)
- treasurer of the Heart Institute Graduate Students Association (HIGSA), (2000-2001)
- member of the Jewish Students Association (JSU-Hillel)

Publications

- Stamler, C.J., **Breznan, D.**, Neville, T.A., Viau, F.J., Camlioglu, E., and D.L. Sparks. 2000. Phosphatidylinositol Promotes Cholesterol Transport *in vivo*. J. Lipid Res. 41: 1214-21.

- **Breznan, D.**, Veereswaran, V., Viau, F., Neville, T.A-M., and Daniel L. Sparks. 2004. The Lipid Composition of HDL Affects its Reabsorption by Renal Proximal Tubule Cells. Biochem. J. 379 (Pt. 2): 343-9.

- Chauhan, V., **Breznan, D.**, Goegan, P., Nadeau, D., Karthikeyan S., Brook, JR., and R. Vincent. 2004. Effect of Airborne Particulate Matter on Nitric Oxide Production in Macrophage Cell Lines. Cell. Biol. Toxicol. 20: 221-39. (co-author, equivalent contribution)

- Chauhan, V., **Breznan, D.**, Thomson, E., and R. Vincent. 2005. Effects of Ambient Air Particles on Endothelin System in Human Pulmonary Epithelial Cells (A549). Cell. Biol. Toxicol. 21: 191-205. (co-author, equivalent contribution)

Presentations

- 11th International Congress of Toxicology (ICT XI). 2007. Montreal, QC
- Health Canada Research Forum: From Science to Policy. 2002, 2003, 2006 and 2007. Ottawa, ON
- Canada-US Border Air Quality (BAQS) Joint Meeting of Health Canada and US EPA. 2005. Detroit, Michigan
- Society of Toxicology of Canada (STC) Annual Symposium. 2004. Montreal, QC
- Federation of American Societies for Experimental Biology (FASEB) Conference. 2003. San Diego, California
- 46th Annual Meeting of the Canadian Federation of Biological Societies (CFBS). 2003. Ottawa, ON
- Canadian Lipoprotein Conference. 2002. White Rock, BC

Scholarly Activities

- Presentations at the Annual Research Day of the Department of Biochemistry, Microbiology and Immunology, University of Ottawa (2000-2007)
- PhD Graduate Students Research Presentation, University of Ottawa (2003, 2006)
- MSc Graduate Students Research Presentation, University of Ottawa (2001)
- Second Annual Celebration of Excellence Research Presentation of the Faculty of Medicine, University of Ottawa (2000)
- University of Ottawa Heart Institute Research Day, University of Ottawa (2000)
- Annual Research Day of the Department of Pathology and Laboratory Medicine, University of Ottawa (1999-2000)